

UC Berkeley

UC Berkeley Electronic Theses and Dissertations

Title

Homological mirror symmetry for the genus 2 curve in an abelian variety and its generalized Strominger-Yau-Zaslow mirror

Permalink

<https://escholarship.org/uc/item/88g945z7>

Author

Cannizzo, Catherine Kendall Asaro

Publication Date

2019

Peer reviewed|Thesis/dissertation

Homological mirror symmetry for the genus 2 curve in an abelian variety and its
generalized Strominger-Yau-Zaslow mirror

by

Catherine Kendall Asaro Cannizzo

A dissertation submitted in partial satisfaction of the

requirements for the degree of

Doctor of Philosophy

in

Mathematics

in the

Graduate Division

of the

University of California, Berkeley

Committee in charge:

Professor Denis Auroux, Chair

Professor David Nadler

Professor Marjorie Shapiro

Spring 2019

Homological mirror symmetry for the genus 2 curve in an abelian variety and its
generalized Strominger-Yau-Zaslow mirror

Copyright 2019
by
Catherine Kendall Asaro Cannizzo

Abstract

Homological mirror symmetry for the genus 2 curve in an abelian variety and its generalized Strominger-Yau-Zaslow mirror

by

Catherine Kendall Asaro Cannizzo

Doctor of Philosophy in Mathematics

University of California, Berkeley

Professor Denis Auroux, Chair

Motivated by observations in physics, mirror symmetry is the concept that certain manifolds come in pairs X and Y such that the complex geometry on X mirrors the symplectic geometry on Y . It allows one to deduce information about Y from known properties of X . Strominger-Yau-Zaslow (1996) described how such pairs arise geometrically as torus fibrations with the same base and related fibers, known as SYZ mirror symmetry. Kontsevich (1994) conjectured that a complex invariant on X (the bounded derived category of coherent sheaves) should be equivalent to a symplectic invariant of Y (the Fukaya category). This is known as homological mirror symmetry. In this project, we first use the construction of SYZ mirrors for hypersurfaces in abelian varieties following Abouzaid-Auroux-Katzarkov, in order to obtain X and Y as manifolds. The complex manifold comes from the genus 2 curve as a hypersurface in its Jacobian torus, and we equip the SYZ mirror manifold with a symplectic form. We then describe an embedding of the category on the complex side into a cohomological Fukaya-Seidel category of Y as a symplectic fibration. While our fibration is one of the first nonexact, non-Lefschetz fibrations to be equipped with a Fukaya category, the main geometric idea in defining it is the same as in Seidel's construction for Fukaya categories of Lefschetz fibrations.

I dedicate my thesis to my father, John Kendall Cannizzo, with all my love.

Thank you for being the sunlight in my life. May you rest in peace.

Contents

Contents	ii
List of Figures	iii
1 Introduction, background, and set-up	1
1.1 Statement of thesis result and approach	1
1.2 The B-side manifold	3
1.3 Background on toric varieties	13
1.4 The A-side manifold	23
1.5 The definition of the symplectic form	38
2 The symplectic form ω is nondegenerate	44
2.1 Putting bounds on the bump function derivatives	44
2.2 Converting to polar coordinates	47
2.3 Showing ω nondegenerate: \mathbb{C}^3 patch	49
2.4 Showing ω nondegenerate: away from \mathbb{C}^3 patch	68
3 HMS for V and V^\vee abelian varieties	70
4 The Fukaya category	82
4.1 The Fukaya-Seidel category of Y : introduction	82
4.2 Background for defining $H^0(FS(Y, v_0))$	91
4.3 Moduli spaces needed to define $H^0(FS(Y, v_0))$	94
4.4 $H^0(FS(Y, v_0))$: definition and independence of choices	110
5 The main theorem	114
5.1 HMS computation	114
5.2 Proof: fully-faithful embedding $D^bCoh(H) \hookrightarrow H^0(FS(Y, v_0))$	130
6 Notation	131
Bibliography	132

List of Figures

1.1	Quotient by Γ_B	11
1.2	The (0,0) tile delimited by the tropical curve	26
1.3	$\text{Trop}(1 + x_1 + x_2) = 0$	27
1.4	Moment polytope $\subset \mathbb{R}^3$	27
1.5	Moment polytope for central fiber of (Y, v_0) when $H = \Sigma_2$	28
1.6	In one dimension lower, the boundary of $\Delta_{\tilde{Y}}$ is the moment map image of a string of \mathbb{P}^1 's. In the polytope, $ v_0 $ increases in the (0, 1) direction. In the fibration v_0 , $ v_0 $ is the radius of the circle in the base.	29
1.7	Depiction of $\Delta_{\tilde{Y}}$ in the Σ_2 case. The coordinates indicate a Γ_B -action which we motivate and define in the next sections. Magenta parallelogram = fundamental domain for Γ_B action, with diagonal \mathbb{P}^1 at center. Each vertex is a \mathbb{C}^3 chart. Coordinate transitions will be explained in Lemma 1.4.9. Expressions in the center of tiles indicate e.g. $\eta \geq \varphi(\xi) = -\xi_1 - 1$ over that tile. Equations of the 6 edges imply tile _(0,0) is given by $(\xi_1, \xi_2) \in \{(\xi_1, \xi_2) \mid -1 \leq \xi_1, \xi_2, -\xi_1 + \xi_2 \leq 1\}$	30
1.8	Delineate regions in $\Delta_{\tilde{Y}}$ around a vertex	35
1.9	Zoom in on region I/II in left/right figures respectively	37
1.10	Interpolate between three potentials: $F = \alpha_1 g_{xy} + \alpha_2 g_{xz} + (1 - \alpha_1 - \alpha_2) g_{yz}$, $0 \leq \alpha_1, \alpha_2 \leq 1$. Region VII is where $\alpha_1 = \alpha_2 = 1/3$ and $F = \frac{1}{3}(g_{xy} + g_{xz} + g_{yz}) \approx \frac{2}{3}((Tr_x)^2 + (Tr_y)^2 + (Tr_z)^2)$ via the log approximation.	38
1.11	How the three angular directions vary	41
2.1	L) Number of potentials interpolated between. R) Zoomed in region about vertex.	49
2.2	The three angular directions	54
3.1	A triangle in the elliptic curve case and representative of the T^4 case	77
4.1	Monodromy in fiber, thought of as a section over the parallelogram $(\xi_1, \xi_2) \mapsto (\theta_1(\xi_1, \xi_2), \theta_2(\xi_1, \xi_2))$	85
4.2	Example of strip-like end	92
4.3	Flow chart for working with moduli spaces in Fukaya categories	96
4.4	2-skeleton of cell complex from construction of T^4 as a quotient of a 4-cube	97
4.5	$L_i =$ parallel transport ℓ_i around U-shaped curves in base of v_0	111

5.1	Leibniz rule	116
5.2	The homotopy between ∂ (left) and the count of discs we compute (right)	116
5.3	Plan for computation	117

Acknowledgments

This work was partially supported by NSF grants DMS-1264662, DMS-1406274, and DMS-1702049, and by a Simons Foundation grant (# 385573, Simons Collaboration on Homological Mirror Symmetry). I would like to thank my advisor Denis Auroux for the immeasurable academic support and guidance on this thesis project. I would also like to thank Mohammed Abouzaid, Melissa Liu, Katrin Wehrheim, Sheel Ganatra, Heather Lee, Roberta Guadagni, Jingyu Zhao, Sara Venkatesh, Wolfgang Schmaltz, Zhengyi Zhou, Benjamin Filippenko, and the MSRI Derived Categories program [APS] for fruitful mathematical discussions. I thank Jo Nelson, Ailsa Keating, Bahar Acu, Ziva Myer, Yu Pan, Morgan Weiler, and Anastasia Chavez for invaluable advice and support during the application process and in my career trajectory. I also thank the Noetherian Ring and UC Berkeley math department staff. Lastly I would like to thank my parents for their unwavering support.

Chapter 1

Introduction, background, and set-up

1.1 Statement of thesis result and approach

In this work, the pronoun “we” is used to denote the author along with the reader.

Theorem 1.1.1 ([Can]). *Let $\iota : H := \Sigma_2 \hookrightarrow V$ be a genus 2 curve embedded into an abelian variety V of complex dimension 2. There exists a mirror (Y, v_0) , which is a symplectic fibration with fiber denoted V^\vee that is mirror to V , and V^\vee is also an abelian variety of complex dimension 2. Then there is a commutative diagram as below, where vertical arrows are cohomologically fully faithful embeddings as functors between categories:*

$$\begin{array}{ccc}
 D^b\text{Coh}(V) & \xrightarrow{i^*} & D^b\text{Coh}(H) \\
 \text{HMS} \downarrow & \curvearrowright & \downarrow \text{HMS (C.)} \\
 H^0(\text{Fuk}(V^\vee)) & \xrightarrow{\cup} & H^0(\text{FS}(Y, v_0))
 \end{array} \tag{1.1}$$

Remark 1.1.2 (Explanation of the diagram). The top row is a functor between bounded derived categories of coherent sheaves. It will suffice to consider line bundles in our case. The bottom row is a functor between the Fukaya and Fukaya-Seidel categories. The morphism spaces in these categories are chain complexes and morphisms are not associative but satisfy associativity relations that involve arbitrarily many morphisms, hence are A_∞ -categories. The statement discussed in this thesis concerns the cohomological Fukaya categories where we pass to cohomology in the morphisms groups, hence obtaining an actual category. The construction of the diagram with A_∞ -functors, namely checking that higher order composition maps match in addition to objects, morphisms and composition, is a future direction.

Remark 1.1.3. Note that HMS for abelian varieties of arbitrary dimension and quotient lattice was discussed in [Fuk02] using more advanced machinery. We present a different argument for this particular case.

Remark 1.1.4. (Previous work on HMS for the genus 2 curve) Seidel proved HMS with the A-model of the genus 2 surface [Sei11], i.e. the symplectic side, so we consider the B-model or complex structure on the genus 2 curve. The complex mirror Seidel constructs is a crepant resolution of $\mathbb{C}^3/\mathbb{Z}_5$, quotienting by the rotation group, so the singularity at zero is resolved while preserving the first Chern class), and it is equipped with a superpotential. The critical locus of the superpotential in his paper and the mirror in this paper are the same. One future direction is to further explore how his mirror is related to the mirror considered in this paper. Note: we are not in the exact case as in [Sei08], namely ω is not exact because we have compact fibers in a symplectic fibration with nonzero volume, and we are not in monotone case, which is discussed later. We are in the Calabi-Yau setting on the mirror, $c_1 = 0$, and it is a Landau-Ginzburg model.

Outline of proof of Theorem 1.1.1. The approach we take is:

- Embed the genus 2 curve as a hypersurface in an abelian variety V .
- Blow up $V \times \mathbb{C}$ along $\Sigma_2 \times \{0\}$ so Σ_2 is the critical locus of a holomorphic function on the blow-up X , as described in [AAK16] for obtaining SYZ mirrors for hypersurfaces of toric varieties. This comes equipped with a Lagrangian torus fibration.
- Use SYZ to get a complex mirror Y two dimensions higher than Σ_2 and equip that mirror with a holomorphic function v_0 that encodes behavior that is mirror to Σ_2 .
- Both sides are Kähler so instead consider the B-model on the genus 2 curve and construct an A-model on the mirror. Note that involutivity is expected when the pair is Calabi-Yau, so one could have started with the mirror as the A-model and construct X as in [AAK16, §8] or [CLL12].
- Prove the existence of the fully-faithful embedding on the cohomological level for the mirror abelian varieties.
- Prove the same for Σ_2 and (Y, v_0) .
- Future directions: prove the subcategory of Lagrangians considered generates the Fukaya category. Prove an A_∞ -equivalence instead of an equivalence on cohomological categories.

□

Remark 1.1.5. We are in the general type case where $c_1 < 0$ on the genus 2 curve, that's why the mirror is a noncompact LG model. Also because of the blow-up, we are in the setting of a non-toric Lagrangian fibration. This is because toric means it comes from a moment map, and here we start with a moment map but then perform operations on the base which still give a Lagrangian torus fibration but no longer from a moment map. In [AAK16] for example the last coordinate comes from a moment map, but not the rest of it. The Fukaya category on X would be the setting of M. Liu and J. Hicks. Conversely in

[CLL12], they take the SYZ mirror on Y and account for sphere bubbles that show up in that case.

1.2 The B-side manifold

Complex geometry

Remark 1.2.1 (The input for building a SYZ mirror is a Lagrangian torus fibration). Given a Lagrangian torus fibration on a symplectic manifold, the SYZ construction [SYZ96] produces a candidate mirror complex manifold by prescribing dual fibers over the same base. The points of a dual fiber are parametrized by unitary flat connections on the trivial line bundle on the original fiber. This process is discussed explicitly in [Aur07].

Constructing a suitable Lagrangian torus fibration is a hard problem. R. Guadagni's thesis finds Lagrangian torus fibrations on central fibers of toric degenerations, which will be the setting of the mirror Y in our case. However there is not an obvious Lagrangian torus fibration on, or toric degeneration to, Σ_2 . Abouzaid-Auroux-Katzarkov [AAK16] construct Lagrangian torus fibrations on blow-ups of hypersurfaces in toric varieties, which we adapt to the abelian variety case here.

Definition 1.2.2 (Definition of abelian variety). The abelian variety V is topologically T^4 and its complex structure is defined as follows:

$$\begin{aligned} V &:= (\mathbb{C}^*)^2 / \Gamma_B \\ \Gamma_B &:= \mathbb{Z} \langle \gamma', \gamma'' \rangle \subset \mathbb{Z}^2, \quad \gamma' := \begin{pmatrix} 2 \\ 1 \end{pmatrix}, \gamma'' := \begin{pmatrix} 1 \\ 2 \end{pmatrix} \\ \Gamma_B \curvearrowright (\mathbb{C}^*)^2, \quad \gamma \cdot (x_1, x_2) &:= (\tau^{-\gamma_1} x_1, \tau^{-\gamma_2} x_2) \end{aligned} \tag{1.2}$$

where $\gamma \in \Gamma_B$ has \mathbb{Z}^2 -coordinates (γ_1, γ_2) and $\tau \in \mathbb{R}$ parametrizes a family of complex structures, which will be mirror to a family of symplectic structures on the mirror. The complex structure is the Γ_B -quotient of the usual J_0 that is multiplication by i on $(\mathbb{C}^*)^2$ at every point.

Remark 1.2.3 (Additive and multiplicative lattice viewpoints of abelian variety). There are equivalent ways to describe an abelian variety: the lattice can act multiplicatively as above, or equivalently it can act additively as we will describe below. This latter viewpoint allows us to understand the cohomology of V and is described in [BL04] and [Pol03].

The following lattice Γ acts additively on \mathbb{C}^2 , and the quotient gives a product torus denoted $T_B \times T_F$, which corresponds to the norms and angles of the multiplicative complex coordinates previously described on V . We define the lattices for T_B and T_F first, and then Γ .

$$\Gamma_B := \mathbb{Z} \left\langle \begin{pmatrix} 2 \\ 1 \end{pmatrix}, \begin{pmatrix} 1 \\ 2 \end{pmatrix} \right\rangle, \quad \Gamma_F := \mathbb{Z}^2, \quad \Gamma := -\log \tau \cdot \Gamma_B + 2\pi i \Gamma_F \subset \mathbb{C}^2 \tag{1.3}$$

Now we define the abelian variety with additive structure:

$$V_+ := \mathbb{C}^2/\Gamma \cong \mathbb{R}_{u_1, u_2}^2/\Gamma_B \times \mathbb{R}_{v_1, v_2}^2/\Gamma_F =: T_B \times T_F$$

The additive structure maps to the multiplicative structure under the exponential map:

$$V_+ = \mathbb{C}^2/\Gamma \ni (-u_1 \log \tau + 2\pi i v_1, -u_2 \log \tau + 2\pi i v_2) \xrightarrow{\exp} (\tau^{-u_1} e^{2\pi i v_1}, \tau^{-u_2} e^{2\pi i v_2}) \in V = (\mathbb{C}^*)^2/\Gamma_B$$

We see that u_1 and u_2 encode the norms of the complex coordinates (x_1, x_2) on V while v_1 and v_2 are the angles. The reason for the subscript B is to denote the base of a moment map from the standard T^2 -rotation action $(\alpha_1, \alpha_2) \cdot (x_1, x_2) := (e^{2\pi i \alpha_1} x_1, e^{2\pi i \alpha_2} x_2)$ and F the fiber, i.e. obtained from rotating angles under an orbit for fixed norms $(|x_1|, |x_2|)$. In particular, the Γ_F no longer acts in the multiplicative setting. So in the T_F direction, properties on V_+ should be trivial in order to pass to V under the exponential map.

In the reverse direction $(-\frac{1}{\log \tau} |\log(\underline{x})|, \frac{1}{2\pi i} (\log(\underline{x}) - \log|\underline{x}|))$ gives the isomorphism $V \xrightarrow{\cong} T_B \times T_F$ where $\underline{x} = (x_1, x_2)$ so this is written in vector notation. Typically τ is small, e.g. $\tau = e^{-2\pi}$. As τ goes to zero the primitive lattice vectors in $-\log \tau \cdot \Gamma_B$ lengthen.

Claim 1.2.4 (Cohomology of abelian variety V). $H^n(V; \mathbb{Z}) \cong \wedge^n \text{Hom}(\Gamma, \mathbb{Z})$

Sketch, c.f. [BL04, §1.3]. It suffices to work with V_+ since it is homeomorphic to V .

$$\Gamma = \pi_1(V_+) = H_1(V_+; \mathbb{Z}) \therefore H^1(V_+; \mathbb{Z}) = \text{Hom}(\Gamma, \mathbb{Z})$$

The second equality follows because Γ is abelian and H_1 is the abelianization of π_1 . The third equality follows from the universal coefficient theorem and lack of torsion. So using the Künneth formula, its compatibility with the cup product, and the de Rham isomorphism we obtain a map which is an isomorphism of rings by induction:

$$\bigwedge^n \text{Hom}(\Gamma, \mathbb{Z}) \cong \bigwedge^n H^1(V; \mathbb{Z}) \xrightarrow{\cup} H^n(V; \mathbb{Z})$$

□

Corollary 1.2.5 ([Pol03, §1]). *Complex line bundles on V are topologically classified by their first Chern class, which is a skew-symmetric bilinear form $E : \Gamma \times \Gamma \rightarrow \mathbb{Z}$.*

Proof. For a complex line bundle, $c_1(L) \in H^2(V; \mathbb{Z}) \cong \wedge^2 \text{Hom}(\Gamma, \mathbb{Z})$ by the previous claim, and $\wedge^2 \text{Hom}(\Gamma, \mathbb{Z}) \cong \text{Hom}(\wedge^2 \Gamma, \mathbb{Z})$. □

We want to determine which forms E arise as the first Chern class of a *holomorphic* line bundle. These are precisely the L for which $c_1(L) \in H^{1,1}(V)$. So the next step is to consider $\text{Pic}(V)$ and the Hodge decomposition on abelian varieties, then find a description in terms of the lattice Γ as we did above for the topological cohomology.

Claim 1.2.6. Holomorphic line bundles on V are classified by

$$H^1(\pi_1(V_+); H^0(\mathcal{O}_{\tilde{V}_+}^*)) \cong H^1(V_+, \mathcal{O}^*) \quad (1.4)$$

Sketch from [BL04]. This theory is from [BL04, Appendix B], where elements of the left hand side of Equation 1.4 are referred to as *factors of automorphy*. This isomorphism is the analogue of the equivalence of Cartier divisors and line bundles on complex manifolds, but with the addition of Γ -equivariance. In other words, factors of automorphy are functions whose vanishing set, i.e. divisor, is Γ -invariant. The notion of a group action is equivalent to the notion of a cocycle, hence this invariance is encoded in the cohomology group $H^1(\pi_1(V_+); H^0(\mathcal{O}_{\tilde{V}_+}^*))$. The right hand side $H^1(V_+, \mathcal{O}^*) \cong \text{Pic}(V_+)$ consists of holomorphic line bundles on \mathbb{C}^2/Γ . Note that $\tilde{V}_+ = \mathbb{C}^2$.

Let $\pi : \mathbb{C}^2 \rightarrow V_+$ be the universal covering. The isomorphism of Equation 1.4 is constructed as follows, c.f. [BL04, Proposition B.1]. Line bundles over V_+ have a nice description because the cocycle condition on charts over V_+ is equivalent to the condition that Γ has a group action on \mathbb{C}^2 on a collection of charts in the universal cover, each one a lift of an open set on the base. We now describe this.

- Let $\{U_i\}$ be a covering of V_+ . A holomorphic line bundle is defined by gluing $U_i \times \mathbb{C}$ to $U_j \times \mathbb{C}$ by a holomorphic transition function g_{ij} acting on the \mathbb{C} factor. Alternatively, we can lift each U_i to W_i so that $\pi|_{W_i} : W_i \rightarrow U_i$ is a biholomorphism. In particular, $\pi_i^{-1}(x)$ and $\pi_j^{-1}(x)$ are two lifts of the same point, so by definition of the universal cover they differ by some element $\gamma_{ij} \in \Gamma$.
- Thus we can alternatively think of the transition functions as a function f of one of the lifts and the γ_{ij} that records the change between $\pi_i^{-1}(x)$ and $\pi_j^{-1}(x)$. Namely $\pi_j^{-1}(x) = \gamma_{ij}\pi_i^{-1}(x)$ for some $\gamma_{ij} \in \Gamma$. Then define

$$f(\gamma_{ij}, \pi_i^{-1}(x)) := g_{ij}$$

- Because Γ acts on \mathbb{C}^2 , the group action implies $\gamma_{ij}\gamma_{jk} = \gamma_{ik}$. The fact that such a g_{ij} is a cocycle on a line bundle implies

$$\begin{aligned} g_{ij}g_{jk} &= g_{ik} \\ \therefore f(\gamma_{ij}, \pi_i^{-1}(x))f(\gamma_{jk}, \pi_j^{-1}(x)) &= f(\gamma_{ik}, \pi_i^{-1}(x)) \\ \therefore f(\gamma_{ij}, \pi_i^{-1}(x))f(\gamma_{jk}, \gamma_{ij}\pi_i^{-1}(x)) &= f(\gamma_{ij}\gamma_{jk}, \pi_i^{-1}(x)) \\ &\iff [f] \in H^1(\Gamma, H^0(\mathcal{O}_{\mathbb{C}^2}^*)) \end{aligned} \quad (1.5)$$

i.e. f is a factor of automorphy.

- Concretely, by considering what cocycles and coboundaries map to under $g_{ij} \mapsto f(\gamma_{ij}, \pi_i^{-1}(\cdot))$ we obtain Čech cohomology groups with the discrete topology on Γ and taking values in the sheaf $\mathcal{O}_{\mathbb{C}^2}^*$. In particular the image gives a representative of a class in $H^1(\pi_1(V_+); H^0(\mathcal{O}_{\tilde{V}_+}^*))$.

- A trivial line bundle implies transition functions are of the form $g_{ij} = h_j/h_i$. So letting $g_{ij} = f(\gamma_{ij}, \pi_i^{-1}) = h_j/h_i$ we can define a function h on the universal cover by

$$h(\pi_i^{-1}(x)) := h(\pi_j^{-1}(x)) \cdot \frac{h_i}{h_j}$$

- So this corresponds to a coboundary $(\gamma, \tilde{x}) \mapsto h(\gamma \cdot \tilde{x})h(\tilde{x})^{-1}$ for some $h \in H^0(\mathcal{O}_{\mathbb{C}^2}^*)$.
- This correspondence is an isomorphism on cohomology, see [BL04, Proposition B.1].
- Note that there is an analogous result for all higher degree cohomology as well.

□

Claim 1.2.7. $H^{1,1}(V_+) \cong \text{Hom}_{\mathbb{C}}(\mathbb{C}^2, \mathbb{C}) \otimes \text{Hom}_{\overline{\mathbb{C}}}(\mathbb{C}^2, \mathbb{C})$

Proof. On the complex vector space \mathbb{C}^2 , recall we have a decomposition $(\mathbb{C}^2)^{1,0} \oplus (\mathbb{C}^2)^{0,1}$ [Huy05, Lemma 1.2.5]. Then $(T^{1,0}\mathbb{C}^2)^* = \text{Hom}_{\mathbb{C}}(\mathbb{C}^2, \mathbb{C})$ and $(T^{0,1}\mathbb{C}^2)^* = \text{Hom}_{\overline{\mathbb{C}}}(\mathbb{C}^2, \mathbb{C})$ see [BL04, Theorem 1.4.1]. If t_v is translation by v on the torus, we can extend (p, q) forms on \mathbb{C}^2 to all of the torus by pulling back by dt_{-v} . So $H^{1,1}(V_+) \cong \text{Hom}_{\mathbb{C}}(\mathbb{C}^2, \mathbb{C}) \otimes \text{Hom}_{\overline{\mathbb{C}}}(\mathbb{C}^2, \mathbb{C})$. □

Corollary 1.2.8 (C.f [BL04, Proposition 2.1.6]). *A complex line bundle \mathcal{L} admits a holomorphic structure if and only if the class $c_1(\mathcal{L})$ is a $(1, 1)$ form, i.e. $E(i\cdot, i\cdot) = E(\cdot, \cdot)$, and $E(\Gamma, \Gamma) \subseteq \mathbb{Z}$. In particular, holomorphic line bundles on V_+ correspond with 2×2 hermitian matrices with the same integral property.*

Remark 1.2.9. The exponential short exact sequence of sheaves $0 \rightarrow \mathbb{Z} \rightarrow \mathcal{O} \xrightarrow{\exp} \mathcal{O}^* \rightarrow 1$ gives a long exact sequence containing $H^1(V, \mathcal{O}^*) \cong \text{Pic}(V) \xrightarrow{-c_1} H^2(V; \mathbb{Z}) \subseteq H^2(V; \mathbb{C}) = H^{0,2}(V) \oplus H^{1,1}(V) \oplus H^{2,0}(V)$. In particular, $c_1(\mathcal{L}) \in H^{1,1}(V)$ if and only if taking a wedge product with generators of $H^{0,2}$ and $H^{2,0}$ gives zero.

Note that $H(\cdot, \cdot) := E(i(\cdot), \cdot) + iE(\cdot, \cdot)$ is a Hermitian form, see [Huy05, Lemma 1.2.15]. Define \mathcal{L} by *multiplicators* e_γ (or *factors of automorphy* in [BL04]) i.e. $\Gamma \rightarrow \mathcal{O}^*(V)$ which describe the necessarily Γ -periodic gluing functions of the line as we go around elements of $\pi_1(V)$.

Lemma 1.2.10 (C.f. [Pol03, Theorem 1.3] and [BL04, Appell-Humbert Theorem 2.2.3]). *The Picard group $\text{Pic}(V_+)$ of holomorphic line bundles on V_+ is isomorphic to the set of all pairs (H, α) for Hermitian forms $H : \mathbb{C}^2 \times \mathbb{C}^2 \rightarrow \mathbb{C}$ and $\text{Im } H(\Gamma, \Gamma) \subseteq \mathbb{Z}$ and $\alpha : \Gamma \rightarrow U(1)$ satisfying $\alpha(\gamma + \tilde{\gamma}) = \exp(\pi i E(\gamma, \tilde{\gamma}))\alpha(\gamma)\alpha(\tilde{\gamma})$, where $E = \text{Im } H$.*

Sketch proof from [Pol03, Chapter 2] and [BL04, Chapter 2]. In [Pol03, §2.3] Polishchuk describes how the holomorphic structures are parametrized by an $\alpha : \Gamma \rightarrow U(1)$ that satisfies

$$\alpha(\gamma + \tilde{\gamma}) = \exp(\pi i E(\gamma, \tilde{\gamma}))\alpha(\gamma)\alpha(\tilde{\gamma})$$

as do [BL04, Proposition 2.2.2]. (Note that α in the former is denoted χ in the latter.) Then the factor of automorphy for a choice of (H, α) (where $E = \text{Im } H$) is

$$(\gamma, v) \mapsto \alpha(\gamma) \exp(\pi H(v, \gamma) + \frac{\pi}{2} H(\gamma, \gamma))$$

This factor of automorphy is a natural definition from the perspective of [BD16] where we have the notion of *generalized Heisenberg groups*. In our case the relevant group is the semi-direct product $U(1) \times \mathbb{C}^2$ with group law

$$(\gamma, v) \cdot (\tilde{\gamma}, \tilde{v}) = (\exp(\pi i E(v, \tilde{v})) \gamma \tilde{\gamma}, v + \tilde{v})$$

The key point about Heisenberg groups is a uniqueness of unitary irreducible representations, a theorem due to Stone and von Neumann. The Fock representation gives the factor of automorphy from above.

Conversely, suppose we have a factor of automorphy f for a holomorphic line bundle \mathcal{L} . Because it is nonvanishing we can express $f = \exp(2\pi i g)$ for some holomorphic function g . Then by [BL04, Theorem 2.1.2] the first Chern class corresponds to the alternating form

$$E_{\mathcal{L}}(\gamma, \tilde{\gamma}) = g(\tilde{\gamma}, v + \gamma) + g(\gamma, v) - g(\gamma, v + \tilde{\gamma}) - g(\tilde{\gamma}, v)$$

for all $\gamma, \tilde{\gamma} \in \Gamma = -\log \tau \Gamma_B + 2\pi i \Gamma_F$ and any choice of $v \in \mathbb{C}^2$ (it turns out this expression is independent of v). As we saw above, E corresponds to a Hermitian form when \mathcal{L} is holomorphic, and also $E(\Gamma, \Gamma) \subseteq \mathbb{Z}$. We can also construct an $\alpha : \Gamma \rightarrow U(1)$ as described at the bottom of [BL04, pg 31].

So this completes the sketch of the isomorphism in the Lemma. □

Example 1.2.11. Recall that for a complex line bundle on an abelian variety, $c_1(L)$ can be represented by an alternating form $E : \Gamma \times \Gamma \rightarrow \mathbb{Z}$ for $\Gamma \subset \mathbb{C}^2$. Thus taking \mathbb{R} linear combinations we can extend this to an \mathbb{R} -linear form $E : \mathbb{C}^2 \times \mathbb{C}^2 \rightarrow \mathbb{R}$. With respect to the basis given by the generators of Γ_B and Γ_F in Remark 1.3, this gives a 4 by 4 skew-symmetric matrix with respect to $\Gamma_B \times \Gamma_F$.

In the example of our setting here, we want the line bundle to be trivial in the T_F directions. That is, $E(iv, iw) = 0$ for $v, w \in \mathbb{Z}^2$. When L is a holomorphic line bundle, we saw in Corollary 1.2.8 that this implies $E(iv, iw) = E(v, w)$. Hence E is a block matrix

$$\begin{matrix} & \Gamma_B & \Gamma_F \\ \Gamma_B & \begin{pmatrix} 0 & * \\ -* & 0 \end{pmatrix} \\ \Gamma_F & & \end{matrix}$$

This produces a corollary of Corollary 1.2.8 above.

Corollary 1.2.12. *Holomorphic line bundles on V_+ that pass under \exp to holomorphic line bundles on V correspond with real integral symmetric 2×2 matrices.*

Proof. On V_+ we can input generic elements of $\Gamma_B + i\Gamma_F$ as $E(\gamma + iw, \tilde{\gamma} + iv)$. By the above, this is $\text{Im } H$ for some hermitian form $H = \begin{pmatrix} a & b \\ \bar{b} & a \end{pmatrix}$ so $a \in \mathbb{R}$.

$$(\gamma_1 + iw_1 \quad \gamma_2 + iw_2) \begin{pmatrix} a & b + ic \\ b - ic & d \end{pmatrix} \begin{pmatrix} \tilde{\gamma}_1 + iv_1 \\ \tilde{\gamma}_2 + iv_2 \end{pmatrix} \quad (1.6)$$

In particular, since $E(iw, iv) = 0$ we find that

$$\begin{aligned} E(iw, iv) &= \text{Im } H(iw, iv) = \text{Im}(aw_1v_1 + bw_1v_2 + icw_1v_2 + bw_2v_1 + dw_2v_2 - icv_1w_2) \\ &= c(w_1v_2 - v_1w_2) = 0 \quad \forall w, v \in \mathbb{Z}^2 \\ \therefore c &= 0 \end{aligned}$$

and H is real hence symmetric. □

Corollary 1.2.13. *We can express a holomorphic line bundle on V with a factor of automorphy given by*

$$(\gamma, x) \mapsto x^{\lambda(\gamma)} \tau^{\kappa(\gamma)}$$

where $\lambda \in \text{hom}(\Gamma_B, \mathbb{Z}^2) = \text{hom}(\Gamma_B, \Gamma_F^*)$ corresponds to the first Chern class and $\kappa(\gamma)$ is a real degree 2 polynomial whose quadratic part is determined by the first Chern class and whose linear part determines the holomorphic structure.

Proof. The factor of automorphy as described above (or see [Pol03, Equation (1.2.2)] and following discussion) corresponds with a choice of (H, α) and equals

$$(\gamma, v) \mapsto \alpha(\gamma) \exp(\pi H(v, \gamma) + \frac{\pi}{2} H(\gamma, \gamma))$$

We calculate the expression in the exponential (note that an element in the Γ of this particular situation is $\gamma + iw \in \Gamma_B + i\Gamma_F$)

$$\begin{aligned} &\pi H\left(-\frac{1}{\log \tau} \log x, \gamma + iw\right) + \frac{\pi}{2} H(\gamma + iw, \gamma + iw) \\ &= \pi \left[-\frac{1}{\log \tau} (\log x)^T H \gamma + \frac{1}{2} H(\gamma, \gamma) + \frac{1}{2} H(w, w) \right] + i\pi \left(-\frac{1}{\log \tau} \right) [(\log x)^T H w] \\ &= \pi \left[\left(-\frac{1}{\log \tau} \right) (\log x)^T H \gamma + \frac{1}{2} H(\gamma, \gamma) \right] \end{aligned}$$

where the second line follows because H is real and symmetric, and in the third line we've taken $w = 0$ since the result should not depend on the angle Γ_F directions. So we can set

$$\begin{aligned} (-\log \tau)\lambda(\gamma) &:= H\gamma \\ \kappa(\gamma) &:= \frac{1}{2}H(\gamma, \gamma) + \log(\alpha(\gamma)) \end{aligned} \tag{1.7}$$

for $H(\Gamma_B, \Gamma_B) \subseteq (-\log \tau)\mathbb{Z}$. We will give the choice of H used in this thesis in an example below. □

Example 1.2.14. Recall Example 1.2.11. Let

$$H := (-\log \tau) \begin{pmatrix} 2 & 1 \\ 1 & 2 \end{pmatrix}^{-1}$$

Then this defines

$$\begin{aligned} \mathcal{L} &\rightarrow V \\ \mathcal{L} &= (\mathbb{C}^*)^2 \times \mathbb{C}/\Gamma_B, \quad \gamma \cdot (x_1, x_2, v) := (\tau^{-\gamma_1}x_1, \tau^{-\gamma_2}x_2, \tau^{\kappa(\gamma)}x^{\lambda(\gamma)}v) \\ \text{Hom}(\Gamma_B, \mathbb{Z}^2) &\ni \lambda : \gamma' \mapsto \begin{pmatrix} 1 \\ 0 \end{pmatrix}, \gamma'' \mapsto \begin{pmatrix} 0 \\ 1 \end{pmatrix} \\ \kappa(n_1\gamma' + n_2\gamma'') &:= -\frac{1}{2} \begin{pmatrix} n_1 & n_2 \end{pmatrix} \begin{pmatrix} 2 & 1 \\ 1 & 2 \end{pmatrix} \begin{pmatrix} n_1 \\ n_2 \end{pmatrix} \end{aligned}$$

Claim 1.2.15.

$$\kappa(n_1\gamma' + n_2\gamma'') = -\frac{1}{2}n^T \begin{pmatrix} 2 & 1 \\ 1 & 2 \end{pmatrix} n$$

satisfies the cocycle condition.

Proof. We want the above definition of κ to satisfy the requirements of a group action $\gamma^2 \cdot (\gamma^1 \cdot (x, v)) = (\gamma^2 \circ \gamma^1) \cdot (x, v)$.

$$\begin{aligned} (x_1, x_2, v) &\xrightarrow{\gamma^1} (\tau^{-\gamma_1^1}x_1, \tau^{-\gamma_2^1}x_2, \tau^{\kappa(\gamma^1)}x^{\lambda(\gamma^1)}v) \\ (x_{new}, v_{new}) &:= (\tau^{-\gamma_1^1}x_1, \tau^{-\gamma_2^1}x_2, \tau^{\kappa(\gamma^1)}x^{\lambda(\gamma^1)}v) \xrightarrow{\gamma^2} (\tau^{-\gamma_1^2-\gamma_1^1}x_1, \tau^{-\gamma_2^2-\gamma_2^1}x_2, \tau^{\kappa(\gamma^2)}x_{new}^{\lambda(\gamma^2)}v_{new}) \\ &= (\tau^{-\gamma_1^2-\gamma_1^1}x_1, \tau^{-\gamma_2^2-\gamma_2^1}x_2, \tau^{\kappa(\gamma^2)}(\tau^{-\gamma^1}x)^{\lambda(\gamma^2)}(\tau^{\kappa(\gamma^1)}x^{\lambda(\gamma^1)}v)) \\ &= (\tau^{-\gamma^1-\gamma^2}x, \tau^{\kappa(\gamma^1)+\kappa(\gamma^2)-\langle \gamma^1, \lambda(\gamma^2) \rangle}x^{\lambda(\gamma^1)+\lambda(\gamma^2)}v) \end{aligned}$$

On the other hand, applying $\gamma_2 \circ \gamma_1$

$$(x_1, x_2, v) \mapsto (\tau^{-\gamma^1-\gamma^2}x, \tau^{\kappa(\gamma^1+\gamma^2)}x^{\lambda(\gamma^1+\gamma^2)}v)$$

and we know λ is a homomorphism. So to check the two maps agree we need to check that

$$\kappa(\gamma^1) + \kappa(\gamma^2) - \langle \gamma^1, \lambda(\gamma^2) \rangle = \kappa(\gamma^1 + \gamma^2)$$

This is satisfied by a quadratic form, so we make a choice of form $M := \begin{pmatrix} 2 & 1 \\ 1 & 2 \end{pmatrix}$ so that the geometry of the diagrams later on are in a standard form. Define

$$\kappa(n_1\gamma' + n_2\gamma'') = -\frac{1}{2}n^T \begin{pmatrix} 2 & 1 \\ 1 & 2 \end{pmatrix} n$$

Then both sides equal $-\frac{1}{2}n^1 M n^1 - \frac{1}{2}n^2 M n^2 - n^1 M n^2$ because $\gamma^1 = M n^1$ and $\lambda(\gamma^2) = n^2$ by definition. □

Claim 1.2.16. Sections of lines bundles on V are functions on $(\mathbb{C}^*)^2$ with the periodicity property

$$s(\gamma \cdot x) = \tau^{\kappa(\gamma)} x^{\lambda(\gamma)} s(x)$$

so have a Fourier expansion.

Proof. A section $s : V \rightarrow \mathcal{L}$ must have the same transition functions as the line bundle, if we consider the Cartier data.

$$s(\gamma \cdot x)/s(x) = \tau^{\kappa(\gamma)} x^{\lambda(\gamma)}$$

□

Corollary 1.2.17. Let \mathcal{L} be the degree $(1, 1)$ line bundle defined above. Then $H^0(V, \mathcal{L}^{\otimes l})$ has the following basis of sections:

$$s_{e,l} := \sum_{\gamma} \tau^{-l\kappa(\gamma + \frac{\gamma_{e,l}}{l})} x^{-l\lambda(\gamma) - \lambda(\gamma_{e,l})}$$

where $\gamma_{e,l} = s\gamma' + t\gamma''$, $0 \leq s, t < l$.

Claim 1.2.18 (Genus 2 curve). $H = \Sigma_2$ is a hypersurface in V defined by the vanishing of the section $s : V \rightarrow \mathcal{L}$:

$$s(x) = \sum_{\gamma \in \Gamma_B} x^{-\lambda(\gamma)} \tau^{-\kappa(\gamma)} \tag{1.8}$$

Proof. By the adjunction formula, $T^*H = K_H \cong (K_V \otimes \mathcal{L})|_H$. Since V is an abelian variety, its tangent bundle is trivializable so $K_H \cong \mathcal{L}|_H$. Recall $\deg(K_H) = \int_H c_1(K_H) = \int_H c_1(\mathcal{L}) = 2g - 2$. Since \mathcal{L} is obtained by winding once in the x_1 and x_2 directions respectively, it has degree 2 and hence $g = 2$. Alternatively, see Figure 1.1 where the solid blue denotes the behavior of the vanishing of $s(x)$ where $|x_i| =: \tau^{-\xi_i}$ is very large or equivalently $\tau \approx 0$

for variables ξ_i defined as $-\log_\tau |x_i|$. In the limit as $\tau \rightarrow 0$ the limit of the vanishing of s is denoted by the dotted line. So identifying opposite ends of the fundamental domain parallelogram and rotating by 2π gives a genus 2 curve. This limiting behavior is described in more detail below using the notion of the *tropicalization of a function*. □

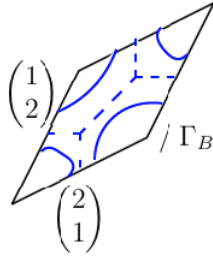


Figure 1.1: Quotient by Γ_B

Remark 1.2.19. The Γ_B lattice chosen above produces the blue curve of horizontal and vertical line segments in Figure 1.1, which we use throughout this thesis. A different choice of generators would give rise to different pictures but the methods used here should be the same.

Relation between invariants on X and H

Theorem 1.2.20 (Construction of Lagrangian torus fibration from [AAK16, §4]). *Recall $x = (x_1, x_2)$ are the periodic coordinates on V . Let $y \in \mathbb{C}$ be the coordinate on the \mathbb{C} factor and $s : V \rightarrow \mathcal{L}$ the function defined above. Then define*

$$\begin{aligned}
 X &:= Bl_{H \times \{0\}} V \times \mathbb{C} \subset \mathbb{P}(\mathcal{L} \oplus \mathcal{O}) \\
 &= \overline{\text{graph}[s(x) : y]} \\
 &= \overline{\{(x, y, [s(x) : y]) \in (\mathbb{P}(\mathcal{L} \oplus \mathcal{O}) \rightarrow V \times \mathbb{C})\}} \\
 &= \{(x, y, [u : v]) \mid s(x)v = yu\}
 \end{aligned} \tag{1.9}$$

a subset of the \mathbb{P}^1 -bundle $\mathbb{P}(\mathcal{L} \oplus \mathcal{O})$ on $V \times \mathbb{C}$. The claim is that X admits a Lagrangian torus fibration.

Idea of proof. A toric variety has a natural torus action (with an orbit that is dense in the variety) so this torus action naturally gives a Lagrangian torus fibration from the moment map. There is also an S^1 rotation action on the y -coordinate. Using cut and paste methods on the base of the moment map which correspond to blowing-up the total space, one produces a Lagrangian torus fibration on X . □

Lemma 1.2.21. $H = \text{Crit}(y)$.

Proof. The zero fiber is the union of the proper transform of V and the exceptional divisor. Let p be the blow-down map:

$$p : X \rightarrow V \times \mathbb{C}, \quad (x, y, (u : v)) \mapsto (x, y)$$

The definition of the proper transform is

$$\tilde{V} := \overline{p^{-1}(V \setminus H \times \{0\})}$$

Geometrically \tilde{V} is a copy of V , i.e. the closure of the part of V away from H in the blow-up which fills in the rest of the V copy. Also define the \mathbb{P}^1 -bundle coming from the blow-down map over H , and a section s^p of that bundle.

$$\begin{aligned} \text{exceptional divisor } E &:= \{(x, 0, (u : v)) \mid x \in H\} = p^{-1}(H \times \{0\}) \\ p|_E : E &\rightarrow H \times \{0\} \\ s^p : H &\rightarrow E, \quad s^p(x) := (x, 0, (1 : 0)) \end{aligned}$$

Now we can see H as the critical locus of the y fibration, as the fixed point set of the S^1 -action that rotates y , namely $(x, e^{i\theta}y, (e^{-i\theta}u : v))$.

$$\begin{aligned} y^{-1}(0) &= \{(x, 0, (u : v)) \mid s(x)v = 0 \cdot u\} \\ &= \{(x, 0, (1 : 0))\} \cup \{(x, 0, (u : v)) \mid s(x) = 0\} \\ &= \tilde{V} \cup E \end{aligned}$$

The claim is that \tilde{V} and E intersect in $s^p(H) \cong H$. Being in E implies $s(x) = 0 \therefore x \in H$. Being in \tilde{V} implies $v = 0$ hence we can scale $u \neq 0$ so that $u = 1$. Thus

$$\tilde{V} \cap E = s^p(H) \cong H = \text{Crit}(y)$$

□

Symplectic invariants

Remark 1.2.22. If $\dim_{\mathbb{C}} V = 1$, then the zero fiber of $y : X \rightarrow \mathbb{C}$ involves a normal crossings divisor of the form $ab = 0$, which for dimensional reasons produces a Lefschetz singularity. Hence Seidel's Fukaya category of Lefschetz fibrations [Sei08] can be used, and in this case $H = \text{a point}$. We would want an analogue of that Fukaya category with $H = \Sigma_2$ as the critical locus, which requires going up a dimension.

Proposition 1.2.23 (Proposing a Fukaya category of Morse-Bott fibration [AAK16]). *The normal bundle to $H \times 0$ in $V \times \mathbb{C}$ is $\mathcal{L} \oplus \mathcal{O}$. Once we blow up along $H \times \{0\}$, then $H = \Sigma_2$ is the intersection of two divisors in a normal crossing singularity and forms the critical locus of a Morse-Bott fibration given by $y : (x, y, (u : v)) \mapsto y$. Then $\text{Fuk}(H)$ is conjectured by [AAK16, Corollary 7.8] to be equivalent to a Fukaya category $F_s(X, y)$ which AAK describe, because Lagrangians in H can be parallel transported from the central fiber to obtain non-compact Lagrangians in X admissible with respect to the superpotential y .*

Complex invariants

The bounded derived category of coherent sheaves on X and H are related as follows.

Lemma 1.2.24 (Orlov [APS]). *There is a semi-orthogonal decomposition*

$$D^b\text{Coh}(X) = \langle D^b\text{Coh}(H), D^b(V \times \mathbb{C}) \rangle$$

Dependence on choice of genus 2 curve

Claim 1.2.25. Any genus 2 curve can be embedded into an abelian variety of complex dimension 2.

Proof. Fixing a point $x_0 \in \Sigma_2$ the map $\Sigma_2 \ni x \mapsto \mathcal{O}(x - x_0) \in \text{Pic}^0(\Sigma_2)$ is injective [Huy05, Proposition 2.3.34]. Then $\text{Pic}^0(\Sigma_2)$ is isomorphic to the Jacobian of Σ_2 , which is an abelian variety, [For91, §21.7]. Explicitly, let $\{\omega_1, \omega_2\} \in H^{1,0}(\Sigma_2)$ be a basis and take $\alpha_1, \dots, \alpha_4 \in H_1(\Sigma_2; \mathbb{Z})$ to be a basis on homology. Let c be a chain on Σ_2 so that $\partial c = x - x_0$. Then the embedding is

$$\Sigma_2 \ni x \mapsto \left(\int_c \omega_1, \int_c \omega_2 \right) \in \text{Jac}(\Sigma_2) = \mathbb{C}^2 / \text{Per}(\omega_1, \omega_2), \quad \text{Per}(\omega_1, \omega_2) := \mathbb{Z} \left\{ \left\langle \left(\int_{\alpha_i} \omega_1, \int_{\alpha_i} \omega_2 \right) \right\rangle \right\}_i$$

Note that the definition of $\text{Pic}(\Sigma_2)$ as holomorphic line bundles [Huy05] versus as divisors modulo principal divisors [For91, §21.6] are equivalent: any complex curve can be embedded into projective space using sections of a line bundle of suitably high degree [For91, Theorem 17.22], Hence the map $\text{Div}(\Sigma_2) \ni D \rightarrow \mathcal{O}(D) \in \text{Pic}(\Sigma_2)$ is surjective [Huy05, Corollary 5.3.7].

□

Corollary 1.2.26. *Varying the genus 2 curve corresponds with varying the complex structure parameters of V (and hence of X). The complex structure limit has an enumerative meaning in the mirror map, see [CLL12]. Thus this will also vary the Kähler parameters of Y via the mirror map.*

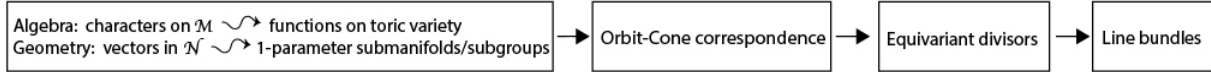
1.3 Background on toric varieties

The SYZ mirror Y is defined using the machinery of toric varieties to obtain a variety \tilde{Y} and then $Y := \tilde{Y}/\Gamma_B$. Toric varieties are a combinatorial way to produce charts and transition functions defining a manifold.

We will then define a symplectic form on Y , the first step in equipping Y with a Fukaya category and then proving HMS with that category. Since Y is locally toric, as a quotient

of a toric variety \tilde{Y} by a discrete group, and toric varieties constructed from a polytope naturally come with a line bundle, we use sections of that line bundle to define a metric that will give rise to the symplectic form.

We build the theory needed to define that line bundle. Here is the plan of action.



The background here is based on [CLS11, p 59, p128] and [Ful93, Chapter 1].

Characters and 1-parameter subgroups

Let Y_Δ be the toric variety associated to a polytope Δ as will be described. In this thesis we will use the following theory for $Y_\Delta = \mathbb{CP}^2(3)$ i.e. \mathbb{CP}^2 blown up at three points, as well as a related *toric variety of infinite type* [KL19] described later. The Orbit-Cone correspondence explains how combinatorial data (cones) gives geometric data (orbits). The data is encoded in a vector space of characters $M_{\mathbb{R}}$ which are functions on Y_Δ , and a vector space $N_{\mathbb{R}}$ of “co-characters” that generates 1-parameter subgroups (PS) in Y_Δ , respectively. The subscript \mathbb{R} means we tensor a lattice with \mathbb{R} . In particular M is the “algebra” and N is the “geometry” in this algebraic geometry setting of toric varieties.

Definition 1.3.1 (Notation). We fix some notation. We will consider examples of $n = 2$ and $n = 3$ below.

- Geometry: $N := \mathbb{Z}^n$ vectors encode the 1-PS parametrized by \mathbb{C}^* in the torus $T_N := (\mathbb{C}^*)^n$ which is dense in the toric variety. $N \otimes_{\mathbb{Z}} \mathbb{C}^* = T_N$ and $N_{\mathbb{R}} := N \otimes_{\mathbb{Z}} \mathbb{R}$.
- Algebra: $M = \text{Hom}_{\mathbb{Z}}(N, \mathbb{Z})$ encodes both linear functionals on N (combinatorial level) and functions on the toric variety (manifold level). In [AAK16] elements of M are called *weight vectors* because exponentiating them gives *toric monomials* which are *characters* i.e. functions on the toric variety.
- $M_{\mathbb{R}} = \mathbb{R}^n$ and define a nondegenerate pairing $M_{\mathbb{R}} \times N_{\mathbb{R}} \rightarrow \mathbb{R}$ by $\langle e_i, f_j \rangle = f_j(e_i) = \delta_{ij}$.

Definition 1.3.2 (Cone). A *cone* $\sigma \subset N_{\mathbb{R}}$ is an intersection of half spaces $H_u^+ := \{n \in N_{\mathbb{R}} \mid \langle u, n \rangle \geq 0\}$ for a set of normal vectors $u \in M$. For example, take $u_1 = e_1$ and $u_2 = e_2$ to get the first quadrant $e_1, e_2 \geq 0$. Then σ consists of convex linear combinations of lattice vectors called *rays* ρ , the set of which is denoted $\sigma(1)$.

The *dual cone* $\sigma^\vee \subset M_{\mathbb{R}}$ is defined to be the intersection of dual half-spaces as follows.

$$\sigma^\vee := \{m \in M_{\mathbb{R}} \mid \langle m, n \rangle \geq 0 \forall n \in \sigma\} = \bigcap_{n \in \sigma(1)} \{m \in M_{\mathbb{R}} \mid \langle m, n \rangle \geq 0\}$$

Definition 1.3.3 (Strongly convex rational polyhedral cone). *Strongly convex* means σ is not generated by $\pm e$ for any direction e (or equivalently $\sigma \cap -\sigma = \{0\}$), and *rational* means σ has integral generators, namely they are in \mathbb{Z}^n .

Remark 1.3.4. If m_1, \dots, m_s generate σ^\vee , then these are the normal vectors of the half-spaces in σ i.e. $\sigma = H_{m_1}^+ \cap \dots \cap H_{m_s}^+$. So the upshot is that σ^\vee encodes the collection of these normal vectors, where its edges are facets of σ . More generally a face τ in σ corresponds to one, call it τ^* , of complementary dimension in σ^\vee namely $\tau^\perp \cap \sigma^\vee$, and conversely.

Definition 1.3.5 (Character). Let $S_\sigma := \sigma^\vee \cap M$ be the lattice points in the dual cone. Then elements of the coordinate ring $\mathbb{C}[S_\sigma]$ are functions locally defined on Y_Δ called *characters* or *toric monomials*. They are \mathbb{C} -linear combinations of elements in the set $\{\chi^u \mid u \in S_\sigma\}$. Define an open set on the toric variety as:

$$U_\sigma := \text{Spec } \mathbb{C}[S_\sigma]$$

In particular, because S_σ is a semi-group, meaning we can add elements and it contains zero, then the set of elements χ^u has a natural ring structure as one expects for the coordinate ring of functions.

Remark 1.3.6 (Notation). We will use the letter u to denote lattice elements in N . We will reserve the letter m to refer to points in $M_{\mathbb{R}}$ or M and n will denote elements of $N_{\mathbb{R}}$. This is to be consistent with [CLS11].

Definition 1.3.7 (Affine charts and functions). An *affine or local chart* on Y_Δ is $\text{Spec } \mathbb{C}[S_\sigma]$. In particular, all local charts contain the dense torus $(\mathbb{C}^*)^n = \text{Spec } \mathbb{C}[\chi^{\pm e_1}, \dots, \chi^{\pm e_n}]$ because

$$M = \text{Span}_{\mathbb{Z}_+} \langle \pm e_1, \dots, \pm e_n \rangle \supset \{u \in \sigma^\vee(1)\}$$

and rays generate the semi-group S_σ . A *local function* is given by characters χ^u as follows. A character is a homomorphism from the dense torus to \mathbb{C}^* :

$$\chi^u : (\mathbb{C}^*)^n \rightarrow \mathbb{C}^*, \quad (t_1, \dots, t_n) \mapsto t^u := t_1^{u_1} \cdot \dots \cdot t_n^{u_n}, \quad u = \sum_{i=1}^n u_i e_i$$

Fix a basis $\{u_1, \dots, u_k\}$ for S_σ in the sense that $\{\pm u_1, \dots, \pm u_l, u_{l+1}, \dots, u_k\}$ generates S_σ over \mathbb{Z}_+ and $\{u_1, \dots, u_k\}$ has no relations (the *minimal generators*). This gives the coordinate chart with *local complex coordinates* $\chi^{u_1}, \dots, \chi^{u_k}$ if σ is a strongly convex cone:

$$(\chi^{u_1}, \dots, \chi^{u_k}) : U_\sigma \rightarrow \mathbb{C}^k$$

Remark 1.3.8. This chart has image given by a potentially singular n -dimensional subvariety of \mathbb{C}^k . In particular for maximal cones, $k = n$, the u_i form a \mathbb{Z} -basis of M , and we obtain a smooth variety and an affine manifold chart in the usual sense, mapping U_σ to the

local model \mathbb{C}^n .

In the other case when the u_i are not a \mathbb{Z} -basis for M , we will have some relations among them. In particular,

$$\mathbb{C}[S_\sigma] \cong \mathbb{C}[\chi^{u_1}, \dots, \chi^{u_k}]/I$$

where I is a *toric ideal* that records these relations. In the example of \mathbb{CP}^2 below, Example 1.3.13, we will not need to quotient by toric ideals.

A suitable closure of this chart gives the toric variety. Later we will look at when a character extends to a function on the whole toric variety, i.e. a partial or full compactification of $(\mathbb{C}^*)^n$, meaning we let the coordinates tend to 0 or infinity. This illustrates how M gives rise to functions.

Definition 1.3.9 (Toric variety). Recall that cones σ give affine charts. A fan is a collection of cones arranged in a way that tell us how to glue local charts, namely what the transition functions on the manifold are. A *fan* is a collection of cones $\sigma_i \subset N_{\mathbb{R}}$ so that

- every face of a cone is a cone
- $\tau_{ij} := \sigma_i \cap \sigma_j$ is a face of both σ_i, σ_j hence we glue U_{σ_i} to U_{σ_j} along $U_{\tau_{ij}}$

Suppose σ_1 and σ_2 are two maximal cones so that $\tau = \sigma_1 \cap \sigma_2$ is $(n - 1)$ -dimensional.

Claim 1.3.10. $\tau = H_m \cap \sigma_1 = H_m \cap \sigma_2$ for $m \in \sigma_1^\vee \cap (-\sigma_2)^\vee \cap M$.

In particular, the semi-group S_τ now has the $\pm m$ direction whereas σ_1 only had m and σ_2 only had $-m$. This corresponds to inverting the coordinate χ^m in the two charts from $\mathbb{C}[S_{\sigma_1}]$ and $\mathbb{C}[S_{\sigma_2}]$, which will now be required to be nonzero. We glue these two charts along

$$U_\tau = (U_{\sigma_1})_{\chi^m} = (U_{\sigma_2})_{\chi^{-m}}$$

We can see how N gives rise to 1 parameter subgroups.

Definition 1.3.11 (1 parameter-subgroup (PS)). Given $v = \sum_{i=1}^n v_i f_i \in N$, we get a 1-PS λ^v via the multiplicative homomorphism:

$$\lambda^v : \mathbb{C}^* \rightarrow (\mathbb{C}^*)^n, \quad t \mapsto (t^{v_1}, \dots, t^{v_n})$$

For example $v = (1, 1)$ gives the complex 1-PS $(t, t)_{t \in \mathbb{C}^*} \subset (\mathbb{C}^*)^2$. This gives a 1-dimensional submanifold in U_σ by taking the image of $(\chi^{u_1}, \dots, \chi^{u_k})$ on $\{\lambda^v(t)\}_{t \in \mathbb{C}^*}$.

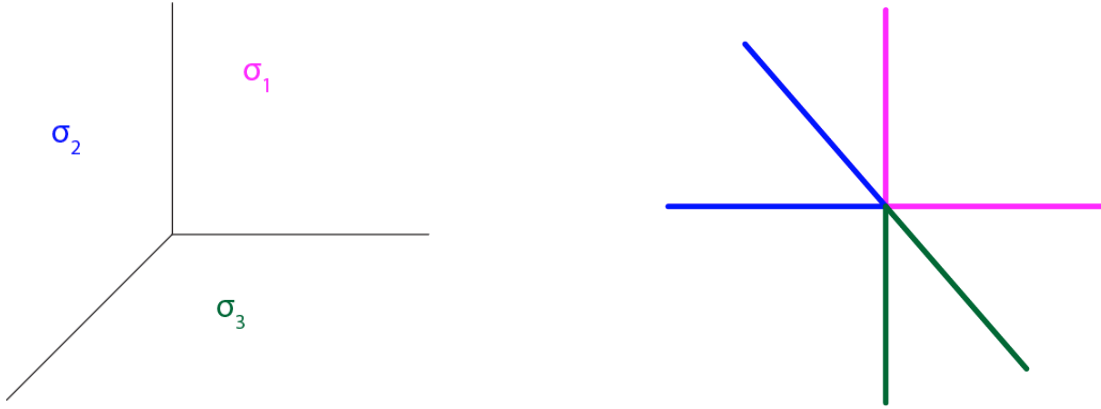
Remark 1.3.12. We can compose characters and 1-PS to get a character of \mathbb{C}^* by

$$\chi^u \circ \lambda^v(t) = t^\ell, \quad \ell = \langle u, v \rangle$$

In particular we can see N geometrically as the dense torus by collecting all the 1-PS via

$$N \otimes_{\mathbb{Z}} \mathbb{C}^* : v \otimes t \mapsto \lambda^v(t)$$

Example 1.3.13 (\mathbb{CP}^2). The fan has three cones, with rays generated by $v_1 = f_1, v_2 = f_2$, and $v_3 = -f_1 - f_2$ in $N_{\mathbb{R}}$.



Dual cones of functionals non-negative on the original cones are

$$\begin{aligned}\sigma_1^\vee &= \text{span}(e_1, e_2) \\ \sigma_2^\vee &= \text{span}(-e_1, -e_1 + e_2) \\ \sigma_3^\vee &= \text{span}(-e_2, e_1 - e_2)\end{aligned}$$

The vectors in these pairs don't have relations between them, so they correspond to variables of an affine chart isomorphic to $\mathbb{C}[x, y]$. In other words, we don't need to quotient by a toric ideal I that would record relations between the generators. The choice of generator in each case gives a complex coordinate on the chart.

$$\begin{aligned}U_{\sigma_1} &= \text{Spec } \mathbb{C}[\chi^{1,0}, \chi^{0,1}] \cong \mathbb{C}^2 \ni (\chi^{1,0}, \chi^{0,1}) \\ U_{\sigma_2} &= \text{Spec } \mathbb{C}[\chi^{-1,0}, \chi^{-1,1}] \cong \mathbb{C}^2 \ni (\chi^{-1,0}, \chi^{-1,1}) \\ U_{\sigma_3} &= \text{Spec } \mathbb{C}[\chi^{0,-1}, \chi^{1,-1}] \cong \mathbb{C}^2 \ni (\chi^{0,-1}, \chi^{1,-1})\end{aligned}$$

If $\tau = \sigma_1 \cap \sigma_2$, then this corresponds to inverting $\chi^{1,0}$ and τ^\vee is $H_{(1,0)}^+$. A choice of generators gives a choice of coordinates, and the two different natural choices give us the coordinate change.

$$\mathbb{C}[S_{\sigma_1}] = \mathbb{C}[\chi^{(1,0)}, \chi^{(0,1)}] \subset \mathbb{C}[\chi^{\pm(1,0)}, \chi^{(0,1)}] = \mathbb{C}[S_\tau] \rightsquigarrow \text{Spec } \mathbb{C}[\chi^{\pm(1,0)}, \chi^{(0,1)}] \rightarrow \text{Spec } \mathbb{C}[\chi^{(1,0)}, \chi^{(0,1)}]$$

and

$$\mathbb{C}[\chi^{-(1,0)}, \chi^{(-1,1)}] \subset \mathbb{C}[\chi^{\pm(1,0)}, \chi^{(-1,1)}] \rightsquigarrow \text{Spec } \mathbb{C}[\chi^{\pm(1,0)}, \chi^{(-1,1)}] \rightarrow \text{Spec } \mathbb{C}[\chi^{-(1,0)}, \chi^{(-1,1)}]$$

Note that $\mathbb{C}[\chi^{\pm(1,0)}, \chi^{(0,1)}] = \mathbb{C}[\chi^{\pm(1,0)}, \chi^{(-1,1)}]$ and under Spec we get U_τ . The choice of generators give us an identification with $\mathbb{C}^* \times \mathbb{C}$ which then includes, as the identity map, into \mathbb{C}^2 in the two charts. The two different choices of this identification give us the transition map.

$$g_{12}(\chi^{(1,0)}, \chi^{(0,1)}) := \left(\frac{1}{\chi^{(1,0)}}, \frac{\chi^{(0,1)}}{\chi^{(1,0)}} \right)$$

This recovers how we think about $\mathbb{CP}^2 \ni [z_0 : z_1 : z_2]$ with $\chi^{(1,0)} = z_1/z_0$ and $\chi^{(0,1)} = z_2/z_0$.

Orbit-cone correspondence

To understand equivariant divisors, we need to understand how the combinatorial data gives us the geometric data. Divisors correspond to the vanishing of a coordinate on the variety. This can be read off from the fan via the ‘‘Orbit-Cone Correspondence.’’

Lemma 1.3.14 (Orbit-Cone correspondence). *There is a 1-1 correspondence between $n - k$ dimensional $(\mathbb{C}^*)^n$ -orbits of a point in the toric variety, and k dimensional cones of the fan, e.g. between divisors and rays.*

Proof. The idea is ‘‘every 1-parameter subgroup corresponding to a point in the interior of a cone in N limits to the same limit point.’’ (Recall the correspondence between points of N and 1-parameter subgroups in Definition 1.3.11.) That point gives the vector that defines the direction of the 1-PS. By algebraic geometry, a point on a toric variety is a semigroup homomorphism $S_\sigma = \mathbb{C}[\sigma^\vee \cap M] \rightarrow \mathbb{C}$ i.e. a map $\text{Spec } \mathbb{C} \rightarrow U_\sigma$. Recall that M encodes the functions on the toric variety. So such an assignment is determining what all the functions equal at the point; knowing all the functions at a given point is the same information as knowing the point. Given $v \in \sigma \cap N$ we can assign coordinates to the associated point using the following map on a basis of $\sigma^\vee \cap M$:

$$\sigma^\vee \cap M \ni u \mapsto \lim_{t \rightarrow 0} \chi^u(\lambda^v(t)) = t^{\langle u, v \rangle} \in \mathbb{C}$$

Now we use the following claim to see why all vectors of a cone give the same limit point, hence giving the Orbit-Cone correspondence by taking the orbit of that cone’s limit point.

Claim 1.3.15. All 1-PS arising from directions $v \in \text{int}(\sigma) \cap N$ limit to the same point.

Proof. For clarification we will use subscripts u_{bdry}, u_{int} to differentiate between the two cases of functions we need to check on each v (namely u not in the interior of the dual cone $\sigma^\vee \subset M$ and u in the interior). We see that:

1. $u_{bdry} \in \sigma^\vee \cap \sigma^\perp$ implies $\langle u_{bdry}, v \rangle = 0$ for all $v \in \sigma$ hence

$$\lim_{t \rightarrow 0} \chi^u(\lambda^v(t)) = t^{\langle u, v \rangle} = 1$$

2. $u_{int} \in \sigma^\vee \setminus (\sigma^\vee \cap \sigma^\perp)$ implies that, on the one hand $\langle u_{int}, v \rangle \geq 0$ for all $v \in \text{int}(\sigma) \cap N$ by definition of σ^\vee but on the other hand $\langle u_{int}, v \rangle \neq 0$ for v in the interior of σ and $u_{int} \notin \sigma^\perp$. Thus

$$\lim_{t \rightarrow 0} \chi^u(\lambda^v(t)) = t^{\langle u, v \rangle} = 0$$

□

To finish the proof of the Orbit-Cone correspondence, we let the orbit corresponding to the cone σ be $(\mathbb{C}^*)^n \cdot p$ where p is the point $\lim_{t \rightarrow 0} (\chi^{u_1}(\lambda^v(t)), \dots, \chi^{u_k}(\lambda^v(t)))$ for some $v \in \sigma$ and u_1, \dots, u_k generators for S_σ . We can choose any v by the previous claim.

□

Example 1.3.16 ($\mathbb{C}\mathbb{P}^2$). The fan has cones and dual cones:

$$\begin{aligned} \{0\}, \{0\}^\vee &= M_{\mathbb{R}} \cong \mathbb{R}^2 \\ \rho_1 &= \langle (1, 0) \rangle, \rho_2 = \langle (0, 1) \rangle, \rho_3 = \langle -1, -1 \rangle \\ \rho_1^\vee &= \langle \pm(0, 1), (1, 0) \rangle, \rho_2^\vee = \langle \pm(1, 0), (0, 1) \rangle, \rho_3^\vee = \langle \pm(-1, 1), (-1, 0) \rangle \\ \sigma_1 &= \langle (1, 0), (0, 1) \rangle, \sigma_2 = \langle (1, 0), (-1, -1) \rangle, \sigma_3 = \langle (0, 1), (-1, -1) \rangle \\ \sigma_1^\vee &= \langle (1, 0), (0, 1) \rangle, \sigma_2^\vee = \langle (0, 1), (1, -1) \rangle, \sigma_3^\vee = \langle (-1, 0), (-1, 1) \rangle \end{aligned}$$

The limit points γ_σ that generate the orbits corresponding to cones σ are the points sending vectors $m \in \sigma^\perp \cap \sigma^\vee$ to 1 and the rest of σ^\vee to 0. Let $(t_1, t_2) \in (\mathbb{C}^*)^2$ be coordinates on the dense toric orbit. The generators taken for S_{ρ_i} are listed below in the exponents.

$$\begin{aligned} \lambda^{(0,0)}(t) &= (1, 1), & \gamma_{\{0\}} &= \lim_{t \rightarrow 0} (\chi^{(1,0)}(1, 1), \chi^{(0,1)}(1, 1)) = (1, 1) \implies (\mathbb{C}^*)^2 \\ \lambda^{(1,0)}(t) &= (t, 1), & \gamma_{\rho_1} &= \lim_{t \rightarrow 0} (\chi^{(0,1)}(t, 1), \chi^{(1,0)}(t, 1)) = (1, 0) \implies \mathbb{C}^* \times \{0\} \\ \lambda^{(0,1)}(t) &= (1, t), & \gamma_{\rho_2} &= \lim_{t \rightarrow 0} (\chi^{(1,0)}(1, t), \chi^{(0,1)}(1, t)) = (1, 0) \implies \mathbb{C}^* \times \{0\} \\ \lambda^{(-1,-1)}(t) &= (t^{-1}, t^{-1}), & \gamma_{\rho_3} &= \lim_{t \rightarrow 0} (\chi^{(-1,1)}(t^{-1}, t^{-1}), \chi^{(-1,0)}(t^{-1}, t^{-1})) = (1, 0) \implies \mathbb{C}^* \times \{0\} \end{aligned}$$

Taking the closures in the toric variety, we have three toric divisors, i.e. divisors invariant under the $(\mathbb{C}^*)^n$ action.

Claim 1.3.17. Let $O(\sigma)$ denote the orbit corresponding to a cone σ under the Orbit-Cone correspondence. Then the toric divisor given by the closure of an orbit has the following description:

$$\overline{O(\tau)} = \bigcup_{\tau \leq \sigma} O(\sigma)$$

Notation: $N(\sigma)$ is lattice points in N modulo those in $\sigma \cap N =: N_\sigma$.

Divisors, line bundles and polytopes

The divisor-ray correspondence is a special case of the Orbit-Cone correspondence, and by complex geometry [Huy05, §2.3] the defining functions of a divisor give transition functions for line bundles. Below we introduce the notion of a polytope and explain why it determines a line bundle. We'll see that it is constructed so its edges are perpendicular to rays in a fan, and the size of it governs the coefficient on each irreducible toric divisor (corresponding to the rays of a fan). Then this divisor gives the line bundle corresponding to that polytope.

Definition 1.3.18 (Polytope). A *polytope* $P \subset M_{\mathbb{R}}$ is

$$P := \{m \in M_{\mathbb{R}} \mid \langle m, \nu_i \rangle \geq -a_i\} \subset M_{\mathbb{R}}$$

for finitely many i , where the $\nu_i \in N$ generate rays ρ_i of a fan Σ . With infinitely many i we get more generally a *polyhedron*.

Definition 1.3.19 (Faces, facets). Codimension 1 faces in the polytope are called *facets*, $\langle u, v_i \rangle = -a_i$ for some i and $\langle u, v_j \rangle > -a_j$ for $j \neq i$. Higher codimension faces have $\langle u, v_i \rangle = -a_i$ for more than one i .

Definition 1.3.20 (Obtaining fan from P : vertices of full dimensional lattice polytope correspond with toric charts, c.f. [CLS11, p 76]). Given polytope P with vertices \mathbf{v} , we translate each vertex to the origin and take the cone spanned by its edges, namely $C_{\mathbf{v}} := \text{Cone}(P \cap M - \mathbf{v}) \subset M_{\mathbb{R}}$. The corresponding cone of the fan is defined to be

$$\sigma_{\mathbf{v}} := C_{\mathbf{v}}^{\vee} = \text{Cone}(\nu_i \mid \text{ith face contains } \mathbf{v}) \subset N_{\mathbb{R}}$$

Thus the chart $U_{\sigma_{\mathbf{v}}} = \text{Spec } \mathbb{C}[\text{Cone}(P \cap M - \mathbf{v}) \cap M]$. (More generally for a face Q of the polytope, we have σ_Q is the cone on the ν_i of faces containing Q .) So the upshot is “local coordinates of a toric variety can be read off from edges to a vertex of the corresponding polytope.”

The collection of all the cones σ_Q can be checked to give a fan which we define to be Σ_P .

Remark 1.3.21. For a discussion of the analogue of dualizing $\sigma \rightarrow \sigma^{\vee}$ on the level of polytopes (polytope \rightarrow polar polytope), see [Ful93, §1.5, p 26]. One can pass between a polytope P in $M_{\mathbb{R}}$ to a cone given by $\text{Cone}(P \times \{1\}) \subset M_{\mathbb{R}} \times \mathbb{R}$, then take the dual $^{\vee}$ on cones to get a cone in $N_{\mathbb{R}} \times \mathbb{R}$, and show that this is a cone on the *polar* P^0 of P , i.e. of the form $\text{Cone}(P^0 \times \{1\})$ for the dual polytope $P^0 \subset N_{\mathbb{R}}$.

Definition 1.3.22 (Equivariant divisor). An *equivariant or T -divisor* is a linear combination of closures of toric orbits.

Claim 1.3.23. A T -divisor is a linear combination of divisors corresponding to facets.

Proof. Rays of a fan correspond to equivariant divisors. Indeed, given a ray ρ its orthogonal ρ^{\perp} has codimension 1, which means the distinguished point γ_{ρ} has $n - 1$ ones and 1 zero (from the one direction generated by ρ sending the codimension 1 space ρ^{\perp} to zero). So the $(\mathbb{C}^*)^n$ -orbit is dimension $n - 1$. Taking the closure of this gets the divisor D_{ρ} . Namely

$$D_{\rho} = \overline{O(\rho)} = \bigcup_{\rho \leq \sigma} O(\sigma)$$

We get a divisor from the vanishing of a coordinate. □

Remark 1.3.24 (Notation). Since we now know that the i in ν_i and a_i are indexed by facets F of the polytope, we can use F to index them.

Definition 1.3.25 (A distinguished divisor). Let $P := \{m \in M_{\mathbb{R}} \mid \langle m, \nu_i \rangle \geq -a_i\} \subset M_{\mathbb{R}}$ be an integral polytope, namely $a_i \in \mathbb{Z}$. By the Orbit-Cone correspondence we can take the closure of the corresponding orbit of each ray ν_F in Σ_P to obtain the toric divisor D_F .

We may then construct a toric variety Y_P from this fan. Finally we define the distinguished divisor in Y_P to be

$$D := \sum_F a_F D_F$$

Remark 1.3.26. The integral condition allows us to define the divisor and later embed Y_P into projective space since D will correspond to an ample line bundle.

Claim 1.3.27 (Sections of $\mathcal{O}(D)$, [CLS11][Proposition 4.3.3]). The sections of $\mathcal{O}(D)$ are given by

$$\Gamma(Y_P, \mathcal{O}(D)) = \bigoplus_{m \in P \cap M} \mathbb{C} \cdot \chi^m$$

where $P := \{m \in M_{\mathbb{R}} \mid \langle m, \nu_F \rangle \geq -a_F\} \subset M_{\mathbb{R}}$ and $D = \sum_{F \text{ facet}} a_F D_F$.

Proof. By definition

$$\Gamma(Y_P, \mathcal{O}(D)) = \{f \in \mathbb{C}(Y_P)^* \mid \text{div}(f) + D \geq 0\} \cup \{0\}$$

where $\mathbb{C}(Y_P)^*$ consists of invertible rational functions on Y_P . Note that

$$\text{Supp}(D) \cap T_N = \emptyset$$

because T_N is the orbit where all coordinates are nonzero and $\text{Supp}(D)$ consists of D_F , which contain orbits where at least one coordinate is zero. Hence $D|_{T_N} = 0$ and $\text{div}(f)|_{T_N} \geq 0$ i.e. f is a regular function on $T_N = \text{Spec } \mathbb{C}[M]$. We deduce that $f \in \text{Spec } \mathbb{C}[M]$ and thus

$$\Gamma(Y_P, \mathcal{O}(D)) \subset \mathbb{C}[M]$$

Write $f = \sum_{m \in \mathcal{A}} c_m \chi^m$ over some subset $\mathcal{A} \subset M$ and complex coefficients c_m . Note that $\Gamma(Y_P, \mathcal{O}(D))$ is a T_N -invariant subset, under the action

$$\begin{aligned} T_N \curvearrowright \Gamma(Y_P, \mathcal{O}(D)) : t \cdot f &:= f \circ t^{-1} \\ T_N \curvearrowright T_N : t \cdot p &:= (t_1 p_1, \dots, t_n p_n) \end{aligned}$$

because D_F are T_N -invariant and f and $f \circ t^{-1}$ have the same vanishing set. In particular, let

$$B = \text{span}\{\chi^m \mid m \in \mathcal{A}\}$$

Since $\chi^m : T_N \rightarrow \mathbb{C}^*$ is a homomorphism, we see that T_N preserves the space spanned by χ^m because

$$t \cdot \chi^m(p) = \chi^m(t^{-1} \cdot p) = \chi^m(t^{-1}) \chi^m(p) \therefore t \cdot \chi^m = \chi^m(t^{-1}) \chi^m$$

so $W := B \cap \Gamma(Y_P, \mathcal{O}(D))$ (which is finite dimensional because f is a finite sum), as an intersection of T_N -invariant subspaces is also T_N -invariant. Now we apply some results of linear algebra. Note that the T_N -action consists of linear maps on the finite-dimensional space W , so gives rise to commuting finite-dimensional matrices (as T_N is a commutative

group) so the matrices can all be simultaneously diagonalized, i.e. we can find a basis of eigenvectors for W . In particular, by representation theory we can write the representation $T_N \rightarrow \mathrm{GL}(W)$ as a direct sum of 1-dimensional representations, namely characters χ^m . So the upshot is that, $f \in W$ is expressed as a sum of characters in $\mathbb{C}[M]$ and also as a sum of characters in W , but by uniqueness those two expressions are the same. So $\chi^m \in W$ for $m \in \mathcal{A}$ and $f \in \bigoplus_{\chi^m \in \Gamma(Y_P, \mathcal{O}(D))} \mathbb{C} \cdot \chi^m$ thus

$$\Gamma(Y_P, \mathcal{O}(D)) = \bigoplus_{\chi^m \in \Gamma(Y_P, \mathcal{O}(D))} \mathbb{C} \cdot \chi^m$$

The final step is as follows. Pick a global section χ^m . The condition $\mathrm{div}(\chi^m) + D \geq 0$, looking at coefficients, is equivalent to the statement

$$\langle m, \nu_F \rangle + a_F \geq 0$$

In other words, this is equivalent to $m \in P$. But since χ^m is a character that means $m \in M$ hence this is equivalent to $m \in P \cap M$ and we get the final result

$$\Gamma(Y_P, \mathcal{O}(D)) = \bigoplus_{m \in P \cap M} \mathbb{C} \cdot \chi^m$$

□

Claim 1.3.28 (Basepoint free, [CLS11][Proposition 6.1.1].) There does not exist a point $p \in Y_P$ where $\chi^{m_i}(p) = 0$ for all $m_i \in P \cap M$. In other words, $\mathcal{O}(D)$ is *basepoint free*, because $\Gamma(Y_P, \mathcal{O}(D)) = \bigoplus_{m_i \in P \cap M} \chi^{m_i}$.

Proof. Recall that faces $Q \subset P$ give cones σ_Q that describe the fan of the polytope Σ_P . We show that for each affine piece U_{σ_Q} , there is a global section which does not vanish on that piece. Since the U_{σ_Q} cover the toric variety, that will suffice.

Write the face $Q = \bigcap_{F \supset Q} F$ as an intersection of facets. Hence

$$Q := \{m \in M_{\mathbb{R}} \mid \langle m, \nu_F \rangle = -a_F, \forall F \supset Q\} \subset M_{\mathbb{R}}$$

Pick a lattice point $m_Q \in Q$, e.g. a vertex. Then χ^{m_Q} is a global section of $\mathcal{O}(D)$ by Claim 1.3.27. Furthermore $\langle m_Q, \nu_F \rangle + a_F = 0$ for $F \supset Q$ means that the order of vanishing of $\chi^{m_Q} + D$ along U_{σ_Q} is zero.

$$(\mathrm{div}(\chi^{m_Q}) + D)|_{U_{\sigma_Q}} = \sum_{F \supset Q} (\langle m_Q, \nu_F \rangle + a_F) D_F = 0$$

In other words, $\chi^{m_Q}(U_{\sigma_Q}) \neq 0$.

□

Corollary 1.3.29 (Definition of a symplectic form, [Huy05][Example 4.1.2]). *Recall by Claim 1.3.27 that*

$$\Gamma(Y_P, \mathcal{O}(D)) = \bigoplus_{m_i \in P \cap M} \chi^{m_i}$$

Because $\mathcal{O}(D)$ is basepoint free by Claim 1.3.28, these basis elements do not simultaneously vanish at any point $p \in Y_P$. Hence we can define a Kähler form by

$$\omega_P := \frac{i}{2\pi} \bar{\partial} \partial h, \quad h = \frac{1}{\sum_{i=1}^s |\chi^{m_i}|^2}$$

where $|\cdot|$ refers to the standard norm in \mathbb{C} since χ^{m_i} are complex coordinates.

Remark 1.3.30. $\mathcal{O}(D)$ is an ample line bundle, which implies that Y_Δ can be viewed as a variety in a projective space. The reason it is ample can be found in [CLS11], and is because of the combinatorics of the polytope. Some multiple kP of the polytope is normal (Chapter 2) which implies the polytope is ample (definition in Chapter 2) which is seen later to be equivalent to the line bundle being ample (Chapter 6). A very ample polytope intuitively has enough lattice points, corresponding to there being enough sections to define an embedding.

1.4 The A-side manifold

We have the toric background, so the next step is to describe the tools we use to construct the polytope for \tilde{Y} . Since (Y, v_0) for a suitable holomorphic function v_0 should be mirror to $H = \Sigma_2 \subset V$, we would expect that the polytope is built from information about the genus 2 curve. We can glean combinatorial data from the defining section s by taking its tropicalization.

Tropicalization of theta function

Definition 1.4.1 (Tropicalization). Let $f(x) = \sum_{a \in A \subset \mathbb{Z}^n} c_a x^a \tau^{\rho(a)}$. Let $\xi = (\xi_1, \dots, \xi_n)$ be Log coordinates so defined by

$$|x_i| = \tau^{-\xi_i}$$

Then

$$f = \sum_a c_a \left(\frac{x}{|x|} \right)^a \tau^{\rho(a) - \langle a, \xi \rangle}$$

In particular, the *tropical limit* corresponds to $\tau \rightarrow 0$, i.e. rescaling $|x_i|$ so that ξ_i remains constant. As $\tau \rightarrow 0$ we see that the leading order term in f is the one with the smallest exponent on τ . Then the *tropicalization of f* is the negative of this, namely

$$\text{Trop}(f) := - \min_{a \in A} \rho(a) - \langle a, \xi \rangle = \max_{a \in A} \langle a, \xi \rangle - \rho(a)$$

Claim 1.4.2. Let s be the theta function above. The tropicalization $\varphi := \text{Trop } s$ satisfies the following periodicity property

$$\varphi(\xi + \tilde{\gamma}) = \varphi(\xi) - \kappa(\tilde{\gamma}) + \langle \xi, \lambda(\tilde{\gamma}) \rangle \quad (1.10)$$

Proof. Recall

$$s(x) = \sum_{\gamma \in \Gamma_B} \tau^{-\kappa(\gamma)} x^{-\lambda(\gamma)}$$

where

$$\begin{aligned} \kappa(\gamma) &= -\frac{1}{2} \lambda(\gamma)^T M \lambda(\gamma), & M &= \begin{pmatrix} 2 & 1 \\ 1 & 2 \end{pmatrix} \\ \lambda(\gamma') &= \begin{pmatrix} 1 \\ 0 \end{pmatrix}, & \lambda(\gamma'') &= \begin{pmatrix} 0 \\ 1 \end{pmatrix} \end{aligned}$$

Let $x = \tau^\xi$. Then this becomes

$$s(x) = \sum_{\gamma \in \Gamma_B} \tau^{-\kappa(\gamma) - \langle \xi, \lambda(\gamma) \rangle}$$

So letting $\tau \rightarrow 0$ we see that the leading term is the minimum exponent or the maximum of its negative, namely

$$\varphi(\xi) := \text{Trop}(s)(\xi) := \max_{\gamma} \kappa(\gamma) + \langle \xi, \lambda(\gamma) \rangle \quad (1.11)$$

Since κ is negative definite of degree 2 and λ is positive of degree 1, this should have a maximum. We have the following periodicity property:

$$\begin{aligned} \varphi(\xi + \tilde{\gamma}) &= \max_{\gamma} \kappa(\gamma) + \langle \xi + \tilde{\gamma}, \lambda(\gamma) \rangle \\ &= \max_{\gamma} \kappa(\gamma) + \langle \xi, \lambda(\gamma) \rangle + \langle \tilde{\gamma}, \lambda(\gamma) \rangle \end{aligned}$$

We know that

$$\kappa(\gamma - \tilde{\gamma}) = \kappa(\gamma) + \kappa(\tilde{\gamma}) + \lambda(\gamma)^T M \lambda(\tilde{\gamma})$$

and

$$M \lambda(\tilde{\gamma}) = \tilde{\gamma}$$

by the above convention for $\lambda(\gamma)$. So we can rewrite the expression for the tropicalization as

$$\begin{aligned} \varphi(\xi + \tilde{\gamma}) &= \max_{\gamma} \langle \xi, \lambda(\gamma) \rangle + [\kappa(\gamma - \tilde{\gamma}) - \kappa(\tilde{\gamma})] \\ &= \left(\max_{\gamma} \kappa(\gamma - \tilde{\gamma}) + \langle \xi, \lambda(\gamma - \tilde{\gamma}) \rangle \right) - \kappa(\tilde{\gamma}) + \langle \xi, \lambda(\tilde{\gamma}) \rangle \end{aligned}$$

This implies that

$$\varphi(\xi + \tilde{\gamma}) = \varphi(\xi) - \kappa(\tilde{\gamma}) + \langle \xi, \lambda(\tilde{\gamma}) \rangle$$

□

Definition 1.4.3 (Vanishing set of tropicalization). The *vanishing of* $\text{Trop}(f)$, denoted $V(\text{Trop}(f))$, is defined to be where two leading order exponents are equal because they can cancel each other out in the limit to get zero.

Claim 1.4.4. $V(\text{Trop } s) \subset \mathbb{R}^2$ is a honeycomb shape that is a tiling by hexagons.

Proof. Let $\xi = 0$. Then $\text{Trop}(s)(0)$ is the maximum over γ of $\kappa(\gamma)$. Note that $\kappa(\gamma)$ is a negative definite form so at most it can be zero. Hence $\varphi(0) = 0$, and since the maximum continues to be achieved by $\gamma = 0$ for ξ in a neighborhood of the origin, the function φ is identically zero in a neighborhood of the origin, which we call the $(0,0)$ tile. We let the (m,n) tile be obtained by moving m times in the γ' direction and n times in the γ'' direction from the $(0,0)$ tile. Now we want to know what happens when we change tiles in order to find the vanishing of the tropicalization.

In what follows in this section ξ is always in the $(0,0)$ tile, and we translate by elements of Γ_B and use the periodicity property of φ to see how its value changes. Let $\tilde{\gamma} = \gamma' := (2,1)$. Then the above equation tells us that for ξ in the $(0,0)$ tile

$$\varphi(\xi + \gamma') = 0 + \frac{1}{2}(1,0)M(1,0)^T + \xi_1 = \xi_1 + 1$$

So setting this equal to 0 we should find where the two piecewise linear components meet. $\xi_1 + 1 = 0 \implies \xi_1 = -1$. Since $\xi_1 = -1$ exactly when the first component of $\xi + \gamma'$ is equal to $-1 + 2 = 1$, we find that the $(0,0)$ and $(1,0)$ tiles meet along the line $\xi_1 = 1$.

Similarly we see what happens when we move in the $\gamma'' = (1,2)$ direction. For ξ in the $(0,0)$ tile

$$\varphi(\xi + \gamma'') = 0 + \frac{1}{2}(0,1)M(0,1)^T + \xi_2 = \xi_2 + 1$$

and similarly we find that the $(0,0)$ tile and $(0,1)$ tile intersect along $\xi_2 = 1$.

Next we consider moving in the negative γ' and γ'' directions. Then

$$\varphi(\xi - \gamma') = 0 + \frac{1}{2}(-1,0)M(-1,0)^T - \xi_1 = -\xi_1 + 1$$

so $-\xi_1 + 1 = 0 \implies \xi_1 = 1$ so the two tiles intersect along the line $\xi_1 = -1$. And similarly along $\xi_2 = -1$ for the $(0,0)$ and $(0,-1)$ tile.

We almost have the hexagonal shape of \mathbb{CP}^2 blown up in three points. We just check $\gamma'' - \gamma'$ and $\gamma' - \gamma''$ when ξ is again in the $(0,0)$ tile.

$$\varphi(\xi + \gamma'' - \gamma') = \varphi(\xi + \gamma'') + \frac{1}{2}(-1,0)M(-1,0)^T + \langle \xi + \gamma'', \lambda(-\gamma') \rangle = \xi_2 + 1 + 1 - \xi_1 - 1 = -\xi_1 + \xi_2 + 1$$

which, setting equal to 0 we get $\xi_1 - \xi_2 = 1$. This line is parametrized as $(t+1, t)$ which means the vanishing of the tropicalization there is $(t+1, t) + \gamma'' - \gamma' = (t+1, t) + (1, 2) - (2, 1) = (t+1, t) + (-1, 1) = (t, t+1)$. This intersects the line $\xi_1 = -1$ when $t = -1$ and the line $\xi_2 = 1$ when $t = 0$ so those are the bounds i.e. the line segment from $(-1, 0)$ to $(0, 1)$.

Final edge:

$$\varphi(\xi + \gamma' - \gamma'') = \varphi(\xi + \gamma') + \frac{1}{2}(0, -1)M(0, -1)^T + \langle \xi, \lambda(-\gamma'') \rangle = \xi_1 + 1 + 1 - \xi_2 - 1 = \xi_1 - \xi_2 + 1$$

so $(t, t+1) + (2, 1) - (1, 2) = (t, t+1) + (1, -1) = (t+1, t)$ which intersects $\xi_1 = 1$ at $t = 0$ and $\xi_2 = -1$ at $t = -1$ so we get the line segment from $(0, -1)$ to $(1, 0)$.

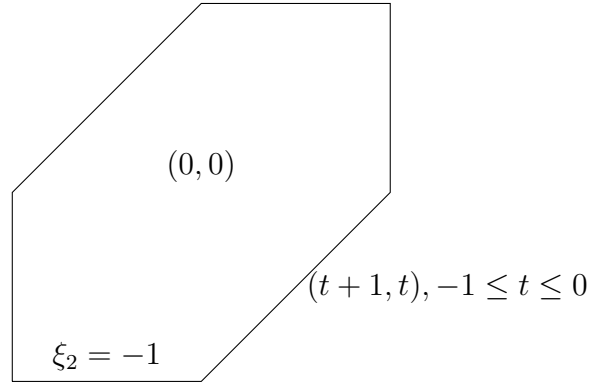


Figure 1.2: The $(0,0)$ tile delimited by the tropical curve

So by periodicity, this picture tiles the plane, and the slope of the (m, n) tile is going to be $m\xi_1 + n\xi_2 + \kappa(m\gamma' + n\gamma'')$ by Equation 1.11. \square

Outline: definition of (Y, v_0) and ω

The smooth manifold Y is constructed as a portion of a toric variety \tilde{Y} quotiented by Γ_B acting properly discontinuously via holomorphic maps. The defining polytope is

$$\begin{aligned} \Delta_{\tilde{Y}} &:= \{(\xi_1, \xi_2, \eta) \in \mathbb{R}^3 \mid \eta \geq Trop(s)(\xi)\} \\ \Delta_Y &:= (\Delta_{\tilde{Y}})|_{\eta \leq T^l} / \Gamma_B \text{ where} \\ \gamma \cdot (\xi_1, \xi_2, \eta) &:= (\xi_1 + \gamma_1, \xi_2 + \gamma_2, \eta - \kappa(\gamma) + \langle \xi, \lambda(\gamma) \rangle) \\ \because Trop(s)(\xi + \gamma) &= Trop(s)(\xi) - \kappa(\gamma) + \langle \xi, \lambda(\gamma) \rangle \end{aligned} \tag{1.12}$$

The polytope $\Delta_{\tilde{Y}}$ is illustrated in Figure 1.7, where η is bounded below by the expression in the center of the tile, and comes out of the page. We discuss the complex coordinates on Y below. For now we give a definition.

Definition 1.4.5 ([AAK16][Definition 1.2]). (Y, v_0) is a *generalized SYZ mirror* for $H = \Sigma_2$.

Remark 1.4.6. Note that one can apply SYZ in the reverse direction by starting with a Lagrangian torus fibration on Y minus a divisor to recover X as its complex mirror, see [AAK16, §8] or [CLL12].

Pair of pants: the local model

We describe an illustrative example of generalized SYZ that is the local model of our setting.

Example 1.4.7 ([AAK16][§9.1]). Suppose $H \subset V$ is the pair of pants $f(x_1, x_2) := 1 + x_1 + x_2 = 0$ in $V = (\mathbb{C}^*)^2$. This is a pair of pants because $x_1 \in \mathbb{C}^* \setminus \{-1\}$ and a cylinder minus a point is a pair of pants. Recall the definition of $\text{Trop}(f)$ in Definition 1.4.1.

So in the pair of pants example, $\rho \equiv 0$ and $A = \{(0, 0), (1, 0), (0, 1)\}$ hence $\text{Trop}(f)(\xi_1, \xi_2) = \max\{0, \xi_1, \xi_2\}$. If $\xi_1, \xi_2 < 0$ then 0 is the maximum, if $\xi_1 > \xi_2 > 0$ then ξ_1 is the maximum and if $\xi_2 > \xi_1 > 0$ then ξ_2 is the maximum. So the zero set (Definition 1.4.3) of $\text{Trop}(f)$ is the following picture

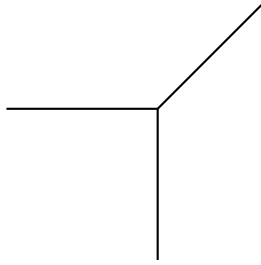


Figure 1.3: $\text{Trop}(1 + x_1 + x_2) = 0$

and the moment polytope is $\Delta := \{(\xi, \eta) \mid \eta \geq \text{Trop}(f)(\xi)\} \subset \mathbb{R}^{n+1}$ which gives

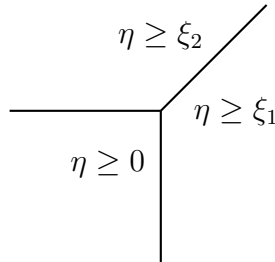


Figure 1.4: Moment polytope $\subset \mathbb{R}^3$

Under a linear transformation on (ξ_1, ξ_2, η) this polytope becomes $\mathbb{R}_{\geq 0}^3$. Then the corresponding toric variety is $\text{Spec } \mathbb{C}[x, y, z] = \mathbb{C}^3$. The superpotential is $v_0 = xyz$ and we get the expected mirror to the pair of pants, (\mathbb{C}^3, xyz) .

ω determines Γ_B -action on complex coordinates

We want to construct a symplectic form ω so that 1) it is Kähler i.e. compatible with the complex structure inherited from the complex toric coordinates, 2) $v_0 := xyz$ is a symplectic fibration and 3) it is toric, i.e. invariant under the torus action.

Because of 3), it suffices to define the symplectic form in terms of the norms of the complex coordinates. To ensure 1), we define ω locally as $\frac{i}{2\pi}\partial\bar{\partial}$ of a suitable Kähler potential, where $\partial\bar{\partial}$ is taken with respect to the local complex toric coordinates. To ensure 2) we need all fibers to be symplectic when we restrict the symplectic form. The central fiber is the toric variety with moment polytope given by the hexagon in Figure 1.5, quotiented by Γ_B . This comes equipped with a symplectic form as described in the theory of Section 1.3 with the toric variety $\mathbb{C}\mathbb{P}^2(3 \text{ points})$. As we move away from $v_0 = 0$ but still near a vertex of the polytope, the toric variety is locally modelled on the (\mathbb{C}^3, xyz) picture that was the local model of Example 1.4.7. So we will use bump functions to interpolate between the toric symplectic form of $\mathbb{C}\mathbb{P}^2(3 \text{ points})$ and the standard form on \mathbb{C}^3 .

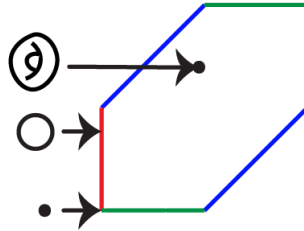


Figure 1.5: Moment polytope for central fiber of (Y, v_0) when $H = \Sigma_2$.

We explain the pictorial motivation for how the symplectic form is constructed in the one dimension down case.

Example 1.4.8. Let H be a point inside an elliptic curve. Then the polytope $\Delta_{\tilde{Y}}$ is two-dimensional, so we can draw it.

A fiber of $v_0 : \tilde{Y} \rightarrow \mathbb{C}$ is topologically a cylinder with necks getting pinched in a periodic way as $|v_0| \rightarrow 0$, degenerating to a string of \mathbb{P}^1 's over the central fiber. Around the widest parts of the cylinder, it looks like a portion of a sphere, and \mathbb{P}^1 comes canonically equipped with the Fubini-Study form. On the other hand, neighborhoods of the vertices of the polytope give charts \mathbb{C}^2 and the local picture of the Lefschetz fibration $\mathbb{C}^2 \rightarrow \mathbb{C}$, $(x, y) \mapsto xy$ where cylinders degenerate to a cone over zero. In particular, \mathbb{C}^2 comes canonically equipped with the standard form ω_{std} . When the toric coordinates are very small, the Fubini-Study form and the standard form are approximately the same by a Taylor expansion of \log . So a symplectic form can be constructed by interpolating between these two Kähler forms.

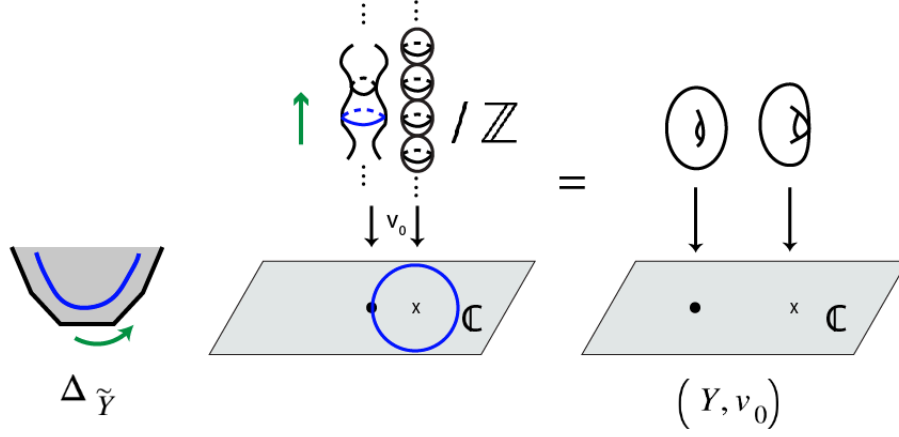


Figure 1.6: In one dimension lower, the boundary of $\Delta_{\tilde{Y}}$ is the moment map image of a string of \mathbb{P}^1 's. In the polytope, $|v_0|$ increases in the $(0, 1)$ direction. In the fibration v_0 , $|v_0|$ is the radius of the circle in the base.

Lemma 1.4.9. *Let $r_x = |x|$ etc. and $0 < T \ll 1$ be a constant. In the case of $H = \Sigma_2$, the symplectic form will interpolate between $(\mathbb{C}^3, \omega_{std})$ with Kähler potential $\frac{1}{3}T^2(r_x^2 + r_y^2 + r_z^2)$ from charts locally around the vertices, and the toric Kähler form induced by the hexagon as $\mathbb{C}\mathbb{P}^2(3 \text{ points})$, the blow-up at three points. The Kähler potential is the logarithm of the sum of squares of suitably scaled sections corresponding to lattice points, as described in Corollary 1.3.29.*

Set $g_{xy} := \log(1 + |T^a x|^2)(1 + |T^b y|^2)(1 + |T^c xy|^2)$ for some (a, b, c) . Then $(a, b, c) = (1, 1, 2)$ has the correct symmetries for ω to be compatible with the Γ_B -action and define a symplectic form on the quotient \tilde{Y}/Γ_B .

Remark 1.4.10. When Tr_x and Tr_y are both small, we have $g_{xy} \approx (Tr_x)^2 + (Tr_y)^2$.

Remark 1.4.11. Consider Figure 1.7, depicting the three dimensional $\Delta_{\tilde{Y}}$ of this thesis. By toric geometry we know (x, y) must map to some scaling of (y^{-1}, xy) as drawn in that figure. We will define a suitable (α, β) in what follows so that the scaling is $(x, y) \mapsto (T^\alpha y^{-1}, T^\beta xy)$.

Definition 1.4.12. Define $G = \mathbb{Z}/6 \curvearrowright \tilde{Y}$ to rotate the hexagon clockwise as follows, where g is the generator of G :

$$g \cdot (x, y) = (T^\alpha y^{-1}, T^\beta xy) \quad (1.13)$$

More specifically, this action on (x, y) determines an action on \tilde{Y} by prescribing it to restrict to an action on a fiber of v_0 , either a generic one or the degenerate central one. In other words, the action on the z coordinate is $g \cdot z = T^{-\alpha-\beta} yz$ so that $v_0 = xyz \mapsto T^{\alpha+\beta-\alpha-\beta} y^{-1} \cdot xy \cdot yz = xyz$ is preserved.

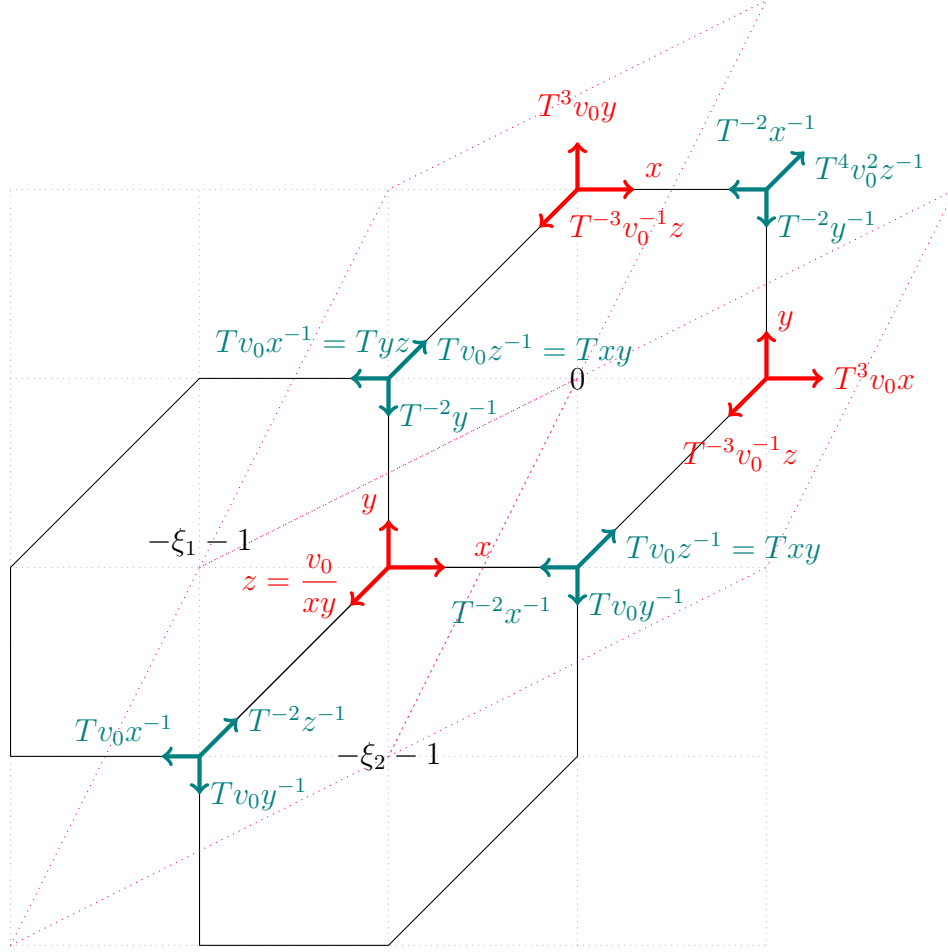


Figure 1.7: Depiction of $\Delta_{\tilde{\gamma}}$ in the Σ_2 case. The coordinates indicate a Γ_B -action which we motivate and define in the next sections. Magenta parallelogram = fundamental domain for Γ_B action, with diagonal \mathbb{P}^1 at center. Each vertex is a \mathbb{C}^3 chart. Coordinate transitions will be explained in Lemma 1.4.9. Expressions in the center of tiles indicate e.g. $\eta \geq \varphi(\xi) = -\xi_1 - 1$ over that tile. Equations of the 6 edges imply $\text{tile}_{(0,0)}$ is given by $(\xi_1, \xi_2) \in \{(\xi_1, \xi_2) \mid -1 \leq \xi_1, \xi_2, -\xi_1 + \xi_2 \leq 1\}$.

Claim 1.4.13. Under G , if g_{xy} maps to a Kähler potential that differs by a harmonic function, namely by $\log |T^{\alpha/2}y|^2$, then the symplectic area of the \mathbb{P}^1 along the y -axis is 1.

Proof. We consider the calculation along the z -axis, which suffices because that along the y -axis is analogous once we have the symmetries. Note that the symplectic area of the \mathbb{P}^1 along the z -axis is 1, by Stokes' theorem. Recall \mathbb{P}^1 has an open covering U_0, U_∞ and charts ϕ_0 and ϕ_1 sending $[z_0 : z_1]$ to z_1/z_0 and z_0/z_1 respectively. We want to split up the integration over \mathbb{P}^1 into these two charts, but only the portion of the chart up to where they intersect (else we integrate over too much). So we have z is the coordinate on $\phi_0(U_0) \cong \mathbb{C}$ then it is

$1/(T^\alpha z)$ on $\phi_\infty(U_\infty)$ and $|z| = |1/T^\alpha z| \implies |z| = 1/T^{\alpha/2}$. Then let D_0 be the disc in $\phi_0(U_0)$ and D_∞ the corresponding in the other one. Let F_0, F_∞ be the Kähler potential in the two charts.

$$\begin{aligned}
\int_{\mathbb{P}^1} \frac{i}{2\pi} \partial \bar{\partial} F &= \frac{i}{2\pi} \left[\int_{\phi_0^{-1}(D_0)} d(\bar{\partial} F) + \int_{-\phi_\infty^{-1}(D_\infty)} d(\bar{\partial} F) \right] \\
&= \frac{i}{2\pi} \left[\int_{\partial D_0} \bar{\partial}(\phi_0^{-1})^* F - \int_{\partial D_\infty} \bar{\partial}(\phi_\infty^{-1})^* F \right] \\
&= \frac{i}{2\pi} \int_{C_{1/T^{\alpha/2}}} \bar{\partial}(F_0 - F_\infty) \\
&= \frac{i}{2\pi} \int_{C_{1/T^{\alpha/2}}} \bar{\partial} \log(|T^{\alpha/2} z|^2) = \frac{i}{2\pi} \int_{C_{1/T^{\alpha/2}}} \frac{T^\alpha z d\bar{z}}{|T^{\alpha/2} z|^2} \\
&= \frac{i}{2\pi} \int_0^{2\pi} e^{i\theta} (-i) e^{-i\theta} d\theta = 1
\end{aligned}$$

□

Proof of main Lemma 1.4.9.

$$\begin{aligned}
g^* \log(1 + |T^a x|^2)(1 + |T^b y|^2)(1 + |T^c xy|^2) &= \log(1 + |T^{a+\alpha} y^{-1}|^2)(1 + |T^{b+\beta} xy|^2)(1 + |T^{c+\alpha+\beta} x|^2) \\
g_{xy} &= \log(1 + |T^a x|^2)(1 + |T^b y|^2)(1 + |T^c xy|^2)
\end{aligned}$$

We expect the two potentials to differ by $\log |T^b y|^2$ because y becomes y^{-1} under g . So comparing exponents we obtain:

$$\begin{aligned}
b &= -a - \alpha \\
a &= c + \alpha + \beta \\
c &= b + \beta
\end{aligned}$$

We have 5 unknowns and 3 equations so should be able to reduce to 2 unknowns. Namely write (a, b, c) in terms of (α, β) and then, requiring $x \leftrightarrow y$ symmetry, we impose $a = b$ and determine α in terms of β .

$$\begin{aligned}
a = c + \alpha + \beta &= (b + \beta) + \alpha + \beta = (-a - \alpha) + \alpha + 2\beta \\
\implies a &= \beta \\
\implies b &= -\alpha - \beta \\
a = b &\therefore \alpha = -2\beta \\
\implies c &= b + \beta = 2\beta
\end{aligned}$$

$$\therefore g_{xy} = \log(1 + |T^\beta x|^2)(1 + |T^\beta y|^2)(1 + |T^{2\beta} xy|^2)$$

$$\text{Choose } \beta = 1 \implies g_{xy} = \log(1 + |Tx|^2)(1 + |Ty|^2)(1 + |T^2 xy|^2)$$

Since we set $\beta = 1$, we see that along the x axis (so y and z axes by symmetry), the complex modulus changes by T^{-2} . So the value of y becomes large when we apply g , but the new coordinate system there, called (x'', y'', z'') later on, will have the same small values as at (x, y, z) . □

We see in the next section why $(\alpha, \beta) = (-2, 1)$ and $g \cdot (x, y) = (T^{-2}y^{-1}, Txy)$ determine the Γ_B -action depicted in Figure 1.7. Then this allows us to define Y as the quotient \tilde{Y}/Γ_B where \tilde{Y} is constructed from $\Delta_{\tilde{\gamma}}$ as explained in Section 1.3.

The definition of Y

Remark 1.4.14 (Convention). The convention is that moving up and right in Figure 1.7 is negative since the powers of $T \ll 1$ are positive, hence decreasing values in the coordinates corresponds with moving in the negative direction of the group action. That is, the actions of γ' and γ'' map the coordinates (x, y, z) to the charts centered at $(-2, -1)$ and $(-1, -2)$ respectively in Figure 1.7.

Definition 1.4.15 (Definition of the Γ_B -action). The Γ_B -action on (x, y, z) can be read off from the $\mathbb{Z}/6$ -action defined above in Definition 1.4.12 as follows. Namely, g^2 maps (x, y, z) to the coordinate system centered at $(\xi_1, \xi_2) = (1, 2)$ as $-\gamma''$ would, but it permutes the coordinate directions by a rotation. Indeed, g sends $(x, y, z) \mapsto (T^{-2}y^{-1}, Txy, Tyz)$. After undoing this permutation in g so the directions are preserved, i.e. $(x, y, z) \mapsto (Tyz, T^{-2}y^{-1}, Txy) = (Tv_0x^{-1}, T^{-2}y^{-1}, Tv_0z^{-1})$, we can define the Γ_B -action by similarly permuting the resulting coordinates from applying g^2 :

$$(-\gamma'') \cdot (x, y, z) := (x, T^3v_0y, T^{-3}v_0^{-1}z)$$

Definition 1.4.16 (Definition of Y). Now we may define Y via the quotient \tilde{Y}/Γ_B :

$$\begin{aligned} \Delta_{\tilde{\gamma}} &:= \{(\xi_1, \xi_2, \eta) \in \mathbb{R}^3 \mid \eta \geq \text{Trop}(s)(\xi)\} \\ \Delta_Y &:= (\Delta_{\tilde{\gamma}})|_{\eta \leq T^l} / \Gamma_B \text{ where Equation 1.10 implies} \\ \gamma \cdot (\xi_1, \xi_2, \eta) &:= (\xi_1 + \gamma_1, \xi_2 + \gamma_2, \eta - \kappa(\gamma) + \langle \xi, \lambda(\gamma) \rangle) \end{aligned} \tag{1.14}$$

Every vertex of $\Delta_{\tilde{\gamma}}$ corresponds to three complex coordinates which we can write in terms of (x, y, z) (and $v_0 = xyz$). Figure 1.7 lists these coordinates, which we gather here for clarity as charts U_{n, g^k} where $\gamma = n_1\gamma' + n_2\gamma''$ denotes the center of the tile in $\Delta_{\tilde{\gamma}}$ we are looking at, when projected to the first two coordinates, and g^k denotes how far around the hexagon we are. The g^k allows us to index the charts, but as noted in Definition 1.4.15 the coordinates are a permutation of the coordinates $g^k \cdot (x, y, z)$ so the subscript is mainly for indexing. The transition maps are

$$(x, y, z) \mapsto \sigma_{g^n} \cdot (g^n \circ \gamma) \cdot (x, y, z), \quad n \in \mathbb{Z}/6, \gamma \in \Gamma_B$$

for a suitable permutation σ_{g^n} on the coordinates that depends on n , see Definition 1.4.15. Going clockwise around on the $(0, 0)$ tile from (x, y, z) :

- $U_{\underline{0}, g^0} : (x, y, z)$
- $U_{\underline{0}, g} : (Tv_0x^{-1}, T^{-2}y^{-1}, Tv_0z^{-1}) =: (x'', y'', z'')$
- $U_{\underline{0}, g^2} : (x, T^3v_0y, T^{-3}v_0^{-1}z) =: (-\gamma'') \cdot (x, y, z)$
- $U_{\underline{0}, g^3} : (T^{-2}x^{-1}, T^{-2}y^{-1}, T^4v_0^2z^{-1})$
- $U_{\underline{0}, g^4} : (T^3v_0x, y, T^{-3}v_0^{-1}z) =: (-\gamma') \cdot (x, y, z)$
- $U_{\underline{0}, g^5} : (T^{-2}x^{-1}, Tv_0y^{-1}, Tv_0z^{-1}) =: (x', y', z')$
- Going along the z axis we get to the g^{-1} vertex in the $(-1, 0)$ tile:
- $U_{(-1, 0), g^{-1}} : (Tv_0x^{-1}, Tv_0y^{-1}, T^{-2}z^{-1}) =: (x''', y''', z''')$

The upshot is that for $|v_0| = T^l$ with $T \ll 1$ and l sufficiently small, Γ_B acts properly discontinuously and holomorphically so the quotient is a well-defined complex manifold Y .

Calculation of coordinates from $\mathbb{Z}/6$ action. Since $g \cdot (x, y) = (T^{-2}y^{-1}, Txy)$, applying the group action twice we find

$$(x, y) \sim (T^{-2}y^{-1}, Txy) \sim (T^{-2}(T^{-1}x^{-1}y^{-1}), T(T^{-2}T^{-1})(Txy)) = (T^{-3}x^{-1}y^{-1}, x)$$

In particular Γ_B fixes $v_0 = xyz$ so we may rewrite the transformed y -coordinate as T^3v_0y to obtain the γ'' action, after suitable permutation σ_{g^2} :

$$\sigma_{g^2} \cdot g^2 \cdot (x, y, z) =: -\gamma'' \cdot (x, y, z) = (x, T^3v_0y, T^{-3}v_0^{-1}z)$$

The γ' calculation is similar. To find the coordinate system (x''', y''', z''') , we first move down and left by γ' action to be in the $(0, -1)$ tile, then rotate by g^{-1} and finally apply a suitable permutation. Since $g^{-1} \cdot (x, y) = (Txy, T^{-2}x^{-1})$ we obtain $g^{-1} \cdot (x, y, z) = (Tv_0z^{-1}, T^{-2}x^{-1}, Tv_0y^{-1})$. Then:

$$\begin{aligned} \gamma' \cdot (x, y, z) &= (T^{-3}v_0^{-1}x, y, T^3v_0z) \\ g^{-1} \cdot (T^{-3}v_0^{-1}x, y, T^3v_0z) &= (Tv_0(T^3v_0z)^{-1}, T^{-2}(T^{-3}v_0^{-1}x)^{-1}, Tv_0y^{-1}) \\ &= (T^{-2}z^{-1}, Tv_0x^{-1}, Tv_0y^{-1}) \\ \therefore (x''', y''', z''') &:= \sigma_{g^{-1}} \cdot g^{-1} \cdot \gamma' \cdot (x, y, z) = (Tv_0x^{-1}, Tv_0y^{-1}, T^{-2}z^{-1}) \end{aligned}$$

The calculations to obtain the remaining coordinates in the charts listed above are similar. \square

Remark 1.4.17. Note that the symmetry properties required for ω told us what complex structure was needed (it produces a product complex structure), which by mirror symmetry will correspond to a specific symplectic form on A-model of X . We label some of the green chart coordinates of Figure 1.7 with new primed-variables in the list in Definition 1.4.16 above.

Corollary 1.4.18 (Complex structure on Y). *The complex structure is obtained by first identifying toric charts for each vertex of the polytope $\Delta_{\tilde{Y}}$ by gluing (x, y, z) to the new coordinate system of each of the other vertices. Then we quotient by the action of Γ_B , which rescales the coordinates while preserving $v_0 = xyz$, so that the fibers of v_0 on the quotient are abelian varieties. In terms of the complex coordinates the Γ_B -action is:*

$$\begin{aligned} (x, y, z) &\sim (T^3 v_0 x, y, T^{-3} v_0^{-1} z) \\ (x, y, z) &\sim (x, T^3 v_0 y, T^{-3} v_0^{-1} z) \end{aligned}$$

Remark 1.4.19. Note that before the Γ_B -action quotient the fibers would be $(\mathbb{C}^*)^2$ after gluing all the toric charts together. The Γ_B -action in complex coordinates corresponds to passing from $\Delta_{\tilde{Y}}$ to $\Delta_Y = \Delta_{\tilde{Y}}/\Gamma_B$. We still glue toric charts by identifying monomials according to the polytope, but we allow rescaling to happen when gluing the complex coordinates. (E.g. in a lower dimension for $\mathbb{C}^* \ni x \mapsto Tx$ we glue a unit circle with a radius T circle, giving a torus.)

Remark 1.4.20 (Terminology). The toric variety \tilde{Y} is referred to as a toric variety of “infinite-type” by [KL19], because of the infinitely many facets, where the neighborhood of the toric divisor there is the same as our restriction to $|v_0|$ small, i.e. η small.

Definition 1.4.21 (Superpotential). The *superpotential* v_0 is the holomorphic function $Y \rightarrow \mathbb{C}$ defined to be

$$v_0(x, y, z) := xyz \tag{1.15}$$

which is well-defined as a global function on Y because it is invariant under the Γ_B action.

Remark 1.4.22. We will equip v_0 with the structure of a symplectic fibration in Section 2, which we then equip with a Fukaya-Seidel category in Section 4.1.

Remark 1.4.23. The Γ_B -action on complex coordinates here is different than that described in [AAK16, §10.2]. That means that Y is mirror to X with a different symplectic form than the one considered in their paper. The complex structure there is

$$\mathbf{v}^m \sim v_0^{\langle \lambda(\gamma), m \rangle} T^{\langle \gamma, m \rangle} \mathbf{v}^m \tag{1.16}$$

where they use complex coordinates $\mathbf{v} = (v_1, v_2)$. Thus setting $(x, y, z) = (v_1^{-1}, v_2^{-1}, v_0 v_1 v_2)$, their complex structure arises from the following Γ_B -action:

$$\begin{aligned} \gamma' \cdot (x, y, z) &= (T^{-2} v_0^{-1} x, T^{-1} y, T^3 v_0 z) \\ \gamma'' \cdot (x, y, z) &= (T^{-1} x, T^{-2} v_0^{-1} y, T^3 v_0 z) \end{aligned}$$

Delineating polytope into regions

Recall the polytope $\Delta_{\tilde{\gamma}}$ of Figure 1.7. We will start by defining ω in a neighborhood of a vertex. It will be defined in terms of a new set of local real radial and angular coordinates d and θ on \tilde{Y} in each delineated region of Figure 1.9.

The delineations are defined in terms of the following variables. We fix $|v_0| (= |xyz|) = T^l$ for $T \ll 1$ and l a large positive constant. In the support of Figure 1.9, we have $r_x, r_y, r_z \ll 1$ so the approximations of Equation 1.18 are valid.

We define functions ϕ_x, ϕ_y, ϕ_z which will be crucial in understanding calculations to follow.

$$\begin{aligned}\phi_x(x, y, z) &:= \log_T \frac{1 + |Tx|^2}{1 + |T^2yz|^2} \\ \phi_y(x, y, z) &:= \log_T \frac{1 + |Ty|^2}{1 + |T^2xz|^2} \\ \phi_z(x, y, z) &:= \log_T \frac{1 + |Tz|^2}{1 + |T^2xy|^2}\end{aligned}\tag{1.17}$$

Now we can define the the local radial and angular coordinates we'll do calculations with. Their subscripts indicate which region of Figure 1.4 they are defined in:

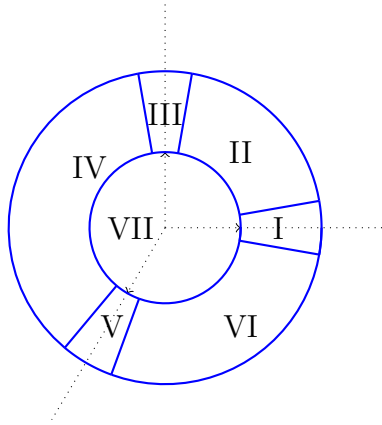


Figure 1.8: Delineate regions in $\Delta_{\tilde{\gamma}}$ around a vertex

$$\begin{aligned}
d_I &:= \phi_x - \frac{1}{2}(\phi_y + \phi_z) \\
&= \log_T \left(\frac{1 + |Tx|^2}{1 + |T^2 v_0 x^{-1}|^2} / \sqrt{\frac{1 + |Ty|^2}{1 + |T^2 v_0 y^{-1}|^2} \cdot \frac{1 + |Tz|^2}{1 + |T^2 v_0 z^{-1}|^2}} \right) \\
&\approx (Tr_x)^2 - \frac{1}{2} \left((Tr_y)^2 + (Tr_z)^2 \right) \text{ for } r_x, r_y, r_z \ll 1 \\
\theta_I &:= \phi_y - \phi_z \\
&= \log_T \left(\frac{1 + |Ty|^2}{1 + |Tz|^2} \cdot \frac{1 + |T^2 xy|^2}{1 + |T^2 xz|^2} \right) \approx (Tr_y)^2 - (Tr_z)^2
\end{aligned} \tag{1.18}$$

$$\begin{aligned}
d_{IIA} &:= \phi_x - \frac{1}{2}(\phi_y + \phi_z) + \frac{3}{2}\alpha_6(\theta_{II}) \cdot \phi_y \approx T^2[r_x^2 - \frac{1}{2}(r_y^2 + r_z^2) + \frac{3}{2}\alpha_6(\theta_{II}) \cdot r_y^2] \\
d_{IIB} &:= \phi_x + \phi_y - \frac{1}{2}\phi_z \\
d_{IIC} &:= \phi_y - \frac{1}{2}(\phi_x + \phi_z) + \frac{3}{2}\alpha_6(-\theta_{II}) \cdot \phi_x \\
\theta_{II} &:= \log_T r_y - \log_T r_x
\end{aligned} \tag{1.19}$$

where α_6 is a cut-off function in the angular direction that we define below. Lastly, we define

$$\begin{aligned}
d_{III} &:= \phi_y - \frac{1}{2}(\phi_x + \phi_z) \\
\theta_{III} &:= \phi_z - \phi_x \\
d_V &:= \phi_z - \frac{1}{2}(\phi_x + \phi_y) \\
\theta_V &:= \phi_x - \phi_y
\end{aligned} \tag{1.20}$$

Along the axes in the top diagram of Figure 1.9 we have $r_y = r_z < r_x$ for the $(1, 0)$ direction, $r_x = r_z < r_y$ for the $(0, 1)$ direction and $r_x = r_y < r_z$ for the $(-1, -1)$ direction.

Definition 1.4.24 (Definition of regions in Figure 1.9). The curves delineating region I are: on the left and right d_I is constant and on the top and bottom θ_I is constant. We can approximate these as r_x constant and r_y constant respectively, letting the other two variables vary while $|xyz| = T^l$ remains constant. Over the origin in region VII $|x| = |y| = |z| = T^{l/3}$ because the three coordinates are equal and their product is $|v_0| = T^l$. We define the following, for a value of p sufficiently large.

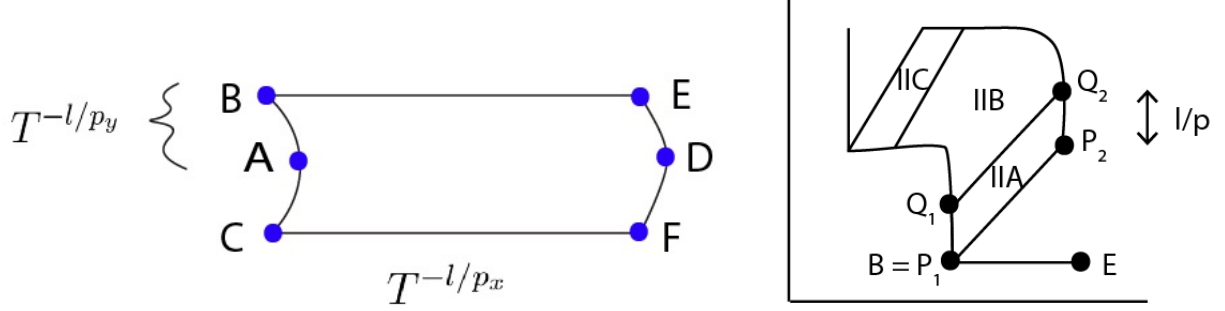


Figure 1.9: Zoom in on region I/II in left/right figures respectively

Region I

- $A(r_x, r_y, r_z) = (T^{l/4}, T^{3l/8}, T^{3l/8})$
- $B(r_x, r_y, r_z) \approx (T^{l/4}, T^{3l/8-l/p}, T^{3l/8+l/p})$.
- $C(r_x, r_y, r_z) \approx (T^{l/4}, T^{3l/8+l/p}, T^{3l/8-l/p})$
- $D(r_x, r_y, r_z) = (T^{l/4-l/p}, T^{3l/8+l/2p}, T^{3l/8+l/2p})$.
Here r_x has increased while maintaining $r_y = r_z$.
- $E(r_x, r_y, r_z) \approx (T^{l/4-l/p}, T^{3l/8-l/p}, T^{3l/8+2l/p})$.
- $F(r_x, r_y, r_z) \approx (T^{l/4-l/p}, T^{3l/8+2l/p}, T^{3l/8-l/p})$

The curves delineating region II are θ_{II} constant for the radially outward lines, and d_{IIA} or d_{IIB} constant along angular curves. Note that d_{IIA} constant here is approximately r_x constant.

Region II

- $P_1 = B \approx (T^{l/4}, T^{3l/8-l/p}, T^{3l/8+l/p})$
- $P_2 \approx (T^{l/4-l/p}, T^{3l/8-2l/p}, T^{3l/8+3l/p})$.

This follows because the sliver from P_1 to P_2 is $\theta_{II} = \log_T r_y - \log_T r_x$ constant, while P_2 is obtained by moving E up along constant $d_I \approx (Tr_x)^2$ so $r_x(P_2) \approx T^{l/4-l/p}$. Then constant θ_{II} implies:

$$\begin{aligned}
 \theta_{II}(P_1) &\approx 3l/8 - l/p - l/4 = l/8 - l/p \\
 &= \theta_{II}(P_2) \approx \log_T r_y - (l/4 - l/p) \\
 \implies \log_T r_y &\approx 3l/8 - 2l/p
 \end{aligned}$$

- $Q_1 \approx (T^{l/4}, T^{3l/8-2l/p}, T^{3l/8+2l/p})$
From P_1 to Q_1 along d_{IIA} constant we increase r_y by a factor of $T^{-l/p}$ keeping r_x approximately constant.
- $Q_2 \approx (T^{l/4-l/p}, T^{3l/8-3l/p}, T^{3l/8+4l/p})$
From Q_1 to Q_2 we have θ_{II} is constant and at Q_1 we have $\theta_{II}(Q_1) \approx 3l/8 - 2l/p - l/4 = l/8 - 2l/p$. From P_2 to Q_2 we have r_x approximately constant hence $\log_T r_x$ at Q_2 is approximately $l/4 - l/p$ so

$$\log_T r_y \approx (l/8 - 2l/p) + (l/4 - l/p) = 3l/8 - 3l/p$$

The r_z coordinate is determined by $r_x r_y r_z = T^l$.

Now finally we get a condition on p . We want $r_x \gg r_y$ everywhere in region IIA so that contour lines for d_{IIA} look roughly as they are drawn and approximations for d_{IIA} are valid. Looking at Q_1 this means $T^{l/4} \gg T^{3l/8-2l/p}$ and Q_2 gives the same constraint. Hence we need $1/8 - 2/p > 0$ or $p > 16$. E.g. take $p = 17$.

The rest of the regions are defined by symmetry.

1.5 The definition of the symplectic form

Now we define the symplectic form in the case of $H = \Sigma_2$.

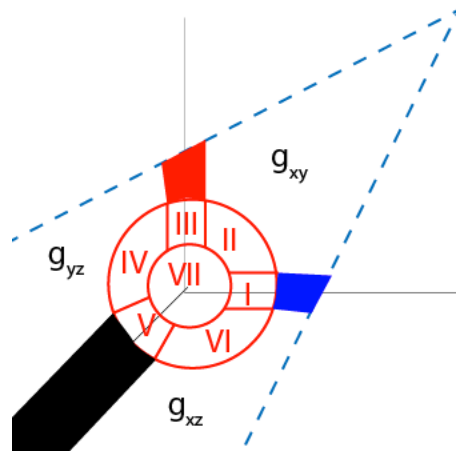


Figure 1.10: Interpolate between three potentials: $F = \alpha_1 g_{xy} + \alpha_2 g_{xz} + (1 - \alpha_1 - \alpha_2) g_{yz}$, $0 \leq \alpha_1, \alpha_2 \leq 1$. Region VII is where $\alpha_1 = \alpha_2 = 1/3$ and $F = \frac{1}{3}(g_{xy} + g_{xz} + g_{yz}) \approx \frac{2}{3}((Tr_x)^2 + (Tr_y)^2 + (Tr_z)^2)$ via the log approximation.

Definition 1.5.1 (Definition of symplectic form). We set $\omega = \frac{i}{2\pi}F$ where F is defined locally as follows in terms of the coordinates in Equation 1.18 and

$$\begin{aligned} g_{yz} &= \log(1 + |Ty|^2)(1 + |Tz|^2)(1 + |T^2yz|^2) \\ g_{xz} &= \log(1 + |Tx|^2)(1 + |Tz|^2)(1 + |T^2xz|^2) \\ g_{xy} &= \log(1 + |Tx|^2)(1 + |Ty|^2)(1 + |T^2xy|^2) \end{aligned} \quad (1.21)$$

We introduce new bump functions $\alpha_3, \dots, \alpha_6$ as follows:

$$\frac{2}{3} \leq \alpha_3(d_I) = \alpha_1 + \alpha_2 \leq 1, \quad -\frac{1}{2} \leq \alpha_4(\theta_I) \leq \frac{1}{2}, \quad 0 \leq \alpha_5(d_I) \leq 1, \quad 0 \leq \alpha_6(\theta_{II}) \leq 1$$

$$\alpha_4(\theta_I) \cdot \alpha_5(d_I) = \frac{1}{2}(\alpha_1 - \alpha_2)$$

These bump functions are smooth, increasing as functions of the specified variable, and near the ends of their domain of definition they are constant at the bounds given. We also require that α_4 is an odd function. See the subsection below ‘‘Motivating the definition’’ for an explanation of the properties of these bump functions. Now the definition is as follows, noting that $g_{xz} - g_{yz} = \phi_x - \phi_y$ and similarly permuting (x, y, z) :

Regions $g_{*\bullet}$ in Fig 1.10: $F = g_{xy}, F = g_{yz}, F = g_{xz}$ respectively

$$\text{Region I: } F = g_{yz} + \alpha_3(d_I)d_I + \alpha_4(\theta_I)\alpha_5(d_I)\theta_I$$

$$\text{Region IIA: } F = g_{yz} - \alpha_6(\theta_{II})\phi_y + \alpha_3(d_{IIA})d_{IIA} + \frac{1}{2}\alpha_5(d_{IIA})(\phi_y - \phi_z - \alpha_6(\theta_{II})\phi_y)$$

$$\text{Region IIB: } F = (g_{yz} - \phi_y) + \alpha_3(d_{IIB})d_{IIB} - \frac{1}{2}\alpha_5(d_{IIB})\phi_z$$

$$\text{Region IIC: } F = g_{xz} - \alpha_6(-\theta_{II})\phi_x + \alpha_3(d_{IIC})d_{IIC} + \frac{1}{2}\alpha_5(d_{IIC})(\phi_x - \phi_z - \alpha_6(-\theta_{II})\phi_x) \quad (1.22)$$

$$\text{Region I to Region IIA: } F = g_{yz} + \alpha_3(d_I) \cdot d_I + \frac{1}{2}\alpha_5(d_I) \cdot \theta_I$$

$$= g_{yz} + \alpha_3(d_{IIA})d_{IIA} + \frac{1}{2}\alpha_5(d_{IIA}) \cdot \theta_I$$

$$\text{Region VII: } F = \frac{1}{3}(g_{xy} + g_{xz} + g_{yz})$$

These formulas match at the boundaries, which allows us to define the rest of the regions III – VI similarly to I and II by symmetry, via permuting the coordinates (x, y, z) . For example, one can check that the formula for region IIA agrees with that for region VII when $\alpha_3 = \frac{2}{3}$ and $\alpha_5 = 0$; with that for region I when $\alpha_6 = 0$ and $\alpha_4 = \frac{1}{2}$; with that for region IIB when $\alpha_6 = 1$; and with g_{xy} when $\alpha_3 = \alpha_5 = 1$. The calculation is similar for the other regions.

Along the coordinate axes (namely the regions shaded red, blue, and black) we interpolate between the relevant $g_{*\bullet}$ ’s using the same formulas as in regions I, III, and V, with $\alpha_3 \equiv 1$. E.g. along the r_x -axis (blue region) the formula is $F = \frac{1}{2}(g_{xy} + g_{xz}) + \alpha_4(\theta_I)(g_{xy} - g_{xz})$ and similarly for the other edges.

Since we have defined the Kähler potential locally, and it is symmetric in (x, y, z) over a neighborhood of the origin in (ξ_1, ξ_2) coordinates, we may define the Kähler form everywhere by requiring it to be invariant under both the $\mathbb{Z}/6$ action described earlier, and the Γ_B -action. The consistency condition for this to happen is verified in Claim 1.5.2 below.

This completes the definition of the symplectic form.

Motivating the definition

We can rearrange terms of the initial expression of F depending on α_1 and α_2 to motivate the definitions of α_3 and $\alpha_4 \cdot \alpha_5$, as well as of the d and θ in each region. The choice of α_6 and the variables in region II are chosen to interpolate between the definition of F in either side, namely in regions I and III.

$$\begin{aligned}
F &= \alpha_1 g_{xy} + \alpha_2 g_{xz} + (1 - \alpha_1 - \alpha_2) g_{yz} \\
&= \alpha_1 \log(1 + |Tx|^2)(1 + |Ty|^2)(1 + |T^2xy|^2) + \alpha_2 \log(1 + |Tz|^2)(1 + |Tx|^2)(1 + |T^2xz|^2) \\
&\quad + (1 - \alpha_1 - \alpha_2) \log(1 + |Tz|^2)(1 + |Ty|^2)(1 + |T^2yz|^2) \\
&= g_{yz} + (\alpha_1 + \alpha_2) \phi_x - \left(\frac{\alpha_1 + \alpha_2}{2} - \frac{\alpha_1 - \alpha_2}{2} \right) \cdot \phi_y - \left(\frac{\alpha_1 + \alpha_2}{2} + \frac{\alpha_1 - \alpha_2}{2} \right) \cdot \phi_z \\
&= g_{yz} + (\alpha_1 + \alpha_2) \left(\phi_x - \frac{1}{2}(\phi_y + \phi_z) \right) + \frac{1}{2}(\alpha_1 - \alpha_2)(\phi_y - \phi_z)
\end{aligned}$$

Note that $\alpha_1, \alpha_2, 1 - \alpha_1 - \alpha_2$ is asymmetric but all three should be treated symmetrically, hence we collect them as done above. In other words, if we rotate (α_1, α_2) thought of as a vector by $\pi/4$, we get something proportional to

$$\begin{pmatrix} 1 & -1 \\ 1 & 1 \end{pmatrix} \begin{pmatrix} \alpha_1 \\ \alpha_2 \end{pmatrix} = \begin{pmatrix} \alpha_1 - \alpha_2 \\ \alpha_1 + \alpha_2 \end{pmatrix}$$

Define $\alpha_3 = \alpha_1 + \alpha_2$. To obtain its bounds, we consider the geometry and how α_1, α_2 vary. In the center region VII, $\alpha_1 = \alpha_2 = 1/3$. As we move through region I and reach the end along the r_x direction, there should not be a g_{yz} contribution, meaning that $\alpha_3 = \alpha_1 + \alpha_2 = 1$ there. Hence α_3 goes from $2/3$ to 1 in region I.

We use $\alpha_1 - \alpha_2$ to define a bump function α_4 that varies in the angular direction, which we'll denote θ_I and define below. There is a caveat. Note that at the start of region I, $\alpha_1 = \alpha_2 = 1/3$ so $\alpha_1 - \alpha_2$ goes from 0 to 0 as we trace out the angle θ_I , but at the end of region I we go from $(\alpha_1, \alpha_2) = (0, 1)$ at the bottom to $(\alpha_1, \alpha_2) = (1, 0)$ at the top, so that $\alpha_1 - \alpha_2$ goes between -1 and 1 . Thus we need to multiply $\alpha_4(\theta_I)$ by another bump function $\alpha_5(d_I)$ that goes from 0 to 1 and depends on a variable d_I that increases along increasing r_x , which we'll define next. Hence we scale the interval that α_4 varies in. We require α_4 to be

an odd function for symmetry reasons. Let $\alpha_4 \cdot \alpha_5 = \frac{1}{2}(\alpha_1 - \alpha_2)$ so that:

$$F = g_{yz} + \alpha_3(\phi_x - \frac{1}{2}(\phi_y + \phi_z)) + \alpha_4 \cdot \alpha_5(\phi_y - \phi_z)$$

The crux of the calculation that follows is that bump functions will be multiplied by the variable they are a function of. The α_i vary according to “how far around the circle” we are, an angular direction, and “how far out from center” we are, a radial direction. So we will introduce a set of coordinates d and θ which can be read off from the expression for F above: $d_I = \phi_x - \frac{1}{2}(\phi_y + \phi_z)$ and $\theta_I = \phi_y - \phi_z$. We motivate geometrically why they make sense.

We are trying to construct a symplectic form whose moment polytope is the same as the toric polytope by Delzant’s theorem. What we can read off from the picture is how r_x, r_y and r_z compare to each other; even if we can’t specify their values we can observe how they compare to one another. In particular, in Figure 1.11 we see that e.g. $T^2(r_y^2 - r_z^2)$ increases in the upward vertical direction and $(Tr_x)^2$ increases in the rightward horizontal direction. This motivates our choices for the angular and radial variables, which we can approximate using leading order terms.

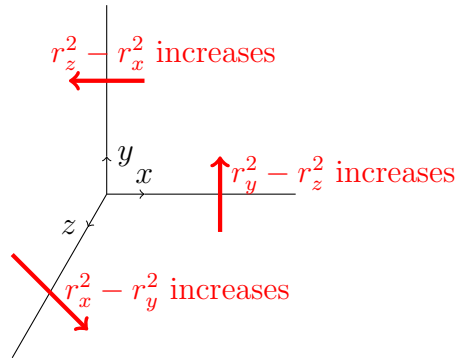


Figure 1.11: How the three angular directions vary

In region I, d should increase with x . In particular $d_I := \phi_x - \frac{1}{2}(\phi_y + \phi_z)$ will still be increasing with x because $r_x \gg r_y, r_z$ when Region I starts. (Since $v_0 = xyz$, if we fix a fiber then $|x|$ increasing means that $|yz|$ decreases accordingly.)

For the angle directions, note that in the expression $\phi_x := \log(1 + |Tx|^2)/(1 + |T^2yz|^2)$, the leading order term is $|Tx|^2$. Thus $\theta_I = \phi_y - \phi_z$ should be the angle coordinate as we saw above and we obtain:

$$F = g_{yz} + \alpha_3(d_I) \cdot d_I + \alpha_4(\theta_I) \cdot \alpha_5(d_I) \cdot \theta_I$$

We’ve now defined the Kähler potential in region I. This will define it in the corresponding regions of III and V, by symmetry in (x, y, z) . Then region II will interpolate between these.

ω extends over the central fiber and descends to Y

Because of the construction of ω , the form extends to one on the total space including the zero fiber. If we draw a disc around a vertex and consider all $|v_0|$ values over that disc, we get a patch in \mathbb{C}^3 with a Kähler form which approximates the standard symplectic form for r_x, r_y, r_z small, i.e. we've transplanted part of the (\mathbb{C}^3, xyz) model fibration, which we know is a smooth manifold and has a well-defined symplectic form. If we take a disc shape centered in the middle of the hexagon where only one Kähler potential is at play, and then consider all $|v_0|$ above that, we get the model toric Kähler form in the fiber, to which we will add a term from the base of the fibration v_0 , to get a product symplectic form.

In the regions interpolating between these two, we get a convex linear combination of two positive-definite Kähler potentials. In particular, we can pick ϵ sufficiently small that adding ϵ to either of these two metrics will not affect positive-definiteness. Then fix a value of l , for some $|v_0| = T^l$ so that all bump function derivatives described below are less than epsilon. Then we can let $|v_0| = T^{l'}$ tend to zero, and the bounds will still hold because if they hold for l they will only get smaller as $l' \rightarrow \infty$. In other words, once we have enough space for the bump function derivatives, we can define them to have the same support for all $v_0 \rightarrow 0$ fibers and be constant on the rest.

Furthermore, ω extends to all of \tilde{Y} in a Γ_B invariant manner (and also in a $\mathbb{Z}/6$ -invariant manner) – by using the group actions to define it in the other coordinate charts U_{n,g^k} introduced in Definition 1.4.16. Then these formulas match on the overlaps of the charts and give a well-defined 2-form on \tilde{Y} . Moreover it descends to a well-defined 2-form on the quotient Y as follows.

Claim 1.5.2. The form ω descends to a well-defined 2-form on the quotient $Y = \tilde{Y}/\Gamma_B$.

Proof. We saw above that the local model for ω is well-defined because all local definitions agree on the boundaries. This is noted at the end of Definition 1.5.1. Furthermore, when we glue coordinate charts U_{n,g^k} (see Definition 1.4.16) at each vertex of $\Delta_{\tilde{Y}}$ and in the center of the hexagon tiles, the formulas agree. E.g. in Lemma 1.4.9 we show g_{xy} is symmetric under the $\mathbb{Z}/6$ -action. Lastly, the definitions along the edges must be compatible. In other words, extending beyond regions I, III and V into the shaded black, red, and blue regions of Figure ?? after setting $\alpha_3 = \alpha_5 = 1$, we check that the transformation is consistent. By symmetry, it suffices to check along the r_z -axis. In the notation of Definition 1.4.16, this is a transformation between the main chart U_{0,g^0} with coordinates (x, y, z) and the chart $U_{(-1,0),g^{-1}}$ with coordinates $(x''', y''', z''') = (Tyz, Txz, T^{-2}z^{-1})$.

Let F denote the Kähler potential for the symplectic form in the unprimed coordinates and F''' that in the triple-primed coordinates. In the region we consider, F is given by the formula for region V after setting $\alpha_3 = \alpha_5 = 1$.

$$\begin{aligned}
F_V &= g_{xy} + d_V + \alpha_4(\theta_V) \cdot \theta_V \\
g_{xy} + d_V &= \log_T(1 + |Tx|^2)(1 + |Ty|^2)(1 + |T^2xy|^2) \cdot \left(\frac{1 + |Tz|^2}{1 + |T^2xy|^2} \cdot \sqrt{\frac{1 + |T^2xz|^2}{1 + |Ty|^2} \cdot \frac{1 + |T^2yz|^2}{1 + |Tx|^2}} \right) \\
&= \frac{1}{2} \log_T(1 + |Tx|^2)(1 + |Ty|^2)(1 + |T^2xz|^2)(1 + |T^2yz|^2) + \log_T(1 + |Tz|^2)
\end{aligned}$$

$$\begin{aligned}
\theta_V &= \phi_x - \phi_y \\
\therefore g_{xy}''' &= \left(\frac{1}{2} \log_T(1 + |T^2yz|^2)(1 + |T^2xz|^2)(1 + |Ty|^2)(1 + |Tx|^2) + \log_T(1 + |T^{-1}z^{-1}|^2) \right) \\
&\quad + \alpha_4(-\theta_V) \cdot (-\theta_V) \\
&= g_{xy} - \log_T(|Tz|^2)
\end{aligned}$$

where the last equality follows because in the first term, pulling back by the coordinate change between (x, y, z) and (x''', y''', z''') just amounts to permuting the factors, and in the second term we use that $\alpha_4(-\theta) = -\alpha_4(\theta)$. Also note that θ_V''' corresponds to $-\theta_V$ under the coordinate chart. Thus to go from one chart to the other we add $\log_T(|Tz|^2)$ which is harmonic because $\log(Tz)$ is holomorphic and its conjugate is antiholomorphic. \square

Lemma 1.5.3. *The definition of ω produces a well-defined symplectic form on Y .*

The full proof of this is in the next chapter, showing positive-definiteness.

Chapter 2

The symplectic form ω is nondegenerate

The goal of this chapter is to show:

Lemma 2.0.1. *The ω defined in Section 1.5 is non-degenerate on fibers of the Landau-Ginzburg model given by $v_0 : Y \rightarrow \mathbb{C}$.*

Corollary 2.0.2. *By adding a term from the base, this implies we obtain a non-degenerate form ω on Y .*

2.1 Putting bounds on the bump function derivatives

Claim 2.1.1 (Logarithmic derivatives facilitate finding estimates). Let α be any of $\alpha_3, \dots, \alpha_5$ and let μ be the appropriate d or θ variable. Then one can ensure that the logarithmic derivative $\alpha'^{\log} = \mu\alpha'(\mu)$ is bounded by a constant over $\log(T^l)$, and similarly for the second derivative. The argument for α_6 is different because its argument is already a function of \log of the norms of the complex coordinates, so we can control the regular derivative.

In particular, Log_T derivatives can be made small. This is the power of writing the Kähler potential in the form $\alpha(\mu) \cdot \mu$ for suitable α and μ . In this section we consider derivatives of the bump functions. So the first order derivatives will pick up terms of the form

$$\alpha'(\mu) \cdot \mu_* \cdot \mu = \mu_* d\alpha/d(\log_T \mu) \approx (\text{small}) \cdot \Delta\alpha/\Delta \log_T \mu$$

where μ_* is some derivative of μ with respect to one of the coordinates. Recall that μ will be approximated by a sum of squares of T times a norm. The norms are very small, on the order of T^l . However $\log_T T^l = l$ so that both the numerator and the denominator change by $O(1)$ terms, which is then multiplied by something that can be made very small. In particular, we divide by l which we can make as large as we like.

Remark 2.1.2 (Checking enough space to make derivatives small, see Figure 1.9). In region I, $d \approx T^2[r_x^2 - \frac{1}{2}(r_y^2 + r_z^2)] > 0$ because r_x is many orders of magnitude bigger than r_y and r_z get in that region. However, in the calculation for α_4 , we end up dividing by θ . So α_4 will need to be constant for a short while in the middle, so we don't divide by zero. This will be detailed below.

Also, there is enough space in θ_{II} and $\log d_{IIA}$ for α_6 and α_3, α_5 respectively. Recall

$$d_{IIA} \approx T^2[r_x^2 - \frac{1}{2}(r_y^2 + r_z^2) + \frac{3}{2}\alpha_6 \cdot r_y^2]$$

Since everywhere in region IIA we have $r_x \gg r_y$, the leading order term in d_{II} is $(Tr_x)^2$. Likewise since θ_{II} is linear in $\log_T r_y - \log_T r_x$, for it to stay constant we find that both $\log_T r_y$ and $\log_T r_x$ increase the same amount along contour lines. At P_1 and P_2 , $\theta_{II} \approx T^{3l/8-2l/p}$. At Q_1 and Q_2 , $\theta_{II} \approx T^{l/8-2l/p}$. Thus the change is $2l/8 = l/4$ and $\alpha_6' \approx \Delta\alpha_6/\Delta\theta_{II} \approx 4/l$. This can be made small.

Now we check d_{IIA} for α_3 and α_5 . At the smaller value we have $d_{IIA} \approx (Tr_x)^2$ at P_1 which has exponent $l/2$. At the larger value we get $l/2 - 2l/p$. So the change is $2l/p$ and the derivatives in α_3 and α_5 are approximately $p/2l$ times whatever the full range of α_i is. Again this can be made small.

Second-order derivatives also have enough space. In the bump functions $\alpha_3, \dots, \alpha_6$ the variable we're taking the derivative with respect to has space $k \cdot l$ for some $k > 0$ to move while each of the bump functions moves through an amount $1/3$ or 1 . By making l really big, we can ensure that while this is happening, the second derivative doesn't get too big. The graph of the bump functions won't be linear because they have to level off at the endpoints of their support. But with enough space, we can make sure they don't turn too quickly from horizontal to linear.

The argument that there is enough space in IIC follows from IIA by swapping r_x and r_y in the calculations. The only variable in region IIB is d_{IIB} and we take the two radial curves to be where d_{IIB} is constant, with the same amount of change in the variable as in d_{IIA} . Note that when $r_x \gg r_y$ we see that $d_{IIB} \approx T^2[r_x^2 + r_y^2 - \frac{1}{2}r_z^2] \approx (Tr_x)^2$. So initially, constant d_{IIB} is approximately the same thing as constant r_x . At some point we increase r_y enough to equal r_x . Likewise, coming from region IIC we have that constant d_{IIB} means, initially, approximately the same thing as constant r_y . So in the middle the curve interpolates between vertical (constant r_x) and horizontal (constant r_y). The derivatives for functions of d_{IIB} have enough space because d_{IIB} goes through the same amount as d_{IIA} and d_{IIC} .

Checking enough space for $\alpha_3'^{\log}$ and $\alpha_5'^{\log}$ sufficiently small. Since α_3 is a function of $T^2[d_I \approx r_x^2 - \frac{1}{2}(r_y^2 + r_z^2)] \approx (Tr_x)^2$ in region I, we need to see how $\log_T(Tr_x)^2$ changes. Recall that r_x changed by l/p_x orders of magnitude, so $\log_T(Tr_x)^2$ changes by approximately $2l/p_x$.

Thus the log derivative can be made as small as possible, as explained above.

For $\alpha_3''^{\log}$ we want to know the change in slope over $\log d$ time. The derivative goes from 0 to $\frac{1}{3l}$ in approximately $l \log$ time. Think of a bump function from $2/3$ to 1. Hence all terms involving a derivative of α_3 are bounded by a constant times T^2/l .

Checking enough space for log derivatives across axes. Recall Figure 1.9 and that from A to B r_y moves through l/p orders of T magnitude while from D to E it moves through $3l/2p$ which is a lot more for small T .

In the calculations above, we have cut out a region where $T < (r_y/r_z)^2 < T^{-1}$. In this region $\alpha_4 \equiv 0$. To do this, we need to make sure that we have at least one order of magnitude difference between r_y and r_z . This is fine in region I because we have r_y and r_z many orders of magnitude apart at B and C , with even more discrepancy as we move out to E and F . (Note however, the reverse would have happened in region II. In other words, r_z gets smaller as we move out, so r_x and r_y get bigger, and constant $r_y^2 - r_x^2$ means they will get closer and closer together as we move out.)

Checking $\alpha_4'^{\log}$, function of θ_I . This one is a function of $\theta_I \approx T^2[r_y^2 - r_z^2]$ or its negative. Furthermore, we're taking out a sliver around the axis where $T < (r_y/r_z)^2 < 1/T$. So we need to check there's enough space left. At the bottom where C and F are, $\theta_I \approx -r_z^2$ which is on the order of $-T^{2(3l/8-l/p_y)}$ as seen above. Then we stop when $r_z/r_y = 1/\sqrt{T}$. At this point r_z and r_y are basically equal, since they are only about one T -order of magnitude apart and both really small. At some fixed d_I , we have $r_x \approx T^{l/4-tl/p_x}$ where t is fixed at some number between 0 and 1. So $r_z = \sqrt{T^{-1}}r_y$ and:

$$r_x r_y r_z = T^l \implies T^{l/4-tl/p_x} \cdot r_y \cdot \sqrt{T^{-1}}r_y = T^l \implies r_y^2 = \sqrt{T} \cdot T^{3l/4+tl/p_x}$$

Hence

$$\begin{aligned} \theta_I \approx T^2[r_y^2 - r_z^2] &= T^2 r_y^2 \left(1 - \left(\frac{r_z}{r_y} \right)^2 \right) \approx T^2 \sqrt{T} \cdot T^{3l/4+tl/p_x} (1 - T^{-1}) \\ &\approx -T^{3l/4+tl/p_x+3/2} \cdot T \ll 1 \end{aligned}$$

We are checking how θ_I changes when we cut out this sliver to make sure α_4 has enough space for the log derivatives. We find θ_I decreases from order of magnitude $3l/4 - 2l/p_y$ to order of magnitude $3l/4 + tl/p_x + 3/2$. This means a net change of

$$(3l/4 - 2l/p_y) - (3l/4 + tl/p_x + 3/2) = -l \left(\frac{2}{p_y} + \frac{t}{p_x} \right) + 3/2$$

with a multiple of l , so we're still okay for the log derivative of α_4 because this is the denominator of the log derivative which can be made very large because of the l . Note that we only care about α_4 in region I since it's constant at $1/2$ when we exit the region and move into region II.

2.2 Converting to polar coordinates

To define the metric, we will convert to polar coordinates where it is easier. Locally the symplectic form is $\frac{i}{2\pi}\partial\bar{\partial}F$ where F is a function of $|x|$ and $|y|$. So we want to transform the derivatives in $\partial\bar{\partial}$ using the real transformation $(r_x, \theta_x) \leftrightarrow (x_1, x_2)$ where $x = x_1 + ix_2 = r_x e^{i\theta_x}$, and similarly for y . Recall $\partial_x = \frac{1}{2}(\partial_{x_1} - i\partial_{x_2})$. Hence $\partial_{x_i} = \partial_{x_i}(r_x)\partial_{r_x} + \partial_{x_i}(\theta_x)\partial_{\theta_x}$ implies that

$$\begin{aligned}\frac{\partial}{\partial x} &= \frac{1}{2} \left(\frac{\partial}{\partial x_1} - i \frac{\partial}{\partial x_2} \right) \\ &= \frac{1}{2} \left(\left[\frac{\partial r_x}{\partial x_1} - i \frac{\partial r_x}{\partial x_2} \right] \frac{\partial}{\partial r_x} + \left[\frac{\partial \theta_x}{\partial x_1} - i \frac{\partial \theta_x}{\partial x_2} \right] \frac{\partial}{\partial \theta_x} \right)\end{aligned}$$

We next re-express each real partial derivatives in terms of polar coordinates $r_x^2 = x_1^2 + x_2^2$ and $\theta_x = \tan^{-1}(x_2/x_1)$, and similarly for y . Recall that the derivative of $\arctan(t) = 1/(1+t^2)$.

$$\begin{aligned}\frac{\partial}{\partial x_1} &= \frac{\partial r_x}{\partial x_1} \frac{\partial}{\partial r_x} + \frac{\partial \theta_x}{\partial x_1} \frac{\partial}{\partial \theta_x} \\ r_x \frac{\partial r_x}{\partial x_i} &= x_i \implies \frac{\partial r_x}{\partial x_i} = \frac{x_i}{r_x} \\ \frac{\partial \theta_x}{\partial x_1} &= -\frac{x_2}{r_x^2}, \quad \frac{\partial \theta_x}{\partial x_2} = \frac{x_1}{r_x^2} \\ \implies \frac{\partial}{\partial x} &= \frac{1}{2} [e^{-i\theta_x} \partial_{r_x} - ie^{-i\theta_x}/r_x \partial_{\theta_x}] \\ \frac{\partial}{\partial \bar{x}} &= \frac{1}{2} [e^{i\theta_x} \partial_{r_x} + ie^{i\theta_x}/r_x \partial_{\theta_x}]\end{aligned}$$

Similarly for y . We also need to rewrite the differentials $dx = dx_1 + idx_2$ and $d\bar{x}$. Use

$$\begin{aligned}x_1 &= r_x \cos \theta_x \\ x_2 &= r_x \sin \theta_x \\ \therefore dx &= e^{i\theta_x} dr_x + ir_x e^{i\theta_x} d\theta_x \\ d\bar{x} &= e^{-i\theta_x} dr_x - ir_x e^{-i\theta_x} d\theta_x\end{aligned}$$

Now we can convert $\partial\bar{\partial}F$ into polar coordinates.

$$\begin{aligned}
i\partial\bar{\partial}F &= \sum_{i,j=1}^3 \frac{\partial^2 F}{\partial z_i \partial \bar{z}_j} dz_i \wedge d\bar{z}_j \\
&= i \sum_{i,j} \left(\frac{1}{2} e^{-i\theta_{z_i}} \left[\partial_{r_{z_i}} - i/r_{z_i} \partial_{\theta_{z_i}} \right] \right) \left(\frac{1}{2} e^{i\theta_{z_j}} \left[\partial_{r_{z_j}} + i/r_{z_j} \partial_{\theta_{z_j}} \right] \right) (F) (e^{i\theta_i} (dr_i + ir_i d\theta_i)) \\
&\quad \wedge (e^{-i\theta_j} (dr_j - ir_j d\theta_j)) \\
&= i \frac{1}{4} \sum_{i,j} e^{-i\theta_i} \left[e^{i\theta_j} \partial_{r_i r_j}^2 F - \frac{i}{r_i} \partial_{r_j} F \delta_{ij} e^{i\theta_j} \right] (e^{i\theta_i} (dr_i + ir_i d\theta_i)) \wedge (e^{-i\theta_j} (dr_j - ir_j d\theta_j)) \\
&= i \frac{1}{4} \left[\sum_i (\partial_{r_i}^2 F + \frac{1}{r_i} \partial_{r_i} F) (dr_i + ir_i d\theta_i) \wedge (dr_i - ir_i d\theta_i) \right] \\
&\quad + \frac{1}{4} \left[\sum_{i \neq j} (\partial_{r_i r_j}^2 F) (dr_i + ir_i d\theta_i) \wedge (dr_j - ir_j d\theta_j) \right]
\end{aligned}$$

In order for this to arise from a metric, we need compatibility with J_0 where J_0 is induced from multiplication by i on the complex coordinates (x, y, z) in the toric chart where they are defined. But ω is compatible with J because it comes from a Kähler potential. J is multiplication by i , which commutes with $\partial\bar{\partial}$.

Next we need positive-definiteness, namely $\omega(v, Jv) > 0$ for all $v \neq 0$.

$$\begin{aligned}
\partial_{r_1} &= \frac{\partial x_1}{\partial r_1} \partial_{x_1} + \frac{\partial x_2}{\partial r_1} \partial_{x_2} \\
&= \cos \theta_1 \partial_{x_1} + \sin \theta_1 \partial_{x_2} \\
\partial_{\theta_1} &= -r_1 \sin \theta_1 \partial_{x_1} + r_1 \cos \theta_1 \partial_{x_2} \\
J(\partial_{x_1}) &= \partial_{x_2}, \quad J(\partial_{x_2}) = -\partial_{x_1} \\
\implies J(\partial_{r_1}) &= \frac{1}{r_1} \partial_{\theta_1} \\
J(\partial_{\theta_1}) &= -r_1 \partial_{r_1}
\end{aligned}$$

We want $g(u, v) := \omega(u, Jv)$ to be a metric, so positive definite. In the 3d case, this gives a 6 by 6 matrix which we want to be positive definite. It'll be block diagonal with the r block and the θ block. The entries along the diagonal in the r block will be

$$g_{ii} = \omega(\partial_{r_i}, J\partial_{r_i}) = \omega(\partial_{r_i}, \frac{1}{r_i} \partial_{\theta_i}) = \frac{1}{r_i} \omega(\partial_{r_i}, \partial_{\theta_i}) = \frac{1}{2} (\partial_{r_i}^2 F + \frac{1}{r_i} \partial_{r_i} F)$$

which will pick up the $dr_i \wedge d\theta_i$ term, which looking back at $\partial\bar{\partial}F$ above is $\frac{2}{4}r_i dr_i \wedge d\theta_i$ times the F derivative term. Similarly

$$\begin{aligned} g_{ij} &= \omega(\partial_{r_i}, J\partial_{r_j}) = \frac{1}{r_j} \omega(\partial_{r_i}, \partial_{\theta_j}) \\ &= \frac{1}{2} (\partial_{r_i r_j}^2 F) \end{aligned}$$

2.3 Showing ω nondegenerate: \mathbb{C}^3 patch

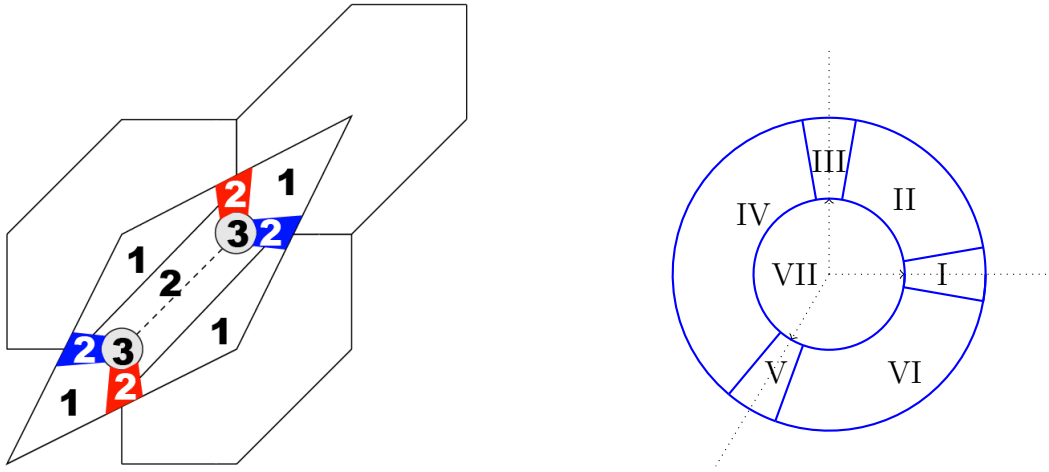


Figure 2.1: L) Number of potentials interpolated between. R) Zoomed in region about vertex.

Leading order Region I terms

First we look at the terms with no derivatives of the bump functions. This should give us a positive definite matrix so we get a metric. Then it will be enough to show that all the remaining terms can be expressed in terms of (log-derivatives of the bump functions) \cdot (bounded terms), which can be made as small as we like by making l as large as we like. First, recall that this is the metric in polar coordinates:

$$\begin{pmatrix} \partial_{r_x}^2 F + \frac{1}{r_x} \partial_{r_x} F & \partial_{r_x r_y}^2 F & \partial_{r_x r_z}^2 F \\ \partial_{r_x r_y}^2 F & \partial_{r_y}^2 F + \frac{1}{r_y} \partial_{r_y} F & \partial_{r_y r_z}^2 F \\ \partial_{r_x r_z}^2 F & \partial_{r_y r_z}^2 F & \partial_{r_z}^2 F + \frac{1}{r_z} \partial_{r_z} F \end{pmatrix}$$

$$\begin{aligned}
F &= f + \alpha_3 d + \alpha_4 \cdot \alpha_5 \theta \\
d &\approx T^2 [r_x^2 - \frac{1}{2} (r_y^2 + r_z^2)] \\
\theta &\approx T^2 [r_y^2 - r_z^2] \\
f &\approx T^2 [r_y^2 + r_z^2]
\end{aligned}$$

Note that because everywhere r_x appears is as r_x^2 , applying $\partial_{r_x r_x}^2$ is the same as applying ∂_{r_x}/r_x . Here are the terms that do not involve derivatives of the α_i , where for ease of notation subscript x means ∂_{r_x} :

$$\begin{aligned}
&\begin{pmatrix} 2(f_{xx} + \alpha_3 d_{xx} + \alpha_4 \alpha_5 \theta_{xx}) & f_{xy} + \alpha_3 d_{xy} + \alpha_4 \alpha_5 \theta_{xy} & f_{xz} + \alpha_3 d_{xz} + \alpha_4 \alpha_5 \theta_{xz} \\ & \text{“} & \text{“} \\ & 2(f_{yy} + \alpha_3 d_{yy} + \alpha_4 \alpha_5 \theta_{yy}) & f_{yz} + \alpha_3 d_{yz} + \alpha_4 \alpha_5 \theta_{yz} \\ & \text{“} & \text{“} \\ & & 2(f_{zz} + \alpha_3 d_{zz} + \alpha_4 \alpha_5 \theta_{zz}) \end{pmatrix} \\
&\approx T^2 \begin{pmatrix} 4\alpha_3 & 0 & 0 \\ 0 & 4 - 2\alpha_3 + 4\alpha_4 \alpha_5 & 0 \\ 0 & 0 & 4 - 2\alpha_3 - 4\alpha_4 \alpha_5 \end{pmatrix}
\end{aligned}$$

Derivatives of the higher order terms in the expansions above will have variables Tr_* so will be negligible. This is bounded below assuming we restrict the region a little, each entry is bounded below. One of the coordinates does go to zero as the bump functions reach their bounds. However, the one that goes to zero in the xy -plane is the z term and similarly in the xz -plane it's the y term. Since we add a term $|xyz|^2$ for the base, this will ensure positive definiteness away from the zero fiber.

Terms with derivatives of bump functions in Region I

The terms that produce derivatives of the bump functions are $\alpha_3(d_I)d_I$ and $\alpha_4(\theta_I)\alpha_5(d_I)\theta_I$. Note that d in region I close to where $r_x = r_y = r_z$ is approximately linear in $(Tr_x)^2$, $(Tr_y)^2$, and $(Tr_z)^2$.

Some notation: Let $d \equiv d_I$ in this section. We want to allow the variable we're taking the derivative with respect to to vary among $\{r_x, r_y, r_z\}$. So we denote those variables to be $\{r_\star, r_\bullet\} \in \{r_x, r_y, r_z\}$. Furthermore, $'\log$ means we take the log derivative $d\alpha_3/d(\log(d_I)) = \alpha_3' \cdot d$. The following calculation for the second derivative applies to α_5 as well, and α_4 if we

replace d with θ .

$$\begin{aligned} \frac{d^2 \alpha_3}{d(\log d)} &= (\alpha'_3 \cdot d)' \cdot d = (\alpha''_3 \cdot d + \alpha'_3) d \\ \implies \alpha''_3 \cdot d + \alpha'_3 &= \frac{1}{d} \cdot \frac{d^2 \alpha_3}{d(\log d)^2} \\ \implies \alpha''_3 &= \frac{1}{d^2} \cdot \left(\frac{d^2 \alpha_3}{d(\log d)^2} - \frac{d \alpha_3}{d(\log d)} \right) \end{aligned}$$

Derivatives of $\alpha_3 d$

First order derivative $\frac{1}{r_*} \partial_{r_*} (\alpha_3 d)$: the term $\alpha'_3 d = \alpha_3'^{\log}$ is a log derivative so can be made arbitrarily small.

Second order derivatives:

A second order derivative of $\alpha_3 d$ involves a first order derivative of $r_* \alpha'_3 d$, which involves terms like $\alpha'_3 d$ from before, as well as $r_* (\partial_{\bullet} d) (\alpha''_3 d + \alpha'_3)$ up to powers of T i.e. proportional to $T^2 r_* r_{\bullet} (\alpha''_3 d + \alpha'_3)$ because d is approximately linear in $(Tr_x)^2, (Tr_y)^2, (Tr_z)^2$. Thus we get

$$T^2 \frac{r_* r_{\bullet}}{d} \alpha_3''^{\log}$$

If we divide numerator and denominator by r_x^2 we get $\frac{(r_* r_{\bullet}) / (r_x)^2}{1 - \frac{1}{2}((r_y/r_x)^2 + (r_z/r_x)^2)}$ which is close to 1 on the bottom, and small or 1 on the top, because $r_x \gg r_y, r_z$. So we get something bounded times something small. Thus all derivatives involving α_3 lead to small terms for a fixed sufficiently large l . Here are the calculations.

Diagonal terms for $\alpha_3(d) \cdot d$:

$$\begin{aligned} d &\approx T^2 [r_x^2 - \frac{1}{2} (r_y^2 + r_z^2)] \\ d_{r_*} &\approx \lambda T^2 r_*, \quad d_{r_* r_*} \approx \lambda T^2, \quad \lambda \in \{2, -1\} \\ \left(\frac{1}{r_*} \partial_{r_*} + \partial_{r_* r_*}^2 \right) (\alpha_3(d) \cdot d) &= \frac{1}{r_*} (\alpha'_3 d_{r_*} d + \alpha_3(d) \cdot d_{r_*}) \\ &\quad + (\alpha''_3 d_{r_*}^2 d + \alpha'_3 d_{r_* r_*} d + 2\alpha'_3(d) d_{r_*}^2 + \alpha_3(d) \cdot d_{r_* r_*}) \\ &\approx \frac{1}{r_*} (\alpha'_3 \lambda T^2 r_* d + \alpha_3(d) \cdot \lambda T^2 r_*) \\ &\quad + (\alpha''_3 (\lambda T^2 r_*)^2 d + \alpha'_3 \lambda T^2 d + 2\alpha'_3(d) (\lambda T^2 r_*)^2 + \alpha_3(d) \cdot \lambda T^2) \\ &= \lambda T^2 [\alpha'_3 d + \alpha_3 + \lambda T^2 \alpha''_3 r_*^2 \cdot d + \alpha'_3 d + 2\lambda T^2 \alpha'_3 r_*^2 + \alpha_3(d)] \\ &= 2\lambda T^2 [\alpha'_3 (d + (\lambda - 1) T^2 r_*^2) + T^2 r_*^2 (\alpha''_3 d + \alpha'_3)] + 2\lambda T^2 \alpha_3 \\ &= 2\lambda T^2 [\alpha_3'^{\log} (1 + \frac{(\lambda - 1) T^2 r_*^2}{d}) + \frac{T^2 r_*^2}{d} \alpha_3''^{\log}] + 2\lambda T^2 \alpha_3 \end{aligned}$$

$$\alpha_3^{\prime \log} \approx \frac{\Delta \alpha_3}{\Delta \log d} \approx \propto \frac{1}{l}$$

$$\frac{T^2 r_*^2}{d} \approx \frac{T^2 r_*^2}{T^2 [r_x^2 - \frac{1}{2}(r_y^2 + r_z^2)]} = \frac{r_*^2}{r_x^2 - \frac{1}{2}(r_y^2 + r_z^2)} = \frac{r_*^2/r_x^2}{1 - \frac{1}{2}(\frac{r_y^2}{r_x^2} + \frac{r_z^2}{r_x^2})} \approx 1 \text{ or } 0 \because r_x \gg r_y, r_z$$

$$\alpha_3^{\prime \prime \log} \approx \propto \frac{1}{l^2}$$

Off-diagonal terms for $\alpha_3(d) \cdot d$ where $* \neq \star$:

$$\begin{aligned} d_{r_* r_*} &= 0 \\ \partial_{r_* r_*}^2 (\alpha_3 \cdot d) &= \partial_{r_*} (\alpha_3' d_{r_*} d + \alpha_3(d) \cdot d_{r_*}) \\ &= \alpha_3'' d_{r_*} d_{r_*} d + \alpha_3' d_{r_* r_*} d + 2\alpha_3' d_{r_*} d_{r_*} + \alpha_3 \cdot d_{r_* r_*} \\ &= T^4 \lambda \mu r_* r_* \alpha_3'' d + 0 + 2T^4 \lambda \mu r_* r_* \alpha_3' + 0, \quad \lambda, \mu \in \{2, -1\} \\ &= T^4 \lambda \mu \frac{r_* r_*}{d} d (\alpha_3'' d + \alpha_3' + \alpha_3') \\ &= T^4 \lambda \mu \frac{r_* r_*}{d} (\alpha_3^{\prime \prime \log} + \alpha_3^{\prime \log}) \\ \frac{T^2 r_* r_*}{d} &\approx \frac{r_* r_* / r_x^2}{1 - \frac{1}{2}((r_y/r_x)^2 + (r_z/r_x)^2)} \approx 0 \text{ or } 1 \end{aligned}$$

Again we see that all the derivatives of the bump functions are log derivatives and all the terms are bounded by a constant times T^2/l .

Derivatives of $\alpha_4 \alpha_5 \theta$

For $\alpha_4 \alpha_5 \theta$, the first order derivative terms (dividing by whatever variable we take the derivative with respect to) involve $\alpha_5(\alpha_4' \theta)$, which is an $O(1)$ term (recall α_5 goes from 0 to 1) times a log derivative, as well as $\alpha_4(\alpha_5' \theta) = \alpha_4(\alpha_5^{\prime \log} \cdot \frac{\theta}{d})$ because α_5 is a function of d . So we need to check that θ/d is bounded, independent of l . Dividing by r_x^2 gets a small expression on top and close to 1 on the bottom. So these are both okay.

From first derivatives we have $r_* \alpha_5(\alpha_4' \theta)$ and $r_* \alpha_4(\alpha_5' \theta)$. Differentiating the r_* with respect to r_\bullet gives terms we already know are small from the previous paragraph, or zero if $\bullet \neq \star$. So we put it out front and differentiate the remaining expression. Keep in mind α_4 is a function of θ and α_5 is a function of d .

- $r_* r_\bullet \alpha_4' \alpha_5' \theta = \frac{r_* r_\bullet}{d} \alpha_4^{\prime \log} \alpha_5^{\prime \log}$

We multiplied and divided by a d to get the α_5 log derivative.

- $r_* r_\bullet \alpha_5 (\alpha_4'' \theta + \alpha_4') = \alpha_5 \cdot \frac{r_* r_\bullet}{\theta} \alpha_4^{\prime \prime \log}$

The r_\bullet comes from $\partial_\bullet \theta$. In particular, if $r_\bullet = r_x$ then we get zero because $\theta \approx T^2 [r_y^2 - r_z^2]$ which means that $\theta_{r_x} \approx 0$.

- $r_\star r_\bullet \alpha_4(\alpha_5'' \theta) = \alpha_4 \cdot \frac{r_\star r_\bullet}{d} (\alpha_5''^{\log} - \alpha_5'^{\log}) \cdot \frac{\theta}{d}$
- $r_\star r_\bullet \alpha_4(\alpha_5') = \frac{r_\star r_\bullet}{d} \cdot \alpha_4 \alpha_5'^{\log}$

We've already seen above that $T^2 \frac{r_\star r_\bullet}{d}$ and hence $\frac{\theta}{d}$ are bounded. So it remains to check that $T^2 \frac{r_\star r_\bullet}{\theta}$ is bounded. Also, we only need to consider the cases where the numerator does not involve r_x by the comment above that we get zero otherwise and that second-order partial derivatives are symmetric. So we have to bound the following expressions:

$$\frac{r_y^2}{r_y^2 - r_z^2}, \frac{r_z^2}{r_y^2 - r_z^2}, \frac{r_y r_z}{r_y^2 - r_z^2}$$

We are considering the top half of region I, where $r_y > r_z$. We declare that α_4 is constant in the region $1 < \left(\frac{r_y}{r_z}\right)^2 < \frac{1}{T}$. So the support of α_4 is where $\left(\frac{r_y}{r_z}\right)^2 > \frac{1}{T}$. In particular, we see that

$$\frac{1}{\left(\frac{r_y}{r_z}\right)^2 - 1} < \frac{1}{T^{-1} - 1} = \frac{T}{1 - T} \approx T$$

So these terms are bounded, which can be seen dividing top and bottom by r_z^2 . Here is the explicit calculation.

Diagonal terms $\frac{1}{r_\bullet} \partial_{r_\bullet} + \partial_{r_\bullet}^2$ and off-diagonal terms $\partial_{r_\bullet r_\star}^2$.

$$\begin{aligned} \theta &\approx T^2(r_y^2 - r_z^2) \\ d &\approx T^2(r_x^2 - \frac{1}{2}(r_y^2 + r_z^2)) \\ \theta_{r_\bullet} &\approx \lambda_\bullet T^2 r_\bullet, \quad \lambda_\bullet \in \{0, \pm 2\} \\ d_{r_\bullet} &\approx \mu_\bullet T^2 r_\bullet, \quad \mu_\bullet \in \{2, -1\} \\ \frac{1}{r_\bullet} \partial_{r_\bullet}(\alpha_4 \alpha_5 \theta) &= \frac{1}{r_\bullet} (\alpha_4' \theta_{r_\bullet} \alpha_5 \theta + \alpha_4 \alpha_5' d_{r_\bullet} \theta + \alpha_4 \alpha_5 \theta_{r_\bullet}) \\ &= T^2 (\lambda_\bullet \alpha_4'^{\log} \alpha_5 + \mu_\bullet \alpha_4 \alpha_5'^{\log} \frac{\theta}{d} + \lambda_\bullet \alpha_4 \alpha_5) \end{aligned}$$

$$\begin{aligned}
\partial_{r_* r_\bullet}^2(\alpha_4 \alpha_5 \theta) &= T^2 \partial_{r_*} [r_\bullet \lambda_\bullet \alpha_4' \theta \alpha_5 + r_\bullet \mu_\bullet \alpha_4 \alpha_5' \theta + r_\bullet \lambda_\bullet \alpha_4 \alpha_5] \\
&= T^2 [\partial_{r_*} r_\bullet \lambda_\bullet \alpha_4' \theta \alpha_5 + T^2 r_\bullet \lambda_\bullet \alpha_4'' \theta_{r_*} \alpha_5 + T^2 r_\bullet \lambda_\bullet \alpha_4' \theta_{r_*} \alpha_5 + T^2 r_\bullet \lambda_\bullet \alpha_4' \theta \alpha_5' d_{r_*} \\
&\quad + \partial_{r_*} (r_\bullet) \alpha_4 \alpha_5' \theta + T^2 r_\bullet \mu_\bullet \alpha_4' \theta_{r_*} \alpha_5' \theta + T^2 r_\bullet \mu_\bullet \alpha_4 \alpha_5'' d_{r_*} \theta + T^2 r_\bullet \mu_\bullet \alpha_4 \alpha_5' \theta_{r_*} \\
&\quad + \partial_{r_*} (r_\bullet) \lambda_\bullet \alpha_4 \alpha_5 + T^2 r_\bullet \lambda_\bullet \alpha_4' \theta_{r_*} \alpha_5 + T^2 r_\bullet \lambda_\bullet \alpha_4 \alpha_5' d_{r_*}] \\
&= T^2 [\delta_{\bullet*} \lambda_\bullet \alpha_4'^{\log} \alpha_5 + T^2 [\lambda_\bullet \lambda_* \frac{r_\bullet r_*}{\theta} (\alpha_4''^{\log} - \alpha_4'^{\log}) \alpha_5 + \lambda_\bullet \lambda_* \frac{r_\bullet r_*}{\theta} \alpha_4'^{\log} \alpha_5 + \lambda_\bullet \mu_* \frac{r_\bullet r_*}{d} \alpha_4'^{\log} \alpha_5'^{\log}] \\
&\quad + \delta_{\bullet*} \frac{\theta}{d} \alpha_4 \alpha_5'^{\log} + \mu_\bullet \lambda_* \frac{T^2 r_\bullet r_*}{d} \alpha_4'^{\log} \alpha_5'^{\log} + \frac{T^2 r_\bullet r_* \theta}{d^2} \alpha_4 (\alpha_5''^{\log} - \alpha_5'^{\log}) + \mu_\bullet \lambda_* \frac{T^2 r_\bullet r_*}{d} \alpha_5'^{\log} \\
&\quad + \delta_{\bullet*} \lambda_\bullet \alpha_4 \alpha_5 + \lambda_\bullet \lambda_* \frac{T^2 r_\bullet r_*}{\theta} \alpha_4'^{\log} \alpha_5 + \lambda_\bullet \mu_* \frac{T^2 r_\bullet r_*}{d} \alpha_4 \alpha_5'^{\log}]
\end{aligned}$$

We see $\frac{T^2 r_\bullet r_*}{\theta}$, $\frac{T^2 r_\bullet r_*}{d}$, $\frac{\theta}{d}$ are bounded as above and the derivatives are log derivatives.

Setting up region III and V to match Region I

In region I, r_x was the dominating coordinate. In region III, r_y will dominate and in region V, r_z will dominate. So we take the analogous data for half regions of III and V, by modeling I.

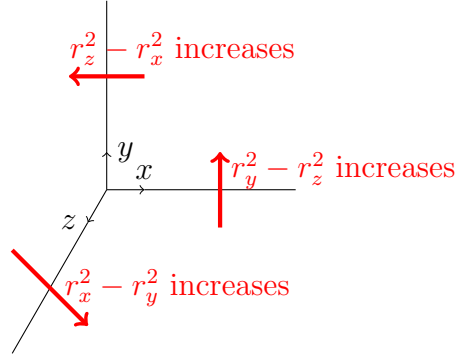


Figure 2.2: The three angular directions

$$\begin{aligned}
g_{yz} &= g_{yz} + \alpha_3(d_I) \cdot d_I + \alpha_4(\theta_I) \alpha_5(d_I) \cdot \theta_I \\
g_{yz} &\approx T^2 [r_y^2 + r_z^2] \\
\theta_I &\approx T^2 [r_y^2 - r_z^2] \\
d_I &\approx T^2 [r_x^2 - \frac{1}{2}(r_y^2 + r_z^2)]
\end{aligned}$$

$$\begin{aligned}
g_{xy} &= g_{xy} + \alpha_3(d_{III}) \cdot d_{III} + \alpha_4(\theta_{III})\alpha_5(d_{III}) \cdot \theta_{III} \\
g_{xy} &\approx T^2[r_x^2 + r_z^2] \\
\theta_{III} &\approx T^2[r_z^2 - r_x^2] \\
d_{III} &\approx T^2[r_y^2 - \frac{1}{2}(r_x^2 + r_z^2)]
\end{aligned}$$

$$\begin{aligned}
F_V &= f_V + \alpha_3(d_V) \cdot d_V + \alpha_4(\theta_V)\alpha_5(d_V) \cdot \theta_V \\
f_V &\approx T^2[r_x^2 + r_y^2] \\
\theta_V &\approx T^2[r_x^2 - r_y^2] \\
d_V &\approx T^2[r_z^2 - \frac{1}{2}(r_x^2 + r_y^2)]
\end{aligned}$$

Given that we know we start out with $\alpha_1 g_{xy} + \alpha_2 g_{xz} + (1 - \alpha_1 - \alpha_2) g_{yz}$ and we know we want to end up with the above expressions in *III* and *V*, this will determine what α_3 and $\alpha_4 \cdot \alpha_5$ are in those regions because the angular and radial directions are determined as above by symmetry.

In region *III*: we want

$$\begin{aligned}
F &= g_{xy} + \alpha_3(d_{III}) \cdot d_{III} + \alpha_4(\theta_{III})\alpha_5(d_{III}) \cdot \theta_{III} \\
&= g_{xz} + \alpha_3 \left(\frac{1}{2}(g_{yz} - g_{xz}) + \frac{1}{2}(g_{xy} - g_{xz}) \right) + \alpha_4\alpha_5(g_{yz} - g_{xy}) \\
&= g_{xz}(1 - \alpha_3) + g_{xy} \left(\frac{\alpha_3}{2} - \alpha_4\alpha_5 \right) + g_{yz} \left(\frac{\alpha_3}{2} + \alpha_4\alpha_5 \right) \\
&= \alpha_1 g_{xy} + \alpha_2 g_{xz} + (1 - \alpha_1 - \alpha_2) g_{yz} \\
\implies \alpha_3 &= 1 - \alpha_2, \quad \alpha_4 \cdot \alpha_5 = \frac{1}{2} - \frac{\alpha_2}{2} - \alpha_1
\end{aligned}$$

In region *V*: we want

$$\begin{aligned}
F &= f_V + \alpha_3(d_V) \cdot d_V + \alpha_4(\theta_V)\alpha_5(d_V) \cdot \theta_V \\
&= g_{xy} + \alpha_3 \left(\frac{1}{2}(g_{xz} - g_{xy}) + \frac{1}{2}(g_{yz} - g_{xy}) \right) + \alpha_4\alpha_5(g_{xz} - g_{yz}) \\
&= g_{xy}(1 - \alpha_3) + g_{xz} \left(\frac{\alpha_3}{2} + \alpha_4\alpha_5 \right) + g_{yz} \left(\frac{\alpha_3}{2} - \alpha_4\alpha_5 \right) \\
&= \alpha_1 g_{xy} + \alpha_2 g_{xz} + (1 - \alpha_1 - \alpha_2) g_{yz} \\
\implies \alpha_3 &= 1 - \alpha_1, \quad \alpha_4 \cdot \alpha_5 = \alpha_2 - \frac{1}{2} + \frac{\alpha_1}{2}
\end{aligned}$$

Again in both cases, α_3 goes from $2/3$ to 1 and α_4 goes from $-1/2$ to $1/2$ while α_5 scales it by going from 0 to 1 . All the calculations carry through as before with $f + \alpha_3 d + \alpha_4 \alpha_5 \theta$ since we've set up everything to be symmetric in (r_x, r_y, r_z) . The issue now is that $\alpha_{\geq 3}$ are functions of d and θ , and these two variables have different definitions in each of the three regions. So we will patch together the d coordinate across regions II, IV and VI.

The reason we only care about patching together the d is because at the boundaries of the odd-numbered regions, α_4 has leveled out to either $1/2$ or $-1/2$, and α_3, α_5 only depend on d . So we take another bump function α_6 , going from 0 to 1 , that allows us to interpolate between the two definitions of d by adding increasing amounts of the θ -coordinate in the even-numbered regions. So just to recap in II, IV, VI: α_3 and α_5 are functions of d , which in turn is a function of $\alpha_6(\theta_{\text{even}}) \cdot \theta_{\text{even}}$. So we're going to need to apply two levels in the chain rule when taking derivatives with respect to r_x, r_y, r_z .

Leading order Region IIA terms

First we get the terms not involving derivatives of the bump functions. These will form the nondegenerate part of the metric on region II and we will show the rest of the terms can be made sufficiently small. Since everything not a bump function is approximately linear in $(Tr_x)^2, (Tr_y)^2$ and $(Tr_z)^2$, we again have that $\frac{1}{r_x} \partial_{r_x} = \partial_{r_x r_x}^2$. Recall $2/3 \leq \alpha_3 \leq 1$ and $0 \leq \alpha_5, \alpha_6 \leq 1$. Fix ϕ terms in first line.

$$F \approx T^2[(r_y^2 + r_z^2 - \alpha_6(\theta_{II}) \cdot r_y^2) + \alpha_3(d_{IIA}) \cdot (r_x^2 - \frac{1}{2}(r_y^2 + r_z^2) + \frac{3}{2}\alpha_6(\theta_{II}) \cdot r_y^2) + \frac{1}{2}\alpha_5(d_{IIA}) \cdot (r_y^2 - r_z^2 - \alpha_6(\theta_{II}) \cdot r_y^2)]$$

Off-diagonal terms $\partial_{r_\bullet r_\star}^2$ for $\star \neq \bullet$ are zero because derivatives of non-bump functions means differentiating r_\star^2 for some \star . Diagonal terms we get $\frac{1}{r_\star} \partial_{r_\star} + \partial_{r_\star r_\star}^2 = 2\partial_{r_\star r_\star}^2$ which, applied to $(Tr_\star)^2$ is $2T^2$. So in the (\star, \star) entry of the matrix, the leading terms are $4T^2$ times the coefficients on r_\star^2 . Need to fix y one.

$$\begin{aligned} x : T^2(4\alpha_3) &\geq T^2 8/3 \\ y : T^2(4 - 4\alpha_6 - 2\alpha_3 + 6\alpha_3\alpha_6 + 2\alpha_5 - 2\alpha_5\alpha_6) &= T^2[4 + (2 - 2\alpha_6)(\alpha_5 - \alpha_3) + 4\alpha_6(\alpha_3 - 1)] \\ &\geq T^2[4 + 2(0 - 2/3) + 4(-1/3)] = T^2 \cdot \frac{4}{3} \\ z : T^2(4 - 2\alpha_3 - 2\alpha_5) \end{aligned}$$

Note that when $\alpha_3 = \alpha_5 = 1$ the z term goes to zero. However, it is bounded below in a region where α_3, α_5 are bounded away from 1 . In the region where it goes to 1 , we add a term to F from the base, i.e. $|xyz|^2$, to maintain nondegeneracy. Because xyz is bounded below in the region where we add it, we can take the partial derivatives and get something positive definite.

Terms with derivatives of bump functions in Region IIA

Now we show that the bump function derivative terms can be made small. For reference:

$$\begin{aligned}
F &\approx (g_{yz} - \alpha_6 \cdot (Tr_y)^2) + \alpha_3(d_{IIA})d_{IIA} + \frac{1}{2}\alpha_5(d_{IIA}) \cdot ((Tr_y)^2 - (Tr_z)^2 - \alpha_6(Tr_y)^2) \\
g_{yz} &\approx T^2[r_y^2 + r_z^2] \\
d_I &\approx T^2[r_x^2 - \frac{1}{2}(r_y^2 + r_z^2)] \\
d_{IIA} &\approx T^2[r_x^2 - \frac{1}{2}(r_y^2 + r_z^2)] + \frac{3}{2}\alpha_6(\log r_y - \log r_x) \cdot (Tr_y)^2 \\
\theta_I &\approx T^2[r_y^2 - r_z^2] \\
\theta_{II} &= \log(r_y/r_x)
\end{aligned}$$

Bump function terms in F are: $\alpha_6 \cdot (Tr_y)^2$, $\alpha_3 \cdot d_{IIA}$, $\{\alpha_5(Tr_*)^2\}_{*=y,z}$, $\alpha_5\alpha_6 \cdot (Tr_y)^2$

$$\text{1st term: } \alpha_6(\log(r_y/r_x)) \cdot (Tr_y)^2$$

First derivative divided by r_* :

$$\begin{aligned}
\frac{1}{r_x} \partial_{r_x} [\alpha_6(\log r_y - \log r_x)(Tr_y)^2] &= -\frac{1}{r_x^2} \alpha'_6 \cdot (Tr_y)^2 = -T^2 \cdot \frac{r_y^2}{r_x^2} \alpha'_6, \quad \left| \frac{r_y^2}{r_x^2} \right| < 1 \\
\frac{1}{r_y} \partial_{r_y} [\alpha_6(\log r_y - \log r_x)(Tr_y)^2] &= \frac{1}{r_y^2} \alpha'_6 \cdot (Tr_y)^2 + \alpha_6 \cdot (2T^2 r_y) = T^2 \alpha'_6 + 2T^2 \alpha_6 r_y \\
\frac{1}{r_z} \partial_{r_z} [\alpha_6(\log r_y - \log r_x)(Tr_y)^2] &= 0 \\
\alpha'_6 &\approx \propto \frac{1}{l}
\end{aligned}$$

So all bump function derivative terms from first order derivatives of this term can be made small.

Second derivative $\partial_{* \bullet}^2$:

$$\begin{aligned}
\partial_{r_x r_x}^2 (\alpha_6 (Tr_y)^2) &= \partial_{r_x} \left(-\frac{(Tr_y)^2}{r_x} \alpha'_6 \right) = \frac{(Tr_y)^2}{r_x^2} (\alpha'_6 + \alpha''_6) < T^2 (\alpha'_6 + \alpha''_6) \approx \propto T^2 \left(\frac{1}{l} + \frac{1}{l^2} \right), \quad \text{small} \\
\partial_{r_x r_y}^2 (\alpha_6 (Tr_y)^2) &= \partial_{r_y} \left(-\frac{(Tr_y)^2}{r_x} \alpha'_6 \right) = \frac{-T^2 r_y}{r_x} (2\alpha'_6 + \alpha''_6), \quad \text{norm} < T^2 (2\alpha'_6 + \alpha''_6) \\
\partial_{r_y r_y}^2 (\alpha_6 (Tr_y)^2) &= \partial_{r_y} (T^2 \alpha'_6 r_y + 2T^2 \alpha_6 r_y^2) = T^2 (\alpha'_6 + \alpha''_6 + 2\alpha'_6 r_y + 4\alpha_6 r_y) < T^2 (3\alpha'_6 + \alpha''_6 + 4\alpha_6 r_y)
\end{aligned}$$

because r_y is small in region II. Note the first derivative α'_6 goes from 0 to a maximum of $1/l + \epsilon$ at the half way point of $l/2$ so the change in slope is roughly like $1/l^2$, still small. (Really $(1/l + \epsilon)(2/l)$.) So everything is ok with the term $\alpha_6 r_y^2$.

$$\text{2nd term: } \alpha_3(d_{IIA})d_{IIA}$$

First derivative. $\frac{1}{r_\star} \partial_{r_\star} (\alpha_3 d_{IIA}) = (\alpha'_3 d_{IIA} + \alpha_3) \cdot \frac{d_{IIA\star}}{r_\star}$.

Here are the partial derivatives of d_{IIA} .

$$\begin{aligned} d_{IIA} &\approx T^2 \left[r_x^2 - \frac{1}{2}(r_y^2 + r_z^2) \right] + \frac{3}{2} \alpha_6 (\log r_y - \log r_x) \cdot (Tr_y)^2 \\ \frac{(d_{IIA})_x}{r_x} &= \frac{T^2}{r_x} \left[2r_x + \frac{3}{2} \left(\alpha'_6 \cdot \frac{-1}{r_x} \cdot r_y^2 \right) \right] = T^2 \left[2 + \frac{3}{2} \left(\alpha'_6 \cdot \frac{-r_y^2}{r_x^2} \right) \right] \\ \frac{(d_{IIA})_y}{r_y} &= \frac{T^2}{r_y} \left[-r_y + \frac{3}{2} \left(\alpha'_6 \cdot \frac{1}{r_y} \cdot r_y^2 + 2r_y \alpha_6 \right) \right] = T^2 \left[-1 + \frac{3}{2} (\alpha'_6 + 2\alpha_6) \right] \\ \frac{(d_{IIA})_z}{r_z} &= \frac{T^2}{r_z} [-r_z] = -T^2 \end{aligned}$$

Hence the terms in $\frac{1}{r_\star} \partial_{r_\star} (\alpha_3 d_{IIA}) = (\alpha'_3 d_{IIA} + \alpha_3) \cdot \frac{d_{IIA\star}}{r_\star}$ are as follows:

- Multiplying $\alpha'_3 d_{IIA}$ by possible terms in $\frac{d_{IIA\star}}{r_\star}$:
 - $\alpha'_3 d_{IIA}$: \star anything, from constant terms in each $\frac{d_{IIA\star}}{r_\star}$
 - $\alpha'_3 d_{IIA} \alpha_6$: $\star = y$, since α_6 only shows up in $\star = y$ derivative
 - $\alpha'_3 d_{IIA} \alpha'_6$: $\star = y$, ”
 - $\alpha'_3 d_{IIA} \alpha'_6 \cdot \left(\frac{r_y}{r_x} \right)^2$: $\star = x$ only
- Multiplying α_3 by $\frac{d_{IIA\star}}{r_\star}$:
 - α_3 : \star anything
 - $\alpha_3 \alpha_6$: $\star = y$
 - $\alpha_3 \alpha'_6$: $\star = y$
 - $\alpha_3 \alpha'_6 \cdot \left(\frac{r_y}{r_x} \right)^2$: $\star = x$

Everything here is ok because we either get $\alpha_3^{\prime \log} = \alpha'_3 d_{IIA}$ or a regular derivative of α_6 , which may be multiplied by $(r_y/r_x)^2$ but $r_x > r_y$ in region IIA, so derivative terms can be made small.

Second derivative terms. We differentiate each of the first derivative terms. Let's say P is a term in the list above. Then we want to differentiate $r_\star P$ because above we divided by r_\star . Thus using the product rule with a differential operator $D = \partial_{r_\bullet}$ we get $D(r_\star)P + r_\star D(P)$. The first term gives 0 or 1 times P , which we already know is small by the above item for each P on the list. So we'll only need to consider $r_\star D(P)$ for the 8 choices of P listed above.

1. $P = \alpha'_3 d_{IIA}$

Then this term contributes to $\partial_{r_\bullet}^2(F)$ via $r_\star \partial_{r_\bullet}(P)$ i.e.

$$\begin{aligned} r_\star \partial_{r_\bullet}(\alpha'_3 d_{IIA}) &= r_\star \alpha_3'' \cdot (d_{IIA})_\bullet \cdot d_{IIA} + r_\star \alpha'_3 (d_{IIA})_\bullet = \frac{r_\star (d_{IIA})_\bullet \alpha_3'' \log}{d_{IIA}} \\ (d_{IIA})_\bullet \text{ terms: } \{T^2 r_\bullet, T^2 \alpha_6 r_y, T^2 \alpha'_6 r_y, T^2 \alpha'_6 \frac{r_y^2}{r_x}\} &< T^2 r_\bullet, \because \alpha_6 \leq 1, \alpha'_6 \approx \alpha \frac{1}{l}, \frac{r_y}{r_x} < 1 \\ \frac{T^2 r_\star r_\bullet}{d_{IIA}} &\approx \frac{r_\star r_\bullet}{r_x^2 - \frac{1}{2}(r_y^2 + r_z^2) + \frac{3}{2}\alpha_6 r_y^2} = \frac{r_\star r_\bullet / r_x^2}{1 - \frac{1}{2}((r_y/r_x)^2 + (r_z/r_x)^2) + \frac{3}{2}\alpha_6 (r_y/r_x)^2} \\ &\approx \frac{r_\star r_\bullet}{r_x^2} \approx \in \{0, 1\} \because r_x \gg r_y, r_z \text{ in region IIA} \\ \therefore r_\star \partial_{r_\bullet}(P) &= \frac{r_\star (d_{IIA})_\bullet \alpha_3'' \log}{d_{IIA}} \approx (\text{bounded}) \cdot \frac{1}{l^2} \end{aligned}$$

2. $P = \alpha'_3 d_{IIA} \alpha_6$ term from differentiating F first wrt y , i.e. $\partial_{r_y}(F)$

$$\begin{aligned} r_y \partial_{r_\bullet}(\alpha'_3 d_{IIA} \alpha_6) &= r_y \partial_{r_\bullet}(\alpha'_3 d_{IIA}) \cdot \alpha_6 + r_y (\alpha'_3 d_{IIA}) \cdot \partial_{r_\bullet}(\alpha_6) \\ &= (\text{above case}) \cdot \alpha_6 \pm \alpha_3'^{\log} \alpha'_6 \cdot c r_y, \quad c \in \left\{ \frac{1}{r_x}, \frac{1}{r_y}, 0 \right\} \\ &= \text{small} + \text{small} \end{aligned}$$

3. $\alpha'_3 d_{II} \alpha'_6$ term from differentiating first wrt y . Same as 2, replacing α_6 with α'_6 .

4. $\alpha'_3 d_{II} \alpha'_6 \cdot \left(\frac{r_y}{r_x}\right)^2$ from differentiating first wrt x

$$\begin{aligned} r_x \partial_{r_\bullet}(\alpha'_3 d_{II} \alpha'_6 \cdot \left(\frac{r_y}{r_x}\right)^2) &= r_x \partial_{r_\bullet}(\alpha'_3 d_{II} \alpha'_6) \cdot \left(\frac{r_y}{r_x}\right)^2 + r_x (\alpha'_3 d_{II} \alpha'_6) \cdot \partial_{r_\bullet} \left(\frac{r_y}{r_x}\right)^2 \\ &= \frac{r_y}{r_x} \cdot r_y \partial_{r_\bullet}(\alpha'_3 d_{II} \alpha'_6) \pm (\alpha_3'^{\log} \alpha'_6) \cdot c r_x, \quad c \in \{2r_y^2/r_x^3, 2r_y/r_x^2, 0\} \\ &= (\text{small})(\text{previous case}) + (\text{small})(r_y/r_x)^i, \quad i \in \{1, 2\} \\ &= \text{small} \because r_x \gg r_y \end{aligned}$$

5. $P = \alpha_3$: shows up in first derivative of F wrt any variable

Taking another derivative gives $r_\star \partial_{r_\bullet} \alpha_3 = r_\star \alpha'_3 (d_{IIA})_\bullet = \alpha_3'^{\log} \cdot (r_\star (d_{IIA})_\bullet) / d_{IIA}$. So we want $(r_\star (d_{IIA})_\bullet) / d_{IIA}$ to be bounded. This was checked in 1.

6. $P = \alpha_3 \alpha_6$: shows up in first derivatives of F wrt y

$$r_y \partial_{r_\bullet}(\alpha_3 \alpha_6) = r_y ((\alpha_3)_\bullet \alpha_6 + \alpha_3 (\alpha_6)_\bullet)$$

The term involving the derivative of α_3 is included in the previous case. The second term gives $\alpha_3\alpha'_6$ times one of zero, $r_y/r_x \approx 0$ or 1 so that term is a bounded term times a small term hence also small.

7. $P = \alpha_3\alpha'_6$: $\star = y$. Replace α_6 with α'_6 in the previous case.
8. $P = \alpha_3\alpha'_6(r_y/r_x)^2$: $\star = x$. The calculation for this is identical to 4, where now the “already-checked” part is $\alpha_3\alpha'_6$ instead of $\alpha'_3 d_{II}\alpha'_6$.

This concludes our check of the first and second order derivatives of $\alpha_3(d_{IIA})d_{IIA}$.

$$\text{3rd term: } \alpha_5 \cdot (Tr_\star)^2 \text{ for } \star \in \{y, z\}$$

We run through the same argument as with $\alpha_3 \cdot d_{IIA}$ above, replacing d_{IIA} with $(Tr_\star)^2$ in the second term.

First derivative. $\frac{1}{r_\star} \partial_{r_\star} (\alpha_5 (Tr_\star)^2) = \frac{1}{r_\star} \alpha'_5 (d_{IIA})_\star (Tr_\star)^2 + \alpha_5 \cdot \frac{((Tr_\star)^2)_\star}{r_\star}$.
The partial derivatives of $(Tr_\star)^2$ are $\frac{1}{r_\star} \partial_{r_\star} ((Tr_\star)^2) = 2T^2$ or 0.

Hence the nonzero terms in $\frac{1}{r_\star} \partial_{r_\star} (\alpha_5 (Tr_\star)^2)$ are $2T^2 \alpha_5$ and

$$\frac{1}{r_\star} \alpha'_5 (d_{IIA})_\star (Tr_\star)^2 = \alpha'_5 \frac{\log T^2 r_\star^2 (d_{IIA})_\star}{d_{IIA} r_\star}$$

Note that $\frac{T^2 r_\star^2}{d_{IIA}}$ and $\frac{(d_{IIA})_\star}{r_\star}$ are bounded. The latter was already checked in item 2.3. For the former:

$$\frac{r_\star^2}{r_x^2 - \frac{1}{2}(r_y^2 + r_z^2) + \frac{3}{2}\alpha_6 r_y^2} = \frac{r_\star^2/r_x^2}{1 - \frac{1}{2}((r_y/r_x)^2 + (r_z/r_x)^2) + \frac{3}{2}\alpha_6(r_y/r_x)^2} \approx 0 \because r_x \gg r_y, r_z$$

Note that $\star \in \{y, z\}$. So first derivatives are ok since they are either non-bump function derivatives or something bounded times a small log derivative.

Second derivative terms. We differentiate each of the first derivative terms. They are $\alpha'_5 (d_{IIA})_\star (Tr_\star)^2$ and $2T^2 r_\star \alpha_5$. Let's say Pr_\star is one of these terms, i.e. P was considered in the previous item. Thus using the product rule with a differential operator $D = \partial_{r_\bullet}$ we get $D(r_\star)P + r_\star D(P)$. The first term gives 0 or 1 times P , which we already know is small by the above item for each P on the list. So we'll only need to consider $r_\star D(P)$ for these 2 choices of P .

1. $P = \alpha'_5 (Tr_\star)^2 \frac{(d_{IIA})_\star}{r_\star}$. This involves the following terms, where we multiply $\alpha'_5 (Tr_\star)^2$ by the four possible types of terms showing up in $\frac{(d_{IIA})_\star}{r_\star}$, and check second derivatives arising from each.

(i) $\alpha'_5(Tr_*)^2$: this term contributes to $\partial_{r_*}^2(F)$ via $r_*\partial_{r_*}(P)$ i.e.

$$\begin{aligned} r_*\partial_{r_*}(\alpha'_5(Tr_*)^2) &= r_*\alpha''_5 \cdot (d_{IIA})_\bullet \cdot (Tr_*)^2 + r_*\alpha'_5((Tr_*)^2)_\bullet \\ &= (\alpha''_5^{\log} - \alpha'_5^{\log}) \frac{r_* \cdot (d_{IIA})_\bullet \cdot (Tr_*)^2}{d_{IIA}^2} + \alpha'_5 \frac{2T^2 r_\bullet r_*}{d_{IIA}} \end{aligned}$$

$$\text{Already checked bounded: } \frac{r_*(d_{IIA})_\bullet}{d_{IIA}} \because (1), \frac{(Tr_*)^2}{d_{IIA}} \because (\text{above}), \frac{T^2 r_\bullet r_*}{d_{IIA}} \because (1)$$

$$\therefore r_*\partial_{r_*}(\alpha'_5(Tr_*)^2) = (\text{small})(\text{bounded}) + (\text{small})(\text{bounded})$$

(ii) $\alpha'_5(Tr_*)^2\alpha_6$: term from differentiating F first wrt y , i.e. $\partial_{r_y}(F)$

$$\begin{aligned} r_y\partial_{r_*}(\alpha'_5(Tr_*)^2\alpha_6) &= r_y\partial_{r_*}(\alpha'_5(Tr_*)^2) \cdot \alpha_6 + r_y(\alpha'_5(Tr_*)^2) \cdot \partial_{r_*}(\alpha_6) \\ &= (\text{above case}) \cdot \alpha_6 \pm \alpha'_5 \frac{(Tr_*)^2}{d_{IIA}} \alpha'_6 \cdot cr_y, \quad c \in \left\{ \frac{1}{r_x}, \frac{1}{r_y}, 0 \right\} \\ &= (\text{small})(\text{bounded}) + (\text{small})(\text{bounded}) \end{aligned}$$

(iii) $\alpha'_5(Tr_*)^2\alpha'_6$: term from differentiating first wrt y . Same as previous, replacing α_6 with α'_6 .

(iv) $\alpha'_5(Tr_*)^2\alpha'_6 \cdot \left(\frac{r_y}{r_x}\right)^2$: from differentiating first wrt x

$$\begin{aligned} r_x\partial_{r_*}(\alpha'_5(Tr_*)^2\alpha'_6 \left(\frac{r_y}{r_x}\right)^2) &= r_x\partial_{r_*}(\alpha'_5(Tr_*)^2\alpha'_6) \cdot \left(\frac{r_y}{r_x}\right)^2 + r_x(\alpha'_5(Tr_*)^2\alpha'_6) \cdot \partial_{r_*} \left(\frac{r_y}{r_x}\right)^2 \\ &= \frac{r_y}{r_x} \cdot r_y\partial_{r_*}(\alpha'_5(Tr_*)^2\alpha'_6) \pm (\alpha'_5 \frac{(Tr_*)^2}{d_{IIA}} \alpha'_6) \cdot cr_x, \quad c \in \left\{ \frac{2r_y^2}{r_x^3}, \frac{2r_y}{r_x^2}, 0 \right\} \\ &= (\text{small})(\text{previous case}) + (\text{small})(r_y/r_x)^i, \quad i \in \{1, 2\} \\ &= \text{small} \because r_x \gg r_y \end{aligned}$$

2. $P = 2T^2\alpha_5$: shows up in first derivative of F wrt any variable

Taking another derivative gives $r_*\partial_{r_*}2T^2\alpha_5 = r_*2T^2\alpha'_5(d_{IIA})_\bullet = 2T^2\alpha_5^{\log} \cdot (r_*(d_{IIA})_\bullet)/d_{IIA}$. So we want $(r_*(d_{IIA})_\bullet)/d_{IIA}$ to be bounded. This was checked in 1.

This concludes our check of the first and second order derivatives of $\alpha_5(d_{IIA})d_{IIA}$. We have one more remaining type of term showing up in F that we have to check first and second order derivatives of.

$$\text{4th term: } \alpha_5\alpha_6 \cdot (Tr_y)^2$$

$$\frac{1}{r_*}\partial_{r_*}(\alpha_5(Tr_y)^2) \cdot \alpha_6 + \alpha_5(Tr_y)^2 \cdot \frac{1}{r_*}\partial_{r_*}\alpha_6 = (\text{previous}) \cdot \alpha_6 \pm \alpha_5(Tr_y)^2 \cdot \frac{c}{r_*^2}\alpha'_6$$

$$\text{2nd term: } \star = z \implies c = 0, \quad \star = x \implies \approx 0 \because r_x \gg r_y, \quad \star = y \implies \frac{r_y^2}{r_*^2} = 1$$

So ok on first derivatives. Finally, we check second order derivatives.

$$\begin{aligned} \partial_{r_\bullet}[\partial_{r_\star}(\alpha_5(Tr_y)^2) \cdot \alpha_6 + \alpha_5(Tr_y)^2 \cdot \partial_{r_\star}(\alpha_6)] &= \partial_{r_\bullet r_\star}^2(\alpha_5(Tr_y)^2) \cdot \alpha_6 + \partial_{r_\star}(\alpha_5(Tr_y)^2) \partial_{r_\bullet} \alpha_6 \\ &\quad + \partial_{r_\bullet}(\alpha_5(Tr_y)^2) \partial_{r_\star} \alpha_6 + \alpha_5(Tr_y)^2 \cdot \partial_{r_\bullet} \partial_{r_\star}(\alpha_6) \end{aligned}$$

1st term ok by previous check on $\alpha_5(Tr_y)^2$

$$\begin{aligned} \text{Terms 2,3: } \partial_{r_\star}(\alpha_5(Tr_y)^2) \cdot \partial_{r_\bullet} \alpha_6 &= (\alpha_5^{\prime \log} \frac{(d_{IIA})_\star}{d_{IIA}}(Tr_y)^2 + 2\alpha_5 T^2 \delta_{y^\star r_y}) \cdot \frac{\pm 1}{r_x \text{ or } r_y} \cdot \alpha_6' \\ &= \pm [T^2 \alpha_5^{\prime \log} \frac{(d_{IIA})_\star r_y}{d_{IIA}} \cdot \frac{r_y}{r_x \text{ or } r_y} \cdot \alpha_6' + 2\alpha_5 T^2 \frac{r_y}{r_x \text{ or } r_y} \cdot \alpha_6'] \end{aligned}$$

$$\begin{aligned} \text{4th term: } \alpha_5(Tr_y)^2 \partial_{r_\bullet} \left(\frac{\alpha_6'}{r_x \text{ or } r_y} \right) &= \alpha_5(Tr_y)^2 \left[\alpha_6'' \cdot \frac{\pm 1}{r_x \text{ or } r_y} \cdot \frac{1}{r_x \text{ or } r_y} - \alpha_6' \frac{1}{r_x^2 \text{ or } r_y^2} \right] \\ &= T^2 \alpha_5 \alpha_6'' \frac{\pm r_y^2}{r_x^2, r_x r_y, \text{ or } r_y^2} - T^2 \alpha_5 \alpha_6' \frac{r_y^2}{r_x^2 \text{ or } r_y^2} \\ &= \text{small,} \quad \because r_x \gg r_y \\ \implies \partial_{r_\bullet} \partial_{r_\star}(\alpha_5 \alpha_6 \cdot (Tr_y)^2) &= (\text{small}) \text{ by 1} \end{aligned}$$

So the upshot is: all terms involving derivatives of bump functions can be made arbitrarily small because they are multiplied by expressions which are bounded (taking either log derivatives of α_3, α_5 or regular derivatives of α_6 .) So we get a positive-definite form, because the terms not involving derivatives of bump functions are $O(1)$ so they dominate, and we already showed they give something positive-definite.

Determining functions on region IIB

We just checked in region IIA hence by symmetry region IIC, and similarly IVA, C and VIA, C by symmetry. Swap $r_x \leftrightarrow r_y$ to get to IIC and subscripts I become III.

Region IIA:

$$\begin{aligned} F &\approx (g_{yz} - \alpha_6 \cdot (Tr_y)^2) + \alpha_3(d_{IIA})d_{IIA} + \frac{1}{2}\alpha_5(d_{IIA}) \cdot ((Tr_y)^2 - (Tr_z)^2 - \alpha_6(Tr_y)^2) \\ g_{yz} &\approx T^2[r_y^2 + r_z^2] \\ d_I &\approx T^2[r_x^2 - \frac{1}{2}(r_y^2 + r_z^2)] \\ d_{IIA} &\approx T^2[r_x^2 - \frac{1}{2}(r_y^2 + r_z^2)] + \frac{3}{2}\alpha_6(\log r_y - \log r_x) \cdot (Tr_y)^2 \\ \theta_I &\approx T^2[r_y^2 - r_z^2] \\ \theta_{II} &= \log(r_y/r_x) \end{aligned}$$

Region IIC:

$$\begin{aligned}
F &= (g_{xy} - \alpha_6 \cdot (Tr_y)^2) + \alpha_3(d_{IIC})d_{IIC} + \frac{1}{2}\alpha_5(d_{IIC}) \cdot ((Tr_x)^2 - (Tr_z)^2 - \alpha_6(Tr_x)^2) \\
g_{xy} &\approx T^2[r_x^2 + r_z^2] \\
d_{III} &\approx T^2[r_y^2 - \frac{1}{2}(r_x^2 + r_z^2)] \\
d_{IIC} &\approx T^2[r_y^2 - \frac{1}{2}(r_x^2 + r_z^2)] + \frac{3}{2}\alpha_6(\log r_x - \log r_y) \cdot (Tr_x)^2 \\
\theta_{III} &\approx T^2[r_x^2 - r_z^2] \\
\theta_{II} &= \log(r_y/r_x)
\end{aligned}$$

At the end of region IIA when $\alpha_6 \equiv 1$ we get:

$$\begin{aligned}
F &\approx (g_{yz} - (Tr_y)^2) + \alpha_3(d_{IIA})d_{IIA} + \frac{1}{2}\alpha_5(d_{IIA}) \cdot (-(Tr_z)^2) \\
g_{yz} &\approx T^2[r_y^2 + r_z^2] \\
d_I &\approx T^2[r_x^2 - \frac{1}{2}(r_y^2 + r_z^2)] \\
d_{IIA} &\approx T^2[r_x^2 + r_y^2 - \frac{1}{2}r_z^2]
\end{aligned}$$

At the end of region IIC when $\alpha_6 \equiv 1$ (where α_6 is still defined as a function of θ_{II}):

$$\begin{aligned}
F &\approx (g_{xy} - (Tr_y)^2) + \alpha_3(d_{IIC})d_{IIC} + \frac{1}{2}\alpha_5(d_{IIC}) \cdot (-(Tr_z)^2) \\
g_{xy} &\approx T^2[r_x^2 + r_z^2] \\
d_{III} &\approx T^2[r_y^2 - \frac{1}{2}(r_x^2 + r_z^2)] \\
d_{IIC} &\approx T^2[r_y^2 + r_x^2 - \frac{1}{2}r_z^2]
\end{aligned}$$

So F on region IIB should equal what it does on the two ends of IIA and IIC. Note d_{IIA} equals d_{IIC} on the ends, so we take d_{IIB} to be this common approximation $d_{IIB} \approx T^2[r_x^2 + r_y^2 - \frac{1}{2}r_z^2]$. The non-bump function at the start is $(Tr_z)^2$ for both. And finally the factor multiplying α_5 is also symmetric in x and y , namely $-(Tr_z)^2$.

Region IIB:

$$\begin{aligned}
F &\approx T^2r_z^2 + \alpha_3(d_{IIB})d_{IIB} + \frac{1}{2}\alpha_5(d_{IIB}) \cdot (-r_z^2) \\
d_{IIB} &\approx T^2[r_x^2 + r_y^2 - \frac{1}{2}r_z^2]
\end{aligned}$$

Note that on the other ends IIA should glue to region I and IIC should glue to region III. At the end of region IIA when $\alpha_6 \equiv 0$ we get:

$$\begin{aligned}
F &\approx g_{yz} + \alpha_3(d_{IIA})d_{IIA} + \frac{1}{2}\alpha_5(d_{IIA}) \cdot \theta_I \\
g_{yz} &\approx T^2[r_y^2 + r_z^2] \\
\theta_I &\approx (Tr_y)^2 - (Tr_z)^2 \\
d_I &\approx T^2[r_x^2 - \frac{1}{2}(r_y^2 + r_z^2)] \\
d_{IIA} &\approx T^2[r_x^2 - \frac{1}{2}(r_y^2 + r_z^2)] \\
\therefore d_I &= d_{IIA}
\end{aligned}$$

At the end of region IIC when $\alpha_6 \equiv 0$:

$$\begin{aligned}
F &\approx g_{xy} + \alpha_3(d_{IIC})d_{IIC} + \frac{1}{2}\alpha_5(d_{IIC}) \cdot (-\theta_{III}) \\
g_{xy} &\approx T^2[r_x^2 + r_z^2] \\
\theta_{III} &\approx (Tr_z)^2 - (Tr_x)^2 \\
d_{III} &\approx T^2[r_y^2 - \frac{1}{2}(r_x^2 + r_z^2)] \\
d_{IIC} &\approx T^2[r_y^2 - \frac{1}{2}(r_x^2 + r_z^2)] \\
\therefore d_{III} &= d_{IIC}
\end{aligned}$$

Note that the region III angle here is negative what we found on the other half of region III. This is because the two angles need to equal $-(Tr_z)^2$ in the middle of region II to glue. If we define the symplectic form in coordinates (x'', y'', z'') the same way we did with (x, y, z) , then the form glues correctly. The only remaining item is to check in region IIB, which has different behavior than the previously checked regions.

Region IIB

The characteristics in region IIB which we did not have in regions IIA and C are 1) r_x and r_y go from $r_x \gg r_y$ to $r_y \gg r_x$, passing through $r_x = r_y$ and 2) $\alpha_6 \equiv 1$. All of r_x, r_y, r_z are still small so we still have an approximation for the Kähler potential:

$$\begin{aligned}
F &\approx T^2 r_z^2 + \alpha_3(d_{IIB})d_{IIB} + \frac{1}{2}\alpha_5(d_{IIB}) \cdot (-(Tr_z)^2) \\
d_{IIB} &\approx T^2[r_x^2 + r_y^2 - \frac{1}{2}r_z^2]
\end{aligned}$$

Let's repeat the calculations above for $\alpha_3(d_{IIA}) \cdot d_{IIA}$ and $\alpha_5 \cdot (Tr_z)^2$ with region IIB, and see if they relied on $r_x \gg r_y$. What we know in region IIB is that $r_x, r_y \gg r_z$.

1st term: $\alpha_3(d_{IIB})d_{IIB}$

First derivative. $\frac{1}{r_\star} \partial_{r_\star} (\alpha_3 d_{IIB}) = (\alpha'_3 d_{IIB} + \alpha_3) \cdot \frac{d_{IIB\star}}{r_\star}$.
Here are the partial derivatives of d_{IIB} .

$$\begin{aligned} d_{IIB} &\approx T^2[r_x^2 + r_y^2 - \frac{1}{2}r_z^2] \\ \frac{(d_{IIB})_x}{r_x} &\approx \frac{T^2}{r_x}(2r_x) = \frac{T^2}{2} \\ \frac{(d_{IIB})_y}{r_y} &\approx \frac{T^2}{2} \\ \frac{(d_{IIB})_z}{r_z} &\approx -\frac{T^2}{4} \end{aligned}$$

Hence the terms in $\frac{1}{r_\star} \partial_{r_\star} (\alpha_3 d_{IIB}) = (\alpha'_3 d_{IIB} + \alpha_3) \cdot \frac{d_{IIB\star}}{r_\star}$ are proportional to $\alpha'_3 d_{IIB}$ (a log derivative, so small) and α_3 (not a derivative). So first derivatives are ok.

Second derivative terms. We differentiate each of the first derivative terms. Let's say P is a term in the list above. Then we want to differentiate $r_\star P$ because above we divided by r_\star . Thus using the product rule with a differential operator $D = \partial_{r_\bullet}$ we get $D(r_\star)P + r_\star D(P)$. The first term gives 0 or 1 times P , which we already know is small by the above item for each P on the list. So we'll only need to consider $r_\star D(P)$ for the 2 choices of P listed above.

1. $P = \alpha'_3 d_{IIB}$

Then this term contributes to $\partial_{r_\star r_\bullet}^2(F)$ via $r_\star \partial_{r_\bullet}(P)$ i.e.

$$r_\star \partial_{r_\bullet} (\alpha'_3 d_{IIB}) = r_\star \alpha''_3 \cdot (d_{IIB})_\bullet \cdot d_{IIB} + r_\star \alpha'_3 (d_{IIB})_\bullet = \frac{r_\star (d_{IIB})_\bullet}{d_{IIB}} \alpha''_3 \log$$

$(d_{IIB})_\bullet$ terms : $T^2 r_\bullet$.

$$\frac{T^2 r_\star r_\bullet}{d_{IIB}} \approx \frac{r_\star r_\bullet}{r_x^2 + r_y^2 - \frac{1}{2}r_z^2} = \frac{r_\star r_\bullet / r_x^2}{1 + (r_y/r_x)^2 - \frac{1}{2}(r_z/r_x)^2} \approx \frac{r_\star r_\bullet / r_x^2}{1 + (r_y/r_x)^2}$$

$$(\star, \bullet) \in \{(r_x, r_x), (r_x, r_z), (r_z, r_z)\} \implies \frac{r_\star r_\bullet}{r_x^2} \in \{1, \text{small}\} \because r_x \gg r_z$$

$$(\star, \bullet) = (r_y, r_z) \implies \frac{r_y r_z}{r_x^2} < \frac{r_y}{r_x}$$

$$(\star, \bullet) \in \{(r_x, r_y), (r_y, r_y)\} \text{ suffices to bound: } \frac{a}{1+a^2}, \frac{a^2}{1+a^2}, \quad a = r_y/r_x$$

$$\frac{a^2}{1+a^2} \leq 1, \quad a < 1 \implies \frac{a}{1+a^2} < 1, \quad a \geq 1 \implies \frac{a}{1+a^2} \leq \frac{a^2}{1+a^2} \leq 1$$

$\therefore r_\star \partial_{r_\bullet} (\alpha'_3 d_{IIB}) = (\text{bounded})(\text{small})$

2. $P = \alpha_3$

Taking another derivative gives $r_\star \partial_{r_\bullet} \alpha_3 = r_\star \alpha'_3 (d_{IIB})_\bullet = \alpha_3^{\prime \log} \cdot (r_\star (d_{IIB})_\bullet) / d_{IIB}$. So we want $(r_\star (d_{IIB})_\bullet) / d_{IIB}$ to be bounded. This was just checked above.

$$\text{2nd term: } \alpha_5 \cdot (Tr_z)^2$$

We run through the same argument as with $\alpha_3 \cdot d_{IIB}$ above, replacing d_{IIB} with $(Tr_z)^2$ in the second term.

First derivative. $\frac{1}{r_\star} \partial_{r_\star} (\alpha_5 (Tr_z)^2) = \frac{1}{r_\star} \alpha'_5 (d_{IIB})_\star (Tr_z)^2 + \alpha_5 \cdot \frac{((Tr_z)^2)_\star}{r_\star}$.
The partial derivatives of $(Tr_z)^2$ are $\frac{1}{r_\star} \partial_{r_\star} ((Tr_z)^2) = 2T^2$ or 0.

Hence the nonzero terms in $\frac{1}{r_\star} \partial_{r_\star} (\alpha_5 (Tr_z)^2)$ are $2T^2 \alpha_5$ and

$$\frac{1}{r_\star} \alpha'_5 (d_{IIB})_\star (Tr_z)^2 = \alpha_5^{\prime \log} \frac{T^2 r_z^2 (d_{IIB})_\star}{d_{IIB} \cdot r_\star}$$

Note that $\frac{T^2 r_z^2}{d_{IIB}}$ and $\frac{(d_{IIB})_\star}{r_\star}$ are bounded. The latter is approximately constant because d_{IIB} is approximately linear in r_x^2, r_y^2 and r_z^2 . For the former:

$$\frac{r_z^2}{r_x^2 + r_y^2 - \frac{1}{2} r_z^2} = \frac{r_z^2 / r_x^2}{1 + \frac{r_y^2}{r_x^2} - \frac{1}{2} ((r_z / r_x)^2)} \approx \frac{r_z^2 / r_x^2}{1 + \frac{r_y^2}{r_x^2}} \approx 0 \because r_x \gg r_z$$

So first derivatives are ok.

Second derivative terms. We differentiate each of the first derivative terms. They are $\alpha'_5 (d_{IIB})_\star (Tr_z)^2$ and $2T^2 r_\star \alpha_5$. Let's say Pr_\star is one of these terms, i.e. P was considered in the previous item. Thus using the product rule with a differential operator $D = \partial_{r_\bullet}$ we get $D(r_\star)P + r_\star D(P)$. The first term gives 0 or 1 times P , which we already know is small by the above item for each P on the list. So we'll only need to consider $r_\star D(P)$ for these 2 choices of P .

1. $P = \alpha'_5(T r_z)^2 \frac{(d_{IIB})_\star}{r_\star}$. It suffices to consider $\alpha'_5(T r_z)^2$ because $\frac{(d_{IIB})_\star}{r_\star}$ is a constant.

$$\begin{aligned} r_\star \partial_{r_\bullet} (\alpha'_5(T r_z)^2) &= r_\star \alpha''_5 \cdot (d_{IIB})_\bullet \cdot (T r_z)^2 + r_\star \alpha'_5 ((T r_z)^2)_\bullet \\ &= (\alpha''_5{}^{\log} - \alpha'_5{}^{\log}) \frac{r_\star \cdot (d_{IIB})_\bullet \cdot (T r_z)^2}{d_{IIB}^2} + \alpha'_5{}^{\log} \frac{2T^2 r_z r_\star}{d_{IIB}} \end{aligned}$$

Already checked bounded: $\frac{r_\star (d_{IIB})_\bullet}{d_{IIB}}$, $\frac{(T r_z)^2}{d_{IIB}}$ \therefore (above)

$$\frac{T^2 r_z r_\star}{d_{IIB}} \approx \frac{r_z r_\star / r_x^2}{1 + (r_y/r_x)^2 - \frac{1}{2}(r_z/r_x)^2} \approx \frac{r_z r_\star / r_x^2}{1 + (r_y/r_x)^2} < \frac{r_\star / r_x}{1 + (r_y/r_x)^2}$$

$\star = x \implies$ bounded

$\star = y \implies a/(1 + a^2)$ bounded as above

$\star = z \implies$ small

$$\therefore r_\star \partial_{r_\bullet} (\alpha'_5(T r_z)^2) = (\text{small})(\text{bounded}) + (\text{small})(\text{bounded})$$

2. $P = 2T^2 \alpha_5$: shows up in first derivative of F wrt any variable

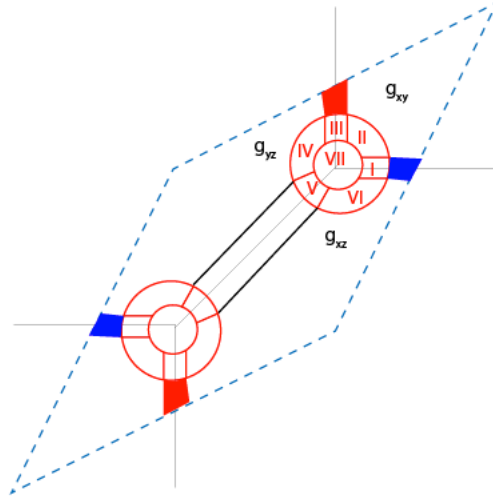
Taking another derivative gives $r_\star \partial_{r_\bullet} 2T^2 \alpha_5 = r_\star 2T^2 \alpha'_5 (d_{IIB})_\bullet = 2T^2 \alpha'_5{}^{\log} \cdot (r_\star (d_{IIB})_\bullet) / d_{IIB}$.
So we want $(r_\star (d_{IIB})_\bullet) / d_{IIB}$ to be bounded, which was already checked above.

This completes the calculation of positive definiteness. We flesh out the details below in checking there's enough space for the log derivatives, by finding approximate values for r_x, r_y, r_z and hence the θ and d variables to make sure their \log_T values vary by an amount proportional to l .

The remainder of \mathbb{C}^3 patch

In the region between region I and region IIA the only bump functions at play are α_3 and α_5 and they are allowed to vary in the same amount of space as checked above, and still $r_x \gg r_y, r_z$ so all the previous estimates apply.

2.4 Showing ω nondegenerate: away from \mathbb{C}^3 patch



All the calculations above involved approximations because r_x, r_y, r_z are all very small near the \mathbb{C}^3 patch. Around each vertex in the unbounded polytope we have some coordinate system with very small coordinates, so we define a symplectic form locally around all the vertices. (An analogue to think about are the coordinates z around 0 and $w = 1/z$ around ∞ in \mathbb{P}^1 . It is true that z gets very large in the w chart, but z and w are both small in the same way so one could take $\log(1 + |\text{coord}|^2)$ which would look the same in each chart.) So what remains to be checked is that the symplectic form glues positive-definitely along e.g. the z axis.

In the green region along the z -axis we no longer have the d_V coordinate because the bump functions α_3, α_5 depending on them have finished their support. However we still have an angular coordinate to allow us to interpolate between g_{xz} and g_{yz} in the unprimed coordinates, or $g_{x'''z'''}$ and $g_{y'''z'''}$ in the tripled primed coordinates at the lower left vertex. So we need to check we have positive definiteness when only α_4 is at play and r_z is large. Note that when there are no bump functions we have positive definite-ness because either we are in region VII where we have the standard Kähler potential or we are in the center of a $\mathbb{C}\mathbb{P}^2(3)$ of the toric variety of $\mathbb{C}\mathbb{P}^2$ blown up at three points, which has a natural potential that can be read off from its lattice points.

We still need to check we get something positive definite when $|z|$ is large. Recall that the equivalence \sim on coordinates is precisely the transition maps coming from thinking of toric charts. As an example think of $\mathbb{C}\mathbb{P}^2$: we have $\mathbb{C} \times \mathbb{C}^*$ sitting inside all the charts as the part where they overlap. The embedding into one is (u, v) and into another is (v^{-1}, uv^{-1}) so this tells us the transition map (u, v) goes to the other one. In my case, we don't deal with homogeneous coordinates first, the picture just goes straight to giving us the transition

maps on toric coordinates.

In particular, we want to find the halfway point in the z coordinate when $|v_0| \neq 0$. When we fix a fiber, this corresponds to a toric chart gluing of $(\mathbb{C}^*)^2$ to itself. That z coordinate maps to $T^{-2}z^{-1}$ and starts at $T^{l/3}$. So we are still gluing two copies of \mathbb{C}^* to each other but actually one starts at the circle of radius $T^{l/3}$ instead of just deleting the point zero. We still get the halfway point is T^{-1} , it's just we are gluing a more punctured plane than before as in \mathbb{CP}^1 . So $|z|$ goes from $T^{l/3}$ to T^{-1} . It suffices to check just on half, because of the gluing property we just checked in the previous item.

Given this, we check that the bump function derivatives are bounded. The Kähler potential is of the form $(f + d) + \alpha_4(\theta) \cdot \theta$. So we just check derivatives of $\alpha_4(\theta) \cdot \theta$. We can use the above calculations for this term by the following reasoning. Although $|z| \leq T^{-1}$, we may assume that $|x|$ and $|y|$ are very small. Thus $|T^2xz| \leq |Tx|$ and $|T^2yz| \leq |Ty|$ hence these quantities are very small and we have again small scale approximations for their logarithms.

$$\begin{aligned} \theta &= \phi_x - \phi_y = \log_T(1 + |Tx|^2) - \log_T(1 + |T^2yz|^2) - \log_T(1 + |Ty|^2) + \log_T(1 + |T^2xz|^2) \\ &\approx 2|Tx|^2 - 2|Ty|^2 \end{aligned}$$

$$\begin{aligned} \frac{1}{r_*} \frac{\partial}{\partial r_*} (\alpha_4 \theta) &= (\alpha'_4 \theta + \alpha_4) \frac{\theta_*}{r_*} \\ \frac{\partial}{\partial r_\bullet} (\alpha'_4 \theta \theta_*) &= \alpha''_4 \theta_\bullet \theta \theta_* + \alpha'_4 \theta_\bullet \theta_* + \alpha'_4 \theta \theta_{*\bullet} = (\alpha''_4 \theta^2 + \alpha'_4 \theta) \cdot \frac{\theta_\bullet \theta_*}{\theta} + \alpha'_4 \log \theta_{*\bullet} \\ \frac{\partial}{\partial r_\bullet} (\alpha_4 \theta_*) &= \alpha'_4 \theta_\bullet \theta_* + \alpha_4 \theta_{*\bullet} = \alpha'_4 \log \frac{\theta_\bullet \theta_*}{\theta} + \alpha_4 \theta_{*\bullet} \end{aligned}$$

Thus we'll need to bound the following three terms, and then check we have enough space for the log derivatives:

- $\frac{\theta_*}{r_*}$

$$\frac{\theta_x}{r_x} \approx 4T^2, \quad \frac{\theta_y}{r_y} \approx -4T^2, \quad \frac{\theta_z}{r_z} \approx 0$$

- $\frac{\theta_\bullet \theta_*}{\theta}$ implies we'll need to consider $\frac{r_\bullet r_*}{r_x^2 - r_y^2}$ so we need to know size constraints so that the support of α_4 is away from a region where $r_x = r_y$. Recall from above that we remove a sliver $T < (r_x/r_y)^2 < 1/T$. Also we get approximately zero unless both $*$ and \bullet are not z , because θ is approximately $2T^2(r_x^2 - r_y^2)$. As above, we divide top and bottom by r_x^2 or r_y^2 depending on which variable is larger, and then the numerator is at most 1 while the denominator is bounded below from the constraint $T < (r_x/r_y)^2 < 1/T$.

- $\theta_{*\bullet}$ is approximately zero unless $* = \bullet$ in which case it's a constant, so bounded.

Note that we will have enough space for log derivatives because $\theta \approx 2T^2(r_x^2 - r_y^2)$ for r_x, r_y very small and this was already checked earlier when $\theta \approx T^2(r_x^2 - r_y^2)$.

Chapter 3

HMS for V and V^\vee abelian varieties

The SYZ mirror of a torus is an example of Family Floer theory, [Fuk02]. In particular, Family Floer theory implies that line bundles should mirror the behavior of Lagrangians. This is because by Serre duality $Ext^1(\mathcal{O}_{p_0}, \mathcal{O}) \cong \mathcal{O}_{p_0}$, while the intersection of the vertical linear Lagrangian on a torus with any other linear Lagrangian of finite slope will have one intersection point. We can define a line bundle at each point to correspond to the 1-dimensional vector space generated by that intersection point on the Floer theory side, and put a holomorphic structure on the result to get a holomorphic line bundle, c.f. [Fuk02]. We can build a rank 1 line bundle from the fact that we have one intersection point for linear finite-slope Lagrangians with L_{pt} .

The Fukaya category $Fuk(V^\vee)$

We consider the following full subcategory of the Fukaya category $Fuk(V^\vee)$, an A_∞ -category.

- Objects: Let $M = \begin{pmatrix} 2 & 1 \\ 1 & 2 \end{pmatrix}$ and $\Gamma_B := M(\mathbb{Z}^2)$. We have affine action-angle coordinates $(\xi_1, \xi_2, \theta_1, \theta_2)$ on a fiber V^\vee of $v_0 : Y \rightarrow \mathbb{C}$, where ξ_i are monotonic in the norms of the complex coordinates and θ_i are their angles. The symplectic form on the fiber in these coordinates is $\omega = d\xi \wedge d\theta$. We consider the subcategory with objects given by the following linear Lagrangians:

$$\ell_i = \{(\xi_1, \xi_2, -i \cdot M^{-1}(\xi))\}_{\xi \in T_B = \mathbb{R}^2 / M(\mathbb{Z}^2)}$$

These are the analogue of the lines of slope i considered on an elliptic curve in [PZ98].

- Morphisms: $|i - j| \geq 1$, then $Hom(\ell_i, \ell_j) := \bigoplus_{p \in \ell_i \cap \ell_j} \mathbb{C} \cdot \{p\} \cong \mathbb{C}^{(i-j)^2}$ by a modular arithmetic argument. Note that this is the same as $h^0(V, \mathcal{L}^{\otimes(j-i)})$ for $j > i$ and $h^2(V, \mathcal{L}^{\otimes(j-i)})$ for $i > j$ which will tell us the morphism groups are isomorphic. If ξ

corresponds to the coordinates on ℓ_i and $\tilde{\xi}$ on ℓ_j then they can only intersect at points where

$$\begin{aligned}
& 1) \xi \equiv \tilde{\xi} \pmod{M(\mathbb{Z}^2)} \\
& 2) i \cdot M^{-1}(\xi) \equiv j \cdot M^{-1}(\tilde{\xi}) \pmod{\mathbb{Z}^2} \\
& \implies i \cdot \xi \equiv j \cdot \tilde{\xi} \equiv j \cdot \xi \pmod{M(\mathbb{Z}^2)} \\
& \implies \xi \in \frac{1}{i-j} M(\mathbb{Z}^2)
\end{aligned} \tag{3.1}$$

So let $\xi = s(2, 1) + t(1, 2)$. Then $(i-j)s$ and $(i-j)t$ can be anything from 0 up to $i-j-1$ and we get $(i-j)^2$ intersection points.

- μ^1 on homs: the differential counts holomorphic bigons between intersection points.

Claim 3.0.1. There are no bigons on T^4 between any two intersection points of the linear Lagrangian submanifolds $\ell_i \cap \ell_j$, for $i \neq j$, so $\mu^1 = 0$.

Proof. From the pair $(T^4, \ell_i \cup \ell_j)$ we have

$$0 = \pi_2(T^4)(= \pi_2(\mathbb{R}^4)) \rightarrow \pi_2(T^4, \ell_i \cup \ell_j) \rightarrow \pi_1(\ell_i \cup \ell_j) \xrightarrow{\cong} \pi_1(T^4)$$

thus $\pi_2(T^4, \ell_i \cup \ell_j)$ is trivial. So any such holomorphic disc is contractible. Pick a bigon $u : D^2 \setminus \pm 1 \rightarrow T^4$ on T^4 between two intersection points p, q with boundary on $\ell_i \cup \ell_j$. Pick lifts $\tilde{\ell}_i$ and $\tilde{\ell}_j$ with lifted intersection point $\tilde{p} = 0$.

$$\tilde{\ell}_i = \{(\xi_1, \xi_2, i \cdot M^{-1}(\xi))\}_{\xi \in \mathbb{R}^2}$$

Let ∂_1 and ∂_2 be the two boundary components of $D^2 \setminus \pm 1$ mapping to ℓ_i and ℓ_j respectively. Pick lifts of $u(\partial_i)$ to \mathbb{R}^4 , call them γ_1, γ_2 such that $\gamma_i(0) = \tilde{p}$ and set $\tilde{q}_i := \gamma_i(1)$. Then by contractibility of discs, $\tilde{q}_1 = \tilde{q}_2$. However

$$\tilde{\ell}_i \cap \tilde{\ell}_j \implies \xi^{(i)} = \xi^{(j)} =: \xi, i\xi = j\xi \therefore \xi = 0$$

since $|i-j| \geq 2$. So there can only be one intersection point, not two as needed for a nontrivial bigon. \square

The hom spaces are dimension $(i-j)^2$ for i and j distinct, matching $h^0(V, L^{j-i})$ only when $j > i$, otherwise they live in Floer degree 2 and match $h^2(V, L^{j-i})$ (a negative line bundle).

Meanwhile, for $i = j$, there typically *are* bigons between ℓ_i and a slight Hamiltonian perturbation of it. However it is still true that $HF(\ell_i, \ell_i) = H^*(T^2)$, and the key geometric fact this relies on is that ℓ_i does not bound any discs in the torus, so self-HF

reduces to classical cohomology.

If $i = j$ then $CF^*(\ell_i, \ell_i) = HF^*(\ell_i, \ell_i)$ from the PSS isomorphism. So $HF^*(\ell_i, \ell_i) \cong H^*(\ell_i) = H^*(T^2)$. Hence in all cases we find that $HF^*(\ell_i, \ell_j) \cong Ext_V^*(\mathcal{L}^{\otimes i}, \mathcal{L}^{\otimes j})$.

- Composition, or μ^2 , on homs (by analogy with the [PZ98] picture for the elliptic curve): we consider lifts $\tilde{\ell}_0, \tilde{\ell}_1, \tilde{\ell}_2$ and look at the possible triangles that can occur. One obtains a sum indexed by elements of Γ , which matches the expansions for multi-theta functions.
- Identity morphism: $hom(\ell_i, \ell_i) \cong H^*(V, \ell_i)$ which naturally carries an identity, but I think this requires more work. The way it's usually done, is to show it's isomorphic to the Morse complex. This is done by taking a Hamiltonian that is the Morse function, and then look at df . Critical points correspond to where $df = 0$ and give intersection points in the Floer setting, also Morse trajectories are Floer trajectories for constant t and the Floer equation and Morse equation end up being the same in this special case. Hamiltonian perturbations are valid in a fiber, although we'll see later not in the total space.

The bounded derived category $D^bCoh(V)$

Definition 3.0.2. The *bounded derived category* is defined as follows. Let \mathcal{A} be the category of coherent sheaves on V . Note that V is an abelian variety, hence a projective variety.

Claim 3.0.3. \mathcal{A} is an abelian category, in particular has kernels and cokernels, so we can define chain complexes of objects.

Definition 3.0.4. Define $Kom(\mathcal{A})$ to be the category of chain complexes in $Coh(V)$, where morphisms are chain maps and composition is composition of chain maps.

Definition 3.0.5. Define $K(\mathcal{A})$ to have objects given by chain complexes as above, and morphisms are identified under an equivalence relation \sim which is homotopy equivalence.

Definition 3.0.6. The derived category $D(\mathcal{A})$ has the same objects as $K(\mathcal{A})$ and a morphism $A^\bullet \rightarrow B^\bullet$ is a roof $A^\bullet \leftarrow C^\bullet \rightarrow B^\bullet$ where $C^\bullet \rightarrow A^\bullet$ is a quasi-isomorphism, i.e. a chain map inducing an isomorphism on homology. Two morphisms are equivalent if they are dominated in $K(\mathcal{A})$ by a third object of the same sort.

Then the bounded derived category is obtained by carrying out this process after starting with $Kom^b(\mathcal{A})$, where we take only bounded chain complexes (zero outside a finite sequence of objects).

Claim 3.0.7. $D^bCoh(V)$ can be enhanced to a dg-category, namely an A_∞ -category where $\mu^{\geq 3} = 0$.

We will not need this here, because in our setting $\mu^1 = 0$ on the Fukaya category so we can show an equivalence of usual categories.

Claim 3.0.8. Recall $\mathcal{L} \rightarrow V$ defined earlier. Then we claim $\mathcal{O}, \mathcal{L}, \mathcal{L}^2$ split-generate $D^b\text{Coh}(V)$.

Remark 3.0.9. While this allows us to reduce to considering only these objects, it comes at the expense of requiring more information about higher A_∞ -products. This is because other objects will come up as complexes built from $\mathcal{O}, \mathcal{L}, \mathcal{L}^2$, but the calculation of cohomology level hom's between these complexes requires knowledge of some chain-level higher compositions among $\mathcal{O}, \mathcal{L}, \mathcal{L}^2$. In particular we would in principle need to know all μ^k 's involving an arbitrary sequence of objects taken from $\mathcal{O}, \mathcal{L}, \mathcal{L}^2$, with as many repetitions as desired among these.

Claim 3.0.10. \mathcal{L} as defined above is an ample line bundle.

Proof. Line bundles on complex tori are characterized by hermitian forms H (see Polishchuk book on Abelian Varieties, [Pol03]). Ample line bundles are equivalently those with $H^0(V, \mathcal{L}^i) \neq 0$ for some i , as is the case in this setting because \mathcal{L}^i for $i > 0$ has i^2 sections, and also the kernel of the map $V \ni x \mapsto t_x^* \mathcal{L} \otimes \mathcal{L}$ is finite, which is equivalent to H being non-degenerate (see [Pol03, Chapter 8.5–8.6]). But here

$$H = \begin{pmatrix} 2 & 1 \\ 1 & 2 \end{pmatrix}$$

has nonzero determinant, i.e. is nondegenerate, so that \mathcal{L} is ample and the claim applies. \square

Corollary 3.0.11. *The abelian variety V is projective.*

For the definition of split-generate, we need some preliminary definitions.

Definition 3.0.12. A category \mathcal{C} is *triangulated* if it contains all mapping cones, i.e. given any morphism f the object $\text{Cone}(f)$ is an object in \mathcal{C} . Rather, it contains the shift functor, the auto-equivalence $A \mapsto A[1]$ and it has a class of distinguished triangles.

Definition 3.0.13. A triangulated subcategory $\mathcal{D} \subset \mathcal{C}$ is *thick* if it closed under taking direct summands, i.e. $E \oplus F \in \text{Ob}(\mathcal{D}) \implies E, F \in \text{Ob}(\mathcal{D})$.

Definition 3.0.14. We say a set of objects $\{G_i\}_{i \in I} \in \text{Ob}(\mathcal{C})$ *split-generate* \mathcal{C} if their thick envelope is \mathcal{C} , namely if we take the smallest triangulated category containing the G_i which is closed under taking direct summands, we get all of \mathcal{C} .

Proof of claim. The following argument is from the MSRI Derived Categories summer school [APS, Lec 5.3]. Every complex is generated by its cohomology, so it suffices to prove that any coherent sheaf F lies in the thick envelope of $\mathcal{O}, \mathcal{L}, \mathcal{L}^2$, because then any element of

$D^b\text{Coh}(V)$ will be reached by the thick envelope, in other words we get that $\mathcal{O}, \mathcal{L}, \mathcal{L}^2$ split-generate.

We saw that V is projective, so that implies $\text{Coh}(V)$ has enough locally frees (reference). In particular, for sufficiently high n we have that $F(n)$ is generated by global sections, i.e. we have a surjective map $\mathcal{O}_X^n \rightarrow F(n)$ so tensoring with $\mathcal{O}(-n)$ and repeating the process with the kernel of $\mathcal{O}_X(-n)^n \rightarrow F$ we get a resolution of F by locally frees:

$$\dots P^{-N} \rightarrow P^{-N+1} \rightarrow \dots \rightarrow P^0 \rightarrow F \rightarrow 0$$

Define Q to be the complex obtained by cutting off in degree N :

$$Q := [P^{-N} \rightarrow \dots \rightarrow P^{-1} \rightarrow P^0]$$

Then Q lies in the thick envelope $\langle \mathcal{O}, \mathcal{L}, \mathcal{L}^2 \rangle$ because all the P^i have \mathcal{L}^i as summands and since $\langle \mathcal{O}, \mathcal{L}, \mathcal{L}^2 \rangle$ is a full exceptional collection (reference) it contains all powers of \mathcal{L} . We have an inclusion of complexes $P^\cdot \rightarrow Q$. The quotient is

$$G[N+1] = \dots \rightarrow P^{-N-1} \rightarrow 0 \rightarrow 0 \dots \rightarrow 0$$

where G is defined to be cohomology in degree $-N-1$ since the rest of the complex is exact. In particular, G is a coherent sheaf and we get a morphism

$$F \rightarrow G[N+1] \in \text{Ext}^{N+1}(F, G) \cong \text{Ext}^{2-N-1}(G, F \otimes \omega)^* = 0$$

by Serre duality. So we have

$$G[N] \longrightarrow Q \longrightarrow F \xrightarrow{0} G[N+1]$$

which implies $Q \cong G[N] \oplus F$. We know Q is in the thick envelope, and since it's thick, i.e. closed under direct summands, we get that F is in it too, hence we are done. \square

So it is enough to prove the fully-faithful embedding of categories by looking at the functor on $\mathcal{O}, \mathcal{L}, \mathcal{L}^2$, though at the expense of needing to know about higher A_∞ -products.

Towards HMS: fully-faithful embedding $D^b\text{Coh}(V) \hookrightarrow \text{Fuk}(V^\vee)$

The functor $D^b\text{Coh}(V) \rightarrow \text{Fuk}(V^\vee)$ is as follows. On objects we map $\mathcal{L}^{\otimes k} \mapsto \ell_k$. Recall Corollary 1.2.17 that $H^0(V, \mathcal{L}^{\otimes l})$ has the following basis of sections:

$$s_{e,l} := \sum_{\gamma} \tau^{-l\kappa(\gamma + \frac{\gamma_{e,l}}{l})} x^{-l\lambda(\gamma) - \gamma_{e,l}}$$

where $\gamma_{e,l} = s\gamma' + t\gamma''$, $0 \leq s, t < l$. So on morphisms the functor does the following (where s_i denotes the choices for $\gamma_{e,l}$):

$$\text{hom}(\mathcal{O}, \mathcal{L}) = H^0(V, \mathcal{L}) \ni s \mapsto p \in \text{hom}(\ell_0, \ell_1) = \bigoplus_{p \in \ell_0 \cap \ell_1} \mathbb{C} \cdot p = \mathbb{C} \cdot p$$

$$\text{hom}(\mathcal{O}, \mathcal{L}^2) = H^0(V, \mathcal{L}^2) \ni (s_1, s_2, s_3, s_4) \mapsto (p_1, p_2, p_3, p_4) \in \bigoplus_{p \in \ell_0 \cap \ell_2} \mathbb{C} \cdot p, \quad |\ell_0 \cap \ell_2| = 4$$

$$\text{hom}(\mathcal{L}, \mathcal{L}^2) \cong \text{hom}(\mathcal{O}, \mathcal{L}^* \otimes \mathcal{L}^2) \cong \text{hom}(\mathcal{O}, \mathcal{L}) = H^0(V, \mathcal{L}) \ni s \mapsto p' \in \text{hom}(\ell_1, \ell_2) = \mathbb{C} \cdot p'$$

Compatible with composition, namely:

$$\begin{aligned} s(x) &= \sum_{\gamma} \tau^{-\kappa(\gamma)} x^{-\lambda(\gamma)} \\ s^2(x) &= \sum_{\tilde{\gamma}, \tilde{\tilde{\gamma}}} \tau^{-\kappa(\tilde{\gamma}) - \kappa(\tilde{\tilde{\gamma}})} x^{-\lambda(\tilde{\gamma}) - \lambda(\tilde{\tilde{\gamma}})} \\ \text{hom}(\mathcal{L}, \mathcal{L}^2) \otimes \text{hom}(\mathcal{O}, \mathcal{L}) \ni s^2(x) &= c_1 s_1 + c_2 s_2 + c_3 s_3 + c_4 s_4 \\ &\leftrightarrow \mu^2(p, p') = c_1 p_1 + c_2 p_2 + c_3 p_3 + c_4 p_4 \end{aligned}$$

In particular, we expect the coefficients c_i to be theta functions $s(x)$ for a particular value of x , analogous to the calculation in [PZ98]. We wish to express $s^2(x)$ in terms of this basis for $H^0(V, \mathcal{L}^2)$. We split the sum above for $s^2(x)$ into four sums, corresponding to the four possible parities of the coefficients on the pair γ', γ'' in $\tilde{\gamma} + \tilde{\tilde{\gamma}}$. We then do a coordinate change

$$\begin{aligned} \gamma &= \frac{1}{2}(\tilde{\gamma} + \tilde{\tilde{\gamma}} - \gamma_e), \eta = \frac{1}{2}(\tilde{\tilde{\gamma}} - \tilde{\gamma} - \gamma_e) \\ \gamma_e &\in \{0, \gamma', \gamma'', \gamma' + \gamma''\} \end{aligned}$$

For example, if $\tilde{\gamma} + \tilde{\tilde{\gamma}} = (n_1 + m_1)\gamma' + (n_2 + m_2)\gamma''$ and $n_1 + m_1$ and $n_2 + m_2$ are both even, that means we can write $\tilde{\gamma} + \tilde{\tilde{\gamma}}$ as 2γ for some $\gamma \in \Gamma_B$. If they are odd and even then we must subtract off γ' , etc. That's how we get the four choices for γ_e . Now we can write $s^2(x)$ in terms of the $s_i(x)$ by separating into four sums corresponding to the four parity choices.

Also recall that the quadratic form κ satisfies $\kappa(\gamma + \eta) = \kappa(\gamma) + \kappa(\eta) - \langle \gamma, \lambda(\eta) \rangle$.

$$\begin{aligned}
s^2(x) &= \sum_{\tilde{\gamma}, \tilde{\gamma}} \tau^{-\kappa(\tilde{\gamma}) - \kappa(\tilde{\gamma})} x^{-\lambda(\tilde{\gamma} + \tilde{\gamma})} \\
&= \sum_{\gamma, \eta} \tau^{-\kappa(\gamma - \eta) - \kappa(\gamma + \eta)} x^{-2\lambda(\gamma)} + \tau^{-\kappa(\gamma + \gamma'/2 - \eta - \gamma'/2) - \kappa(\gamma + \gamma'/2 + \eta + \gamma'/2)} x^{-2\lambda(\gamma)} x_1^{-1} \\
&\quad + \tau^{-\kappa(\gamma + \gamma''/2 - \eta - \gamma''/2) - \kappa(\gamma + \gamma''/2 + \eta + \gamma''/2)} x^{-2\lambda(\gamma)} x_2^{-1} \\
&\quad + \tau^{-\kappa(\gamma + (\gamma' + \gamma'')/2 - \eta - (\gamma' + \gamma'')/2) - \kappa(\gamma + (\gamma' + \gamma'')/2 + \eta + (\gamma' + \gamma'')/2)} x^{-2\lambda(\gamma)} (x_1 x_2)^{-1} \\
&= \sum_{\eta} \tau^{-2\kappa(\eta)} \sum_{\gamma} \tau^{-2\kappa(\gamma)} x^{-2\lambda(\gamma)} + \sum_{\eta} \tau^{-2\kappa(\eta + \gamma'/2)} \sum_{\gamma} \tau^{-2\kappa(\gamma + \gamma'/2)} x^{-2\lambda(\gamma)} x_1^{-1} \\
&\quad + \sum_{\eta} \tau^{-2\kappa(\eta + \gamma''/2)} \sum_{\gamma} \tau^{-2\kappa(\gamma + \gamma''/2)} x^{-2\lambda(\gamma)} x_2^{-1} \\
&\quad + \sum_{\eta} \tau^{-2\kappa(\eta + (\gamma' + \gamma'')/2)} \sum_{\gamma} \tau^{-\kappa(\gamma + (\gamma' + \gamma'')/2)} x^{-2\lambda(\gamma)} (x_1 x_2)^{-1} \\
&= \sum_{\eta} \tau^{-2\kappa(\eta)} s_1 + \sum_{\eta} \tau^{-2\kappa(\eta + \gamma'/2)} s_2 + \sum_{\eta} \tau^{-2\kappa(\eta + \gamma''/2)} s_3 + \sum_{\eta} \tau^{-2\kappa(\eta + (\gamma' + \gamma'')/2)} s_4
\end{aligned}$$

Claim 3.0.15. The coefficients on the s_i match up with the triangle counts, i.e. μ^2 in the Fukaya category.

Proof. Let $\tilde{\cdot}$ denote lifts to the universal cover \mathbb{R}^4 . There are four choices for where to place $\tilde{\ell}_0 \cap \tilde{\ell}_2$ in the triangle (the other choices producing the same triangles on the abelian variety). From the calculation in Equation 3.1, we take these to be $(\gamma_e/2, 2M^{-1}(\gamma_e/2)) = (\gamma_e/2, \lambda(\gamma_e))$ because λ is the linear map M^{-1} .

$$\tilde{p}_e = (\gamma_e/2, \lambda(\gamma_e))$$

We know the lift \tilde{p} of $p = \ell_0 \cap \ell_1$ must lie on $\tilde{\ell}_0$ which goes through \tilde{p}_e . Since there is no change in the second two coordinates along $\tilde{\ell}_0$ this means $\lambda(\gamma_e)$ is the angular coordinates. And \tilde{p} lies above $(0, 0)$ so the first coordinate is some $\eta \in \Gamma_B$.

$$\tilde{p} = (\eta, \lambda(\gamma_e))$$

If \tilde{p} is at $(0, 0)$, then the lift of $p' = \ell_1 \cap \ell_2$ is some $(\xi, M^{-1}(\xi)) = (\xi, \lambda(\xi))$ because $\tilde{\ell}_2$ would go through the origin (assume clockwise ordering of the Lagrangians). Since it is potentially shifted by $(\eta, \lambda(\gamma_e))$, we get that $\tilde{p}' = (\eta, \lambda(\gamma_e)) + (\xi, \lambda(\xi))$ for some ξ . This ξ is determined by the fact that $\tilde{p}'\tilde{p}_e$ lies on $\tilde{\ell}_2$ i.e. the angle changes by 2λ .

$$\begin{aligned}
\tilde{p}'\tilde{p}_e &= \langle \eta + \xi - \gamma_e/2, \lambda(\gamma_e + \xi) - \lambda(\gamma_e) \rangle \\
\implies 2\lambda(\eta + \xi - \gamma_e/2) &= \lambda(\xi) \therefore \xi = \gamma_e - 2\eta \\
\therefore \tilde{p}' &= (\gamma_e - \eta, 2\lambda(\gamma_e - \eta))
\end{aligned}$$

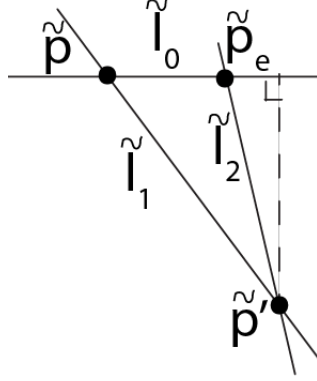


Figure 3.1: A triangle in the elliptic curve case and representative of the T^4 case

Now that we have three points of the triangle, we want to find the area. Motivated the picture in the elliptic curve case (see Figure 3.1), we see that if we extend \tilde{p}_e along the line between \tilde{p}_e and \tilde{p} in the direction away from \tilde{p} by the same distance that \tilde{p} is, we get a right triangle. This can be seen because the three sides form a Pythagorean triple:

$$|\eta - \gamma_e/2|^2 + |\lambda(\gamma_e - 2\eta)|^2 = (\text{length of third side})^2$$

So taking half the length in the base, and the same height, we get the area of the triangle:

$$\frac{1}{2} \int_{\Delta} d\xi \wedge d\theta = \langle (\eta - \gamma_e/2), \lambda(\eta - \gamma_e/2) \rangle = -2\kappa(\eta - \gamma_e/2)$$

This agrees with the exponents on τ on the complex side, and hence completes the proof of the claim. \square

Now we want to prove that multiplication matches up in the more general setting for $i < j < k$. First we consider the line bundles. We have $\text{Hom}(\mathcal{L}^i, \mathcal{L}^j) \cong H^0(V, \mathcal{L}^{j-i})$ so let $l := j - i$ and $l' := k - j$. We take the following basis for \mathcal{L}^l :

$$s_{e,l} := \sum_{\gamma} \tau^{-l\kappa(\gamma + \frac{\gamma_{e,l}}{l})} x^{-\lambda(l\gamma - \gamma_{e,l})}$$

In particular, $\gamma_{e,l} = s\gamma' + t\gamma''$ for some $0 \leq s, t < l$, which gives us l^2 basis elements for $H^0(V, \mathcal{L}^l)$. We want to write the product of two such sections in terms of the basis for $H^0(V, \mathcal{L}^{l+l'})$, and compare coefficients with the triangle count on the other side.

$$s_{e,l} \cdot s_{e,l'} = \sum_{\tilde{\gamma}, \tilde{\gamma}'} \tau^{-l\kappa(\tilde{\gamma} + \frac{\gamma_{e,l}}{l}) - l'\kappa(\tilde{\gamma}' + \frac{\gamma_{e,l'}}{l'})} x^{-\lambda(l\tilde{\gamma} + \gamma_{e,l} + l'\tilde{\gamma}' + \gamma_{e,l'})}$$

We want to write this in terms of the similar basis for $H^0(V, \mathcal{L}^{l+l'})$:

$$s_e := \sum_{\gamma} \tau^{-(l+l')\kappa(\gamma + \frac{\gamma_e}{l+l'})} x^{-(l+l')\lambda(\gamma + \frac{\gamma_e}{l+l'})}$$

Comparing with the powers of x in the product, we define γ by considering the sum $l\tilde{\gamma} + \gamma_{e,l} + l'\tilde{\tilde{\gamma}} + \gamma_{e,l'}$ as an element in $(l+l')\Gamma_B$ plus a remainder γ_e . Namely define this element to be $\gamma \in \Gamma_B$ and denote the remainder as γ_e :

$$(l+l')\gamma + \gamma_e := l\tilde{\gamma} + \gamma_{e,l} + l'\tilde{\tilde{\gamma}} + \gamma_{e,l'}$$

Analogous to the $(i, j, k) = (0, 1, 2)$ case above, we want to find a change of coordinates in terms of new variables A, B satisfying the following equality, as exponents of τ :

$$\left(\tilde{\gamma} + \frac{\gamma_{e,l}}{l}, \tilde{\tilde{\gamma}} + \frac{\gamma_{e,l'}}{l'}\right) = \left(A - \frac{B}{l}, A + \frac{B}{l'}\right)$$

because $-l\kappa(A - \frac{B}{l}) - l'\kappa(A + \frac{B}{l'}) = -(l+l')\kappa(A) - (\frac{1}{l} + \frac{1}{l'})\kappa(B)$. We will want $A = \gamma + \frac{\gamma_e}{l+l'}$, which does hold. And B should be a function of a variable η and a remainder term, so that $\eta \in \Gamma_B$. We make the following definition for which this is true, and the motivation will become clear when counting triangles below.

$$B = \frac{l'l'}{l+l'} \left(\tilde{\gamma} + \frac{\gamma_{e,l}}{l} - \tilde{\tilde{\gamma}} - \frac{\gamma_{e,l'}}{l'}\right) =: \eta - \frac{l\gamma_e}{l+l'}$$

Claim 3.0.16. $\eta \in \Gamma_B$.

Proof.

$$\begin{aligned} \eta &= \frac{l'l'}{l+l'} \left(\tilde{\gamma} + \frac{\gamma_{e,l}}{l} - \tilde{\tilde{\gamma}} - \frac{\gamma_{e,l'}}{l'}\right) + \frac{l\gamma_e}{l+l'} \\ &= \frac{1}{l+l'} (l'l'\tilde{\gamma} + l'\gamma_{e,l} - l\tilde{\tilde{\gamma}} - l\gamma_{e,l'} - l(l+l')\gamma + l^2\tilde{\tilde{\gamma}} + l\gamma_{e,l} + l\tilde{\tilde{\gamma}} + l\gamma_{e,l'}) \\ &= l\tilde{\tilde{\gamma}} + \gamma_{e,l} - l\gamma \in \Gamma_B \end{aligned}$$

□

Corollary 3.0.17.

$$\begin{aligned} s_{e,l} \cdot s_{e,l'} &= \sum_{\tilde{\gamma}, \tilde{\tilde{\gamma}}} \tau^{-l\kappa(\tilde{\gamma} + \frac{\gamma_{e,l}}{l}) - l'\kappa(\tilde{\tilde{\gamma}} + \frac{\gamma_{e,l'}}{l'})} x^{-\lambda(l\tilde{\gamma} + \gamma_{e,l} + l'\tilde{\tilde{\gamma}} + \gamma_{e,l'})} \\ &= \sum_{\gamma, \eta} \tau^{-l\kappa(\gamma + \frac{\gamma_e}{l+l'} - \frac{1}{l}(\eta - \frac{l\gamma_e}{l+l'})) - l'\kappa(\gamma + \frac{\gamma_e}{l+l'} + \frac{1}{l'}(\eta - \frac{l\gamma_e}{l+l'}))} x^{-(l+l')\lambda(\gamma) - \lambda(\gamma_e)} \\ &= \sum_{\eta} \tau^{-\left(\frac{1}{l} + \frac{1}{l'}\right)\kappa(\eta - \frac{l\gamma_e}{l+l'})} \sum_{\gamma} \tau^{-(l+l')\kappa(\gamma + \frac{\gamma_e}{l+l'})} x^{-(l+l')\lambda(\gamma) - \lambda(\gamma_e)} \end{aligned}$$

Claim 3.0.18. The left vertical functor $D^b\text{Coh}(V) \rightarrow \text{Fuk}(V^\vee)$ respects composition.

Proof. We compare the coefficients in the expression for the product of two sections with the triangle count. Take p_1, p_2, p_3 for $\ell_i \cap \ell_k, \ell_i \cap \ell_j$ and $\ell_j \cap \ell_k$ respectively. We have $(l+l')^2$ choices for $\ell_i \cap \ell_k$ as follows:

$$p_1 = \left(\frac{\gamma_e}{k-i}, -\frac{k}{k-i} \lambda(\gamma_e) \right)$$

Then $p_2 \vec{p}_1$ lies on $\tilde{\ell}_i$ so takes the form $(\xi, -i\lambda(\xi))$. Also, p_2 lies on a lift of ℓ_i so is also of this form (we use η/l so $\eta \in \Gamma_B$ will ultimately agree with the η used above in the multi-theta functions), up to a shift by a lattice element, which turns out to be $(0, \lambda(\gamma_e))$.

$$\begin{aligned} p_2 &= \left(\frac{\eta}{l}, -i\lambda\left(\frac{\eta}{l}\right) - \lambda(\gamma_e) \right) \\ p_2 \vec{p}_1 &= \left(\frac{\gamma_e}{k-i} - \frac{\eta}{l}, -\frac{k}{k-i} \lambda(\gamma_e) + i\lambda\left(\frac{\eta}{l}\right) + \lambda(\gamma_e) \right) = (\xi, -i\lambda(\xi)) \end{aligned}$$

Then $p_3(A, B)$ has two conditions as follows.

$$\begin{aligned} p_2 \vec{p}_3 &= \left(A - \frac{\eta}{l}, B + i\lambda\left(\frac{\eta}{l}\right) + \lambda(\gamma_e) \right) \\ \therefore B + i\lambda\left(\frac{\eta}{l}\right) + \lambda(\gamma_e) &= -j\lambda\left(A - \frac{\eta}{l}\right) \\ p_1 \vec{p}_3 &= \left(A - \frac{\gamma_e}{k-i}, B + \frac{k}{k-i} \lambda(\gamma_e) \right) \\ \therefore B + \frac{k}{k-i} \lambda(\gamma_e) &= -k\lambda\left(A - \frac{\gamma_e}{k-i}\right) \\ \implies B &= -k\lambda(A) \\ \implies -k\lambda(A) &= -j\lambda(A) + (j-i)\lambda\left(\frac{\eta}{l}\right) - \lambda(\gamma_e) \\ \implies (k-j)A &= (i-j)\frac{\eta}{l} + \gamma_e \\ \therefore A &= \frac{i-j}{k-j} \frac{\eta}{l} + \frac{1}{k-j} \gamma_e = -\frac{1}{l'} \eta + \frac{1}{l'} \gamma_e \\ B &= -k\lambda(A) \end{aligned}$$

We set $\zeta := -\frac{\eta}{l} + \frac{\gamma_e}{l+l'}$ since the expression shows up in multiple places. To get the symplectic area of the triangle (which is the same under homotopy invariance, i.e. for any holomorphic triangle with these corners), we take $\frac{1}{2} \int_P d\xi \wedge d\theta$ where P is the parallelogram spanned by

$$\vec{a} := p_2 \vec{p}_1 = \left(\frac{\gamma_e}{l+l'} - \frac{\eta}{l}, -i\lambda\left(\frac{\gamma_e}{l+l'} - \frac{\eta}{l}\right) \right) = (\zeta, -i\lambda(\zeta))$$

and to define the other vector $\vec{b} := p_1 \vec{p}_3$ we will consider the following expression, so we simplify it first:

$$-\frac{1}{l'} \eta + \frac{1}{l'} \gamma_e - \frac{\gamma_e}{l+l'} = \frac{l}{l'} \left(-\frac{\eta}{l} + \frac{\gamma_e}{l+l'} \right) = \frac{l}{l'} \zeta$$

hence we define

$$\vec{b} := p_1 \vec{p}_3 = \left(\frac{l}{l'} \zeta, -k\lambda\left(\frac{l}{l'} \zeta\right) \right)$$

because we've set \tilde{l}_k to go through the origin hence points on \tilde{l}_k and vectors parallel to it are both of the form $(\xi, -k\lambda(\xi))$. Finally we can compute the symplectic area.

$$\begin{aligned} \frac{1}{2} \int_P d\xi \wedge d\theta &= \frac{1}{2} (a_\xi \cdot b_\theta - a_\theta \cdot b_\xi) = \frac{1}{2} \left\langle \zeta, -k\lambda\left(\frac{l}{l'} \zeta\right) \right\rangle - \frac{1}{2} \left\langle -i\lambda(\zeta), \frac{l}{l'} \zeta \right\rangle \\ &= \left(\frac{kl}{l'} - \frac{il}{l'} \right) \kappa(\zeta) = \frac{l+l'}{ll'} \kappa \left(-\eta + \frac{l\gamma_e}{l+l'} \right) \end{aligned}$$

We obtain the same exponent as on τ above, namely $-\left(\frac{1}{l} + \frac{1}{l'}\right) \kappa\left(\eta - \frac{l\gamma_e}{l+l'}\right)$, since κ is an even function. □

Note: rename η so doesn't conflict with previous $\eta \geq \phi(\xi)$. Note the latter η only makes sense on \tilde{Y} and doesn't descend to the quotient.

Claim 3.0.19. The triangles described above bounded by ℓ_i, ℓ_j, ℓ_k are holomorphic.

Before we prove this, we recall that Lagrangian Floer theory in the setting of the example of this paper is independent of *regular* or *generic* J , as follows.

Lemma 3.0.20. *There exists a dense set $\mathcal{J}_{reg} \subset \mathcal{J}(Y, \omega)$ of ω -compatible almost complex structures J such that, for all J -holomorphic maps $u : \mathbb{D} \rightarrow Y$ with suitable Lagrangian boundary condition, the linearized $\bar{\partial}$ -operator D_u is surjective.*

We postpone the proof to our discussion of regularity below in more generality.

Lemma 3.0.21. *The counts μ_2 for J_1 and J_2 on V^\vee are equal.*

Sketch. This will rely on arguments from the proof of the previous statement. The argument will be the same, but our Fredholm problem will have an additional $[0, 1]$ factor in the Banach bundle setup. So we will obtain a 1-dimensional manifold. There is no other boundary expected because 1) sphere bubbling happens in codimension 2 so doesn't appear in a 1-dimensional space, 2) strip breaking would break off a bigon but there are no bigons on a torus by parameter translation considerations and dimensional/index reasons (namely all intersection points have the same index and a broken strip would have indices differing by 2, c.f. the Morse analogue with flow lines) and 3) disc bubbling doesn't occur because Lagrangians don't bound discs on a torus (since π_2 is preserved upon taking the universal cover of the torus which has no π_2). Since the signed boundary of a 1-dimensional manifold is zero, we get $\mathcal{M}(3 \text{ pts, homol class}, J_1) = \mathcal{M}(3 \text{ pts, homol class}, J_2)$ for regular J_1 and J_2 . The existence of a dense set of regular paths is similar to the above proof for the existence of regular J . □

Now we can prove that the triangles counted above are J -holomorphic for a particular suitable regular J .

Proof of Claim 3.0.19. To count the triangles, we pick the most convenient J . We want J to properly transform ∂_ξ . If we vary one complex coordinate, keeping the other two constant, that won't work because v_0 can't remain constant, as it should on a fiber. So instead vary one complex coordinate, then keep another and v_0 constant.

Take the J that is off diagonal with $\lambda = \begin{pmatrix} 2 & 1 \\ 1 & 2 \end{pmatrix}^{-1}$, $-\lambda^{-1}$ in lower left and upper right, wrt the ξ, θ coordinates. Squares to $-I$ and can check compatible because multiplying the standard symplectic form from $d\xi \wedge d\theta$ with this J we do indeed get a metric, i.e. positive definite. Taking the universal cover of V^\vee , we split up the resulting linear space into a product of two planes, $P := \langle \zeta, \lambda(\zeta) \rangle$ and P^ω the symplectic orthogonal complement. In particular, P and P^ω are J -holomorphic planes, by definition of J .

We then show that the triangles above, spanned by \vec{a} and \vec{b} which are $(\zeta, 0) \in \langle \partial_{\xi_i} \rangle_i$ and $(0, \lambda(\zeta)) \in \langle \partial_{\theta_i} \rangle_i$ up to sign, are holomorphic with respect to this J . Thus $\tilde{\ell}_i$ is a product, a linear triangle in the $\zeta, \lambda(\zeta)$ plane and a constant in the symplectic orthogonal. The ξ directions and θ directions have a suitable change of variable property because $\theta = -i\lambda(\xi) + c$.

Now that we can work in components P and P^ω , we have a holomorphic disc in P where J is a complex structure (as every almost complex structure is integrable in two dimensions) with a specified Lagrangian boundary condition so by the Riemann mapping theorem it's unique. Also, $\tilde{\ell}_i$ is constant in P^ω so the boundary condition of the projection of the 3-punctured disc to that plane must be constant. A further corollary is that the discs are regular by standard regularity arguments in the plane.

□

Remark 3.0.22. This J is a bit unusual compared to the standard J_0 that is multiplication by i in each component. If one thinks of a soap bubble in the corner of a room, which minimizes area i.e. is J_0 -holomorphic, it will be pulled in quite a bit to the vertex of the corner. However for this J , the area-minimizing triangles are linear.

Chapter 4

The Fukaya category

4.1 The Fukaya-Seidel category of Y : introduction

The Fukaya category for symplectic manifolds, and the Fukaya-Seidel category for symplectic fibrations, are A_∞ -categories. In what follows, we consider a subcategory of the Fukaya-Seidel category of $v_0 : Y \rightarrow \mathbb{C}$. We then prove, passing to the cohomology level where the A_∞ -category becomes a category, that this subcategory is equivalent to the bounded derived category of coherent sheaves on the hypersurface $H = \Sigma_2$.

Remark 4.1.1 (Not exact, not compact, Hamiltonian perturbation method not used). In [Sei08] the Fukaya category of a Lefschetz fibration has Lagrangians given by thimbles obtained by parallel transporting a sphere to the singular point in the Morse singular fiber where it gets pinched to a point. In our situation, the degenerate fiber over 0 is not a Lefschetz singularity (i.e. modeled on $\sum_i |z_i|^2$) but instead the fiber T^4 degenerates by collapsing a family of S^1 's, and also collapsing a T^2 in two points. So instead, we will consider Lagrangians that go around this singular fiber, with suitable behavior at infinity governed by the superpotential v_0 . This is because it is a smoothing of two fiber Lagrangians parallel transported to the central fiber. This is the notion of a U-shaped curve from [AS].

One difference of our set-up to that in [Sei08] is that we are in the non-exact case so there are sphere bubbles. Also the manifold is non-compact in the base of the fibration v_0 , or equivalently we can restrict to a neighborhood of the origin and then it will have boundary. Another difference is that although Seidel in some later papers defines the Fukaya category on U-shaped curves, he uses Hamiltonian perturbations where the symplectic form used is a product on the base and fiber. Since the symplectic form is not a product here, we instead use the notion of *categorical localization* of [AS] and Ganatra's notes.

Example 4.1.2 (Not monotone). We are also not in the monotone setting, which is another standard setting. To define monotone, we illustrate through the following example of Oh of the Clifford torus [Oh93].

Definition 4.1.3 (Maslov index of a map). Given $u : (\mathbb{D}, \partial\mathbb{D}) \rightarrow (M, L)$ we first trivialize u^*TM over the disc. Then the Maslov index counts the rotation of \mathbb{R} around the boundary in this trivialized pullback.

Definition 4.1.4. A *monotone* Lagrangian L in symplectic manifold (M, ω) is such that $[\omega] = k \cdot [\mu(u)]$ for all $u \in \pi_2(M, L)$, for some constant k . Namely, the areas of discs are proportional to the Maslov indices of those discs.

To obtain $\pi_2(M, L)$ in the case of $L \cong T^n$ the Clifford torus and $M := \mathbb{C}\mathbb{P}^n$, we can use the homotopy exact sequence for the pair of manifolds to get a split exact sequence (split because the boundary map has an inverse map by inclusion) and then $\pi_2(\mathbb{C}\mathbb{P}^n)$ follows from the homotopy exact sequence on the fiber bundle $S^1 \rightarrow S^{2n+1} \rightarrow \mathbb{C}\mathbb{P}^n$.

This gives us a basis of $H^2(M, L)$ on which to check that Maslov indices and area are proportional. In fact, we only need to check on two elements because the rest in the Clifford T^n are the same by symmetry. In T^n , the maps $w_k(z) = [1 : \dots : 0 : z : 0 \dots : 0]$ for $k > 0$ have index 2 because we rotate one full rotation, so the line \mathbb{R} is rotated twice.

The difference of Maslov index for two maps u and u' with $u|_{\partial\mathbb{D}} = u'|_{\partial\mathbb{D}}$ is $\int_{u(\mathbb{D}^2) \cup u'(\overline{\mathbb{D}^2})} 2c_1(M)$. Thus the disc map $w_0 : \mathbb{D} \rightarrow M$ defined by $\{[z : 0 : \dots : 0]\}_{z \in \mathbb{D}}$ has Maslov index $2c_1(\mathbb{C}\mathbb{P}^n) = 2(n+1)$; this is because we can think of w_0 as gluing on a constant disc, or equivalently a sphere attached to T^n by a slender tube, via the image of a generator in $\pi_2(\mathbb{C}\mathbb{P}^n)$ under the homotopy long exact sequence. Ultimately we find

$$\frac{\text{Area}(w_1)}{\text{Area}(w_0)} = \frac{1}{n+1} = \frac{\mu(w_1)}{\mu(w_0)}$$

In this thesis, all discs considered have Maslov index 2, but the areas vary as prescribed by a formula of [CO06] which we will elaborate on later.

Now that we've indicated how this set-up differs from those currently in the literature, we give an outline of the sections below that first define the Fukaya-Seidel category and then prove the HMS statement. In Sections 4, 4, and 4 we discuss monodromy around the central fiber in $v_0 : Y \rightarrow \mathbb{C}$ because it will be needed to define the Lagrangians in the subcategory of $FS(Y, v_0)$ we will consider. Then Section 4.2 sets up the background needed to define the structure maps in $H^0FS(Y, v_0)$, and Section 4.3 proves the moduli spaces involved in these structure maps have the required conditions to be put into the definition. Finally we give the definition in Section 4.4 and show it's well-defined for regular choices of datum.

Monodromy background

We define monodromy. This is how we will obtain Lagrangians in the total space, by parallel transporting Lagrangians in the fiber. We will define Darboux coordinates in local

charts, also called action-angle coordinates. This will enable us to do symplectic geometry calculations in the Fukaya category.

Definition 4.1.5. A *symplectic fibration* is a symplectic manifold (Y, ω) with a fibration such that fibers of the fibration are symplectic with respect to ω .

Example 4.1.6. In this paper, we've constructed (Y, ω) so that $v_0 : Y \rightarrow \mathbb{C}$ is a symplectic fibration.

Definition 4.1.7. The *symplectic horizontal distribution* of a symplectic fibration $\pi : Y \rightarrow C$ to a base manifold C is $H \subset TY$ such that if F is a generic fiber of π then $H = TF^\omega$ is the ω -complement, i.e.

$$\omega(H, TF) = 0$$

Definition 4.1.8. Given two points $p_0, p_1 \in C$ and a path $\gamma : I \rightarrow C$ between them (i.e. $\gamma(0) = p_0$ and $\gamma(1) = p_1$), the *parallel transport map* is a symplectomorphism $\Phi : F_{p_0} \rightarrow F_{p_1}$ defined as follows: given $x \in F_{p_0}$ and $v \in T_x F_{p_0}$, we set $\Phi(x)$ to be $\tilde{\gamma}(1)$ where $\tilde{\gamma} : I \rightarrow Y$ such that $\pi \circ \tilde{\gamma} = \gamma$, $d\pi(\tilde{\gamma}') = \gamma'$ and $\tilde{\gamma}'$ is in the horizontal distribution.

Remark 4.1.9. This last condition implies Φ is a symplectomorphism.

Definition 4.1.10. *Monodromy* is parallel transport around a loop going once around a singularity in the base.

The main result of this section is the following, illustrated in Figure 4.1:

Lemma 4.1.11. *The monodromy in each compartment of parallelogram T_B is as follows: away from the tropical curve we obtain $(0, 0)$ in the upper right corner where $r_z^{-1} \gg r_x^{-1}, r_y^{-1}$, then $(0, 1)$ on the right where r_y^{-1} is the largest, $(1, 0)$ on the left where r_x^{-1} largest and thus $(1, 1)$ in the bottom left corner.*

Remark 4.1.12. We say a few words to illuminate the geometry depicted in Figure 4.1. A v_0 -fiber V^\vee can be described in action-angle coordinates $(\xi_1, \xi_2, \theta_1, \theta_2)$. A linear Lagrangian ℓ_i is a graph of a linear function on $\xi := (\xi_1, \xi_2)$. In other words, it is parametrized by the hexagon. When we parallel transport V^\vee about the origin, $\phi(\ell_i)$ is still parametrized by the hexagon but the angles have rotated according to the monodromy. This is calculated below.

Claim 4.1.13. $\phi(\ell_i)$ is Lagrangian in V^\vee with respect to $\omega|_{V^\vee}$, also a symplectic form as v_0 is a symplectic fibration with respect to ω .

Proof. Parallel transport is defined by taking $H := (TF)^\omega$, the symplectic complement of the fiber. Thus the monodromy is a symplectomorphism, e.g. see [MS17], and so preserves Lagrangians. \square

Remark 4.1.14 (Notation). Let $F := V^\vee$ and hereafter F will refer to the Kähler potential function defining the symplectic form, and a fiber of v_0 will be denoted V^\vee .

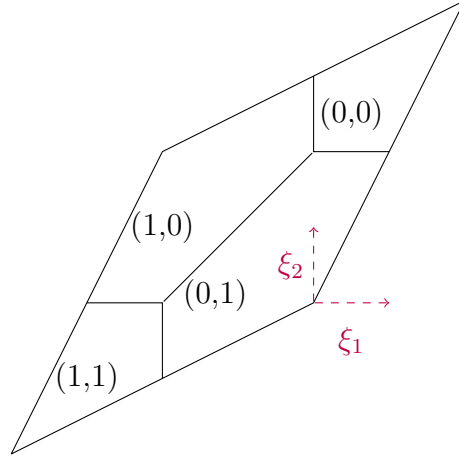


Figure 4.1: Monodromy in fiber, thought of as a section over the parallelogram $(\xi_1, \xi_2) \mapsto (\theta_1(\xi_1, \xi_2), \theta_2(\xi_1, \xi_2))$.

Remark 4.1.15 (Caveat). We next define the action-angle coordinates arising from the symplectic form. We will find that the image of the moment map is the same as the toric polytope, an instance of Delzant's theorem e.g. see [MS17]. Note that a usual moment map would land in \mathbb{R}^n where n is the dimension of the torus, but here the moment map will land in \mathbb{R}^3/Γ_B instead.

Claim 4.1.16 (Definition of action-angle coordinates). Let $\theta_1 := \arg(x)$, $\theta_2 := \arg(y)$, $\theta_3 = \arg(z)$, where x, y, z are the complex toric coordinates. They are defined in the following region: $|v_0| = |xyz| \leq T^\ell$ for sufficiently large ℓ where we remove a branch cut along $v_0 \in \mathbb{R}_-$, and $x, y \in (\mathbb{C}^*)^2/\Gamma_B$. Then there exist coordinates ξ_1, ξ_2 so that $\omega|_{V^\vee} = d\xi_1 \wedge d\theta_1 + d\xi_2 \wedge d\theta_2$, which we may abbreviate as $d\xi \wedge d\theta$. Note that ξ_3, θ_3 are not defined globally, hence the branch cut. We have a third coordinate pair $\eta, \theta_\eta := \arg(v_0)$, where $\eta = \xi_1 + \xi_2 + \xi_3$.

Proof. We have a local T^3 -action, for which we use the symbol α_i as coordinates because θ_i is already used as above.

$$\rho : T^3 \times Y \rightarrow Y, \quad \rho((\alpha_1, \alpha_2, \alpha_3), (x, y, z)) = (e^{2\pi i \alpha_1} x, e^{2\pi i \alpha_2} y, e^{2\pi i \alpha_3} z)$$

In particular on the coordinate v_0 this corresponds to $e^{2\pi i(\alpha_1 + \alpha_2 + \alpha_3)} v_0$. When v_0 has made a full rotation around the origin, the values of θ_1, θ_2 have changed according to the monodromy, thus the S^1 -action on v_0 is not globally defined. That's why we remove the branch cut above.

The infinitesimal action of α_1 and α_2 on Y is expressed by the pushforwards $X_i := d\rho(\partial_{\alpha_i})$ for $i = 1, 2$. If $\iota_{X_i} \omega|_{V^\vee}$ were exact, say dH_i for some function H_i (known as the Hamiltonian), then the torus action would be called a *Hamiltonian group action* and (H_1, H_2) would be the moment map. This leads us to the caveat in Remark 4.1.15. In the setting here, ω

is complicated so computing $\iota_{X_i}\omega|_{V^\vee}$ is involved. However, we do know that differential forms on a torus \mathbb{R}^4/Λ with Λ -periodic coordinates a_1, a_2, a_3, a_4 are generated over \mathbb{C} by da_1, \dots, da_4 , non-exact because the a_i aren't globally defined. Thus there exist Γ_B -periodic functions ξ_1, ξ_2 so that

$$\begin{aligned} \iota_{X_i}\omega|_{V^\vee} = d\xi_i &\implies \omega|_{V^\vee} = d\xi \wedge d\theta \\ \implies \iota_{X_i}\left(\frac{i}{2\pi}\partial\bar{\partial}F\right) &= \frac{i}{2\pi}d\iota_{X_i}\partial F = d\xi_i \\ \therefore \xi_1 &:= \frac{i}{2\pi}\partial F(2\pi ix\partial_x) = -\frac{1}{2}xe^{-i\theta_x}\frac{\partial F}{\partial|x|} \\ \therefore \xi_1 &= -\frac{1}{4}\frac{\partial F}{\partial|x|^2}, \quad \xi_2 = -\frac{1}{4}\frac{\partial F}{\partial|y|^2} \end{aligned}$$

using $\partial\bar{\partial} = -\bar{\partial}\partial = -d\partial$, the conversion to polar coordinates from §2.2 and that F is preserved by rotating x, y, z as it is a function of their norms, hence the Lie derivative $\mathcal{L}_{X_i}\bar{\partial}F = 0$ and also $\partial_{\theta_x}F = 0$. The upshot is that the moment map (ξ_1, ξ_2) provides periodic action-coordinates which are monotonic increasing in $|x|$ and $|y|$ because of how we defined F . (But recall the caveat, we are calling it a moment map but it takes values in a torus instead of affine space, so we are expanding the definition of moment map here to include that case. Typically the ξ_i should not be periodic.) We see that V^\vee is symplectomorphic to (T^4, ω_{std}) .

Note that an orbit is precisely the kernel of $(d\xi_1, d\xi_2)$ so that a preimage of a moment map value is a T^2 -orbit. Said another way, the torus action preserves the moment map. Or said a third way, the tangent space to a fiber of the moment map is $\partial_{\theta_1}, \partial_{\theta_2}$.

Note that the coordinates (ξ_1, ξ_2, η) are periodic by $\xi \sim \xi + \gamma$ and $\eta \geq \varphi(\xi)$, so $\varphi(\xi + \gamma) = \varphi(\xi) - \kappa(\gamma) + \langle \xi, \lambda(\gamma) \rangle$ implies $\eta \sim \eta - \kappa(\gamma) + \langle \xi, \lambda(\gamma) \rangle$, when $\gamma \in \Gamma_B$. \square

Corollary 4.1.17. *The ℓ_k are Lagrangian in a fiber.*

Proof. We have ℓ_k is the graph $\Gamma_{kM^{-1}(\xi)}$. So

$$T\ell_k = \langle \partial_{\xi_i} + kM^{-1}(\partial_{\theta_i}) \rangle_{i=1,2}$$

and

$$\omega(\partial_{\xi_1} + kM^{-1}(\partial_{\theta_1}), \partial_{\xi_2} + kM^{-1}(\partial_{\theta_2})) = 0$$

because ω only picks up terms from $d\xi_1 \wedge d\theta_1$ or $d\xi_2 \wedge d\theta_2$. \square

Remark 4.1.18 (Notation). μ_X refers to S^1 -action in the last coordinate. μ_Y refers to the local T^3 -action.

Claim 4.1.19 ([AAK16]). The function $\mu_X(x, y)$ is equal to the symplectic area of the disc bounded by the orbit of (x, y) .

Proof. We claim $\mu_X(x, y) = \int_D \omega$. The integral over the disc (e.g. the $\mathbb{C}\mathbb{P}^1$ moment map image is a segment over which we can draw an elongated sphere and map a value in the segment to the area of the part traced out in the sphere) is integral over disc with boundary component an orbit (integral flow of $X^\#$) and the line from (x, y) around to the origin. Call this line C . Then we can write the integral as

$$\int_C \iota_{X^\#} \omega = \int_C d\mu_X = \mu_X(x, y) - \mu_X(0, 0) = \mu_X(x, y)$$

□

Remark 4.1.20. We are starting with a polytope, which we want to be the moment map image with respect to some symplectic form that we construct. In particular, we find a symplectic form so that the boundary \mathbb{P}^1 's of the hexagon have length 1.

Monodromy computations

Example 4.1.21 (One dimension down, 2D local case). The case of \mathbb{C}^2 with symplectic fibration $(x, y) \mapsto xy$ is the setting of a Lefschetz fibration, with singular fiber given by two copies of \mathbb{C} from $x = 0$ or $y = 0$, and monodromy is a Dehn twist about the S^1 around the belt of the cylindrical fibers. Reference.

$f(x, y) = xy$ and S^1 -action is $(e^{i\theta}x, e^{-i\theta}y)$. The holomorphic vector field corresponding to this is $iz_1\partial_{z_1} - iz_2\partial_{z_2}$, whose contraction with $\omega = \frac{i}{2}(dz_1 \wedge d\bar{z}_1 + dz_2 \wedge d\bar{z}_2)$ gives Hamiltonian vector field $-\frac{1}{2}(|z_1|^2 - |z_2|^2)$. We have a new set of coordinates on the two dimensional fiber: the moment map coordinate μ and the angle coordinate of the action θ . As we approach $xy = 0$, the orbit at μ -height 0, namely $|x| = |y|$, goes to zero. That's one way to see how we get the picture of a cylinder with the neck pinching to zero.

Example 4.1.22 (3D local case). We do this in steps.

- **Parallel transport for holomorphic fibration.**

$$\begin{aligned} f &= xyz, & |f|^2 &= (x_1^2 + x_2^2)(y_1^2 + y_2^2)(z_1^2 + z_2^2) \\ \nabla_{\omega_0} f &= 2 \langle x|yz|^2, y|xz|^2, z|xy|^2 \rangle \perp (|f|^2)^{-1}(c^2) = \{|xyz| = c\} \end{aligned} \tag{4.1}$$

So the projection of the gradient vector field of $|f|^2$ will be perpendicular to circle in case. In particular, multiplying by i we get something tangent to the circle. The fact that multiplying by i on top gives the correct horizontal lift follows because f is holomorphic so commutes with i . Also we will see that the gradient is a linear combination of elements in the horizontal subspace.

- **Finding horizontal subspace.**

Claim 4.1.23. $X_{\Re(f)}, X_{\Im(f)} \in H$ where H is the horizontal distribution.

Proof. A fiber is precisely a level set of f .

$$\begin{aligned}
\ker(d_p f) &= T_p(f^{-1}(c)), \quad p \in f^{-1}(c) \\
\ker(df) &= \ker(d\Re(f)) \cap \ker(d\Im(f)) \\
\ker(d\Re(f)(\cdot)) &= \ker(\omega_0(X_{\Re(f)}, \cdot)) \ni X_{\Re(f)} \\
f \text{ holo} &\implies \nabla(\Re(f)) = -J\nabla(\Im(f)) \\
&\therefore \nabla(\Re(f)) = -JX_{\Re(f)} = X_{\Im(f)} \implies X_{\Im(f)} \in \ker(d\Re(f)) \\
&\therefore H = \langle X_{\Re(f)}, X_{\Im(f)} \rangle = \langle \nabla(\Re(f)), \nabla(\Im(f)) \rangle
\end{aligned} \tag{4.2}$$

□

- **Calculations for parallel transport.** Integrate horizontal lift of i times the gradient suitably scaled. Because we want to cover the circle in the base.

$$\begin{aligned}
i \nabla(|f|^2) &= 2i \langle \nabla \Re(f), \nabla \Im(f) \rangle \in Hor \\
&= 2i \langle x_1|y|^2|z|^2, x_2|y|^2|z|^2, y_1|x|^2|z|^2, y_2|x|^2|z|^2, z_1|x|^2|y|^2, z_2|x|^2|y|^2 \rangle \\
\int^\theta i \nabla(|f|^2) &= \rho^{i \nabla(|f|^2)}(\theta) = (e^{2i\theta|y|^2|z|^2} x, e^{2i\theta|x|^2|z|^2} y, e^{2i\theta|x|^2|y|^2} z)
\end{aligned} \tag{4.3}$$

We want to find a horizontal lift of $\frac{\partial}{\partial \theta} e^{i\theta} = iw\partial/\partial w$. Namely $df(i(\nabla|f|^2)/g) = iw\partial/\partial w$ for a suitable scalar function g .

$$\begin{aligned}
df &= yzdx + xzdy + xydz \\
\nabla_{g_0}|f|^2 &= 2 \langle x|yz|^2, y|xz|^2, z|xy|^2 \rangle \\
|\nabla|f|^2|^2 &= 4|xyz|^2(|yz|^2 + |xz|^2 + |xy|^2) \\
\implies (|yz|^2 + |xz|^2 + |xy|^2) &= \frac{|\nabla|f|^2|^2}{4|f|^2} \\
X_H &= \frac{2i}{g} \langle x|yz|^2, y|xz|^2, z|xy|^2 \rangle \text{ s.t. } df(X_H) = iw\partial/\partial w \\
\therefore \frac{2i}{g} xyz(|yz|^2 + |xz|^2 + |xy|^2) &= iw = i(xyz) \implies g = 2(|yz|^2 + |xz|^2 + |xy|^2) \\
\therefore X_H &= \frac{i}{|yz|^2 + |xz|^2 + |xy|^2} \langle x|yz|^2, y|xz|^2, z|xy|^2 \rangle \\
\therefore \rho^{X_H}(x, y, z, \theta) &= (e^{i\theta \frac{|y|^2|z|^2}{|y|^2|z|^2 + |x|^2|z|^2 + |x|^2|y|^2}} x, e^{i\theta \frac{|x|^2|z|^2}{|y|^2|z|^2 + |x|^2|z|^2 + |x|^2|y|^2}} y, e^{i\theta \frac{|x|^2|y|^2}{|y|^2|z|^2 + |x|^2|z|^2 + |x|^2|y|^2}} z) \\
&= (e^{i\theta \frac{|x|^{-2}}{|x|^{-2} + |y|^{-2} + |z|^{-2}}} x, e^{i\theta \frac{|y|^{-2}}{|x|^{-2} + |y|^{-2} + |z|^{-2}}} y, e^{i\theta \frac{|z|^{-2}}{|x|^{-2} + |y|^{-2} + |z|^{-2}}} z)
\end{aligned} \tag{4.4}$$

because recall $w = xyz$ on the circle and in the last step we divide by $|f|^2$ to make it easier to see Dehn twisting behavior. This gives the monodromy result, Lemma 4.1.11 at the start of this section.

Example 4.1.24 (In the setting $v_0 : Y \rightarrow \mathbb{C}$ of this paper).

Claim 4.1.25. If $\gamma(t)(v_0) = e^{2\pi it}v_0$ then the horizontal lift of γ' is of the form

$$X_{hor} = \partial/\partial\theta_{v_0} + f(\xi)\partial/\partial\theta_1 + g(\xi)\partial/\partial\theta_2$$

Proof. Note that the Lie bracket on Lie T^3 is zero, so standard theory implies

$$\omega(X_{\zeta_1}, X_{\zeta_2}) = X_{[\zeta_1, \zeta_2]} = 0$$

In particular, if we take $\zeta_1 = (1, 0, 0)$ or $(0, 1, 0)$, namely the angular tangent directions of TF for F a fiber of v_0 , and ζ_2 anything, then we get zero. Furthermore, since $\omega(X_{(1,0,0)}, -) = d\xi_1$ we see that X_{ζ_2} does not have $\partial/\partial\xi_1$ in it, in other words its flow preserves the moment map coordinates ξ_1 and ξ_2 .

In particular, let X_{hor} be the horizontal lift in the statement of the claim. Let $X_{(1,0,0)}$ be the vector field generated by the infinitesimal action of rotating the x coordinate, keeping y and v_0 fixed. Then X_{hor} being horizontal implies (by definition of the moment map ξ_1)

$$d\xi_1(X_{hor}) = \omega(X_{(1,0,0)}, X_{hor}) = 0$$

Thus if ϕ_t is the flow of X_{hor} we see by the Chain rule

$$\frac{d}{dt}(\xi_1 \circ \phi_t) = 0 \therefore \xi_1 \circ \phi_t = \xi_1$$

and similarly with ξ_2 . So parallel transport preserves the moment map coordinates ξ_1, ξ_2 . It also preserves η because we are considering angular parallel transport, so in coordinates $\pi : (\xi_1, \xi_2, \eta, \theta_x, \theta_y, \theta_{v_0}) \rightarrow (|w|, \theta_w) := (|v_0|, \theta_{v_0})$ for w the coordinate on the base \mathbb{C} of $v_0 : Y \rightarrow \mathbb{C}$

$$d\pi(X_{hor}) = \partial/\partial\theta_{v_0} \\ \implies \begin{pmatrix} 0 & 0 & \partial|v_0|/\partial\eta & 0 & 0 & 0 \\ 0 & 0 & 0 & 0 & 0 & 1 \end{pmatrix} \begin{pmatrix} 0 \\ 0 \\ h \\ f \\ g \\ a \end{pmatrix} = \begin{pmatrix} h\partial|v_0|/\partial\eta \\ a \end{pmatrix} = (0, 1)$$

thus $a = 1$ and $h = 0$ because η depends on $|v_0|$. So we get the following form for the horizontal lift:

$$X_{hor} = \partial/\partial\theta_{v_0} + f\partial/\partial\theta_1 + g\partial/\partial\theta_2$$

□

Corollary 4.1.26. $X_{hor} = \partial/\partial\theta_{v_0} + f\partial/\partial\theta_1 + g\partial/\partial\theta_2$ where f and g are functions of ξ_1, ξ_2 only.

Proof. Note we get independence of η by invariance of the moment map under radial parallel transport. Let ρ^t be the flow of the horizontal vector field X_{hor} from angular parallel transport:

$$\rho^t(\xi_1, \xi_2, \eta, \theta_1, \theta_2, \theta_{v_0}) = (\xi_1, \xi_2, \eta, \theta_1 + tf, \theta_2 + tg, \theta_{v_0} + t)$$

Let ϕ_α be the T^2 -action $(e^{2\pi i\alpha_1}x, e^{2\pi i\alpha_2}y, v_0)$. This is a symplectomorphism because it is holomorphic and preserves the norms, so commutes with $\partial\bar{\partial}$ and preserves the Kähler potential F hence $(\phi_\alpha)_*\partial\bar{\partial}F = \partial\bar{\partial}F$. It is also a fiberwise symplectomorphism, since it acts on fibers. So we have:

$$\begin{aligned} 0 &= \phi_\alpha^*\omega(TF, H) = \omega((\phi_\alpha)_*TF, (\phi_\alpha)_*H) = \omega(TF, (\phi_\alpha)_*H) \\ &\quad \therefore (\phi_\alpha)_*H = H \\ d\pi((\phi_\alpha)_*X_{hor}) &= d(\pi \circ \phi_\alpha)(X_{hor}) = d\pi(X_{hor}) \\ \therefore (\phi_\alpha)_*(X_{hor}) \circ \phi_\alpha^{-1} &= X_{hor} \\ \implies d\phi_\alpha\left(\frac{d}{dt}\rho^t\right) \circ \phi_\alpha^{-1} &= \frac{d}{dt}(\phi_\alpha \circ \rho^t) \circ \phi_\alpha^{-1} = \frac{d}{dt}(\rho^t) \\ \implies \phi_\alpha \circ \rho^t &= \rho^t \circ \phi_\alpha \\ &\implies (\xi_1, \xi_2, \eta, \theta_1 + \alpha_1 + tf(\xi, \theta + \alpha), \theta_2 + \alpha_2 + tg(\xi, \theta + \alpha), \theta_{v_0} + t) \\ &\quad = (\xi_1, \xi_2, \eta, \theta_1 + \alpha_1 + tf(\xi, \theta), \theta_2 + \alpha_2 + tg(\xi, \theta), \theta_{v_0} + t) \\ &\implies f(\xi, \theta + \alpha) = f(\xi, \theta), \quad g(\xi, \theta + \alpha) = g(\xi, \theta) \quad \forall \alpha \end{aligned}$$

where we integrate the line with $\frac{d}{dt}$ to get to the next line. Thus we find that f and g are independent of θ_1, θ_2 . A similar argument shows they are independent of θ_{v_0} , i.e. $\phi_\lambda \circ \rho^t = \rho^t \circ \phi_\lambda$ for $\lambda \in S^1$ the action on the v_0 coordinate. \square

Fiber Lagrangians Hamiltonian isotopic to linear Lagrangians

Definition 4.1.27. Let L_i be the parallel transport over a U-shape of the ℓ_i in the fiber.

Claim 4.1.28. The parallel transported ℓ_i is Hamiltonian isotopic to ℓ_{i+1} .

Proof. We construct an isotopy $\psi_t : F \rightarrow F$ in the fiber in coordinates $(\xi_1, \xi_2, \theta_1, \theta_2)$. It maps ℓ_1 to $\phi(\ell_0)$ where ϕ is the monodromy. To prove ψ_t is a Hamiltonian isotopy, i.e. $\iota_{\frac{d}{dt}\psi_t}\omega = dH_t$ for some H_t , Banyaga's result (cf Pascaleff notes) states that it suffices to show that the flux of ω through cylinders traced out by generators of $H_1(F)$ is zero.

$$\left\langle \int_t \iota_{X_t}\omega, [\gamma] \right\rangle = \langle \text{Flux}(\psi_t), [\gamma] \rangle = \int_{\psi_t(\gamma)} \omega = \text{area of cylinder traced out by } \gamma \text{ over time}$$

First we define the isotopy, and set $A := M^{-1}$.

$$\psi_t(\xi_1, \xi_2, \theta_1, \theta_2) := (\xi_1, \xi_2, \theta_1 + t(f(\xi) - A_1\xi), \theta_2 + t(g(\xi) - A_2\xi))$$

We note that $H_1(F)$ has rank four since $F \cong T_B \times T_F$. If we let γ be the loop generated by $(0, 0, 1, 0)$ or $(0, 0, 0, 1)$ the two angular directions, then $\{\psi_t(\gamma)\}_t$ is one dimensional because ξ is constant thus the integral is zero. Now we let

$$\gamma(t) = (2t, t, 0, 0), \quad -\frac{1}{2} \leq t \leq \frac{1}{2}$$

The case of $\gamma(t) = (t, 2t, 0, 0)$ is similar.

$$\begin{aligned} flux &= \int_{\psi_t(\gamma)} \omega = \int_{\gamma} \iota_{X_t} \omega = \int_{\gamma} (d\xi_1 \wedge d\theta_1 + d\xi_2 \wedge d\theta_2)((f - A_1)\partial_{\theta_1} + (g - A_2)\partial_{\theta_2}, -) \\ &= \int_{\gamma} (f - A_1)d\xi_1 + (g - A_2)d\xi_2 \\ &= \int_{-1/2}^{1/2} 2f(2t, t)dt + g(2t, t)dt \end{aligned}$$

where we used that A being a linear map implies symmetry across zero, and it remains to show that the above is zero, namely symmetry across zero in f and g . It suffices to show that $f(-\xi) = -f(\xi)$ and similarly with g .

To do this we recall that f and g are defined by

$$X_{hor} = \frac{\partial}{\partial \theta_{v_0}} + f(\xi) \frac{\partial}{\partial \theta_1} + g(\xi) \frac{\partial}{\partial \theta_2}$$

Also recall that X_{hor} will be preserved by any fiber-preserving symplectomorphism, as we saw above in the example of the T^2 -action. Another fiber-preserving symplectomorphism is $\phi_{neg} : (\xi, \theta) \mapsto (-\xi, -\theta)$ in the fiber. It is a symplectomorphism because $d\xi \wedge d\theta \mapsto d(-\xi) \wedge d(-\theta) = d\xi \wedge d\theta$. Thus

$$\begin{aligned} (\phi_{neg})_*(X_{hor}) &= X_{hor} \circ \phi_{neg} \\ \implies f(-\xi) &= -f(\xi), \quad g(-\xi) = -g(\xi) \end{aligned}$$

So this completes the proof. □

4.2 Background for defining $H^0(FS(Y, v_0))$

The following background is from [Sei08].

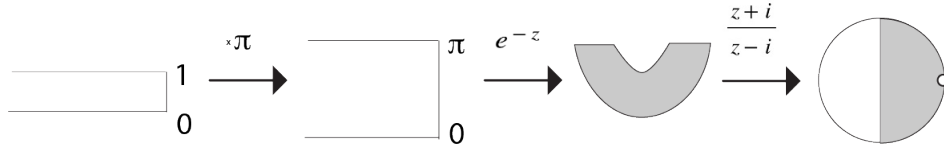


Figure 4.2: Example of strip-like end

Remark 4.2.1 (Notation). We start with the symplectic fibration $v_0 : Y \rightarrow \mathbb{C}$, which is not exact because fibers are compact tori. Although Y does not have boundary, we will restrict to a small disc around the origin, which does have boundary. In particular, in the terminology of [Sei08], we do not have a *horizontal boundary* since fibers are tori, but we do have a *vertical boundary* by taking the preimage of a compact neighborhood in the base.

The class of almost complex structures we consider are 1) compatible with the ω defined above and 2) are equal to the standard J_0 induced from the complex toric coordinates near the boundary. We will denote this set as $\mathcal{J}_{reg}(Y, \partial Y)$. This set is non-empty, because it contains J_0 , and contractible by the same argument as for the set of all ω -compatible almost complex structures.

Definition 4.2.2 (Domains). A *punctured boundary Riemann surface* S is the data of a compact, connected, nonempty boundary Riemann surface with punctures removed on its boundary, and the assignment of an exact Lagrangian to each component of ∂S . We further “*rigidify*” by adding extra structure to S ; denote punctures as “positive” or “negative” and define *strip-like ends* via embeddings $\epsilon : (-\infty, 0]_s \times [0, 1]_t \rightarrow \mathbb{D}$ or $\epsilon : [0, \infty)_s \times [0, 1]_t \rightarrow \mathbb{D}$ for the negative and positive punctures ζ^\pm respectively, such that $\lim_{s \rightarrow \pm\infty} \epsilon(s, t) = \zeta^\pm$. This is called a *Riemann surface with strip-like ends*.

Example 4.2.3. In this thesis, S will be one of the unit disc \mathbb{D} , two discs glued together at a point on their boundary, or a disc union a configuration of spheres, in each case with potentially some punctures. One example of a strip-like end we use later on to glue two discs is $(-\infty, 0] \times [0, 1] \ni (s, t) \mapsto \epsilon^-(s, t) := \frac{e^{-\pi(s+it)+i}}{e^{-\pi(s+it)-i}} = \frac{z+i}{z-i} \circ e^{-z} \circ \pi \cdot (s+it) \in \mathbb{D} \setminus \{1\}$. Note that $-\infty$ is the puncture which would map to $\zeta^- := 1$ in the disc. See Figure 4.2.

Remark 4.2.4. This “rigidifies” because any operation on S must preserve the additional data of strip-like ends, thus placing further restrictions. The strips provide a nice set of coordinates near the punctures (namely s and t) and give a straightforward way to glue two sections by gluing linearly in the (s, t) coordinates. See [Sei08, §(8i) and §(9k)].

Definition 4.2.5 (Maps). Let $J \in \mathcal{J}_{reg}(Y, \partial Y)$. A *pseudo-holomorphic map* is a J -holomorphic map $u : (S, \partial S) \rightarrow (Y, \sqcup_{i \in \pi_0(\partial S)} L_i)$. A *J /pseudo-holomorphic curve* is the image of such a

map. We require

$$\lim_{s \rightarrow \pm\infty} u(\epsilon_{ij}(s, t)) \in L_i \cap L_j$$

for strip-like end ϵ_{ij} limiting to an intersection point of $L_i \cap L_j$.

Remark 4.2.6 (With data of a symplectic fibration, can look at sections). We can think of the above as a section of a trivial fibration with fixed Lagrangian boundary condition. Now we generalize to non-trivial fibrations. Consider a holomorphic polygon in the total space of a fibration with boundary in fiber Lagrangians parallel transported around polygon in the base. If we project down to the base, we obtain a holomorphic polygon. This indicates we should look at holomorphic sections.

Definition 4.2.7 (Sections). We can similarly define pseudo-holomorphic sections. Instead of limiting to an intersection point of the transverse Lagrangians, it limits to a function $u_\zeta(t)$ (for each t) which gives a possibly varying point in M for each t satisfying a suitable derivative condition and on the intersection of two Lagrangian boundary conditions over ∂S .

Remark 4.2.8. The above assumes that Lagrangians intersect transversely. Since Lagrangians are half-dimensional, if they intersect transversely then their intersection is 0-dimensional and we have a discrete set of points. There are a couple ways that have been invented to account for non-transverse intersections. One is by introducing a Hamiltonian function and flowing one Lagrangian along the symplectically dual vector field to the derivative of that Hamiltonian function, until the two Lagrangians intersect transversely. This is what Seidel does in [Sei08]. We can do this on a fiber of the fibration, so we give the background here.

We have a Hamiltonian function H defined on the fiber and 1-form γ defined on the base of v_0 , vanishing on the boundary. In particular, we define γ to be zero near punctures where there is no problem and nonzero near punctures where the Lagrangians do not intersect transversally. Then maps u should satisfy the modified Cauchy-Riemann equation

$$(du - X_H \circ \gamma)^{0,1} = 0$$

with a modified boundary condition in the strip-like ends. Equivalently, u limits to an intersection point of the Lagrangian and the time-1 flow under X_H of the other Lagrangian intersecting non-transversely. We can use this to compute self-homs of Lagrangians ℓ_i in the fiber.

For the total space, we need to use a different method of perturbation, because the symplectic form is not a product of the base and fiber. We instead use the categorical localization method of [AS], described later.

Example 4.2.9. Let t_z be the preimage of a moment map value $(c_1, c_2) \in T_B$, intersected with a fiber. So $t_z = \{c_1, c_2, \theta_1, \theta_2\}_{\theta_i \in [0, 2\pi)}$ which in particular is invariant under parallel

transport because that map rotates the angles. Since $\ell_i \cap t_z$ is the one point of ℓ_i with $(\xi_1, \xi_2) = (c_1, c_2)$, any pseudo-holomorphic section u must limit to that one point over the corresponding puncture in the base.

Example 4.2.10. The intersection in $t_z \cap t_z$ is not transverse, so we'll need to introduce an inhomogeneous Hamiltonian term as above. This is a smooth function on the fiber (that vanishes near the boundary of the fiber, but a torus has no boundary so this doesn't concern us). In our case the time-1 flow of X_H is an automorphism of the fiber that is a graph on the real norms of the coordinates $|x|, |y|, |z|$, chosen so that it descends to a map from the torus to itself. The PSS isomorphism implies $HF^*(t_z, t_z) \cong H^*(t_z; \mathbb{C})$, the cohomology of a 2-torus.

4.3 Moduli spaces needed to define $H^0(FS(Y, v_0))$

Remark 4.3.1 (Reason for moduli spaces in the Fukaya category). The Fukaya category is an A_∞ -category. This means we have objects, morphisms, and structure maps on k morphisms for any natural number k that satisfy A_∞ -relations, which can be thought of as higher order associativity relations on the morphisms. Objects are Lagrangians, morphisms are intersection points, and structure maps count pseudo-holomorphic maps with boundary punctures limiting to k input intersection points and 1 output intersection point. For the Fukaya-Seidel category, the input is a symplectic fibration and we replace “maps” with “sections” in the above description.

To ensure we can make these counts, we first collect the maps into a set modulo reparametrization. Gromov equipped this quotient set with a topology so it is a topological space, known as a moduli space because we mod out by automorphisms of the Riemann surface S . His result of Gromov compactness can compactify this topological space by analyzing what behavior can happen to a limit of pseudo-holomorphic curves, using results from complex analysis that still hold in the pseudo-holomorphic setting such as unique continuation and somewhere injectivity. However, to make a count we would like a 0-dimensional compact manifold. So we use differential geometry on function spaces to put the structure of a compact zero-dimensional smooth manifold on the moduli space, which is a finite number that can be counted. Here is the plan for defining the moduli spaces, fitting them into the framework of the Fukaya-Seidel category, and then working out the HMS computation:

- Immediately below: determine **homology classes in \mathbf{Y}** where curves map to.
- Section §4.3 (current): Prove **existence of regular \mathbf{J}** , for which the moduli spaces in the Fukaya category are compact 0-dimensional manifolds. This will adapt [MS12] from the $S = \mathbb{C}\mathbb{P}^1$ setting to the $S = \mathbb{D}$ setting with Lagrangian boundary conditions, and is also discussed in [Sei08] and [Gan16b].

- Section §4.4: **Define the category** following [AS] and **prove independence of choice of regular J and Hamiltonian isotopy class of the Lagrangian** in $FS(Y, v_0)$, up to quasi-isomorphism, by a standard continuation map argument.
- Chapter §8: **Calculate** the objects, morphisms, differential, and composition to find a subcategory of $H^0(FS(Y, v_0))$ which we can show is isomorphic to the bounded derived category of coherent sheaves on the mirror. In particular, we will need to count the moduli spaces rather than know a count exists. For this we will use non-regular J , and then use results from Gromov-Witten theory [KL19]. An abstract regularization theory will tie the definition and computation together, discussed in Sections 5.1.

The last three steps involve moduli spaces. Figure 4.3 is a flow chart for how to define them and what we hope to do with them.

Lemma 4.3.2 (Homology of Y).

$$H_2(Y) \cong H_2(\mathbb{C}P^2(3)/\Gamma_B) \cong \mathbb{Z}^4$$

where all homology classes will be over \mathbb{Z} .

Proof. Note that Y deformation retracts onto the central fiber over the contractible base. Therefore the homology of Y is the homology of the central fiber.

We view the central fiber as a degeneration of a T^4 fiber to the central fiber, so that we can compute homology by reading off what shrinks to a point in the cell decomposition. We want an analogue of the one dimension lower case where T^2 degenerates to a sphere glued at its ends. This can be seen from the torus as a quotient of a square, where one pair of opposite edges is shrunk to a point, or in the cell decomposition we contract one 1-cell in the construction of the 2-torus from one 0-cell, two 1-cells, and one 2-cell wrapping around the bouquet of two circles.

In Figure 4.4, we aim to illustrate the 2-skeleton of the cell construction of T^4 , viewed as a quotient of a 4-cube. We obtain three 2-tori identified at one S^1 . The 2-skeleton is enough to compute the second homology. So we find that the homology is \mathbb{Z}^3 from each T^2 . In the degeneration to the central fiber, this S^1 shrinks to a point and we get a banana manifold with three banana spheres, which recall is the boundary of the central fiber from the hexagon. We get an additional generator now that the S^1 has shrunk to a point. So the homology is \mathbb{Z}^4 . Note that the fiber is actually $T_B \times T_F$ instead of I^4 but topologically they are the same.

□

Remark 4.3.3. Note that we used intuition from spectral sequences for topological fibrations applied to the fibration $v_0 : Y \rightarrow \mathbb{C}$. Note that it is a fibration in the sense of algebraic geometry but not in the sense of algebraic topology because it does not have the homotopy

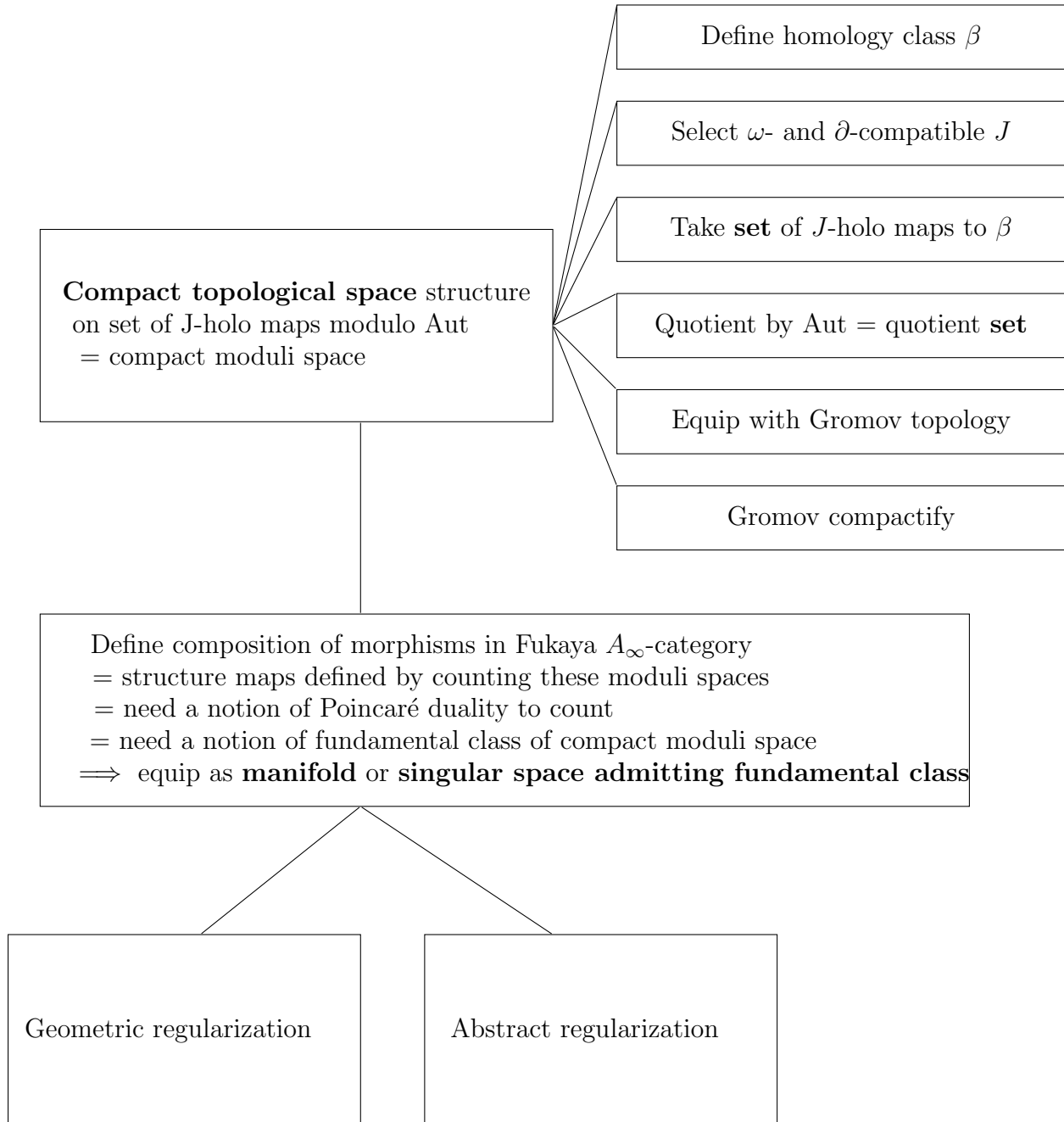


Figure 4.3: Flow chart for working with moduli spaces in Fukaya categories

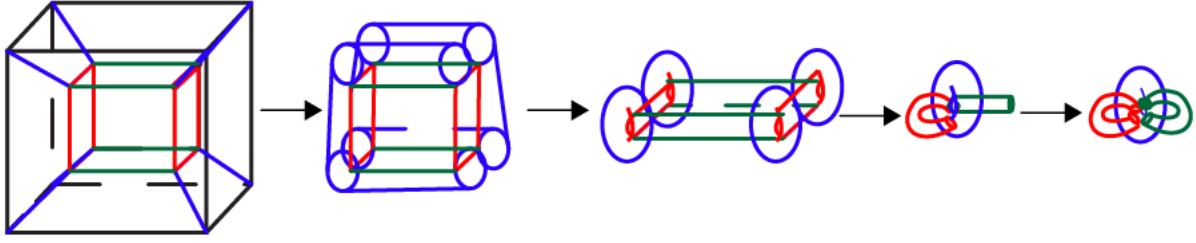


Figure 4.4: 2-skeleton of cell complex from construction of T^4 as a quotient of a 4-cube

lifting property; for example over a disk about the origin we have an S^1 -set of choices to lift it to due to the singularity. Namely we do not have weak homotopy equivalent fibers from T^4 to its degenerated fiber $\mathbb{C}\mathbb{P}^2(3)/\Gamma_B$. If we were in the right situation then the second page would be $E_{p,q}^2 = H_p(\mathbb{C}, H_q(T^4))$.

Algebraically: the homology with local coefficients means we have $C_*(\tilde{X}) \otimes_{\pi} H_q(F)$ where $\pi = \pi_1(\text{base})$ acts on the covering space $H_q(F_b) \mapsto b$ (with discrete topology) so over monodromy in base we might see how an $H_1(F_b)$ element changes, and that will give us the action of π . Then the differential on this chain complex is $\partial \otimes \mathbf{1}$. So in the case of universal cover $\tilde{X} = \text{base} = \mathbb{C}$ being contractible, then π_1 is trivial so the tensor product just recovers usual homology which is zero in degrees $p > 0$ and recovers the homology of the base at $p = 0$.

Remark 4.3.4. Note that an alternative method is to compute homology using the theory of toric varieties from [CLS11]. Inside the toric variety X there is a dense $(\mathbb{C}^*)^n$. This is n cylinders which can be retracted to n circles so π_1 is \mathbb{Z}^n . Moreover, this surjects onto $\pi_1(X)$, which will hence always be some quotient of \mathbb{Z}^3 . For example in this case we \mathbb{Z}^4 before quotienting: we have one \mathbb{P}^1 from the center of the polytope and three more from the blow-ups. Once we quotient we find that the three $\mathbb{C}\mathbb{P}^1$'s in the banana manifold add up to a fiber of the moment map and a pinched T^3 , in particular the fourth generator is a sum of the first three.

Let $Z := \widetilde{\mathbb{C}\mathbb{P}^2(3)}/\sim$ which has polytope given by an infinite tiling of hexagons, i.e. the central fiber of Y . The reason this is the universal cover is that $\pi_1(Z) = 0$ from toric theory. As a result, Hurewicz's theorem implies $\pi_2(Z) = H_2(Z)$ and $\pi_2(\mathbb{C}\mathbb{P}^2(3)/\sim) = \pi_2(Z)$. Thus alternatively to get $H_2(\mathbb{C}\mathbb{P}^2(3)/\sim)$ we may use Mayer-Vietoris as follows.

Cut out an open set in the hexagonal picture, which then retracts onto the boundary. This gives two open sets, which in the moment map picture are a disc and its complement, intersecting in an S^1 .

Let $B := D^2 \times T^2$ correspond to the disc in the moment polytope. Let \tilde{A} be the complement, a string of 6 $\mathbb{C}\mathbb{P}^1$'s in a circle and $A := \tilde{A}/\Gamma_B$ the banana manifold. Let

$$\begin{aligned}
0 &= H_3(\tilde{A}) \oplus H_3(B) \rightarrow H_3(Z) = 0 \\
&\rightarrow H_2(\tilde{A} \cap B) = \mathbb{Z}^3 \xrightarrow{(*)} H_2(\tilde{A}) \oplus H_2(B) = \mathbb{Z}^6 \oplus \mathbb{Z} \rightarrow H_2(Z) \rightarrow 0 \\
H_1(\tilde{A} \cap B) &= \mathbb{Z}^3 \xrightarrow{\cong} H_1(\tilde{A}) \oplus H_1(B) = \mathbb{Z} \oplus \mathbb{Z}^2 \rightarrow H_1(Z) = 0
\end{aligned}$$

where $(*) = \begin{pmatrix} 1 & 0 & 0 \\ 0 & 1 & 0 \\ -1 & 1 & 0 \\ -1 & 0 & 0 \\ 0 & -1 & 0 \\ 1 & -1 & 0 \\ 0 & 0 & 1 \end{pmatrix}$ and the second to last map is the 3-by-3 identity matrix with

respect to the three generators of $H_2(\tilde{A} \cap B) = H_2(S^1 \times T^2)$ (call them b for the S^1 in the moment polytope and T_1, T_2 for the two loops in the 2-torus fiber). Then passing to the quotient $\mathbb{C}\mathbb{P}^2(3)/\sim$ we find that

$$\begin{aligned}
0 &= H_3(A) \oplus H_3(B) \rightarrow H_3(\mathbb{C}\mathbb{P}^2(3)/\sim) = 0 \\
&\rightarrow H_2(A \cap B) = \mathbb{Z}^3 \xrightarrow{(**)} H_2(A) \oplus H_2(B) = \mathbb{Z}^3 \oplus \mathbb{Z} \\
&\rightarrow H_2(\mathbb{C}\mathbb{P}^2(3)/\sim) = \mathbb{Z}^4 \rightarrow \mathbb{Z} \cdot b \subset H_1(A \cap B) = \mathbb{Z}^3 \\
&\xrightarrow{\begin{pmatrix} 0 & 0 & 0 \\ 0 & 0 & 0 \\ 0 & 1 & 0 \\ 0 & 0 & 1 \end{pmatrix}} H_1(A) \oplus H_1(B) = \mathbb{Z}^2 \oplus \mathbb{Z}^2 \rightarrow H_1(\mathbb{C}\mathbb{P}^2(3)/\sim) = 0
\end{aligned}$$

where $(**) = \begin{pmatrix} 0 & 0 & 0 \\ 0 & 0 & 0 \\ 0 & 0 & 0 \\ 0 & 0 & 1 \end{pmatrix}$. So ultimately we look at the projection of the 6 \mathbb{P}^1 's mapping to the three glued \mathbb{P}^1 's. Again we find that the homology is \mathbb{Z}^4 .

Now we have the homology classes of Y where images of sphere bubbles may exist. We also want to know relative H_2 for discs with boundary in a given Lagrangian. Recall our discussion of maps and sections above in the background section. We now define the discs we will consider in this thesis. The homology classes in $\pi_2(Y, L)$ that we consider cover a disc in the base around 0, and pass through the central fiber in one point. Varying this point using the toric geometry of the central fiber allows one to enumerate all the homology classes, done in [CO06]. We will discuss this below when we do the computation of the disc count for a

particular J . Here we will just show existence of moduli spaces for a given homology class β in $H_2(Y, L)$.

Definition 4.3.5 (Section-like maps). We select an open set around the origin, call it U . Then we restrict ourselves to look at almost complex structures that are identically J_0 outside of U . In particular, discs will be sections there. By Riemann mapping theorem, when we compose the J_0 -holomorphic map there to the base via v_0 which is also holomorphic, there is a unique such map if we have J_0 everywhere. To allow enough regularity, we will need to consider J which can vary away from J_0 inside the set U . In particular, we will define all our Lagrangians below to be required to go through the point -1 in the base so if we choose U to be a disc of radius smaller than 1, this allows us to conclude there are no multiply-covered discs because they cannot wrap around the boundary. Take U to be the disc of radius $1/2$ centered at the origin.

We can also exclude disc bubbling and strip-breaking: fibers have no discs because linear Lagrangians in tori have zero relative π_2 i.e. they don't bound discs. A disc can't form that wraps around the boundary of a disc over an open set around the origin, because it must be 1-1 near -1 . So another disk or strip would have to lie over a proper subset of the circle in the base, for which the fibration is trivializable. Assuming the boundary of the disc lies outside of U (but then need to show invariant under Hamiltonian isotopy), or by continuing the 1-1 property near -1 of discs to the rest of the boundary of the disc, we find that such a disc must have boundary given by a point because of the 1-1 property, but there are no spheres in the torus, so it must be constant (or again invoke 1-1 property).

If we did have multiple covers, we may require that J depend on $z \in S$, in which case we replace J with J_z . The text [MS12] lays this foundation for Lagrangian boundary conditions case which is described in [Aur14] and will involve an \mathbb{R} -family of J 's on a strip. But we don't need to do that here.

Corollary 4.3.6. *J -curves have some analogous properties as complex curves. For example, the Carlemann similarity principle: a curve that satisfies almost the CR equation can be modified by post composing with a map, to satisfy it with J_0 . This is in the case of symplectic manifold \mathbb{R}^{2n} . Other corollaries include: unique continuation (if two J -holomorphic maps agree on an open set, or all derivatives agree at a point, then the maps are equal). There are only finitely many points in a preimage and only finitely many critical points. Simple curves have open dense set of injective points.*

Now that we've discussed the homology classes where the curves have their image in Y , we next move to proving existence of regular J , which will allow us to construct a Fredholm problem where the Cauchy-Riemann operator $\bar{\partial}_J$ will cut out the moduli spaces as a section of a Banach bundle, and the implicit function theorem will tell us the preimage of zero is a manifold, which will allow us to put a smooth structure on our moduli spaces.

Example 4.3.7. This is an infinite-dimensional Banach analogue to checking e.g. that the function $f : \mathbb{R}^3 \rightarrow \mathbb{R}$ defined by $f(x, y, z) = x^2 + y^2 + z^2$ is regular for $(x, y, z) \neq 0$ because $df|_{(x,y,z)} = (2x, 2y, 2z)^T|_{(x,y,z) \neq (0,0,0)} : \mathbb{R}^3 \rightarrow \mathbb{R}$ is surjective hence f is a *regular function* and the preimage of 1 is a smooth manifold (a sphere). In the Banach-bundle setting, regular means not only surjective but also a right inverse exists.

The difference here is that the differential operator inputs functions, which lands us in the world of infinite-dimensional Banach spaces. The following theory follows the arguments of [MS12, Chapters 3–10] but for curves with boundary, also discussed in [Sei08]. An example of the geometric regularization theory is implemented in [Weh13] for Gromov non-squeezing, which involves illustrating how to show a family of moduli spaces varying J_t is 1 dimensional (Fredholm), a manifold (transversality/regularity), compact (Gromov compactness) and has boundary. A nice reference for abstract regularization theories is [Weh14].

We now proceed to prove existence of a regular J .

Lemma 4.3.8 (Geometric regularization). *There exists a dense set $\mathcal{J}_{reg}^1 \subset \mathcal{J}(Y, \omega)$ of ω -compatible almost complex structures J that are identically J_0 outside of U such that, for all J -holomorphic maps $u : (\mathbb{D}, \partial\mathbb{D}) \rightarrow (Y, L|_\gamma)$ with Lagrangian boundary condition given by parallel transporting a fiber Lagrangian around a U -shape in the basis from -1 , the linearized $\bar{\partial}$ -operator D_u is surjective.*

Remark 4.3.9. We use the superscript 1 because later we will want existence of slightly smaller sets \mathcal{J}_{reg}^2 and \mathcal{J}_{reg}^3 which are regular for a disc attached to a disc and a disc attached to a sphere, with similar Lagrangian boundary conditions. These will be labelled 2 and 3 and will require not only surjectivity of the linearized operator but also compatible behavior when evaluating at the intersection point.

Sketch adapting the 2nd edition book [MS12, pg 55, proof of Theorem 3.1.6 (ii)]. We give a road map adapting McDuff-Salamon to the setting with Lagrangian boundary conditions. The background for this was also learned from [Weh14, Lecture 9]. Details also discussed in Denis meeting on Sept 8, 2017. Note Theorem C.1.10 in [MS12] proves we have a Fredholm problem for the case of boundary.

Introduction. “Regularization” refers to perturbing the $\bar{\partial}_J$ operator to be equivariantly transverse to the zero section of a Fredholm bundle which we can build so that the operator is a section of the bundle. “Geometric regularization” means the perturbations are obtained by perturbing the almost complex structure J , so are geometric in nature. Namely the perturbations of $\bar{\partial}_J$ are $\bar{\partial}_{J'} - \bar{\partial}_J$ as J' varies. In this setting equivariance will be automatic, as described below. Note that later on, we will need to use a non-regular J for computations and in that case we will use “abstract regularization” by adding abstract perturbations ν which are sections of the same Fredholm bundle but are not necessarily of the form $\bar{\partial}_{J'} - \bar{\partial}_J$.

To prove existence of regular J for discs mapping to fiber Lagrangians parallel-transported over U-shaped curves, we show that there is a dense set of them in $\mathcal{J}_\omega^\ell(Y, U) := \{J \in \Gamma(TY) \mid J^2 = -\mathbf{1}, J|_{Y \setminus U} \equiv J_0, J \in C^\ell\}$. (This is called \mathcal{J}_F^ℓ in [Sei08] where F denotes the Lagrangian boundary condition that is obtained by parallel transporting a fiber Lagrangian, which he refers to as a *moving boundary condition*. This set of J is what's needed in the boundary case, see [MS12, Remark 3.2.3].) First, we define the set of all $W^{k,p}$ maps u and geometric perturbations encoded by varying J :

$$\mathcal{M}_{\mathcal{J}} := \{(u, J) \mid J \in \mathcal{J}_\omega^\ell(Y, U), W^{k,p} \ni u : (\mathbb{D}, \partial D) \rightarrow (Y, L)\}$$

For sufficiently large k , $W^{k,p} \subset C^\ell$. Then elliptic bootstrapping will imply that J -holomorphic maps u are in C^ℓ . This moduli space is called “universal” because we allow J to vary. We use $W^{k,p}$ because it is complete, i.e. a Banach space, which will be needed to invoke Sard-Smale and elliptic regularity in the infinite dimensional setting of function spaces. In particular, we want $\mathcal{M}_{\mathcal{J}}$ to be a $C^{\ell-1}$ separable Banach manifold. Then we can use Sard-Smale on the projection map $(u, J) \rightarrow J$ to prove existence of a dense set of regular J for the disc.

Banach bundle set-up. We want to view $\mathcal{M}_{\mathcal{J}} \subset \mathcal{B}^{k,p} \times \mathcal{J}_\omega^\ell(Y, U) \ni (u, J) \rightarrow J$ as a Fredholm section of a Banach bundle in order to invoke Sard-Smale to get a dense set of regular values. *Fredholm* is a generalization of surjectivity. We also need existence of a right inverse, which is a requirement in the infinite-dimensional setting. E.g. see recent polyfold paper for example where there is no right inverse and why it's not enough. Then an implicit function theorem will imply the set of (u, J) cut out by the zero set of this section is a Banach submanifold of the base and not just a subset. Note that the zero-set consists of (u, J) so that u is J -holomorphic.

Banach manifold structure on $\mathcal{B}^{k,p} \ni u$: we construct a local Banach chart about an arbitrary map u . The local model is $T\Gamma(u^*TY, u^*TL) \ni \xi$ via $u \mapsto \exp_u \xi$. This is well-defined: we always have existence of a metric so that one Lagrangian is totally geodesic [MS12, Lemma 4.3.4] and so one Lagrangian, or two, are totally geodesic from some metric. And at any point considered there are at most two Lagrangians intersecting so this suffices. We need totally geodesic for this to provide a chart in the case of Lagrangian boundary condition: given a point in $\partial\mathbb{D}$, move along the vector ξ planted at that point and the result will be tangent to L so that geodesic remains in L .

Banach manifold structure on $\mathcal{J}_\omega^\ell(Y, U) \ni J$, the second factor of the base of the Banach bundle we are constructing, cf [MS12, §3.2]: again exponentiate to obtain \dot{J} . Three conditions on J become linearized: 1) $J|_{Y \setminus U} \equiv J_0$ implies $\dot{J}|_{Y \setminus U} \equiv 0$ (this is specific to the Lagrangian boundary case), 2) $J^2 = -\mathbf{1}$ implies $\dot{J}J + J\dot{J} = 0$, and 3) $\omega(\cdot, J\cdot) > 0$ and symmetric also gets linearized. A chart is constructed via $J \mapsto J \exp(-JJ)$. C.f. [Sei08]. A fiber of the bundle will not have boundary conditions because it is given by the space where $(du)^{0,1} = \frac{1}{2}(du + J \circ du \circ j)$ lands in, and that doesn't concern the boundary. One doesn't

know what happens to directions tangent to the boundary since J and j could twist them around.

Now we describe how to put the structure of a Banach bundle over open sets in the base. This will mimic the case of [MS12] because there are no boundary conditions on the fiber. We use the exponential map to trivialize the bundle over a neighborhood $\mathcal{N}(u)$ in the first factor of $\mathcal{B}^{k,p} \times \mathcal{J}_\omega^\ell(Y, U)$, and we use parallel transport to trivialize over a neighborhood $\mathcal{N}(J)$. This trivializes the bundle over a neighborhood in the base, and a composition of these gives transition maps that satisfy conditions for a Banach bundle, [MS12] and [Sei08].

Fredholm problem. A *Fredholm problem* is a *Fredholm section* of a Banach bundle. I.e. a section whose linearization is a Fredholm operator, namely $\dim \ker - \dim \text{coker}$ is finite (e.g. the projection to the tangent space of the fiber is surjective) and whose image is closed. More generally it's a set-up of the moduli spaces (main part and Gromov compactifying components that are fiber products) as the zero sets of Fredholm sections. We claim that the section $(u, J) \mapsto \bar{\partial}_J(u)$ is Fredholm. To take the linearization of the $\bar{\partial}$ operator at some map u , we have to see what happens as we vary u infinitesimally by a tangent vector ξ . That is, we differentiate the $\bar{\partial}$ operator in a family and take the derivative at zero. See [MS12, Proposition 3.1.1]. Similarly we will vary J infinitesimally by tangent vector \dot{J} .

$$\mathcal{F}_u : W^{k,p}(S, u^*TY) \rightarrow W^{k-1,p}(S, \Lambda^{1,0} \otimes_j u^*TY)$$

We define D_u as follows: for $D_{u'} \bar{\partial}_J$ for a nearby u' in the exp neighborhood of u , we parallel transport back to the origin of the chart at u , take $\bar{\partial}_J$, then map forward again on the fiber under parallel transport. Then the linearized operator $D_u \xi$ will be the derivative of this operation at the point 0. This is well-defined because of the totally geodesic condition above. This is only when varying u . Varying J as well we get [Weh14, Lecture 9]:

$$D_u \xi + \frac{1}{2} \dot{J} duj$$

In particular, this is surjective with right inverse, so is Fredholm. The reasoning is as follows. Suppose by contradiction the image is not dense. Take a nonzero linear functional η in the orthogonal complement to the image. Taking $\dot{J} = 0$ we see that η is orthogonal to $\text{im}(D_u)$ as well. So it must be orthogonal to $\dot{J} duj$ for all \dot{J} . However, using bump functions, since $\eta \neq 0$ we can construct a perturbation \dot{J} so η integrated on \dot{J} is nonzero, which gives the contradiction, see [MS12, page 65].

It's still possible to do this construction in the Lagrangian boundary setting because the constructed \dot{J} is supported in a small neighborhood around a somewhere injective point so will be zero near the boundary as required. Somewhere injective points are dense so we can find one close to a given point where η is nonzero. In particular there is a neighborhood of them. Use bump functions to construct a \dot{J} so that the integral of $\int_{\mathbb{D}} \eta(\dot{J} duj) > 0$. This is

a contradiction. So η vanishes on the open set of injective points, hence vanishes identically by unique continuation [MS12, Theorem 2.3.2]. This is again a contradiction since $\eta \neq 0$. Thus we find that our original assumption that the image is not dense is false. The image is dense, and since it's closed, it's surjective with right inverse.

Sard-Smale: inverse function theorem. Now that we have a Fredholm problem, we can apply the results of [MS12, Appendix A: Fredholm Theory] for Banach spaces. In particular, we have the hypothesis of the [MS12, Theorem A.5.1 (Sard-Smale Theorem)] which relies on the infinite-dimensional inverse function theorem, [MS12, Theorem A.3.1 (Inverse Function Theorem)]. The result of Sard-Smale is that the set of regular J is dense in the set of all J , which is what we were aiming for. So we have existence of regular J . □

Remark 4.3.10 (Notation). NB: the notation \dot{J} does not mean we can only vary J in one direction as is usually the case with the dot notation. We use the notation as a merely symbolic way to denote tangent vectors to the space of complex structures, which is typically denoted Y in the literature but in this thesis Y is the A-side manifold.

Lemma 4.3.11. *The set of parametrized J -holomorphic discs $u : (\mathbb{D}, \partial\mathbb{D}) \rightarrow (Y, L|_\gamma)$ for $J \in J_{reg}^1(Y, \partial Y)$ is a finite-dimensional manifold.*

Proof from [MS12, Theorem 3.1.6 (i)]. Charts are given using

$$\begin{aligned} \mathcal{F}_u : W^{k,p}(S, u^*TY) &\rightarrow W^{k-1,p}(S, \Lambda^{1,0} \otimes_j u^*TY) \\ \xi &\mapsto \exp_u \xi \end{aligned}$$

and obtaining a diffeomorphism of an open set around u in $\mathcal{F}_u^{-1}(0)$ to the corresponding open set in the Banach space around 0. Regularity of J implies $d\mathcal{F}_u(0) = D_u$ is surjective. The implicit function theorem [MS12, Theorem A.3.3] implies these are smooth manifold charts after restricting to potentially smaller open sets. This does not depend on k, l because J -holomorphic maps u are smooth by elliptic regularity [MS12, Proposition 3.1.10]. Note that [MS12, Appendix B (Elliptic Regularity)] covers the necessary background with *totally real boundary conditions* e.g. the Lagrangian boundary condition case here. We will not rewrite the proofs here but will define the terminology used in that section, see also [Weh13, Lecture 4–6].

- C_0^k : k times continuously differentiable and derivatives up those orders limit to zero at infinity.
- *Schwartz space* ζ of test functions: f such that $f \cdot (\sqrt{1 + |x|^2})^k \in C_0$. It is closed under convolution and is associative. *Tempered distributions* ζ' denotes the dual space. In particular, $\zeta \hookrightarrow \zeta'$ via a continuous dense injection $f \mapsto \int_{\mathbb{R}^n} f \cdot (\cdot) d^n x$.
- The phrase that an equality holds “in a weak sense” means, “true when integrated under all tempered distributions.”

- The Fourier transform is a continuous map on Schwartz space where convolution becomes multiplication.
- Sobolev space $W^{s,2}$: those $\hat{f} \in \zeta'$ s.t. $FT(f) \cdot (\sqrt{1+|x|^2})^k \in L^2$. $W^{k,p}$: derivatives up to order k are in L^p in a weak sense. In particular, there is a Sobolev embedding $W^{k,p} \subset C^l$ with compact support when $k \gg l$.
- The *support* of a function u is the complement of where $u = 0$ in a weak sense. The *singular support* of a distribution means we remove, in a weak sense, $u \in \zeta$ with no local compact smoothness.
- Elliptic regularity: $p(D)u$ smooth is equivalent to singular support of $p(D)$ being empty, which is equivalent to u being smooth. In particular, $\bar{\partial}u = 0$ implies u is smooth. When $p > 2$ then the L^p bound on the derivative gives a compact moduli space. This fails when $p = 2$, i.e. L^2 norm, hence bubbling can occur and not be in the moduli space. So to compactify we will quotient by the automorphism group of the domain and determine what bubbling can occur. This bubbling phenomena will then need to be glued onto the main part to get a compact manifold. See [Weh13, Lecture 7–9] for notes on this phenomena of *Gromov compactness*.

□

Remark 4.3.12. Even for non-regular J , we can still use the above to construct a Fredholm problem by [MS12, Theorem C.1.10 (Riemann-Roch)], which is proven in the case of Lagrangian boundary condition. How we get the smooth structure will be a different matter though, because J is not regular. This is where abstract perturbations may be necessary.

Example 4.3.13 (Moduli space of domains). Deligne-Mumford space: stable curves (genus g and k marked points) to a point. Quotient by reparam. To compactify and get all the possible codimension 1 configurations, namely limits of stable curves, we consider a suitable dual graph. C.f. [Sei08, §9] and Liu reference for dual graphs.

A tree encodes information for how to glue, where interior edges are assigned a gluing length, and semi-infinite edges at either end give the resulting marked points of the final glued disc. The idea is that we can have a family of discs, parametrized in the base by possible cyclic configurations. We also have a gluing parameter for each interior edge. The more interior edges we have the more dimensions the base will have because the more codimensional space do the bubbles take up.

We then compactify the base of this family by adding in all d -leafed trees. If we have second countable and Hausdorff on $\bar{\mathcal{R}}^{d+1}$ then we can define continuity, a topology and smoothness. Claim is that FOOO says it's inherited from being a subset of real locus (because gluing parameter is real) of the Deligne-Mumford space $\bar{\mathcal{M}}_{0,d+1}$. See also [Sei08, §13] for a discussion of regularity of polygons and a sheaf-theoretic interpretation.

Claim 4.3.14. Given the Fredholm section we can compute the expected dimension of the manifold of parametrized curves, and then the moduli space of unparametrized curves will be three less. We also have an induced orientation.

Analogue in Morse theory – when have Morse-Smale data then know the dimension of moduli space by counting eigenvalues. Transverse intersection of unstable of x_- and stable of x_+ . Projection map from unstable to perp of stable. Index of a Fredholm section is spectral flow of Hessian (versus counting eigenvalues of a Hessian matrix as in Morse case.) Spectral flow of $(J_0\partial_t + S_s)_{s \in \mathbb{R}}$ where D_u is this plus ∂_s plus a compact perturbation.

Claim 4.3.15. Aut acts smoothly on the manifold of parametrized curves, hence the moduli space $\hat{\mathcal{M}}/Aut$ is a smooth manifold.

Claim 4.3.16. We can put a smooth structure on the compactified moduli space using gluing. The configurations we glue are precisely those in Gromov compactness. This allows us to obtain the structure of a smooth compact 0-dimensional manifold, which we can then count.

Sketch. This is covered in [MS12] and [Weh13]. Gromov compactness follows from results such as the isoperimetric inequality: $|a(\gamma)| \leq C|\text{length}(\gamma)|^2$, the removable singularity theorem and energy decay. This tells us what the possible limit configurations of discs are: a disc bubble at a boundary point, a sphere bubble, or strip-breaking.

Compactifying as topological space. We then consider any disc bubble, sphere bubble, or strip-breaking and show it is the limit of a sequence of J -holomorphic curves. This is done by first pregluing the maps by pasting them together, which may not give something J -holomorphic, and then Newton iterate it to a J -holomorphic map.

The upshot is that the boundary of the unparametrized moduli spaces (namely $\overline{\hat{\mathcal{M}}/Aut} \setminus \hat{\mathcal{M}}/Aut$) is a fiber product of moduli spaces which agree at their intersection point. E.g. we will have a component for moduli spaces of discs fiber product with moduli spaces of spheres over their common intersection point, to account for sphere bubbling.

Compactifying as smooth manifold: existence of regular J for limit configurations. So to finish up the sketch that the moduli spaces are compact smooth 0-dimensional manifolds, we need to prove the existence of regular J for these additional fiber product configurations. As described above, we can exclude disc bubbling and strip-breaking by the geometry of Y . So we only need to consider sphere bubbling from spheres in the central fiber. The addition of a point where the disc and sphere attach at means we need a notion of additional data to account for these *special points*.

Definition 4.3.17 (Moduli space of stable maps). A *stable map* is given by a tree, where each vertex α is a sphere bubble, except for the original main sphere one. The *stable* refers

to the nontrivial automorphisms; in particular if we fix three points there are no nontrivial automorphisms. A *pseudocycle* is when the image of the boundary of the moduli space has codimension at least two in the total space. The *virtual dimension* is given by the Maslov index minus twice the number of edges in the stable tree. That is, each bubbled off sphere reduces dimension by 2. *Semipositive* means that there are no J -holo spheres of negative Chern number for generic J – this is our setting because it's Calabi-Yau. We define the resulting moduli space by taking a collection of maps, quotient by reparametrization, and then compactify.

Lemma 4.3.18 (Bolzano-Weierstrass analogue for bounded energy curves limit to trees). *The moduli space of stable maps exhibits Gromov convergence.*

C.f. [MS12, Chapter 5]. Let u.c.s. := uniformly on compact subsets. If the derivatives in a fixed homology class are bounded in $W^{1,p}$ for some $p > 2$, then we have a Bolzano-Weierstrass type result that any sequence has a convergent subsequence. However, in the borderline $p = 2$ case, as is the case here, the limit may not be in original class of curves. Gromov convergence to a stable map: for each vertex α of tree we have a family of reparametrizations ϕ'_α . The marked points stay fixed, at least in the limit they do.

We use the following terminology to introduce the objects required to include limits of curves, i.e. to achieve a compact moduli space. Finite energy can still have bubbles because energy is invariant under rescaling, argument rescales inversely whereas differential forms rescale proportionally. However derivative may blow up as in the following example: $\mathbb{C}\mathbb{P}^1 \rightarrow \mathbb{C}\mathbb{P}^2$ given by $[x : y] \mapsto [x^2 : \epsilon y^2 : xy]$. Parametrizes holo curve in $\mathbb{C}\mathbb{P}^2$ given by $ab = \epsilon c^2$. As $\epsilon \rightarrow 0$, we only get curve $[x : 0 : y]$. However the limit of the image is actually two spheres, $ab = 0$ and not just $b = 0$ because of rescaling in $\mathbb{C}\mathbb{P}^2$. Look at $ab = \epsilon c^2$ and let $\epsilon \rightarrow 0$ to get $ab = 0$.

If we remove the bubbling points, then sequence of curves converges u.c.s. to the main component. To find the other bubbled-off components, take a new curve defined by z/R_n where the R_n goes to infinity and add a sequence of points tending to the bubble point. Energies of main plus bubbles should add up to original energy. Energy remains the same in limit.

e_i denotes $\frac{1}{2}|du_i|^2$. To get C_{loc}^∞ convergence to the main component we use the Bolzano-Weierstrass theorem on the energy. And the reason the main component is fully defined on S (even though we removed the bubble points) is because of removable singularity property of pseudo-holomorphic maps. \square

Lemma 4.3.19 (Gromov compactness for stable maps, c.f. [MS12, Equation (5.1.5)]). *The compactification of the moduli space of unparametrized curves (i.e. equivalence classes) is a union over possible bubble trees of unparametrized curves.*

Sketch. The reason is that these are the possible limit configurations. Equation (5.1.5) equips the set with a topology in the situation of special points, and later on discusses gluing and a Fredholm problem in this setting. \square

In particular, we'll need gluing and a discussion of the Fredholm problem for a disc and a sphere. We will then show that the moduli space of a somewhere injective disc union a simple sphere is a manifold of negative dimension, meaning it is empty and can be excluded.

Lemma 4.3.20 (Excluding bubbling in our setting). *There exists a dense set $\mathcal{J}_{reg}^2(Y, \partial Y; \mathbb{D} \cup \mathbb{P}^1)$ of J regular for the moduli space of a simple sphere in the central fiber union a somewhere injective disk, which is section-like hence must be simple.*

Corollary 4.3.21. *The moduli space for the regular J above has negative dimension, this is empty. In particular, the moduli space of any somewhere injective disk passing through the open set U union any configuration of multiply-covered and simple spheres can be excluded.*

Proof of Corollary 4.3.21. The Riemann-Roch theorem [MS12, Appendix] implies the dimension of the manifold cut out by the regular J is of negative dimension, specifically dimension -2 . Lazzarini's result [Laz11] implies any disc can be decomposed into simple discs and his other paper [Laz00] shows that any J -holomorphic disc contains a simple J -holomorphic disc. Thus if we had a nonempty configuration as in the statement of the corollary, we would have a non-constant map in the case of a simple disc union a simple sphere, by factoring through the multiple covers and taking one simple disc that goes through the sphere. But this is a contradiction, so there couldn't have been any such nonempty moduli spaces to begin with. \square

Proof of Lemma 4.3.20. We have dense sets of J regular for each component (the disc and the sphere); the disc was described earlier and the sphere situation is done in [MS12, Chapter 3]. This proof will involve checking that there is still a dense set of J in the intersection of these two dense sets which interact well at the point over 0 where the disc and sphere intersect.

Intersect dense set of regular J for sphere and disc separately. Consider $\mathcal{U} \subset \mathcal{J}_{reg}^2(Y, \partial Y; \mathbb{D} \cup \mathbb{P}^1) \times \mathcal{J}_{reg}^1(Y, \partial Y)$ where $u_{\mathbb{D}}(\mathbb{D}) \not\subseteq u_{\mathbb{P}^1}(\mathbb{P}^1)$ (in contrast with the case of just spheres where we require the images not be equal). We have the pointwise constraint that the sphere and disc are attached at a point. So we need transversality of the evaluation map $\mathcal{U} \rightarrow Y \times Y$.

Using Sard-Smale we can deduce that \mathcal{U} is a manifold, with an additional check involving annihilators on the multiple components as follows. This is from [MS12, Chapter 6]. An L^q form η that annihilates $D_u \xi$ over $W^{1,p}$ test vectors ξ which vanish on the point of intersection of the sphere and disc, thought of either as a point on the sphere (McDuff-Salamon) or on the disc (same proof as in [MS12] but we have less to test because the spaces are smaller due to more geometric constraints) in fact has $W^{k,p}$ regularity. Recall that the elliptic bootstrapping result of [MS12] is proven for Lagrangian boundary conditions. Via integration by

parts we show $D^*\eta = 0$; this is Stokes' theorem and the product rule applied to $\langle \eta, \xi \rangle$ which is evaluation on the 1-form and inner product on the bundles. In particular, η and the test vectors ξ being tangent to the Lagrangian at the boundary ensure that the relevant integral is zero.

The implicit function theorem puts the structure of a Banach submanifold on the cross product $\mathcal{J}_{reg}^2(Y, \partial Y; \mathbb{D} \cup \mathbb{P}^1) \times \mathcal{J}_{reg}^1(Y, \partial Y)$, at which point we use an evaluation map to ensure transversality. Then the preimage of the diagonal is not just a subset but a submanifold, and in particular is the desired dense set of regular J of the lemma. This is done in a series of lemmas in [MS12, §3.4], which are valid when applying the theorems in the appendices because these are done for Lagrangian boundary conditions.

- Want evaluation map to be transverse. The disc and sphere must intersect at 0 in the domain since the central fiber of ν_0 is where H_2 is nonzero. We also fix a point on the boundary of the disc so there are no nontrivial automorphisms.
- To show the evaluation map is transverse, it's enough to construct \dot{J} supported in small balls, one on each component. Each ball should not intersect the other component. Because of the “half-way step” where we looked at \mathcal{U} inside the product of the moduli spaces for each component, that means we can find such open sets.
- This is possible because: 1) the Lagrangian boundary condition implies \dot{J} is zero near the boundary and so if it's only supported on a small ball in the interior it is of this form and 2) we can extend each \dot{J} by zero and then add them. In order to check transversality, we want the linearized map to be surjective. So we select two tangent vectors in codomain at $(0_{\mathbb{D}}, 0_{\mathbb{P}^1})$, and then construct two \dot{J} supported in small balls around the intersection point. This will give us transversality.
- To show existence of these \dot{J} , we need a regularity and vanishing result about forms η that are zero on D_u . Because then we'll get $D_u\xi + \frac{1}{2}\dot{J}duj$ surjects onto $W^{k-1,p}$ spaces which will allow us enough freedom to find the vectors above. With boundary conditions, all the lemmas in the appendix hold as well as integration by parts because taking the adjoint means the boundary term is $d\langle \eta, J\xi \rangle_\omega$ and so on the boundary Lagrangian and using ω -compatibility we find that term vanishes. So everything carries through in this setting.

By Sard-Smale on this subset of the universal space where they respect the pointwise constraint, we get existence of a dense set of regular J for the disc and sphere so that the evaluation map at their intersection is transverse. This concludes the proof of Lemma 4.3.20. \square

Limit configurations form smooth manifold. Now that we have a regular J for the limit configuration, we prove that $\bar{\partial}_J$ cuts out $\hat{\mathcal{M}}_{\mathbb{D}}/Aut \times_0 \hat{\mathcal{M}}_{\mathbb{P}^1}/Aut$ transversally so it is

a manifold. To get a manifold structure, we again want a Fredholm section of a Banach bundle where the linearized operator is surjective with right inverse.

Let Σ be the Riemann surface given by the disc with one fixed boundary point attached to a sphere at the origin. As above, we put a Banach manifold structure on $W^{k,p}(\Sigma, Y)$, via charts modelled off its tangent space, which we know is a Banach manifold. That is, we describe maps “close to” a given map u using the exponential map: given a point u and a tangent direction ξ at that point, we move u along the geodesic (i.e. path where the least action is required) in the tangent direction ξ for time 1 to obtain a new map $W^{k,p}$ map $\exp_u \xi$ that pushes u everywhere slightly in the direction of ξ .

We want to preserve the Lagrangian boundary condition on $u_{\mathbb{D}} : \mathbb{D} \rightarrow Y$, so if ξ is tangent to L and $z \in \partial\mathbb{D}$ then $u_{\mathbb{D}}(z) \in L$ and we want $\exp_{u_{\mathbb{D}}} \xi$ on $\partial\mathbb{D}$ to still be in L . In other words, if we push off u in a direction ξ tangent to L , the new map should still map its boundary to the desired Lagrangians. Said another way: a geodesic that starts in L and initial velocity tangent to L should stay in L . This is precisely the definition of *totally geodesic*. Thus L must be totally geodesic. Recall that geodesics (and minimizing action) only make sense with a metric on Y . So we need a metric on Y for which all Lagrangians involved are totally geodesic. The existence of a metric so that one Lagrangian is totally geodesic is proven by Urs Frauenfelder in his diploma thesis, see [MS12, Lemma 4.3.4]. In general we at most have two Lagrangians at an intersection point, and existence of a metric so that both Lagrangians are totally geodesic is proven in [Mil65, Lemma 6.8], which also has a self-contained account in the lecture notes on the Whitney Trick [Fra10, Lemma 0.6, Lec 11], the proof of which is continued in [Fra10, Lec 12].

For the fiber of the Banach bundle, we don’t need to worry about boundary conditions c.f. [Sei08, §(8h)].

The case of regular J and obtaining a smooth manifold from the zero set of $\bar{\partial}_J$ for curves with pointwise constraints involves a few additional checks from what we did before with just the disc. We list them, and this follows [MS12, §3.4].

- Construct an η locally that lives in a fiber of the Banach bundle.
- Show that η has $W_{loc}^{k,p}$ regularity, which is why in previous step we look at it locally.
- Once we have regularity, we can integrate to get $D_u^* \eta = 0$.
- Then we write out $D_u^* \eta$ and use Carleman similarity principle to see that if η is zero on an open set it must be identically zero.
- This allows us to show that the annihilator of a certain space is zero, whence Hahn-Banach applies to give us denseness so combining that with closedness from the Fredholm property we find that the linearized operator when including \mathcal{J}^l in fact surjects onto $W^{k-1,p}$.

- We are still working on a single component, \mathbb{P}^1 or \mathbb{D} . This surjection tells us that we can find a ξ pointing in a specified direction at a specified point *and* tangent to moduli space. First do former, apply previous bullet point to modify to get latter.
- Moreover one can do this in a small neighborhood around a specified point. Hence we can add vectors that work on *different components*. Now we bring in $\mathbb{P}^1 \cup \mathbb{D}$.
- Since the (linearized) evaluation map is surjective on vectors, the universal moduli space is a manifold hence we have a dense set of regular J , and so the moduli space with a regular J is a manifold.
- Done since elliptic bootstrapping and the implicit function theorem are covered in the appendices of [MS12] for Lagrangian boundary conditions.
- Note: we may encode asymptotic behavior via the C_ϵ^∞ -topology, see [Sei08, Remark 9.9].

We have now excluded all types of bubbling behavior. So the moduli spaces $\hat{\mathcal{M}}/Aut$ are already compact manifolds, and the proof is complete. We can now take their zero-dimensional part to use in the construction of the Fukaya category below. \square

Corollary 4.3.22. *The above is valid for a disc with any number of Lagrangians and punctures with strip-like ends, because of the existence of metrics for which two Lagrangians are totally geodesic, [Mil65, Lemma 6.8].*

4.4 $H^0(FS(Y, v_0))$: definition and independence of choices

Now we arrive at the definition of the Fukaya-Seidel category. Because of the linearity of Lagrangians considered, they have a lift that allows for Maslov grading given by their slope, and they have a Spin structure as well.

Definition 4.4.1. The *Fukaya-Seidel category* $FS(Y, v_0)$ is defined as follows, using the *categorical localization method*, instead of Hamiltonian perturbation methods (as in [Sei08]):

- Objects: the Lagrangians in $FS(Y, v_0)$, i.e. in the total space, are allowed to be non-compact. The Lagrangian L_i is obtained by taking ℓ_i over -1 in the base of v_0 and parallel-transporting it around the singular fiber over zero, along U-shapes as in Figure 4.5.

Specifically, outside of a compact set around the origin, the Lagrangians must project to rays in the plane, and they are fibered meaning the parallel transport of Lagrangians in the fiber.

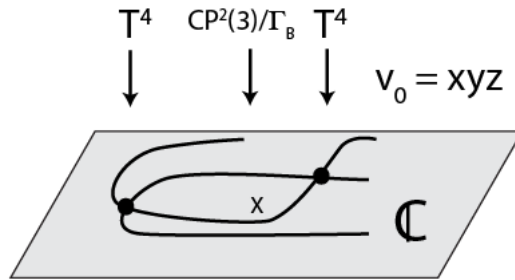


Figure 4.5: $L_i =$ parallel transport ℓ_i around U-shaped curves in base of v_0

- Morphisms: we define a directed category

$$\text{hom}(K, L) = \begin{cases} CF(K, L), & \text{if } K > L \\ \mathbb{C} \cdot 1, & \text{if } K = L \\ 0, & \text{else} \end{cases} \quad (4.5)$$

where the ordering $>$ denotes that, outside a compact set, all the rays of K lie above all the rays of L . If $K = L$, then we push the rays of one copy to lie above the rays of the other copy as in Figure 4.5 and the unit e_L is the count of discs with those Lagrangians as boundary conditions. This pushing procedure gives L^ϵ . We then localize at these e_L , in other words we set them to be isomorphisms. Recall that formally inverting morphisms involves taking equivalence classes of roofs

$$K \leftarrow K^\epsilon \rightarrow L$$

which is the definition of an arrow $K \rightarrow L$ when $K < L$, namely push up to $K^\epsilon > L$ so that the first arrow of the roof is a quasi-isomorphism, and then $K^\epsilon \rightarrow L$ is defined as above.

- The differential (μ^1), composition (μ^2), and higher order μ^k count bigons, triangles, and $(k + 1)$ -gons respectively which are *section-like maps* as defined in Definition 4.3.5, and have the usual Lagrangian boundary conditions from these L_i , and are J -holomorphic for some regular J , which exists by the above. These moduli spaces can be counted by the theory of the previous section.
- Note that here we exclude T_z , the parallel transport of t_z around a circle in the base, as an object of the subcategory of the Fukaya category we are considering, to avoid the use of bounding cochains in defining $\text{hom}(T_z, T_z)$ due to disc bubbling.

Lemma 4.4.2. *Correct position for homs in localized category, via Abouzaid-Seidel, Ganatra's notes, Abouzaid-Auroux.*

Lemma 4.4.3. *The composition of roofs is a roof.*

Proof. See M. Jeffs masters thesis. □

Remark 4.4.4 (Units). In Floer theory $HF(V, V) \cong H(V; \mathbb{K}/2)$. The cohomology ring for the 2-torus (“height zero” part of a T^4 fiber) is \mathbb{Z} in degree zero and two, and $\mathbb{Z} \oplus \mathbb{Z}$ in degree 1 by the Künneth formula. We indeed have the same number of generators on the cochain level.

Definition 4.4.5. The *Donaldson-Fukaya category* is obtained by passing to cohomology on the morphism chain complexes. It is an example of a *topological quantum field theory*, i.e. a functor from manifolds to vector spaces where cobordisms map to vector space homomorphisms.

Lemma 4.4.6. *Let J_1 and J_2 be two regular almost complex structures. Then they give quasi-equivalent Fukaya A_∞ -categories.*

Proof of lemma. Seidel §8 and §(10c). □

Remark 4.4.7. This is discussed in (10a) and (10b) of [Sei08], which go beyond what we need. Section (10c) of [Sei08] contains the argument of an isomorphism of the Donaldson-Fukaya categories.

We can construct an A_∞ functor (which will be the identity as noted above), see the beginning of [Sei08]. Then we don’t need to consider homotopies. This is not true in general because μ^2 could jump, but not here because all intersection points are in degree 0. We have a linear continuation map, and all higher ones are the identity.

The classical approach of FOOO and Floer is to construct a homotopy. See [FOOO09a, p 244]: the algebraic background on homotopies is in section 4.2, then after introducing the virtual fundamental chain the theorem is applied to the Fukaya category setting in Corollary 4.6.3 of the book or Theorem 15.19 of their 2000 preprint.

Seidel upgrades this system to the A_∞ -setting by packaging all the Fukaya categories for varying choices of J indexed by i into a “total” Fukaya category, and showing that each $\mathcal{F}(Y)^i$ fully faithfully embeds into the total while inducing an isomorphism on cohomology using Salamon-Zehnder’s work for an actual category. Thus all $\mathcal{F}(Y)^i$ are quasi-isomorphic to the same thing, hence to each other, and the proof is complete.

Note that [FOOO09a, p 244] discuss J -invariance. Algebraic homotopy invariance is discussed in section 4.2, and the main theorem is in section 4.6. In between these two they setup the geometrical fundamental chain as an application of the algebraic theory in section 4.2

In general, a continuation map argument with a single PDE that interpolates between the two J ’s indicates an isomorphism of Floer groups at each choice, and then Seidel in [Sei08, §(10c)] discusses upgrading this to the A_∞ -category.

Corollary 4.4.8. *This category is independent of regular choices of datum so is well-defined. In particular different values of sufficiently small T , so when defining the complex structure we have a proper holomorphic group action of Γ_B that we can quotient by, give quasi-isomorphic Fukaya categories.*

Proof. Invariance under regular J is given above. Invariance under Hamiltonian perturbations in the fiber has been done before in the literature. This completes the proof that we have a well-defined Fukaya category. □

Remark 4.4.9. We will technically have a mirror correspondence between a family of Fukaya categories over T , so the complex structure J_T involves scaling the standard J , and scaling the symplectic form on the A-side. Showing invariance would involve looking at a connected path in the space of ACS, namely that obtained by scaling this T .

Chapter 5

The main theorem

5.1 HMS computation

Remark 5.1.1. In physics the functor $(Y, v_0) \mapsto H^0(FS(Y, v_0))$ can be referred to as a *topological quantum field theory* or TQFT. That is, the first part of a TQFT is a functor from certain manifolds to vector spaces. For more background, see Segal’s lecture notes [Seg]. We will be considered with the Donaldson-Fukaya category in this thesis, and the full A_∞ -categorical equivalence is a future direction. In order to pass to H^0 , we need to know the differential.

Remark 5.1.2. Recall above that we stated the definition of the Fukaya-Seidel category. However, to prove a fully faithful HMS embedding on the cohomological level, we will need to compute the differential on $FS(Y, v_0)$ to find morphisms groups in $H^0(FS(Y, v_0))$, and not just know the existence of the differential as above. Also, the definition above was with regular J that excluded sphere bubbling, which was proven adapting results of McDuff-Salamon: the philosophy is that, assuming “generic J ” relates to the same generic in “generic intersection”, the union of all points in a zero-dimensional family of spheres is two, and that of discs in a one-dimensional family is three, so generically these two don’t intersect in a six dimensional manifold.

However, when we compute the differential below we will use the standard J_0 , which is multiplication by i in the toric coordinates, and there we cannot exclude sphere bubbling. The reason is because of the nontriviality of $H_2(v_0^{-1}(0))$, the central fiber of Y , which arises from submanifolds that are J_0 -complex since v_0 is holomorphic with respect to J_0 . Nonzero Dolbeaut cohomology implies the spheres are not regular, i.e. by Riemann Roch and fact that cokernel of $\bar{\partial}$ operator is actually Dolbeaut cohomology. We use the theory of Gromov-Witten invariants to describe the computation of spheres given in [KL19] and then show invariance of the Fukaya category for nonregular J by polyfold theory’s use of abstract perturbations of $\bar{\partial}_J$ [BFW17] to show that polyfolds give a quasi-isomorphic Fukaya category

as the one computed directly with J_0 . Thus we can match up the categories of HMS using the direct computation of the differential with J_0 .

Remark 5.1.3 (Notation). Capital M^k denotes structure maps on the total space of Y and lowercase M^k denotes structure maps on the torus fiber.

Lemma 5.1.4. $\partial : CF(\ell_{i+1}, \ell_j)[-1] \rightarrow CF(\ell_i, \ell_j)$ can be computed from the data of $\partial : CF(t_z, \ell_i) \rightarrow CF(t_z, \ell_j)$ over all z .

Proof. Let p_j denote the intersection point of ℓ_j and t_z , and let $t_{i,j}^k$ denote the k th intersection point of $\ell_i \cap \ell_j$, where $0 \leq k < (i-j)^2$ as described in the definition of the Fukaya-Seidel category above. We can compute the first and last vertical arrow of the diagram below, and we want to compute the middle arrow. Let's say the differential maps p_j to $C(z) \cdot p_j$ where $C(z)$, for count, is a count that we will compute, depending on z but not j . This diagram allows us to find the middle vertical arrow. Note that upper case refers to parallel transporting lower case fiber Lagrangians around curves in the base. The crux of this argument is that we use the Leibniz rule. See Figure 5.1.

$$\begin{array}{ccc} \text{hom}(\ell_j, t_z) \otimes \text{hom}(\ell_{i+1}, \ell_j) \ni p_j \otimes t_{i+1,j}^k & \xrightarrow{M^2} & \text{hom}(\ell_{i+1}, t_z) \ni M^2(p_j, t_{i+1,j}^k) \\ \downarrow \partial & & \downarrow \partial \\ \text{hom}(\ell_j, t_z) \otimes \text{hom}(\ell_i, \ell_j) \ni Cp_j \otimes \partial(t_{i+1,j}^k) & \xrightarrow{M^2} & \text{hom}(\ell_{i+1}, t_z) \ni \partial(M^2(p_j, t_{i+1,j}^k)) \end{array}$$

In particular, by the Leibniz rule for differentiating a product we have

$$M^1(M^2(p_j, t_{i+1,j}^k)) = M^2(M^1(t_{i+1,j}^k), p_j) + M^2(t_{i+1,j}^k, M^1(p_j)) = M^2(M^1(t_{i+1,j}^k), p_j)$$

because $M^1(p_j) = 0$, since p_j is of degree 0 and there is nothing in degree 1 at the other intersection points of the two Lagrangians; note that p_i is of degree -1 . Note that $M^1(t_{i+1,j}^k)$ is what we are looking for. Also, the fibration is trivial in the beige region so we can count triangles in a fiber with points at p_i, p_j , and $t_{i+1,j}^k$ to get that $M^2(p_j, t_{i+1,j}^k) = D(z) \cdot p_i$ for some function $D(z)$. Then $M^1(p_i)$ will be computed by the homotopy argument, to get $C(z) \cdot p_j$. So the equation above gives

$$C(z) \cdot D(z) \cdot p_j = M^2(M^1(t_{i+1,j}^k), p_j)$$

from which we can compute $M^1(t_{i+1,j}^k)$.

The reason we would like to use t_z and not some ℓ_j is because this will allow us to count discs with boundary in the preimage of a moment map, as in [CO06]. The Lagrangian T_z obtained by parallel-transporting t_z around U-shaped curves corresponds to evaluation sections at the point z on the mirror side. So once we know the morphisms groups for all t_z , we know homs between any ℓ_i and ℓ_j .

□

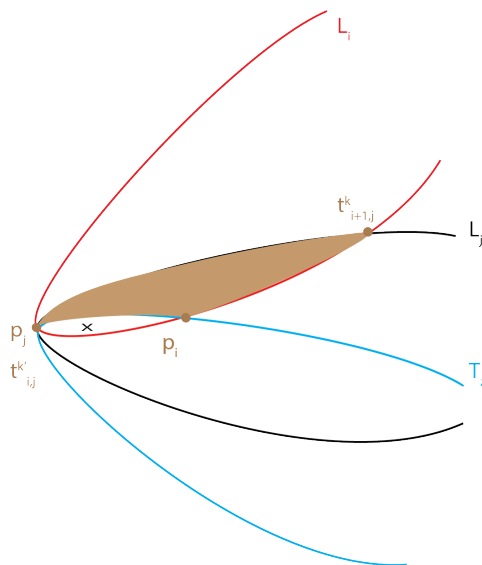


Figure 5.1: Leibniz rule

Now we describe is the homotopy argument that will allow us to find the $M^1(p_i)$. See Figures 5.2 and 5.3.

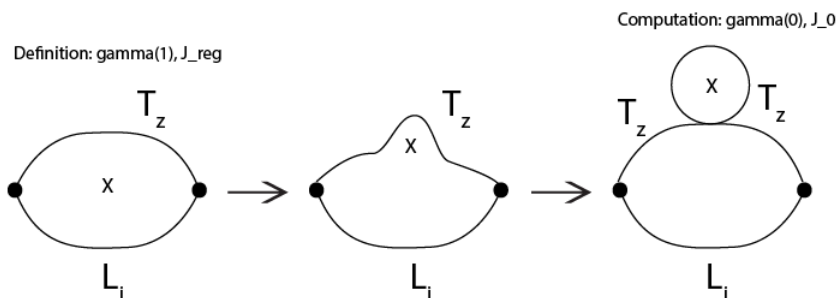


Figure 5.2: The homotopy between ∂ (left) and the count of discs we compute (right)

Remark 5.1.5. In the computation with J_0 , we are using a non-regular J . Thus we will need to use an invariance of J argument that incorporates invariance under non-regular J . We use the abstract regularization methods of polyfolds for this (perturbing $\bar{\partial}_{J_0}$ via a section of the Banach bundle, which may or may not be induced from perturbing J_0 , hence the term “abstract”).

The computation of the Gromov-Witten invariants from [KL19] involves proving that an open Gromov-Witten has an isomorphic Kuranishi structure as a closed Gromov-Witten

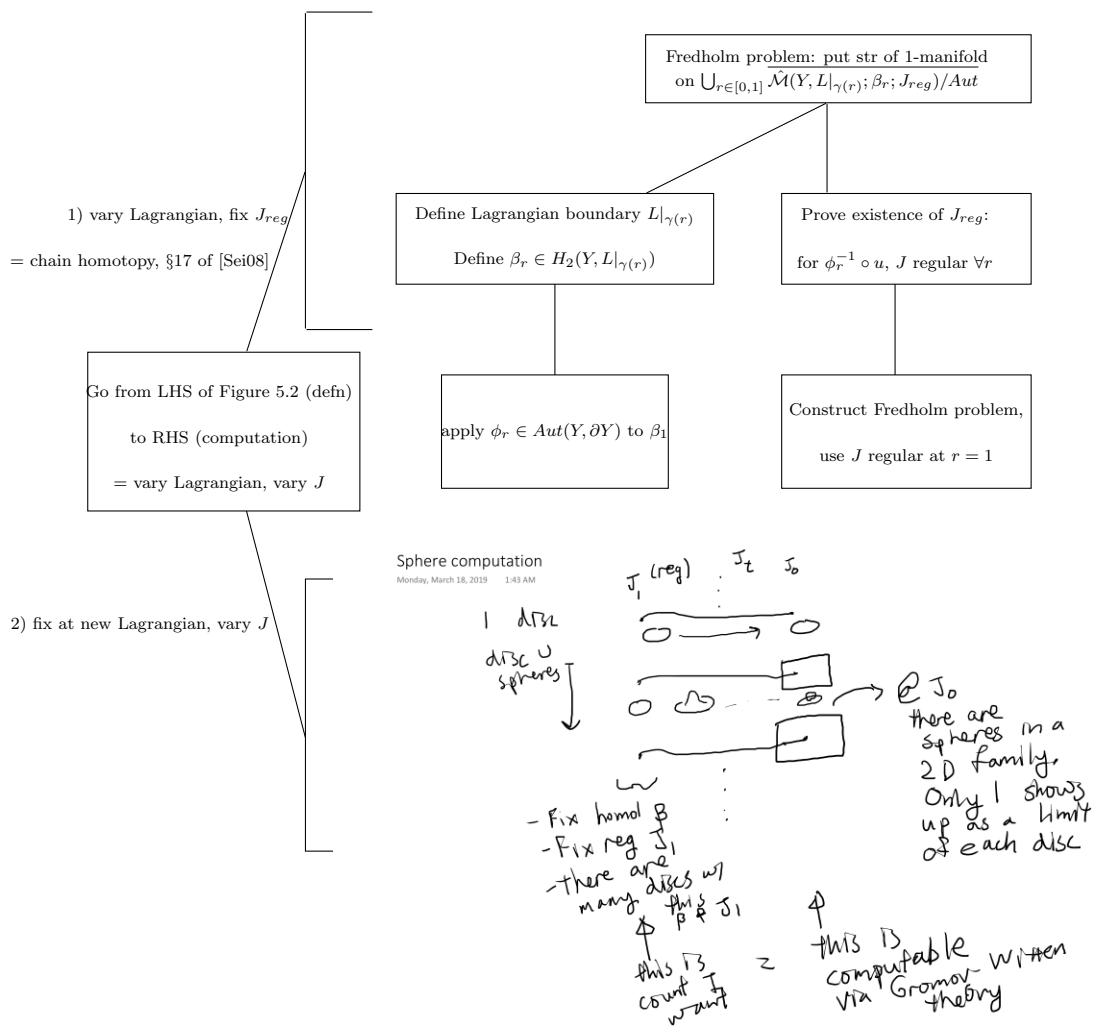


Figure 5.3: Plan for computation

invariant. This uses [Cha11] and will be discussed further. In this section we discuss the homotopy argument. Then we discuss the computation of discs and sphere bubbles. Finally we finish with the polyfold argument for how the computation relates to the definition.

Remark 5.1.6 (Notation). This section uses theory developed in [Sei08, §17g] for counting pseudo-holomorphic polygon sections which pass through singular fibers. In that section, d is called M^1 here. Also L_1, L_2 from Seidel are t_z in this setting and $Q = \ell_i$. This follows from L_2 being isotopic to $\phi(L_1)$. All other maps here should be named the same as Seidel's notation.

Lemma 5.1.7. $M^1 : CF(T_z, L_i) \rightarrow CF(T_z, L_i)$ is homotopic to $M^2(c, -)$ where c is a count of discs times a suitable intersection point p .

Proof. First we note that

$$M^1 : CF(t_z, \ell_i) \rightarrow CF(t_z, \phi(\ell_i)) \xrightarrow[\phi^{-1}]{c} F(\phi^{-1}(t_z), \ell_i) = CF(t_z, \ell_i) \cong \mathbb{C}$$

where ϕ is the monodromy. We've used that applying the diffeomorphism ϕ^{-1} gives a bijection between intersection points, and t_z is invariant under parallel transport because it only rotates angles. So we get $CF(t_z, \ell_i)$, which has only one intersection point.

Open Gromov-Witten invariant theory can count J_0 -holomorphic discs with boundary on a moment map fiber, one marked point, and passing through the singular fiber of Y once (as is the case because recall from the definition, because they are 1-1 and with J_0 we actually get sections of v_0). However, M^1 as is counts bigons through the singular fiber with boundary on T_z and L_i . So following [Sei08, §17g] we deform M^1 . Call the count of J_0 -holomorphic discs with boundary on T_z and marked point p as count $c \cdot p$. This deformation constructs a homotopy l such that

$$M^2(c, \cdot) - M^1(\cdot) = M^1 \circ l - l \circ M^1 = 0$$

where the zero is because $M^1 = 0$ on the torus fiber. See Figure 5.2. Below, we describe the details from his book, filling in as needed the additional information in the slightly different setting of this thesis. In this setting, the analogue of the vanishing cycle that one Dehn twists from Seidel is three families of T^2 's degenerating to S^1 's which intersect at a point. One property we need though to apply his theory is that the monodromy ϕ preserves $t_z = \{(\xi_1, \xi_2, \theta_1, \theta_2)\}_{\theta_1, \theta_2 \in [0, 2\pi)}$, which is still true here.

We start by defining k , a homotopy between $\tilde{d} := M^2(c, -)$ and the zero map, where c is closed hence a Floer homology representative. Set $\tilde{l} = M^2(k(\cdot), \cdot) + M^3(c, \cdot, \cdot)$.

Claim 5.1.8. The claim is that (\tilde{d}, \tilde{l}) satisfy the boxed equations in [Sei08, (17.15)] which express that \tilde{d} is a chain map between the two CF groups on the fiber and \tilde{l} is a homotopy

between $\tilde{d} \circ M^2$ and zero.

Also, isotoping L_1 and L_2 , and taking different choices of (d, l) satisfying these same equations give homotopic maps, so we have a uniqueness statement and can take a limit of choices without changing the theory.

Proof. The equations (17.15) are satisfied by definition of (\tilde{d}, \tilde{l}) . So next we look at how (d, l) depends on L_1 , and similarly in the tilde case. Use continuation maps a and b to go from $CF(Q, L_1)$, $CF(L_0, L_1)$ respectively to the tilde versions. Thus the maps are well-defined, namely they have the same input. Seidel claims also that the continuation maps are compatible with the triangle product up to a chain homotopy. The maps in the moduli spaces of sections for the continuation maps have boundary condition constant over Q or L_1 and realize the isotopy from L_1 to \tilde{L}_1 over the time 1 side of the strip-like end. The moduli space for the chain homotopy h needed in compatibility of the triangle product is as follows: take trivial fibration with boundary Q, L_0, L_1 and glue on the moduli space for a . Similarly do with (Q, L_0, \tilde{L}_1) trivial, glued to b . The chain homotopy h is defined to go between these two. Since the continuation maps are quasi-isomorphisms, we have an isomorphism on cohomology. Likewise we can isotope L_2 and still get isomorphic cohomology.

First we look at moduli spaces interpolating between the Floer complexes. Namely, δ is a map between the two Floer complexes over the two intersection points: $t_z \cap \ell_i$ at each end. And λ is a product map. These new objects δ and λ satisfy equations similar to (17.15) but there are additional $d + \tilde{d}$ and $l + \tilde{l}$ terms respectively. The equations say that the two chain complexes $C' \oplus C \oplus C''$ and the tilde version are isomorphic. Note that (δ, λ) is a construction for varying (\tilde{d}, \tilde{l}) more generally, while (α, β) is a construction from varying d by varying L_1 specifically which introduces more terms than in the first case.

Next we want to see why different choices of (d, l) satisfying (17.15) give homotopic results (a more general result than taking a different choice from isotoping L_1 and L_2). Pick some such (d, l) . We construct a homotopy between d and $\tilde{d} \circ a$, call it α . Similarly call β a chain homotopy between l and \tilde{l} . The continuation maps are quasi-isomorphisms and α, β produce a map between D and \tilde{D} which is a quasi-isomorphism. \square

Claim 5.1.9. We can compute M^1 using $M^2(c, -)$ and obtain quasi-isomorphic Fukaya categories.

Proof. This is a limiting case of the uniqueness statement. Here ξ and ψ pertain to varying the differential and product. And ξ interpolates between what Seidel refers to as d and $M^2(c, -)$. We look at the limit of isotopies on this L_1 . The reason being: that was how we varied L_1 in the previous section and so in particular, that was how we varied d . So we say \tilde{d} is a limiting case of the previous section because of the limiting case of isotoping \tilde{L}_1 : here $\tilde{d} = M^2(c, -)$.

Now to construct the homotopy between the choices for triangle product: we'll look at a parametrized family that has five parts. The first part is l as in the original (d, l) pair. The second family is that associated to $\xi(M^2)$: glue the ξ fibration to a trivial 3-pointed disc. Remember that ξ was the 1-parameter family interpolating between the two differential-like options: d and $M^2(c, -)$. So we get another family, by gluing this family to a 3-pointed disc. Effectively we are making the ξ family into a family that works on the product level. "Large gluing length" implies this is just $\xi(M^2)$. Note that at $r = 0$ we get the l family at $r = 1$. At the other end of the second ξ family, when $r = 1$, we get $M^2(c, M^2(,))$. Take a sufficiently large closed interval $[0; 1] \subset \mathcal{R}^4$.

□

Remark 5.1.10. We have a composition of maps on one side of the homotopy, namely $M^2(c, -)$. Anytime we compose two structure maps in the Fukaya category, geometrically this corresponds to gluing the Fredholm problems producing the moduli spaces that are counted in each structure map. So we will need to discuss gluing in this particular setting. This is another place where our setting differs from that of Seidel. In the book, he deforms the fibrations. However in this setting, the fibration stays the same, while the Lagrangian boundary conditions are deformed. So we will need a gluing argument to deduce the moduli space

$$\bigcup_{r \in [0, 1]} \mathcal{M}(J_{reg}, L_r)$$

is a one dimensional smooth manifold. The following theory follows [Weh14, Lecture 9]. Also Fall 2013, Lecture 14 of Wehrheim's topics course and McDuff-Salamon: First done with J_z . §10.9 deals with case of just J .

Claim 5.1.11.

$$\bigcup_{r \in [0, 1]} \mathcal{M}(J_{reg}, L_r)$$

is a 1-dimensional manifold.

Outline of proof. To prove the existence of a smooth structure, we construct a Fredholm problem. Let γ_r denote the varying path in the base of the fibration indicated in Figure 5.2. Let $\{\phi_r\}_{r \in (0, 1]}$ be an isotopy of diffeomorphisms

$$\phi_r : (Y, L_i \cup T_z|_{\gamma_1}) \xrightarrow{\cong} (Y, L_i \cup T_z|_{\gamma_r})$$

which induces an isomorphism ϕ_{r*} on the corresponding relative second homology groups. Note that when $r = 1$, using methods above we have existence of regular J for the moduli space of curves, and geometrical conditions allow us to exclude bubbling, so we get a compact one-dimensional space. This J then allows us to define a Banach bundle that will be the base of the Fredholm problem:

$$\tilde{\mathcal{B}}^{k,p} := \{(\phi_r^{-1} \circ u, r) \mid u : \mathbb{R} \times [0, 1] \rightarrow (Y, L_i \cup T_z|_{\gamma_r}) \in W^{k,p}\}$$

Alternatively we can classify the tangent space to a path in \tilde{B} as one where the derivative of the path at the boundary is a vector that is a sum of a vector in the tangent space to the Lagrangian boundary and a vector corresponding to the flow of the isotopy ϕ_r . This will give us a 1-manifold structure on the set of maps u so that $\bar{\partial}_J(\phi_r^{-1} \circ u) = 0$, where J is the regular J defined above.

The next step will be to Gromov compactify at the $r = 0$ end. Note that ϕ_r does not have a limit at $r = 0$, as it becomes very degenerate and is not a diffeomorphism. So instead we consider elements as u in this moduli space instead of $\phi_r^{-1} \circ u$. Then we can modify the gluing argument to glue together two homology classes at $r = 0$ to view the glued curve as a limit of $r > 0$ curves. Conversely by Gromov compactness arguments we can reparametrize to deduce that the limit of $r > 0$ maps will be the triangle glued to the disc as shown in Figure 5.2. More concretely, see below.

Gluing domains. In order to preglue: trivialize the normal bundle in a neighborhood of where we want to glue, and then interpolate linearly between the two maps. See [Weh14, lec 3, 1 hr]. Note that even without trivializing, there are scaling functions on the normal bundle. Take r to be the gluing parameter for the two discs in the base, which will be a cross ratio of four points around the neck that is getting pinched to a point. Note that the gluing parameter is $e^{-\ell}$ which goes to zero as the gluing length ℓ goes to infinity, which is the configuration of two discs.

We preglue the domains as follows. We remove a neighborhood of the puncture first. In the (s, t) coordinates on strip-like ends, we glue $(s - \ell, t)$ to (s, t) . That is, we place an amount ℓ in the \mathbb{R} direction on one strip overlapping onto the other strip. The two parts separately give the $r = 0$ case and the two parts glued together is the $r = \epsilon > 0$ case. The embedding that gives the strip-like end embedding is as follows: 1) map $(-\infty, 0] \times [0, 1] \rightarrow (-\infty, 0] \times [0, \pi]$ by $\cdot\pi$. Then map to the lower half of an annulus by e^{-z} , and then lastly to the right half of a disc with a puncture at 1 by $\frac{z+i}{z-i}$. The reason why the preglued map is close to the J -holomorphic glued map is because by continuity $\bar{\partial}_J$ of the glued map is still small; if it were constant on the glued part then it would actually be holomorphic. Since we interpolate slowly, it is indeed close to constant. Note that there is a Gromov topology which gives a distance metric on this space, and metrizable spaces are Hausdorff.

Next we apply Newton iteration to the preglued disc to obtain a J -holomorphic curve. The process of gluing is as follows: take the exponential at the preglued map of the pullback of the tangent bundle, where we can add vectors. The tangent vectors ξ are obtained by Newton iteration (a contraction mapping principle argument), which is applicable on Banach spaces.

The geometry of our setup implies that the moduli spaces of J -holomorphic discs do not

limit to disc bubbling, strip breaking, or sphere bubbling for each $0 < r \leq 1$. At $r = 0$, we do have a disc bubble that forms, and we know this happens by Gromov compactness. That is, we compactify to obtain fiber products on the boundary as the zero set of a Fredholm section. Note that we can find a J which is regular at the $r = 0$ configuration as well. We consider the usual $\bar{\partial}$ operator on each disk component, as well as the difference of the two evaluation maps where they should meet. This also has a Fredholm setup, c.f. [Weh14, Lecture 3, 22 mins].

After this, we then consider gluing maps to the base of $v_0 : Y \rightarrow \mathbb{C}$, versus just the domains as we did above, and finally we use the moment map coordinates $(\xi_1, \xi_2, \eta, \theta_1, \theta_2, \theta_3)$ to glue maps u to the total space.

Thus we have the structure of a compact 1-manifold cobordism between the $r = 0$ and $r = 1$ choices. □

This completes the proof that the homotopy between M^1 and $M^2(c, -)$ is well-defined as the boundary of a 1-dimensional moduli space. □

Computation of discs

In this section we take $J = J_0$ and consider moduli spaces of discs only, for which J_0 is regular. In other words, we only consider homology classes β that arise from disks. Note that since the set of J regular for all configurations is nonempty and dense, and the maps are J_0 sections away from a neighborhood of zero we can claim that J_0 is a limit of such J by the denseness of the regular J . I.e. have a line of J 's limiting to J_0 , so the J 's involve perturbing J_0 near the zero fiber. See the sphere picture in 5.3.

Remark 5.1.12. If we include t_z parallel transported in a circle around the base of $v_0 : Y \rightarrow \mathbb{C}$ as a Lagrangian in the subcategory we are considering, then this Lagrangian bounds nonconstant holomorphic discs. A future direction is to incorporate and define M^0 for the category containing this Lagrangian. Note that M^0 is index 2 in $\mathbb{Z}/2$. In this thesis, we do not include it in the subcategory being considered. We do still want to count the discs and J_0 -spheres, but they will show up only in the c in $M^2(c, -)$ considered as a map on Floer groups.

The following is based on [Aur07] and [CO06].

Definition 5.1.13 (Maslov class of a Lagrangian). $HF(L_0, L_1)$ has a \mathbb{Z}/N grading, up to shifts. Can do relative (up to shifts) or absolute (no shifts). For example, $N = 2$. Suppose $2c_1(M) = 0$, so the square of the anticanonical bundle is trivializable by some section s .

We have a map from LGr to the unit bundle of K^{-2} by taking \det^2 of a basis for each Lagrangian. We can identify that unit bundle with S^1 using the trivializing section s mentioned above. The upshot is that we get a map from $LGr \rightarrow S^1$. The “Maslov class” is the pullback of $[S^1]$ which would imply that we get a homology class in LGr .

Lemma 5.1.14 ([Aur07, §3.1]). *Let (X, ω, J) be a smooth, compact and Kähler manifold. Let $\Omega \in \mathcal{M}^0(X, (T^{*(1,0)}X)^n)$ be a global meromorphic n -form, with poles along an anti-canonical divisor D , e.g. using log coordinates. In other words, Ω^{-1} is a nonzero holomorphic section of the anti-canonical bundle on $X \setminus D$.*

Let L be a Lagrangian submanifold in $X \setminus D$ which is special, i.e. $\Omega|_L$ has constant angle in the function in local holomorphic coordinates. Let $\beta \in \pi_2(X, L)$ be nonzero.

Then: for this special Lagrangian L , $M(\beta)$ is twice the algebraic intersection number $\beta \cdot [D]$.

Proof. The tangent space to L is real since being Lagrangian is defined by $(TL)^\perp = JTL$ with respect to $\omega(-, J-)$. Taking a real basis gives a nonvanishing section of $K_X^{-1}|_L$ which we can scale to unit length. Since we’ve normalized, this section is independent of choice of basis. In particular, its square trivializes the square of the anticanonical bundle, i.e. $2c_1(X \setminus D) = 0$. That is, recall that $M(\beta)$ measures the obstruction to extending the square of this normalized section on L to one on a disc representing β . We can always get grading M by [Sei00], because we have a lift to \mathbb{R} for special Lagrangians, as follows. Ultimately have two nonvanishing unit real sections on TL so they must be the same, one of which is the section (corresponding to divisor D) squared. So the Maslov class of β is, via this squared section, twice the intersection of D and β . \square

Theorem 5.1.15 ([CO06], [Aur07]). *Consider the moduli space of J -holomorphic discs with boundary in L and in the class of β . The virtual dimension is $n - 3 + M(\beta)$. The claim is that these moduli spaces each have one disk in them.*

Proof. The reason for the dimension claim is that $M(\beta)$ should be the dimension by Fredholm theory, but then we add n -marked points and subtract out the reparametrization action (3 points determine an automorphism of the disc).

What we expect for dimensional reasons: since we’re looking at sections, they go through the central fiber which is also the divisor D . They intersect D transversely once so they have Maslov index 2. Then we assume we have one marked boundary point. So the expected dimension is then 2 for Maslov index plus 1 for the marked point minus 3 from quotienting by reparametrization, resulting in an expected dimension of zero. (The disc with boundary on T_z , and fixing a point on the boundary, is a zero dimensional family, otherwise we could rotate the disc by the T^3 action and obtain a family of discs. Fixing a boundary point cuts the dimension down to zero so we can count.)

T_z can be thought of as corresponding to the skyscraper sheaf. Recall before that ℓ_i meant rotating i along the angle directions for one loop in each of the base moment map directions. Rotating only the angle directions and not in the base gives T_z . Namely, fix the moment map coordinates and let the angles vary. This gives the preimage of a moment map coordinate $A = (a_1, a_2, a_3)$ and we let $z = e^{2\pi i A}$ be the exponentiated coordinates. The reason for choosing the letter A is that the formula for counting such discs is discussed in a paper of [CLL12] and that notation agrees with theirs.

Recall that we have complex coordinates on Y as a toric variety. So this carries a natural J_0 . The additional layer of complexity is that this has holomorphic spheres. This will be considered below. We will describe the discs that appear with J_0 , and show this count matches up with the theta function, then discuss a geometric regularization argument with varying J_0 that will exclude the existence of spheres for a nearby J by index and dimension reasons.

The complex dimension of the moduli space of discs with 1 marked point is 1 for the marked point minus 3 from the automorphism group and then plus the Maslov index of the disc class β . Since we want dimension zero, we want $1 - 3 + 2\beta \cap D = 0$ where recall the Maslov index $M(\beta) = 2\beta \cap D$ where D is the union of toric divisors in $v_0^{-1}(0)$. So $\beta \cap D = 1$ implies we only want to consider Maslov 2 discs which intersect the central fiber once. There are no nontrivial Maslov zero discs by the fact that Lagrangians in the fiber do not bound discs.

We can think of the disc in the chart $\mathbb{C}^* \times \mathbb{C}^* \times \mathbb{C}$ (pull back to the universal cover, where we know $\pi = 1$ by toric geometry). Then a disc with boundary in $S^1(r_1) \times S^1(r_2) \times S^1(r_3)$ means it can't show up in the first two components (by the maximum principle) and we obtain a disc in the last v_0 coordinate. It can't be multiply covered because we have Maslov index 2 as the minimum and the maximum. So the discs we count correspond to picking a point A in the moment polytope and drawing a line to a facet, which means $|v_0|$ decreases down to 0.

□

Theorem 5.1.16. *The count of discs equals the defining theta function, up to a change of coordinates.*

Proof. Recall that we weight by $e^{-\int \omega}$ in the count, and now we find the facet equations explicitly.

In 3D we obtain facet equations of

$$\left\langle \nu(F_{m_1, m_2}), \begin{pmatrix} \xi_1 \\ \xi_2 \\ \eta \end{pmatrix} \right\rangle + \alpha(F_{m_1, m_2}) = \langle -m_1, -m_2, 1 \rangle \cdot \langle \xi_1, \xi_2, \eta \rangle + m_1^2 + m_2^2 + m_1 m_2 = 0$$

and the two series are, where x_i are coordinates on the complex side on V and the z_i are $e^{2\pi i a_i}$ where the point in the polytope we measure from is (a_1, a_2, a_3) and the area is $2\pi (\langle \underline{a}, \nu(F_{m_1, m_2}) \rangle + \alpha(F_{m_1, m_2}))$ (or with T Novikov parameter):

$$\begin{aligned} \theta\text{-function} &= \sum_{n \in \mathbb{Z}^2} x_1^{n_1} x_2^{n_2} e^{\frac{1}{2} n^T \begin{pmatrix} 2 & 1 \\ 1 & 2 \end{pmatrix} n} \\ \text{disc count by area} &= z_3 \sum_{n \in \mathbb{Z}^2} z_1^{n_1} z_2^{n_2} e^{\frac{1}{2} n^T \begin{pmatrix} 2 & 1 \\ 1 & 2 \end{pmatrix} n} \end{aligned}$$

Shift origin to middle of tile in polytope, which will get rid of the m_1, m_2 additional terms. The normal to the (m_1, m_2) tile is $\langle -m_1, -m_2, 1 \rangle$. At (m_1, m_2) the tile moving in the $(1, 0)$ direction means we add $\langle 2, 1, z \rangle$ which must be perpendicular to $\langle -m_1, -m_2, 1 \rangle$ hence $z = 2m_1 + m_2$. Similarly moving in the $(0, 1)$ direction from the (m_1, m_2) tile we add $\langle 1, 2, m_1 + 2m_2 \rangle$. To get the equation of each facet, we have the normal but we also need a point on each hexagon. We take the lower left corner, which starts at $(-1, -1, 0)$ in the $(0, 0)$ tile. And we've just found how it increases moving in each direction.

So going from $(0, 0) \rightarrow (1, 0) \rightarrow \dots \rightarrow (m_1, 0)$ tile we add $\langle 2, 1, 0 \rangle$ then $\langle 2, 1, 2 \rangle$ all the way up to $\langle 2, 1, 2(m_1 - 1) \rangle$ hence the total gives $\langle 2m_1, m_1, m_1(m_1 - 1) \rangle$. Then when we go from $(m_1, 0)$ tile to $(m_1, 1)$ tile we add $\langle 1, 2, m_1 \rangle$ as found above and so on until at the end $\langle 1, 2, m_1 + m_2(m_2 - 1) \rangle$. So the total added is $\langle m_2, 2m_2, m_1 m_2 + m_2(m_2 - 1) \rangle$. Hence our distinguished point is

$$\langle 2m_1 + m_2 - 1, m_1 + 2m_2 - 1, m_1(m_1 - 1) + m_2(m_2 - 1) + m_1 m_2 \rangle$$

which we know satisfies

$$\langle -m_1, -m_2, 1 \rangle \cdot \langle \xi_1, \xi_2, \eta \rangle + \alpha(F_{m_1, m_2}) = 0$$

so solving we find $\alpha(F_{m_1, m_2}) = m_1^2 + m_1 m_2 + m_2^2$ or

$$\frac{1}{2} m^T \begin{pmatrix} 2 & 1 \\ 1 & 2 \end{pmatrix} m = \frac{1}{2} m^T (2m_1 + m_2, m_1 + 2m_2) = m_1^2 + m_1 m_2 + m_2^2$$

which is the same as the theta function. □

Remark 5.1.17. We finish the remainder of the plan of computation in Figure 5.3. With J_0 and no α spheres in the homology class, we know the moduli space has 1 disc by invariance. All discs by themselves are regular for J_0 . Then we look at a limit of J_t -holomorphic disks

u_t as t goes to 0, namely they solve the Cauchy-Riemann equation with J_t . After possibly passing to a subsequence, then $\lim_{t \rightarrow 0} u_t =: u_0$ in the Gromov topology, where by Gromov compactness and the exclusion of disk bubbling and strip breaking we find that u_0 is either a disk or a disk union spheres. This is discussed in [CLL12, Proposition 4.30]. In particular, it should be possible to obtain an algebraic relation between these two things similar to the way done above when we found a chain homotopy by varying choices. We instead use polyfold theory to prove well-definedness once we have the count, as it is well-equipped to handle nonregular J , by abstractly perturbations of the $\bar{\partial}_J$ operator.

Remark 5.1.18. More discs with J than J_0 because with J some of them must converge to disc union bubbles with J_0 . Note that [MS12] discuss what happens to maps as we vary J . And in our setting, the homology class also varies when we are varying the Lagrangians. Use invariance: to get moduli spaces with J same as with action applied to J . And then use property of Fukaya category independent of J choices.

Computation of sphere bubbles with J_0 : Gromov-Witten invariants

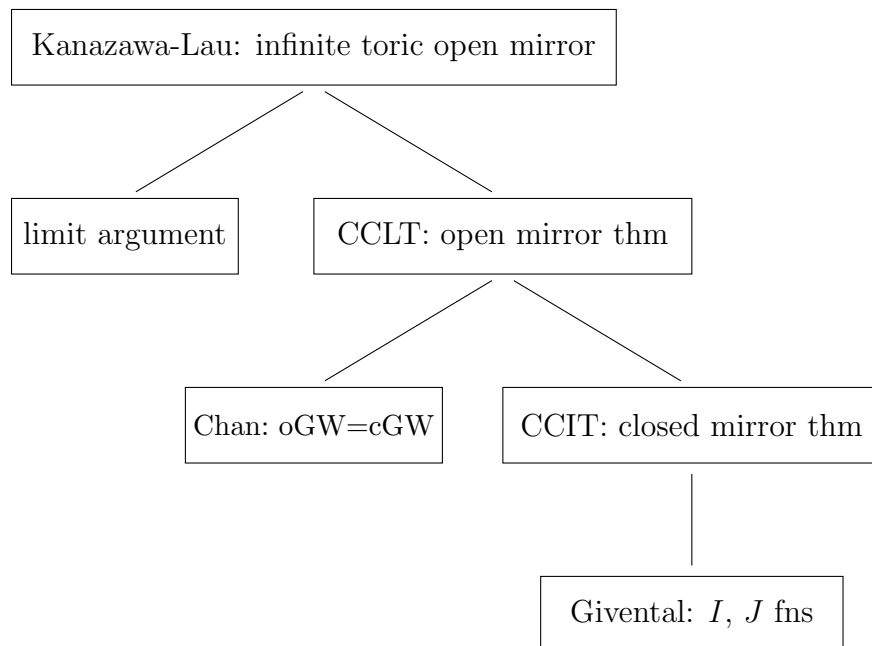
Claim 5.1.19. There are spheres that are not regular for J_0 .

See [Aur07, §4] . T^3 -orbits away from the divisor over 0 are special Lagrangian wrt $\wedge_i d \log x_i$ form. Note: if J is integrable then $\bar{\partial}_J$ is complex linear so the derivative D_u is the same thing. So the cokernel for something with no $(0, 2)$ forms (e.g. in this case true on a Riemann surface in source space) is precisely a Dolbeault cohomology group, degree 1. If that's not zero, then it's not surjective. Hence those problem sphere bubbles over zero are not regular. The index operator gives $n - 3 + c_1$ which is $2 - 3 + 0 = -1$ so dimension -1 can't happen which would imply those spheres do not show up, but we know that they do so it couldn't be regular. They appear in a higher dimensional family so are not of the expected dimension. Only some configurations appear as a limit of moduli spaces while varying J_t . \square

Corollary 5.1.20. *By equivariance, a constant factor appears in our setting which won't affect the quasi-isomorphism class of the resulting Fukaya category.*

Proof of Corollary. Equivariance is discussed in [KL19]. Also, any set-up that produces the moduli spaces will be invariant under the group action Note that [KL19] define a toric Kähler form than here. The complex structures i.e. J_0 are the same. We will be computing the area of spheres in the boundary of the infinite-type toric variety. So a different symplectic form just means that the $\mathbb{C}P^1$'s could be scaled differently. Varying the symplectic parameter would incorporate the Kähler parameters that show up in Gromov-Witten theory, and are called q in [KL19]. Since we fix the symplectic form here, we fix the Kähler parameters q_i . \square

Idea of proof of sphere count. Here is a flow chart indicating the necessary background to understand the sphere count in [KL19]. Note that they use $J = J_0$ as we are using here.



Lemma 5.1.21 (Givental). *Picard-Fuchs can compute GWI and is mirror to combinatorial notion of periods in Hodge structure. Givental introduced the I and J functions.*

Remark 5.1.22 (Closed mirror theorem: [CCIT15]). We provide a collection of resources indicating the timeline and background for understanding Gromov-Witten invariants. J function on one (Gromov-Witten invariants) corresponds to the I function on the other (combinatorial). Builds on Givental: the mirror map is the coefficient on $1/z$. See section 6.3 of [CK99]. Kähler and complex moduli are isomorphic, and mirror map goes between neighborhoods of Kähler large limit point and maximally unipotent monodromy on complex side. Picard-Fuchs is for complex moduli near maximally unipotent monodromy. It is y_k in [CK99]. And q_k is for Kähler moduli. GKZ system is §5.5 in [CK99]. Picard-Fuchs is §5.1.2. Varying complex moduli gives variation of Hodge structure. §2.6.2 introduces Givental's I and J functions. §11.2.5 is Givental's mirror theorem for toric complete intersections. Chapter 10: stack definition of moduli spaces. Equation (10.4) gives the relation between differentials/intersection theory and GW. A reference for an introduction to stacks is [Fan01]. Proposition 10.3.4 of [CK99] gives the relation between the J -function and GW potential. Example of mirror theorem: 11.2.1.3. Theorem 10.3.5: QM differential operator iff Picard-Fuchs operator. Chapter 7 gives the GW definition. Coefficient on $1/z$ statement: [CK99, page 151], z in [KL19] is y_0 in [CK99]. Note: Givental mirror theorem, equivariance, wasn't complete in the original paper [Giv98], according to [CK99]. This is what [CCIT15] discuss. Then [CCLT16] add in the result of [Cha11]:

$$M_X^{open}(\beta + \alpha) = M_X^{closed}(\beta + \alpha)$$

Equivariance was discussed in [CCIT15] because it was in the toric setting.

Definition 5.1.23 (Kuranishi structure). Properties of a Kuranishi neighborhood of p :

- V_p smooth finite-dimensional *manifold*, maybe w/ corners
- $V_p \times E_p \rightarrow V_p$ called *obstruction bundle*. (E_p finite-dimensional real *vector space*.)
- Γ_p finite *group*. Acts smoothly and effectively (no non-trivial elt acts trivially) on V_p , and E_p linearly represents the group.
- *Kuranishi map* s_p is a smooth *section* of $V_p \times E_p$ (smooth map $V_p \rightarrow \Gamma_p$) AND is Γ_p equivariant.
- ψ_p is a *topological chart*, a homeo from local model $s_p^{-1}(0)/\Gamma_p$ to a neighborhood of p in X .
- V_p/Γ_p may also be called a *Kuranishi neighborhood* (rather than the collection of all these pieces of data). In fact, V_p may also be called a Kuranishi neighborhood. So three different things could be called such a nbhd.
- o_p is a point that Kuranishi map sends to zero and chart sends to p .

Gromov-Witten invariants are an example of something that has a Kuranishi structure, since the definition of the structure describes the local picture of such moduli spaces. See also [MTFJ19].

In [KL19] there is a notion of taking a limit to get to the infinite toric case, as mine is. Builds on CCLT open mirror theorem. Kanazawa-Lau do the sphere count: the coefficient of $1/z$ is the mirror map.

Theorem 5.1.24 (Open mirror theorem in [KL19, Theorem 3.10]). *Y is a toric Calabi-Yau manifold of infinite-type. Then*

$$\sum_{\alpha} n_{\beta_l + \alpha} q^{\alpha}(\check{q}) = \exp(g_l(\check{q}))$$

where $q(\check{q})$ is the mirror map and

$$g_l(\check{q}) := \sum_d \frac{(-1)^{(D_l \cdot d)} (-(D_l \cdot d) - 1)!}{\prod_{p \neq l} (D_p \cdot d)!} \check{q}^d$$

This concludes the proof outline for the sphere bubble count of [KL19]. □

Accounting, in definition, for use of non-regular J in computation

At this point, we use polyfolds (with acknowledgement to Benjamin Fillipenko for assistance). The $\overline{\mathcal{M}}_\beta(J)$ we want consider is

$$\overline{\mathcal{M}}_\beta(J) := \{(u, \underline{v}) : (\mathbb{D}, (S^2)^k) \rightarrow Y \mid u(\partial\mathbb{D}) \subset T_z|_{C_r},$$

$$[u\#v] = \beta, (u, \bar{v}) \in C^\infty, ev_{z_0}(0) = ev_{z_1}(z), \bar{\partial}_J(u, v) = 0\} \times \{p\} / \text{Aut}(Y, p)$$

which right now is a set. Define a set \mathcal{B}_β to be the completion of this without the J -holomorphic condition. So similar to the geometric case, however the difference here is the different dimensions and configurations. The whole setup has a polyfold structure, discussed in Jiayong Li's thesis. It contains the set of smooth maps as a dense subset. The bundle on top of \mathcal{B}_β should also have a polyfold structure, and it is defined to be the right thing that $\bar{\partial}_J$ lands in fiberwise.

This has a Fredholm/polyfold setup with suitable section. We can perturb, and there is a cobordism between different perturbations, so it's invariant under perturbations. Also there is a cobordism between varying J . In particular, if we start with a regular J then the perturbation is zero and we get a cobordism between that and the perturbed moduli space which is actually a manifold. Lastly, we use W. Schmaltz's thesis result that the pullback of an admissible perturbation is admissible, under suitable conditions of the map, which the one here satisfy. We find then that all the moduli spaces for different discs have the same configuration of spheres showing up. This uses the machinery of EP groupoids in polyfolds.

By results of [CLL12], we know that the only homology classes that can appear in the compactification are stable trees of the form $D_{ij} + \sum_i n_i \alpha_i$ for some integers n_i and spheres α_i . The goal is then to show that if we fix D_{ij} and compactify, we get the same compactification for any other D_{ij} . Namely that all the moduli spaces are isomorphic as we vary the homology classes; applying the group action gets isomorphic moduli spaces with the same J_0 and we know existence of such moduli spaces by the above discussions. That way, whatever the count is in the compactification with D_{ij} , the compactification with $\gamma(D_{ij})$ will involve isomorphic moduli spaces, so the counts will be the same and we can pull out a common factor.

$$\mathcal{M}(D + \alpha_i, J_0) \cong \mathcal{M}(\gamma(D + \alpha_i), \gamma^* J_0)$$

where the isomorphism is the map given by composition with γ on the cover of Y (before we quotient by Γ_B). Note the result is holomorphic because we use $\gamma^* J_0$, but know that multiplication by scalars is a holomorphic map hence $\gamma^* J_0 = J_0$ and the two moduli spaces are isomorphic.

So both GW theory and polyfold theory give equivalent FS categories as the one we calculated by considering only discs with no spheres. And the count of discs gives the theta function.

5.2 Proof: fully-faithful embedding

$$D^bCoh(H) \hookrightarrow H^0(FS(Y, v_0))$$

On objects we map $\mathcal{L}|_H^{\otimes i} \mapsto L_i$. If ϕ is the monodromy of the symplectic fibration $v_0 : Y \rightarrow \mathbb{C}$ around the origin, then the symmetry of our definition of ω ensures that $\phi(\ell_i)$ is Hamiltonian isotopic to ℓ_{i+1} . Since Floer cohomology is invariant under Hamiltonian isotopy, we can consider linear Lagrangians in the fibers. This allows us to obtain the bottom row of the following diagram, whenever $j \geq i+2$. When $j < i+2$ there are also Ext groups to consider and we get a long exact sequence instead, namely the last horizontal map is not surjective anymore.

$$\begin{array}{ccccccc}
 Hom(\mathcal{L}^{i+1}, \mathcal{L}^j) & \xrightarrow{\otimes s} & Hom(\mathcal{L}^i, \mathcal{L}^j) & \rightarrow & H^0(\mathcal{L}^i, \mathcal{L}^j \otimes \iota_* \mathcal{O}_H) & \rightarrow & 0 \\
 \cong \downarrow & & \cong \downarrow & & \downarrow & & \\
 CF(\ell_{i+1}, \ell_j) & \xrightarrow{\partial} & CF(\ell_i, \ell_j) & \rightarrow & HF(L_i, L_j) & \rightarrow & 0
 \end{array}$$

The map ∂ is part of the Floer differential on $CF(L_i, L_j) \cong CF(\ell_{i+1}, \ell_j)[-1] \oplus CF(\ell_i, \ell_j)$ and counts holomorphic sections of $v_0 : Y \rightarrow \mathbb{C}$ with suitable Lagrangian boundary conditions. The first two vertical isomorphisms on the left come from the abelian variety case. My result is that the left-side square in the diagram commutes, which then implies that the rightmost vertical arrow is an isomorphism as well. More precisely, I show that under the chosen isomorphisms, the Floer differential ∂ agrees with multiplication by $s \in H^0(V, \mathcal{L})$ up to a multiplicative factor (the open Gromov-Witten invariant in [KL19] for a particular choice of Kähler parameter). This provides the desired isomorphism between the morphisms groups for the functor $D^bCoh(H) \rightarrow FS(Y, v_0)$ described above.

Chapter 6

Notation

Section 1.2

- $H = \Sigma_2$ the genus 2 curve
- $V = (\mathbb{C}^*)^2/\Gamma_B$ abelian variety of which H is a hypersurface
- $\mathcal{L} \rightarrow V$ degree $(1, 1)$ line bundle on V
- $s : V \rightarrow \mathcal{L}$ multi-theta function, section of \mathcal{L}
- λ linear form, determines Chern class of \mathcal{L}
- κ quadratic form, determines holomorphic structure of \mathcal{L}

Section 1.3

- M lattice of characters, or functions on toric variety
- N lattice of cocharacters, or 1-parameter subgroups of toric variety
- $M_{\mathbb{R}} = M \otimes_{\mathbb{Z}} \mathbb{R}$, same for N
- m an element of M or $M_{\mathbb{R}}$
- u a lattice element in N

Section 1.4

- $\Delta_{\tilde{Y}}$ polytope defining \tilde{Y}
- $\Delta_Y = \Delta_{\tilde{Y}}/\Gamma_B$
- $(\xi_1, \xi_2, \eta) \in M_{\mathbb{R}}/\Gamma_B \cong \mathbb{R}^3/\Gamma_B$ denote coordinates on the polytope
- $v_0 : Y \rightarrow \mathbb{C}$ superpotential
- $V^\vee \cong (\mathbb{C}^*)^2/\Gamma_B$ fiber of v_0

Bibliography

- [AAK16] Mohammed Abouzaid, Denis Auroux, and Ludmil Katzarkov, *Lagrangian fibrations on blowups of toric varieties and mirror symmetry for hypersurfaces*, Publ. Math. Inst. Hautes Études Sci. **123** (2016), 199–282.
- [Abo09] Mohammed Abouzaid, *Morse homology, tropical geometry, and homological mirror symmetry for toric varieties*, Selecta Math. (N.S.) **15** (2009), no. 2, 189–270.
- [ACGK12] Mohammad Akhtar, Tom Coates, Sergey Galkin, and Alexander M. Kasprzyk, *Minkowski polynomials and mutations*, SIGMA Symmetry Integrability Geom. Methods Appl. **8** (2012), Paper 094, 17.
- [APS] Nicolas Addington, Alexander Polishchuk, and Ed Segal, *Summer graduate school, derived categories*, https://www.msri.org/summer_schools/821.
- [AS] Mohammed Abouzaid and Paul Seidel, *Lefschetz fibration methods in wrapped Floer cohomology*, in preparation.
- [AS10] Mohammed Abouzaid and Ivan Smith, *Homological mirror symmetry for the 4-torus*, Duke Math. J. **152** (2010), no. 3, 373–440.
- [Aur07] Denis Auroux, *Mirror symmetry and T-duality in the complement of an anti-canonical divisor*, J. Gökova Geom. Topol. GGT **1** (2007), 51–91.
- [Aur14] ———, *A beginner’s introduction to Fukaya categories*, Contact and symplectic topology, Bolyai Soc. Math. Stud., vol. 26, János Bolyai Math. Soc., Budapest, 2014, pp. 85–136.
- [BD16] Marco Bonatto and Dikran Dikranjan, *Generalize Heisenberg Groups and Self-Duality*, arXiv e-prints (2016), arXiv:1611.02685.
- [Bej18] Dori Bejleri, *The SYZ conjecture via homological mirror symmetry*, Super-school on derived categories and D-branes, Springer Proc. Math. Stat., vol. 240, Springer, Cham, 2018, pp. 163–182.

- [BFW17] Nate Bottman, Joel Fish, and Katrin Wehrheim, *Polyfold theory towards the Fukaya category, June 12-16, 2017 at UC Berkeley*, http://www.polyfolds.org/index.php?title=RTG_workshop_program, 2017.
- [BJ07] B.H. Bransden and Charles Joachain, *Quantum mechanics (second edition)*, Prentice Hall-Pearson, Harlow, England, January 2007.
- [BL04] Christina Birkenhake and Herbert Lange, *Complex abelian varieties*, second ed., Grundlehren der Mathematischen Wissenschaften [Fundamental Principles of Mathematical Sciences], vol. 302, Springer-Verlag, Berlin, 2004.
- [Can] Catherine Cannizzo, *Homological mirror symmetry for the genus 2 curve in an abelian variety and its generalized Strominger-Yau-Zaslow mirror*, Ph.D. thesis, University of California, Berkeley, in preparation: https://math.berkeley.edu/~cannizzo/Cannizzo_draft_Oct_31.
- [CCIT15] Tom Coates, Alessio Corti, Hiroshi Iritani, and Hsian-Hua Tseng, *A mirror theorem for toric stacks*, *Compos. Math.* **151** (2015), no. 10, 1878–1912.
- [CCLT16] Kwokwai Chan, Cheol-Hyun Cho, Siu-Cheong Lau, and Hsian-Hua Tseng, *Gross fibrations, SYZ mirror symmetry, and open Gromov-Witten invariants for toric Calabi-Yau orbifolds*, *J. Differential Geom.* **103** (2016), no. 2, 207–288.
- [CdLOGP91] Philip Candelas, Xenia C. de la Ossa, Paul S. Green, and Linda Parkes, *A pair of Calabi-Yau manifolds as an exactly soluble superconformal theory*, *Nuclear Phys. B* **359** (1991), no. 1, 21–74.
- [Cha11] Kwokwai Chan, *A formula equating open and closed Gromov-Witten invariants and its applications to mirror symmetry*, *Pacific J. Math.* **254** (2011), no. 2, 275–293.
- [CK99] David A. Cox and Sheldon Katz, *Mirror symmetry and algebraic geometry*, *Mathematical Surveys and Monographs*, vol. 68, American Mathematical Society, Providence, RI, 1999.
- [CLL12] Kwokwai Chan, Siu-Cheong Lau, and Naichung Conan Leung, *SYZ mirror symmetry for toric Calabi-Yau manifolds*, *J. Differential Geom.* **90** (2012), no. 2, 177–250.
- [CLS11] David A. Cox, John B. Little, and Henry K. Schenck, *Toric varieties*, *Graduate Studies in Mathematics*, vol. 124, American Mathematical Society, Providence, RI, 2011.

- [CO06] Cheol-Hyun Cho and Yong-Geun Oh, *Floer cohomology and disc instantons of Lagrangian torus fibers in Fano toric manifolds*, Asian J. Math. **10** (2006), no. 4, 773–814.
- [Fan01] Barbara Fantechi, *Stacks for everybody*, European Congress of Mathematics, Vol. I (Barcelona, 2000), Progr. Math., vol. 201, Birkhäuser, Basel, 2001, pp. 349–359.
- [FOOO09a] Kenji Fukaya, Yong-Geun Oh, Hiroshi Ohta, and Kaoru Ono, *Lagrangian intersection Floer theory: anomaly and obstruction. Part I*, AMS/IP Studies in Advanced Mathematics, vol. 46, American Mathematical Society, Providence, RI; International Press, Somerville, MA, 2009.
- [FOOO09b] ———, *Lagrangian intersection Floer theory: anomaly and obstruction. Part II*, AMS/IP Studies in Advanced Mathematics, vol. 46, American Mathematical Society, Providence, RI; International Press, Somerville, MA, 2009.
- [For91] Otto Forster, *Lectures on Riemann surfaces*, Graduate Texts in Mathematics, vol. 81, Springer-Verlag, New York, 1991, Translated from the 1977 German original by Bruce Gilligan, Reprint of the 1981 English translation.
- [Fra10] J Francis, *Math 465, spring 2010: Topology of manifolds*, <http://math.northwestern.edu/~jnkf/classes/mflds/>, 2010.
- [Fuk02] Kenji Fukaya, *Mirror symmetry of abelian varieties and multi-theta functions*, J. Algebraic Geom. **11** (2002), no. 3, 393–512.
- [Ful93] William Fulton, *Introduction to toric varieties*, Annals of Mathematics Studies, vol. 131, Princeton University Press, Princeton, NJ, 1993, The William H. Roever Lectures in Geometry.
- [Gan16a] Sheel Ganatra, *Automatically generating Fukaya categories and computing quantum cohomology*, arXiv preprint arXiv:1605.07702 (2016).
- [Gan16b] ———, *Math 257b: Topics in symplectic geometry – aspects of fukaya categories*, <https://dornsife.usc.edu/sheel-ganatra/math-257b/>, 2016.
- [GH94] Phillip Griffiths and Joseph Harris, *Principles of algebraic geometry*, Wiley Classics Library, John Wiley & Sons, Inc., New York, 1994, Reprint of the 1978 original.
- [Giv98] Alexander Givental, *A mirror theorem for toric complete intersections*, Topological field theory, primitive forms and related topics (Kyoto, 1996), Progr. Math., vol. 160, Birkhäuser Boston, Boston, MA, 1998, pp. 141–175.

- [GP90] B. R. Greene and M. R. Plesser, *Duality in Calabi-Yau moduli space*, Nuclear Phys. B **338** (1990), no. 1, 15–37.
- [Huy05] Daniel Huybrechts, *Complex geometry*, Universitext, Springer-Verlag, Berlin, 2005, An introduction.
- [KL19] Atsushi Kanazawa and Siu-Cheong Lau, *Local Calabi-Yau manifolds of type \tilde{A} via SYZ mirror symmetry*, J. Geom. Phys. **139** (2019), 103–138.
- [Kon95] Maxim Kontsevich, *Homological algebra of mirror symmetry*, Proceedings of the International Congress of Mathematicians, Vol. 1, 2 (Zürich, 1994), Birkhäuser, Basel, 1995, pp. 120–139.
- [KS01] Maxim Kontsevich and Yan Soibelman, *Homological mirror symmetry and torus fibrations*, Symplectic geometry and mirror symmetry (Seoul, 2000), World Sci. Publ., River Edge, NJ, 2001, pp. 203–263.
- [Laz00] L. Lazzarini, *Existence of a somewhere injective pseudo-holomorphic disc*, Geom. Funct. Anal. **10** (2000), no. 4, 829–862.
- [Laz11] Laurent Lazzarini, *Relative frames on J -holomorphic curves*, J. Fixed Point Theory Appl. **9** (2011), no. 2, 213–256.
- [Mil65] John Milnor, *Lectures on the h -cobordism theorem*, Notes by L. Siebenmann and J. Sondow, Princeton University Press, Princeton, N.J., 1965.
- [MS12] Dusa McDuff and Dietmar Salamon, *J -holomorphic curves and symplectic topology*, second ed., American Mathematical Society Colloquium Publications, vol. 52, American Mathematical Society, Providence, RI, 2012.
- [MS17] ———, *Introduction to symplectic topology*, third ed., Oxford Graduate Texts in Mathematics, Oxford University Press, Oxford, 2017.
- [MTFJ19] Dusa McDuff, Mohammad Tehrani, Kenji Fukaya, and Dominic Joyce, *Virtual fundamental cycles in symplectic topology*, American Mathematical Society, 2019.
- [Oh93] Yong-Geun Oh, *Floer cohomology of Lagrangian intersections and pseudo-holomorphic disks. I*, Comm. Pure Appl. Math. **46** (1993), no. 7, 949–993.
- [Pol03] Alexander Polishchuk, *Abelian varieties, theta functions and the Fourier transform*, Cambridge Tracts in Mathematics, vol. 153, Cambridge University Press, Cambridge, 2003.
- [PZ98] Alexander Polishchuk and Eric Zaslow, *Categorical mirror symmetry: The elliptic curve*, Adv. Theor. Math. Phys. **2** (1998), 443–470.

- [Seg] Graeme Segal, *July-august 1999 itp workshop on geometry and physics: Topological field theory ('stanford notes')*, <http://web.math.ucsb.edu/~drm/conferences/ITP99/segal/>.
- [Sei00] Paul Seidel, *Graded Lagrangian submanifolds*, Bull. Soc. Math. France **128** (2000), no. 1, 103–149.
- [Sei08] ———, *Fukaya categories and Picard-Lefschetz theory*, Zurich Lectures in Advanced Mathematics, European Mathematical Society (EMS), Zürich, 2008.
- [Sei11] ———, *Homological mirror symmetry for the genus two curve*, J. Algebraic Geom. **20** (2011), no. 4, 727–769.
- [SYZ96] Andrew Strominger, Shing-Tung Yau, and Eric Zaslow, *Mirror symmetry is T-duality*, Nuclear Phys. B **479** (1996), no. 1-2, 243–259.
- [Weh13] Katrin Wehrheim, *Berkeley math 278: Analysis of pseudoholomorphic curves*, <https://piazza.com/berkeley/fall2013/berkeleymath278/resources>, 2013.
- [Weh14] ———, *Regularization of moduli spaces of pseudoholomorphic curves*, <https://math.berkeley.edu/~katrin/teach/regularization/lectures.shtml>, 2014.